LEABHARLANN CHOLÁISTE NA TRÍONÓIDE, BAILE ÁTHA CLIATH | TRINITY COLLEGE LIBRARY DUBLIN
Ollscoil Átha Cliath | The University of Dublin

Terms and Conditions of Use of Digitised Theses from Trinity College Library Dublin

Copyright statement

All material supplied by Trinity College Library is protected by copyright (under the Copyright and Related Rights Act, 2000 as amended) and other relevant Intellectual Property Rights. By accessing and using a Digitised Thesis from Trinity College Library you acknowledge that all Intellectual Property Rights in any Works supplied are the sole and exclusive property of the copyright and/or other IPR holder. Specific copyright holders may not be explicitly identified. Use of materials from other sources within a thesis should not be construed as a claim over them.

A non-exclusive, non-transferable licence is hereby granted to those using or reproducing, in whole or in part, the material for valid purposes, providing the copyright owners are acknowledged using the normal conventions. Where specific permission to use material is required, this is identified and such permission must be sought from the copyright holder or agency cited.

Liability statement

By using a Digitised Thesis, I accept that Trinity College Dublin bears no legal responsibility for the accuracy, legality or comprehensiveness of materials contained within the thesis, and that Trinity College Dublin accepts no liability for indirect, consequential, or incidental, damages or losses arising from use of the thesis for whatever reason. Information located in a thesis may be subject to specific use constraints, details of which may not be explicitly described. It is the responsibility of potential and actual users to be aware of such constraints and to abide by them. By making use of material from a digitised thesis, you accept these copyright and disclaimer provisions. Where it is brought to the attention of Trinity College Library that there may be a breach of copyright or other restraint, it is the policy to withdraw or take down access to a thesis while the issue is being resolved.

Access Agreement

By using a Digitised Thesis from Trinity College Library you are bound by the following Terms & Conditions. Please read them carefully.

I have read and I understand the following statement: All material supplied via a Digitised Thesis from Trinity College Library is protected by copyright and other intellectual property rights, and duplication or sale of all or part of any of a thesis is not permitted, except that material may be duplicated by you for your research use or for educational purposes in electronic or print form providing the copyright owners are acknowledged using the normal conventions. You must obtain permission for any other use. Electronic or print copies may not be offered, whether for sale or otherwise to anyone. This copy has been supplied on the understanding that it is copyright material and that no quotation from the thesis may be published without proper acknowledgement.

Functional analyses of a novel leucine-rich repeat-containing protein, Elfn1, in the mouse

Jackie N. Dolan

A thesis submitted for the fulfilment of the Degree of Doctor in Philosophy to Trinity College, University of Dublin.

May 2013

Declaration

I declare that I am the sole author of this thesis and the work presented is entirely my own, unless otherwise stated. I declare that the work has not been submitted previously to this or any other university.

I agree that the library of Trinity College Dublin may lend or copy this thesis upon request.

Thesis 10236

Summary

The functional brain is critically dependent on a highly specific and perfectly timed gene-expression programme that underlies neuronal connectivity. Each step of this process, which includes cell migration, axon guidance, target selection and synaptogenesis, requires a vast number of molecules. While many genes with roles in these processes have been identified to date, the astonishing complexity and specificity of neural connections suggests that further molecules yet-unidentified are involved. Leucine-rich repeat (LRR)-containing proteins are known to play crucial roles in the developing central nervous system. This led to the hypothesis that additional genes from this class of proteins could provide the necessary specificity of cellular interactions involved in neural connectivity.

A comprehensive survey of the entire extracellular LRR (eLRR) proteome was established in the worm, fly, mouse and human using a bioinformatics approach. Only proteins with LRR domains that reside outside the cell, with a potential to function in cell-cell communication, were included. The resultant number of proteins in each species showed that the eLRR superfamily has greatly expanded in mammals (139 proteins in human, 135 in mouse) and to a lesser extent in the flies (66 proteins) compared with the worm (29 proteins). Within species and between species relationships were analysed using a clustering programme which provided accurate classification of related families and subfamilies. Evolutionary analyses identified that a particular group of proteins, which include an Ig or FN3 domain but no other extracellular domains except LRRs (LRR_Ig/FN3 group), contained the highest percentage of mammal-specific subfamilies with many containing multiple members, indicating evolutionary divergence followed by expansion. Analyses of novel proteins by *in situ* hybridisation (ISH) highlighted a family of vertebrate-specific proteins from the LRR_Ig/FN3 group, which consists of two closely related transmembrane proteins characterised by a signal peptide, 6 LRR repeats, an LRR-CT and an FN3 domain extracellularly, a TM domain and a long cytoplasmic tail. We named them Elfn1 and Elfn2. *Elfn1* displayed highly localised expression in particular regions of the brain, a prerequisite for a function in specifying connectivity. A knockout mouse for *Elfn1* was obtained for further investigation. In this line, the full *Elfn1* coding region was replaced by a β-

galactosidase (βgal) reporter labeling the cell bodies. A comprehensive description of *Elfn1* expression using βgal immunohistochemistry in Elfn1$^{+/-}$ brains identified expression in particular regions of the brain including subsets of cells in the hippocampus and the cortex, and discrete nuclei within the habenula. Sylwestrak and Ghosh (2012) have shown that Elfn1 localises to the dendrites of interneurons in the hippocampus, and functions postsynaptically in the elaboration of synaptic properties of glutamatergic synapses from CA1 pyramidal cells. Our expression study established that Elfn1 also localises to long-range GABAergic neurons and excitatory neurons suggesting additional functions for Elfn1 in the presynaptic neuron. Furthermore, comparative immunohistochemistry stainings in Elfn1$^{-/-}$ and Elfn1$^{+/-}$ mice with a pan-Elfn antibody identifed that Elfn1 is present in axons of the fasciculus retroflexus innervating the interpeduncular nucleus and long-range GABAergic neurons that project to the substantia nigra pars compacta.

In a zebrafish screen for molecules involved in extracellular interactions, Elfn1 was found to interact with Robo3, a known axon guidance molecule (Sollner and Wright, 2009). The confirmation of this interaction in mouse is presented here, *in vitro* and *in vivo,* by co-immunoprecipitation and Robo3-AP ISH on mouse brain slices. Comparisons of *Elfn1* and *Robo3* expression patterns by *in situ* hybridisation and *in silico* analysis identified a strong and complementary expression pattern for *Elfn1* and *Robo3* in the habenula, a nucleus identified as an important modulator of monoaminergic activity. No anatomical or connectivity phenotype has been identified thus far by comparing immunohistochemistry staining patterns in Elfn1$^{-/-}$ and Elfn1$^{+/-}$ brain sections. However, preliminary results suggest that there may be altered glutamatergic transmission to the habenula in Elfn1$^{-/-}$ mice, with reduced vGlut2 staining patterns visible in the habenula. Behavioural analyses have revealed that Elfn1$^{-/-}$ mice display spontaneous seizures and abnormalities in motor function. In the open field behaviour test, Elfn1$^{-/-}$ mice exhibited reduced thigmotaxis, an indicator of anxiety, and increased locomotion when compared with Elfn1$^{+/-}$ mice. The increased locomotion was paradoxically attenuated by amphetamine, which occurs in ADHD-like hyperactivity, and therefore Elfn1$^{-/-}$ mice are potentially an animal model of this disorder. In conclusion, these behavioural phenotypes reveal a requirement for Elfn1 in the establishment of the functional circuitry of the brain.

Acknowledgements

I would like to sincerely thank Dr. Kevin Mitchell for allowing me the opportunity to carryout this research. He has supported and guided me throughout this process, including the short pauses in progress when I had my two boys. His massive interest and knowledge in every aspect of neuroscience, is hugely motivating and a great benefit to all his students.

I would like to thank the members of the Mitchell lab, both past and present, for the help, advice and friendship throughout the years. I would like to particularly thank Karen and Niamh; both have given me so much time and help with this project. I also wish to thank Manuela, Olivia and Danny and all my friends for their encouragement, especially over the last couple of months.

I cannot thank my parents enough for the love and support they have always given me. I couldn't have managed without them through the course of this research. Thanks also to my two brothers, Gary and Johnny, for their continued encouragement.

To my three boys; Artie, Ben and Sam. I really couldn't have done this without the full support of my husband. I will always appreciate how well you looked after our boys while I was working, and for encouraging me and distracting me when I needed it. A very special thank you to my two sons, Ben and Sam, for giving me so much happiness and motivating me to make you both proud.

Finally, I would like to dedicate this thesis to my beautiful little sister Amy.

Table of Contents

Table of Contents 1

List of Figures 6

List of Tables 8

List of abbreviations 9

1 **Chapter 1 General Introduction** 11

1.1 Introduction 11

1.2 Leucine-rich repeat structure 11

1.3 Leucine-rich repeat proteins in nervous system development 13

1.3.1 LRR proteins in axon guidance 17

1.3.2 LRR proteins in target selection 18

1.3.3 LRR proteins in synaptogenesis 23

1.3.4 LRR proteins and neurological or psychiatric disorders 27

1.3.5 eLRR proteins display differential patterns of expression in the brain 32

1.4 Aims of this thesis 35

2 **Chapter 2 Materials and Methods** 37

2.1 Database pipeline 37

2.2 LRRscan 38

2.3 RNA *in situ* hybridization 41

2.3.1 RNA in situ hybridization of *Drosophila* embryos 41

2.3.2 Mouse in situ hybridization 42

2.4 Animal Husbandry 43

2.5 Genotyping of mice 43

2.6 Immunohistochemistry 44

2.7 Production of tagged proteins 45

2.8 AP in situ hybridization 47

2.9 Behaviour analysis 47

2.9.1 Wire-hang test 48

2.9.2 Open-field test 48
2.9.3 Drug Administration 49
2.9.4 Seizure observation 49
2.9.5 Data analysis 49

3 **Chapter 3 The extracellular Leucine-Rich Repeat superfamily** 51

3.1 Introduction 51
3.2 Results 54

3.2.1 Bioinformatics strategy 54
3.2.2 Clustering 55
3.2.3 Identification of LRR motifs 56
3.2.4 Identification of extracellular LRR proteins 57
3.2.5 Manual curation of extracellular sequences 58
3.2.6 Defining consensus architectures 59
3.2.7 The eLRR superfamily 60
3.2.8 Subfamily expansion and diversification 61
3.2.9 Clustering of known proteins 71
3.2.10 Novel protein families 72
3.2.11 Genomic clustering 77
3.2.12 Expression analyses 78

3.3 Discussion 82

3.3.1 Methodological issues 83
3.3.2 A comprehensive, curated dataset 83
3.3.3 Hierarchical clustering 85
3.3.4 Nomenclature 86
3.3.5 Comparative analyses of major groups 86
3.3.6 Human-mouse differences 88

3.4 Conclusions 89

4 **Chapter 4 *Elfn1* expression in the mouse brain** 90

4.1 Introduction 90

4.1.1 Elfn genes 90
4.1.2 *Elfn1* 93

4.1.3 Habenula Circuitry 95
4.1.4 Aims of this chapter 99
4.2 Results 99
4.2.1 Investigation of the *Elfn1* knockout model 99
4.2.2 *Elfn1* is expressed in interneurons of the hippocampus and cortex 103
4.2.3 *Elfn1* is expressed in GABAergic cells of the Globus pallidus 105
4.2.4 Elfn1 expression in the Amygdala 110
4.2.5 Elfn1 expression in the Septal Nuclei and islands of Calleja ..110
4.2.6 Elfn1 in the Habenula 117
4.2.7 Elfn1 localises to axons of the fasciculus retroflexus, the IPL and the substantia nigra pars compacta. 117
4.3 Discussion 119
4.3.1 Elfn1 in the cortex and hippocampus 120
4.3.2 Elfn1 in the habenula circuitry 121
4.3.3 Elfn1 and the islands of Calleja 126
4.3.4 Conclusion 126
5 Chapter 5 **Investigation of an interaction between Elfn1 and Robo3** 127
5.1 Introduction 127
5.1.1 Elfn1 interacts with Robo3 in zebrafish 127
5.1.2 Robo3 in the mouse developing nervous system 128
5.1.3 Aims of this chapter 129
5.2 Results 130
5.2.1 *In silico* expression analysis of Robo3 and Elfn1 130
5.2.2 Robo3a binds Elfn1 in mouse 132
5.2.3 Preliminary analysis reveals normal innervation of the IPN by Robo3-expressing axons 137
5.3 Discussion 138
5.3.1 Confirmation of Robo3 as a binding partner for Elfn1 138

5.3.2 Possible role in axon guidance 139
5.3.3 Conclusion 140

6 **Chapter 6 Phenotypic investigation of the *Elfn1* mutant mouse** .. 141

6.1 Introduction 141

6.1.1 Elfn1 functions in synaptic transmission 141
6.1.2 Aims of this chapter 142

6.2 Results 142

6.2.1 No anatomical abnormality detected in the Elfn1$^{-/-}$ mice 142
6.2.2 Gross connectivity in Elfn1$^{-/-}$ mice is normal 142
6.2.3 Reduced vGlut2 immunoreactivity in the habenula of Elfn1$^{-/-}$ mice 147

6.3 Discussion 147

6.3.1 Elfn1$^{-/-}$ mice lack obvious anatomical or connectivity defects . 147
6.3.2 Altered synaptic transmission in the habenula 149
6.3.3 Conclusion 150

7 **Chapter 7 Behavioural analyses of the *Elfn1* mutant mouse** 151

7.1 Introduction 151

7.1.1 Aims of this chapter 155

7.2 Results 156

7.2.1 Seizures in *Elfn1*$^{-/-}$ mice 156
7.2.2 Reduced performance of *Elfn1*$^{-/-}$ mice in motor coordination and strength testing 156
7.2.3 Elfn$^{-/-}$ mice exhibit hyperlocomotion 158
7.2.4 Reduced thigmotaxis in *Elfn1*$^{-/-}$ mice 163
7.2.5 Attenuation of hyperlocomotion with amphetamine 165

7.3 Discussion 168

7.3.1 Behavioural abnormalities in *Elfn1*$^{-/-}$ mice 168
7.3.2 *Elfn1* mice exhibit increased locomotion 169
7.3.3 Reduced thigmotaxis in *Elfn1*$^{-/-}$ mice 171
7.3.4 Psychostimulant-induced attenuation of hyperlocomotion 172

8 **Chapter 8 Conclusions and future directions** 174

8.1 Final conclusions 174

8.1.1 eLRR superfamily 174

8.1.2 The Elfn family 174

8.1.3 Interaction of Elfn1 and Robo3 175

8.1.4 Anatomical investigation of Elfn1$^{-/-}$ mice 176

8.1.5 Behavioural analyses of Elfn1$^{-/-}$ mice 176

8.2 Future directions 178

9 **Chapter 9 Appendix** 180

10 **Chapter 10 References** 184

List of Figures

Figure 1.1 Structure of the leucine-rich repeat (LRR) domain. 12
Figure 1.2 Identified extracellular interactions made by LRR and immunoglobulin superfamily members in the zebrafish. 16
Figure 1.3 Expression of the target recognition molecules, Capricious and connectin, in the fly neuromuscular system. 20
Figure 1.4 Netrin-G-NGL transneuronal interactions between axons and distinct dendritic segments of their target neurons. 23
Figure 1.5 Differential expression patterns of LRRTM family members. 32
Figure 1.6 Differential expression patterns of the Slitrk family members. 33
Figure 1.7 Differential expression patterns of the Lrfn/Salm genes. 34
Figure 3.1 Bioinformatics pipeline. 55
Figure 3.2 Sample from list of all eLRR genes, hierarchically clustered at e^{-40} cutoff. 63
Figure 3.3 eLRR protein predicted architectures (part 1). 66
Figure 3.4 eLRR protein predicted architectures (part 2). 67
Figure 3.5 Group-specific patterns of expansion and diversification. 70
Figure 3.6 Alignment of Elfn proteins. 75
Figure 3.7 Alignment of proteins in Elron cluster. 76
Figure 3.8 Expression of *Elfn* genes in developing mouse brain. 80
Figure 3.9 Expression of Elron cluster genes in developing mouse brain. 81
Figure 3.10 Expression of novel eLRR genes in the *Drosophila* embryo. 82
Figure 4.1 Protein architecture and intracellular sequence alignment for Elfn1 and Elfn2 91
Figure 4.2 Targeted allele of Elfn1. 94
Figure 4.3 Schematic diagram of the dorsal diencephalic conduction (DDC) system. 97
Figure 4.4 βgal immunohistochemistry replicates *Elfn1 in-situ* hybridisation staining patterns (part 1). 101
Figure 4.5 βgal immunohistochemistry replicates *Elfn1 in-situ* hybridisation staining patterns (part 2). 102

Figure 4.6 βgal expression in scattered cells throughout the neocortex and piriform cortex. 104
Figure 4.7 βgal is expressed in a subset of somatostatin-positive cells in the cortex. 105
Figure 4.8 Elfn1 is expressed throughout the rostrocaudal extent of the globus pallidus. 107
Figure 4.9 Elfn1 expressing cells in the globus pallidus are GABAergic. 108
Figure 4.10 Elfn1 expression in the amygdala. 109
Figure 4.11 Elfn1 is expressed in the septal nuclei and the islands of Calleja. ... 112
Figure 4.12 Elfn1 is expressed in interneurons of the medial septum. 113
Figure 4.13 A subset of Elfn1 containing cells are positive for GAD67 in the islands of Calleja. 114
Figure 4.14 Elfn1 expression in a subset of cells in the medial and lateral habenula. 115
Figure 4.15 Elfn1 localises to axons of the fasciculus retroflexus. 118
Figure 4.16 Elfn1 expression in the lateral IPN and the SNc. 119
Figure 4.17 Allen brain atlas habenula connectivity in adult 125
Figure 5.1 Expression of Efn1 and Robo3 in the developing mouse brain. 130
Figure 5.2 Elfn1 and Robo3 expression in the habenula 131
Figure 5.3 In vitro co-imunoprecipitation of Robo3 and Elfn1 proteins. 133
Figure 5.4 Robo3-AP *in situ* hybridisation indentifies robo3-Elfn1 interaction *in vivo* 135
Figure 5.5 Robo3a-AP staining in the habenula and fasciculus retroflexus. 136
Figure 5.6 Normal innervation of Robo3-containing fibres at the IPN. 137
Figure 6.1 Anatomical analyses of the Elfn1$^{-/-}$ mouse brain at P0 (part 1) 143
Figure 6.2 Anatomical analyses of the Elfn1$^{-/-}$ mouse brain at P0 (part 2). 144
Figure 6.3 Phenotypic analysis of neuronal connectivity in Elfn$^{-/-}$ brain. 145
Figure 6.4 Phenotypic analysis of habenulopeduncular connectivity in the Elfn1$^{-/-}$ brain. 146
Figure 6.5 Reduced vGlut2 immunoreactivity in the habenula of Elfn1$^{-/-}$ mice. ... 148
Figure 7.1 Motor performance of *Elfn1*$^{+/-}$ and *Elfn1*$^{-/-}$ mice in the wire-hang test. 157
Figure 7.2 Hyperlocomotion of *Elfn1*$^{-/-}$ mice in experiment 1. 160
Figure 7.3 Increased locomotion in *Elfn1*$^{-/-}$ mice in experiment 2. 161

Figure 7.4 Locomotion of *Elfn1*$^{-/-}$ and *Elfn1*$^{+/-}$ mice over time in experiment 2. ... 162
Figure 7.5 Reduced thigmotaxis in *Elfn1*$^{-/-}$ mice ... 164
Figure 7.6 Reduced locomotion in *Elfn1*$^{-/-}$ mice with Amphetamine. ... 167
Figure 9.1 Nucleotide sequence of Elfn1 showing vector insertion site. ... 180
Figure 9.2 Amino acid sequence alignment of Robo3 isoforms. ... 182

List of Tables

Table 1.1 Summary of the identified interactions made by a selection of LRR-containing proteins. ... 15
Table 1.2 List of eLRR-containing proteins implicated in neurodevelopmental disorders. ... 30
Table 1.3 Genetic mouse models of common neurodevelopmental disorders. ... 31
Table 1.4 Neurological disorders associated with the binding partners of LRR-containing proteins. ... 31
Table 2.1 Primer sequences used for genotyping PCR reactions ... 44
Table 2.2 Description of the PCR genotyping programme ... 44
Table 2.3 List of antibodies used in this study. ... 45
Table 2.4 Primers used to amplify Elfn1 and Elfn2 transcripts for directional cloning into pcDNA3.1 ... 46
Table 3.1 List of LRR_Only singletons. ... 68
Table 3.2 Complement of eLRR proteins by group, localisation and species. ... 69
Table 9.1Elfn1 knockout mice used in the behavioural analyses. ... 183

List of abbreviations

ADHD	Attention-deficit/hyperactivity disorder
AMPH	Amphetamine
Amy	Amygdala
AP	Alkaline phosphatase
BLA	Basolateral amygdala
BMA	Basomedial amygdala
BNST	Bed nucleus of the stria terminalis
CCR	Cytoplasmic conserved region
CeA	Central amygdala
Ctx	Cortex
DBB	Diagonal band of Broca
DCD	Developmental coordination disorder
DDC	Dorsal diencephalic conduction system
DTg	Dorsal tegmental nucleus
eLRR	Extracellular leucine-rich repeat
EP	Entopeduncular nucleus
FN3	Fibronectin type-3 domain
FR	Fasciculus retroflexus
GP	Globus pallidus
HC	Hippocampus
ICj	Islands of Calleja
IG	Immunoglobulin domain
IPN	Interpeduncular nucleus
ISH	*In-situ* hybridisation
LH	Lateral hypothalamus
LHb	Lateral habenula
LRR	Leucine rich-repeat
LRRCT	C-terminal leucine rich-repeat
LRRNT	N-terminal leucine rich-repeat
LS	Lateral septum

MeA	Medial amygdala
MHb	Medial habenula
MS	Medial septum
OL-M	Oriens lacunosum-moleculare
Pir	Piriform cortex
RMTg	Rostromedial tegmental nucleus
SFi	Septofimbrial nucleus
SM	Stria medullaris
SNc	Substantia nigra pars compacta
SP	Substance P
SST	Somatostatin
St	Stria terminalis
Th	Thalamus
TM	Transmembrane
TS	Triangular septal nucleus
vGlut	Vesicular glutamate transporter
VP	Ventral pallidus
VTA	Ventral tegmental area
βgal	βgalactosidase

1 Chapter 1 General Introduction

1.1 Introduction

The brain is an extremely complex system and its development involves a highly conserved programme of gene expression that underlies the establishment of functional neuronal circuits. This process includes neural induction, cell migration, axon guidance, target selection and synapse formation. Indeed, the working brain is crucially dependent on the interconnection of distinct brain regions via fiber pathways that is highly conserved between species and extraordinarily consistent within a species.

The first step towards a functional brain involves neural induction and the differentiation of neurons from progenitor cells (Jessell and Sanes 2000, Kobe and Kajava 2001), followed by the migration of these cells to their final positions (Valiente and Marin 2010). From there, neurons extend axons following highly stereotyped pathways through the brain to appropriate targets (Tessier-Lavigne and Goodman 1996). The molecular mechanisms regulating these aspects of development have been studied extensively; however, the final step in the process has received relatively little attention thus far. How the growing axon recognises its appropriate cellular partner and forms a subcellular-specific synapse remains to be elucidated, and the identification of cell surface ligands and receptors involved in mediating cell-cell communication is ongoing. In recent years, advancement in this area has included the discovery of leucine-rich repeat (LRR) proteins as crucial specifiers of synaptic connectivity (de Wit et al. 2011).

1.2 Leucine-rich repeat structure

Leucine-rich repeats (LRRs) are protein-ligand interaction motifs, first identified in α2-glycoprotein (Putnam and Takahashi 1988) and found in a large number of proteins of diverse structure, localization and function in bacteria, fungi, plants and animals (Kobe and Kajava 2001). Each repeat is about 24-29 amino

acids long and consists of two parts. There is a well-conserved N-terminal stretch of ten amino acids, characterised by precisely-positioned hydrophobic residues (usually leucines) and this part of the motif forms a β-strand. The C-terminal stretch is more variable in sequence and structure and consists of 13-19 amino acids and this part of the repeat forms α-helices. Together, the arrangement of multiple repeats in tandem forms a horseshoe-shaped solenoidal structure, with the β-strands stacking to form the concave surface and the variable stretches forming the convex surface (Figure 1.1). The horseshoe shape arises due to the tightly packed β-strands which forces the solenoid into a curved configuration. The advantage of the curved shape is that it exposes the concave side of the domain, and presents a large surface for protein-protein interactions. Moreover, the sequence and length variability of the convex side can alter the shape of this surface thus allowing huge versatility in the type of ligands it can bind to (Bella et al. 2008).

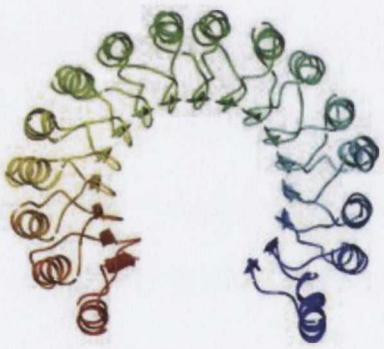

Figure 1.1 Structure of the leucine-rich repeat (LRR) domain. Diagram shows the three-dimensional structure of the porcine ribonuclease inhibitor. The horseshoe shape consists of an outer layer composed of parallel β-strands and the inner layer of α-helices (taken from Kobe and Deisenhofer (1995).

The three-dimensional structures of a number of eLRR proteins have been solved. These include the transmembrane proteins Toll-like receptor 3; (Botos et al. 2011, Bell et al. 2005), Tlr8 (Tanji et al. 2013) and LINGO-1 (Mosyak et al. 2006), the GPI-linked Nogo-receptor (NgR) (He et al. 2003), and the secreted glycoproteins GP1bα (Huizinga et al. 2002), decorin (Scott et al. 2004) and CD14

(Kim et al. 2005). In all cases, the structure of the LRR region has the characteristic horseshoe shape and ligand binding has been shown to occur along the concave surface of the LRR horseshoe, sometimes with protruding loops (Tanji et al. 2013).

The versatility of interactions made by this domain is evident from the large number of LRR-containing proteins with functions in the innate immune system, where the ability to recognise many different exogenous factors encountered by the body is vital for successful immune function (Nurnberger et al. 2004). The brain contains a large number of different cell types, and a staggering amount of inter-cellular connections which is mediatied by molecules involved in cell-cell communications. With this in mind, it may not be surprising that LRR-containing proteins could provide the versatility of interactions needed in this system. Moreover, the evolution of the brain with increased morphological complexity and cellular interactions raises the need for additional molecules functioning in these roles. Indeed, accumulating evidence shows that there are increasing numbers of LRR-containing proteins, especially those with extracellular LRRs (eLRRs), involved in various aspects of nervous system development (Chen et al. 2006).

1.3 Leucine-rich repeat proteins in nervous system development

Studies have shown that there are a large number of LRR-containing proteins expressed in the central nervous system (CNS), a number of which exhibit expression exclusively in the brain or spinal cord; for example, *Lingo2, Lingo4, Ngl1, Salm1, Salm5,* and *TrkB* (Homma et al. 2009). Furthermore, many eLRR proteins are expressed by distinct populations of neurons. In the developing mouse embryo, *Ngl2* was mainly found in specific populations of cells in the CNS and PNS including the telencephalon, rhombencephalon, spinal cord, optic cup and otocyst, and *Islr2* showed restricted expression in caudal regions of the brain and spinal cord (Homma et al. 2009). *Pal* is a retina specific gene, detected by post-natal day 7 (P7) and most abundant at P14 in the rat. More specifically Pal was localised to photoreceptor cells at a time-point coinciding with the appearance of the rod outer segments which are involved in phototransduction (Mandai et al.

2009). *Lrrc3b* expression is restricted to the dendrites of odorant receptor neurons in the olfactory bulb and this expression is regulated by odorant activity (Bennett et al. 2010). *Tpbg* was found in a subset of cells, in a strata-specific manner in both the olfactory bulb and the retina (Imamura et al. 2006). An interesting temporally regulated pattern of expression was detected for *Tlr8* in the developing mouse brain. Expression was first detected by embryonic day 12, followed by an increase in expression until P21 after which expression decreased considerably, coinciding with the completion of neurogenesis and axogenesis. During late embryogenesis, expression was restricted to axonal tracts in the following regions: olfactory nerve fibre layer, cortical intermediate zone, internal capsule, anterior commissure, fimbria of hippocampus, optic chiasm (Ma et al. 2006). An interesting and discrete pattern of expression was identified for *Lgr8* in various thalamic nuclei including the parafascicular nucleus (Pf), the dorsolateral, ventrolateral and posterior thalamic nuclei, and in the medial habenula. Low *Lgr8* levels were also detected in the frontal cortex where thalamic connections are received (Sedaghat et al. 2008).

The binding partners for many of the LRR-containing proteins are beginning to be identified and are structurally diverse, confirming the binding versatility of the LRR domain. Some eLRR proteins have been shown to bind homophilically or with other members of the same subfamily (AMIGOs (Kuja-Panula et al. 2003), FLRTs (Karaulanov et al. 2006), LINGO-1 (Jepson et al. 2012) and SALMs (Nam et al. 2011)). Many eLRRs also bind with other ligands; the Nogo-receptor (NgR) binds OMgp (Wang et al. 2002b), RTN4 and MAG (Barton et al. 2003); RTN3 interacts with the SALM family (Chang et al. 2010) while the SALMs also interact with PSD-95, NMDA and AMPA receptors (Nam et al. 2011). Trk receptors bind neurotrophins (Huang and Reichardt 2003) and the NGL family have been shown to interact with netrin-G1, netrin-G2, LAR, PSD-95 and NMDA receptors (Woo et al. 2009). Additionally, NGL3 binds PTPdelta and PTPsigma (Kwon et al. 2010) and Whirlin (Delprat et al. 2005). LGI1 and LGI4 bind to ADAM22, ADAM23 and ADAM11 (Sagane et al. 2008); LRRTM1 and LRRTM2 bind NEUREXIN (de Wit et al. 2009, Ko et al. 2009); both AMIGO3 and LINGO1 bind NGR1 and p75 (Mi et al. 2004, Ahmed et al. 2013). The secreted LRR-containing Slit proteins are ligands for the Roundabout proteins (Nguyen-Ba-Charvet and Chedotal 2002). Flrt3 interacts with Unc5B (Karaulanov et al. 2009) and Flrt2 binds Unc5d (Yamagishi et

al. 2011). Islr2 interacts with TrkA and Ret RTKs (Mandai et al. 2009) and Flrt3 has been shown to interact with LPHN3 (O'Sullivan et al. 2012) (Table 1.1). The identified interacting proteins have established functions in synaptic transmission, myelination, suppression of regeneration, synaptic plasticity and axon guidance and consequently these eLRR proteins may also function in these crucial CNS developmental roles.

LRR proteins	Homophilic binding	Heterophilic binding
AMIGOs	Yes	NgR1 and p75
LINGO-1	Yes	NgR1 and p75
FLRTs	Yes	Latrophilins (LPHNs)
SALMs	Yes	PSD-95, NMDA and AMPA receptors and RTN3
NgR1	unknown	OMgp, RTN4 and MAG
TRKs	unknown	Neurotrophins (NGF, NT3, NT4, BDNF)
NGLs	unknown	netrin-G1, netrin-G2, LAR, PSD-95, NMDA receptors, Whirlin, PTPdelta, PTPsigma
LGI1 and LGI4	unknown	ADAM22, ADAM23 and ADAM11
LRRTM1 and LRRTM2	unknown	NEUREXIN
Slits	unknown	Robo receptors
Flrt2 and Flrt3	unknown	Unc5B and Unc5D (respectively)
ISLR2	unknown	TrkA and Ret RTKs

Table 1.1 Summary of the identified interactions made by a selection of LRR-containing proteins.

A large *in vitro* screen was recently carried out in the zebrafish to identify novel extracellular protein interactions using neural leucine-rich repeat (LRR) and immunoglobulin (IG) superfamily members (Sollner and Wright 2009). The methodology included an assay developed by the researchers called AVEXIS (Avidity-based Extracellular Interaction screen) and involved testing for

interactions among 150 receptor ectodomains. The resultant screen confirmed the interaction between Flrt and Unc5b while also identifying many novel interactions (Figure 1.2). The newly identified interacting partners included *Elfn1* and Robo3, and Boc and Igsf21 were found to interact with Elfn2. An interesting conclusion that emerged from this study is that many members of the eLRR superfamily interact with IG superfamily proteins. A database for the continuing screen is available online (AVEXIS Receptor Network with Integrated Expression (ARNIE) www.sanger.ac.uk/cgi-bin/teams/team30/arnie).

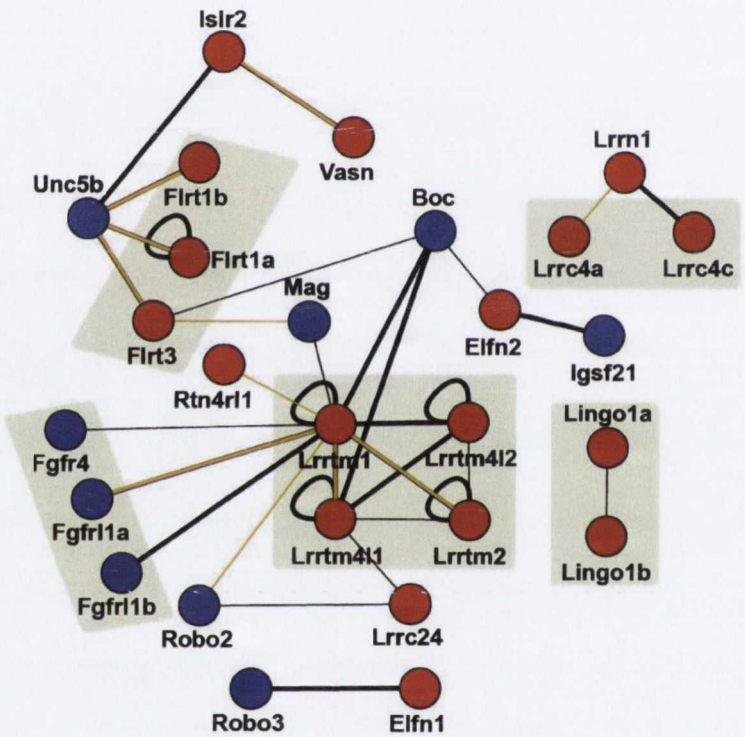

Figure 1.2 Identified extracellular interactions made by LRR and immunoglobulin superfamily members in the zebrafish. Blue nodes are Ig receptors, red nodes are LRR receptors and receptors belonging to the same family are shaded in green. Thick lines represent high confidence interactions; thin lines are interactions of lower confidence. Orange lines represent interactions that were indepedently identified (taken from Sollner and Wright (2009).

1.3.1 LRR proteins in axon guidance

Axons have the amazing ability to travel through the brain along a stereotyped path to find a specific target. This occurs in a series of specific steps, with the axonal tip or growth cone responding to both attractive and repulsive guidance cues in their environment leading the axon along its route. The axon moves with continuing cytoskeletal changes mediated by intracellular signalling in response to the guidance cues (reviewed in (Dent et al. 2011)). The ability to path find through the intricate terrain of the developing brain is governed by the ability of the neuron to assess the relative balance of attractive and repulsive cues to select the right path (Tessier-Lavigne and Goodman 1996). A great number of molecules involved in axon guidance have been identified, such as Ephrins and Eph receptors, Plexins, Semaphorins and Netrins (Kolodkin and Tessier-Lavigne 2011).

The LRR-containing Slits and their Robo receptors have been extensively studied in the fly (reviewed in (Dickson and Gilestro 2006)), in the mouse olfactory system (Cho et al. 2009) and in midline commissural axon guidance in vertebrates (Long et al. 2004, Ypsilanti et al. 2010). In each system, Slit proteins have been shown to have a repulsive effect on neurons expressing Robo receptors. Neurotrophins are involved in neuronal survival, axonal outgrowth and have been shown to stimulate axonal regeneration (reviewed in (Lykissas et al. 2007)). These neurotrophins function through their interaction with two classes of receptors, the p75 neurotrophin receptor and the LRR-containing Trk receptors (Chao 2003). More specifically, nerve growth factor (NGF) binds to TrkA, brain-derived neurotrophic factor (BDNF) and neurotrophin 4 (NT4) bind TrkB and neurotrophin 3 (NT3) to TrkC (Chao 2003). The Trk receptors, when activated, form dimers causing intracellular phosphorylation and activation of intracellular signalling cascades (Ullrich and Schlessinger 1990) producing changes to the actin cytoskeleton and promoting growth cone motility (Lykissas et al. 2007). Linx or *ISLR2* has also been identified as a binding partner for *TrkA* and their direct interaction exerts control over axonal elongation and guidance (Mandai et al. 2009).

In mammals, in vitro studies have identified two subfamilies of LRR proteins, Flrts and Slitrks, and a member of the Amigo family (*Amigo1)* with functions in neuronal growth and guidance. The Flrt proteins function in the process of axon guidance through their interaction with the Unc5 receptor family, which are known repulsive receptors for Netrin (Keleman and Dickson 2001). The interaction between Flrt2 and Unc5D, and Flrt3 with Unc5B was confirmed in cultured neurons where the Flrts activate Unc5 repulsive signalling causing growth cone collapse (Yamagishi et al. 2011). The Slitrk family consists of six structurally related transmembrane proteins in vertebrates and overexpression of Slitrk1 in neuronal culture produced unipolar neurites whereas the other Slitrk proteins inhibited neurite outgrowth. The differing functions have been attributed to the intracellular domain differences in this family which are conserved in Slitrk2-6, but not in Slitrk1 (Aruga and Mikoshiba 2003). The LRR-containing ectodomain of Amigo promoted neurite extension and inhibited fasciculation in hippocampal neurons (Kuja-Panula et al. 2003).

1.3.2 LRR proteins in target selection

When axons have been guided to the vicinity of their final targets, they must locate and select precise cell-types and even subcellular compartments before making a synapse. The ability of axons to recognise these targets is believed to involve a large amount of both pathway- and target-derived cues that are processed by receptors on the growing growth cone. The first evidence of LRR-containing proteins functioning in target selection was identified in experiments using the Drosophila neuromuscular system (Nose et al. 1994). Connectin, a GPI-linked protein containing 11 LRR domains was located in a subset of muscles and the axons that innervate them (Figure 1.2). Loss-of-function of Connectin showed no phenotype in motor axon targeting. However, using ectopic expression, Nose and colleagues showed that Connectin could promote neuromuscular synaptic target selection and that it functioned in a homophilic manner. Ectopic expression of Connectin on all muscles led to ectopic innervation by connectin-expressing axons onto inappropriate, normally Connectin-negative muscles. Subsequent to

this finding, the Drosophila neuromuscular system allowed for the identification of Capricious (*Caps*) and Tartan with targeting functions. In wildtype flies, muscle 12 expresses *Caps*, which is innervated by the *Caps*-positive RP5 motor axon (Figure 1.3). In *Caps* loss-of-function mutants, RP5 neurons target muscle 12 normally but also make ectopic projections onto *Caps*-negative muscle 13 (Shishido et al. 1998). When *Caps* is ectopically expressed on all muscles, RP5 axons make ectopic innervations. Further investigation revealed that filopodia can discriminate between target and non-target axons and that *Caps* is functioning post-synaptically as an active participant in target selection. Kohsaka and colleagues observed a concentration of *Caps* proteins in the tips of the muscular filopodia where it is involved in stabilising appropriate synaptic contacts and in destabilising inappropriate ones (Kohsaka and Nose 2009). The lack of phenotype in the absence of Connectin is suggestive of redundancy in the wiring mechanisms and molecules involved. Indeed, a close paralog of *Caps*, Tartan (Irani et al. 2012), shows a similar axon mistargeting phenotype in the Trn loss-of-function flies (Kurusu et al. 2008). Moreover, the double mutant of *Caps* and Trn displays an enhanced phenotype indicating a redundancy within these molecules in neuromuscular targeting. The molecular redundancy in this system contributes to its robustness during development, but is also suggestive that additional cues yet unidentified are functioning to establish these neuronal circuits.

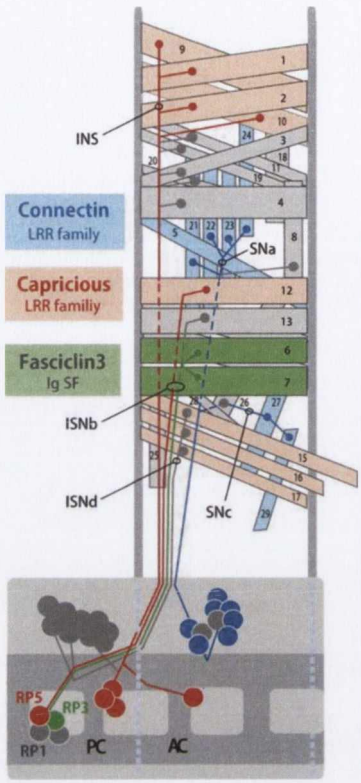

Figure 1.3 Expression of the target recognition molecules, Capricious and connectin, in the fly neuromuscular system.

Homophilic interactions specify neuromuscular connectivity. Caps is expressed in the RP5 motorneurons and its target muscle 12 (*orange*). Con is expressed in external muscles and a group of motorneurons that innervate them (*blue*). Capricious, Caps; Connectin, Conn. (Taken from Nose (2012).

Another LRR-containing protein, Toll, is expressed in a subset of muscles and acts to inhibit synapse formation of the motor neuron axons on inappropriate muscle targets (Halfon et al. 1995, Rose et al. 1997). Toll is normally expressed in a dynamic pattern in several muscle fibres in each hemisegment including muscles 15, 16, 17 and 28, and also by muscle 7 in early stages. At later stages however expression in muscle 7 is lost while expression in muscles 15 and 16 remains high. The timing of this change coincides with the timing of innervation of muscles 6 and 7 by the motoneuron RP3. In *Toll* zygotic mutant animals, errors in RP3 target selection are observed, with occasional failure to innervate muscles 6 and 7 and ectopic innervation of muscles 15 and 16. These findings suggest that Toll is normally acting to inhibit synapse formation by the RP3 neuron on inappropriate targets, which it must normally bypass on its way to muscles 6 and 7. Consistent with this model, ectopic expression of Toll on all muscles leads to a failure of RP3 to innervate muscles 6 and 7. The growth cones still reach and explore the surface of these muscles but fail to form synapses during embryogenesis, though

by late larval stages they have succeeded in doing so. A more recent study demonstrates that Toll is expressed in muscle 13, but not in muscle 12. In toll mutants, axons that would normally innervate muscle 12 ectopically innervate muscle 13 with only a small number of synapses observed in muscle 12. Furthermore, overexpression of Toll in muscle 12 inhibits synapse formation by the axons that innervate them (Inaki et al. 2010). As well as this, Inaki and colleagues (2012) identified a transcription factor Tey, which is specifically expressed in muscle 12 and negatively regulates the inhibitory function of Toll. In Tey mutants, the levels of Toll are strongly increased in muscle 12, and consequently, innervation of axons onto muscle 12 was inhibited. Toll is not expressed by any motor axons and therefore is acting with a heterophilic ligand, however the receptor mediating this effect remains unknown (Rose et al. 1997).

A common theme in these studies is that the removal of an individual cue does not produce substantial targeting errors, and motor axons select their synaptic targets by integrating levels of positive and negative cues from each muscle (Winberg et al. 1998). Due to this, the ectopic expression of potential cues was adopted for identification of additional molecules functioning in target selection. Kurusu and colleagues screened over 400 cell-surface or secreted molecules for defects in neuromuscular connectivity. Of these, 53 were proteins containing LRRs, 16 of which produced defects in motor axon targeting or alterations in the structure of the neuromuscular junction or both (Kurusu et al. 2008). These identified LRR proteins included known molecules such as *Caps*, and its close relative *Tartan*, as well as *18-wheeler,* a member of the Toll-like receptor family and three novel LRR proteins encoded by CG14351 (now called *hattifattener*), CG3413 (*windpipe*) and CG8561 (dALS). Besides the LRR-containing genes, all other domain types were represented by a comparatively low number of genes in this screen. Therefore, this unbiased approach showed a very strong enrichment for genes encoding LRR proteins (Kurusu et al. 2008, Nose 2012).

The involvement of the LRR-protein *Caps* in specifying neuron-neuron connectivity has been identified in the visual and olfactory systems. *Caps* is specifically expressed by R8 photoreceptors and their target neurons in layer M3 of the medulla. Loss of *Caps* function leads to targeting errors of R8 neurons onto

cells in inappropriate layers, while forced expression of *Caps* in R7 photoreceptors is sufficient to cause them to mistarget to the *Caps*-positive neurons in layer M3 (Shinza-Kameda et al. 2006). Therefore, *Caps* is involved in layer-specific targeting of Drosophila photoreceptor axons, and this most likely occurs by homophilic interaction. In the olfactory system, *Caps* instructs glomerus-specific targeting of dendrites. More specifically, *Caps* is expressed in a subset of projection neurons in the olfactory bulb which project their dendrites to specific glomeruli, and in *Caps* mutants dendritic targeting errors were identified. *Caps* overexpression caused normally *Caps*-negative dendrites to project to glomeruli normally innervated by *Caps*-positive dendrites. Also, misexpression of *Caps* in a single projection neuron causes misprojection of its dendrites even in a $Caps^{-/-}$ background (Hong et al. 2009). The expression of *Caps* in the olfactory receptor neurons does not match with *Caps* expression in the projection neurons and therefore a homophilic interaction is unlikely. In this way, the function of Caps in the olfactory system differs from that in the neuromuscular and visual systems. This study also observed that Trn was partially redundant with *Caps,* however, there is likely to be many more molecules involved in the formation of specific-synaptic connections at approximately 50 glomeruli.

In vertebrates, the NGL-NetrinG interaction has been implicated in lamina-specific targeting in the hippocampus (Nishimura-Akiyoshi et al. 2007). Netrin-G1 and netrin-G2 are localised to axons of distinct pathways where axons containing Netrin-G1 innervate the distal region of CA1 pyramidal cells, and Netrin-G2-positive axons innervate the proximal region. The interacting partners for these proteins, NGL-1 and NGL-2, selectively localise to distal and proximal segments within dendrites, which corresponds to the site of termination for axons expressing netrin-G1 and -G2, respectively (Figure 1.4). In netrin-G1 and -G2 mutant mice the lamina-specific clustering of the NGLs was disrupted and the receptors were mislocated along the entire dendrite. This result suggests that the expression of presynaptic Netrin-Gs directly influences the localisation of NGLs to specific dendritic segments.

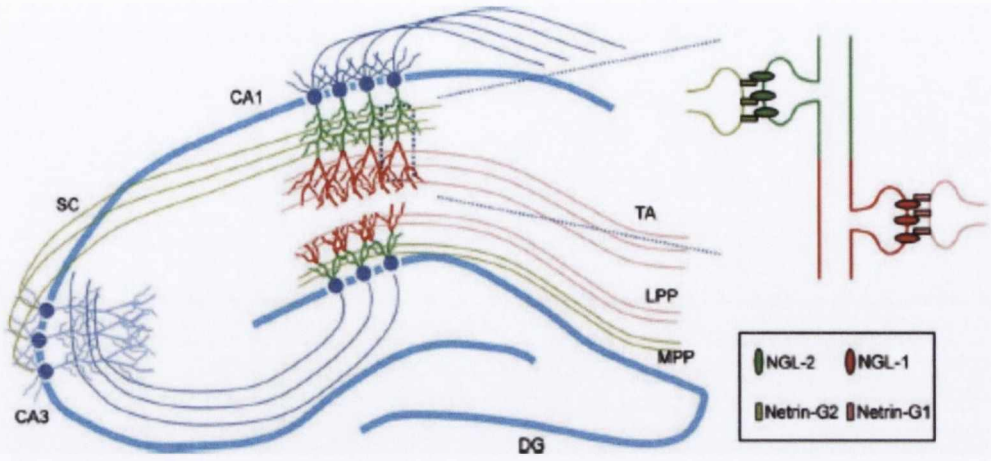

Figure 1.4 Netrin-G-NGL transneuronal interactions between axons and distinct dendritic segments of their target neurons. Netrin-G1 expressing axons induce clustering of NGL-1 in the distal dendritic segments of CA1 pyramidal cells. Netrin-G2 expressing axons induce NGL-2 clustering in proximal dendritic segments of the CA1 pyramidal cells. In the dentate gyrus, dendritic clustering of NGL-1 and NGL-2 in outer and middle molecular layers is induced by Netrin-G1 and Netrin-G2 expressing axons, respectively. (Taken from Woo et al. (2009).

1.3.3 LRR proteins in synaptogenesis

When axons have located their targets, the process of synaptogenesis ensues. This fundamental step in a functioning brain involves the formation of neurotransmitter release machinery in the presynaptic neurons and a receptive system in the postsynaptic cells. Many recent studies have identified synapse-promoting activities for a number of LRR-containing families and proteins; such as the SALMs, NGLs, LRRTMs, SLITRKs, LGI1, NYx, 5T4, and FLRT3.

The SALMs/LRFNs are a family of five vertebrate-specific extracellular LRR-containing proteins. SALMs1, 2, 3 have pdz-binding motifs and interact with the post-synaptic density protein PSD-95 (Ko et al. 2006, Wang et al. 2006, Nam et al. 2011). In vitro experiments in mammalian neuronal cells have identified that *SALM2* localises to excitatory synaptic sites, forms a complex with both NMDA and AMPA receptors and its overexpression increases the number of excitatory

synapses. In addition, knockdown of SALM2 decreases the number of excitatory but not inhibitory synapses (Ko et al. 2006). SALM1 induces surface clustering of NMDA receptors through a direct interaction, and has also been shown to form a coimmunoprecipitable complex with SALM2 and SALM3 (Seabold et al. 2008). Additionally, SALM3 and SALM5 have been shown to induce both excitatory and inhibitory presynaptic activity in contacting axons of cultured hippocampal neurons (Mah et al. 2010). SALM4 and SALM5 are present in both pre- and postsynaptic membranes and can mediate transcellular adhesion homophilically (Seabold et al. 2008). In summary, the SALMs are enriched in synaptic membranes, recruit neurotransmitter receptors to the synapse and interact with the synapse scaffolding protein, PSD-95, all of which establishes their importance in synaptogenesis.

The LRRTM family emerged from an unbiased screen for synaptogenic proteins (Linhoff et al. 2009). Linhoff and colleagues showed that all four members localised to excitatory synapses and exhibited synaptogenic activity. The LRR domain of these proteins was found to be necessary and sufficient for this synaptogenic activity by testing deletion constructs in the co-culture assays. *In vivo*, Lrrtm1$^{-/-}$ mutant mice revealed a synaptic defect in specific regions of hippocampal formation. A selective increase in the size of VGLUT1 puncta in CA1 stratum radiatum and stratum oriens which may indicate a dispersal of synaptic vesicles and reduction in reserved pool vesicles (Linhoff et al. 2009). Further research has identified neurexins as binding partners for LRRTM1 and 2 (de Wit et al. 2009). Neurexins function presynaptically and influence the formation of synapses (Dean and Dresbach 2006). As well as binding to post-synaptic LRRTM1 and LRRTM2, the neurexins also interact with Neuroligins and triple knockdown experiments of the LRRTM1, 2 and neuroligin-3 show that all of these molecules act redundantly to maintain excitatory synapses (Ko 2012).

The NGL (netrin-G ligand) family contains three members, (NGL-1, NGL-2 and NGL-3), and were found to interact with the postsynaptic scaffolding protein (PSD-95) through a PDZ-binding domain in the cytoplasmic tail (Kim et al. 2006). Artificial aggregation of NGL-2 on fibroblasts or beads induced functional presynapses in contacting axons of cocultured neurons, and surface aggregation of NGL-2 in dendrites produced a clustering of excitatory postsynaptic proteins. *In*

vivo, knockdown and genetic deletion of NGL-2 demonstrated that NGL-2 functions in regulating strength of synaptic transmission and spine density at synapses in the hippocampus (DeNardo et al. 2012). A trans-synaptic interaction between postsynaptic NGL-3 and presynaptic LAR (for leukocyte antigen-related) was shown to regulate excitatory synapse formation bidirectionally (Woo et al. 2009). Moreover, NGL-3 was also found to interact with the other two LAR family members PTPδ and PTPσ with roles in regulating excitatory synapse formation (Kwon et al. 2010).

The LGI family consists of four members, LGI1-4, and are all vertebrate-specific secreted glycoproteins. LGI1 localises to glutamatergic synapses (Sirerol-Piquer et al. 2006, Fukata et al. 2006) and has been identified as an important regulator of excitatory synaptic transmission, mutations in which have been shown to cause epilepsy (Kalachikov et al. 2002). LGI1 appears to control synaptic strength at excitatory synapses at postsynaptic sites only, and the addition of soluble LGI1 to hippocampal slices considerably increased the expression of AMPA receptors. Mutant mice expressing a truncated LGI1 showed increased excitatory synaptic transmission due to inhibition of dendritic pruning and an increased spine density (Zhou et al. 2009, Fukata et al. 2006). LGI1 was originally identified as a component of a tripartite protein complex that included PSD-95 and ADAM22 (Fukata et al. 2006). However in a more recent study, LGI1 has been shown to simultaneously bind the postsynaptic ADAM22 and the presynaptic ADAM23 and co-purifies with the presynaptic Kv1.1 potassium channel and the postsynaptic density proteins PSD-95, and is therefore a component of a transsynaptic protein complex. In $LGI1^{-/-}$ mice, the lack of LGI1 causes a disruption to this complex and a specific reduction in synaptic transmission in the hippocampus (Fukata et al. 2010). Subsequently, another member of the LGI family, LGI2, has been shown to interact with the same ADAM receptors as LGI1 but at an earlier stage of synaptic pruning and mutations in this gene are associated with epilepsy (Seppala et al. 2011).

The Sltrk family consists of six transmembrane proteins, which are highly expressed in the CNS (Aruga and Mikoshiba 2003). Slitrk2 was the first member implicated in synaptic function in a coculture assay, where Slitrk2 induced clusters of synapsin in contacting hippocampal axons (Linhoff et al. 2009). Slitrk5 is

localized at synaptic sites and mutant mice for this gene display decreased expression of glutamate receptors and exhibit deficits in corticostriatal neurotransmission (Shmelkov et al. 2010). Subsequently, another member of this family emerged with a function in synaptogenesis. In co-culture experiments, Slitrk3 expression in fibroblasts induced clustering of vGAT in contacting axons, suggesting a function in inhibitory presynaptic differentiation. Moreover, Sitrk3$^{-/-}$ mice showed a reduction in inhibitory synapse number in the hippocampus and increased seizure susceptibility (Takahashi et al. 2012).

The FLRT family has been reported to function in axon guidance however; more recent data suggest an additional function in synaptogenesis for FLRT3. An interaction between FLRT3 and latrophilin3 (LPHN3) has recently been identified. Latrophilins are neuronal receptors for α-latroxilin; a black widow spider toxin that causes the massive release of neurotransmitters (Silva and Ushkaryov 2010) however, the endogenous function of these genes has not been fully elucidated. The interaction of FLRT3 and LPHN3 was investigated in cultured neurons and these proteins were found to interact *in trans*. Disruption of this interaction with knockdown experiments resulted in a decrease in excitatory synapse density. Furthermore, in vivo knockdown of *Flrt3* in rats produced a reduction in the strength of synaptic inputs to dentate granule cells and also a decrease in dendritic spine number (O'Sullivan et al. 2012).

In contrast with many of the LRR proteins already mentioned, the Nogo-66 receptor (NgR) has been shown to limit synaptic plasticity in the mature CNS (McGee et al. 2005). In NgR$^{-/-}$ mice, ocular plasticity continued abnormally past the juvenile age. More recently, the NgR family were found to inhibit excitatory synapse formation *in vitro*, reducing dendritic growth and synapse number (Wills et al. 2012).

Other preliminary studies of individual LRR proteins have attained results hinting at possible roles in synaptogenesis. Nyctalopin (Nyx) is localised post-synaptically in bipolar cells in the outer plexiform layer (OPL) and in postsynaptic neurons in the inner plexiform layer (IPL), and disruption of function in the Zebrafish leads to defects in synaptic transmission in the retina (Bahadori et al. 2006). An expression based study looked at the localisation of LRR and PDZ-domain containing protein 5T4/TPBG in the mouse and found strata-specific

expression in both the olfactory bulb and the retina (Imamura et al. 2006). In the mouse olfactory bulb interneurons, 5T4 overexpression resulted in a significant increase in dendritic branching, while $5T4^{-/-}$ mice displayed reduced dendritic arborisation and this function was show to activity-dependent (Yoshihara et al. 2012).

This summary illustrates that many proteins from the eLRR superfamily function in synaptogenesis. A number of conclusions can be drawn from the literature, the first being that the majority of these eLRR proteins are associated with excitatory synapses while it appears that only Slitrk3 is involved in inhibitory synapse development. Also, most of these proteins have been shown to function in the postsynaptic membrane with the following exceptions; Salm4 and 5 localise to both the pre- and postsynaptic membranes, and LGI1 and 2 are secreted into the synaptic cleft from the presynaptic neuron. Even among family members, the eLRR proteins appear to have distinct functions at the synapse that include functioning as a mechanical link between pre- and postsynaptic cells, and in the formation, function and plasticity of the synapses. Further studies are needed to clarify and identify interacting partners for these proteins and the specific mechanisms of function. At the level of the synapse, there is substantial complexity and specificity in neural connectivity and further synaptic cell adhesion molecules are needed to mediate these connections.

1.3.4 LRR proteins and neurological or psychiatric disorders

The LRR superfamily contains a large amount of proteins that have been implicated in neurological or psychiatric disorders highlighting the importance of this class of proteins in the development of the central nervous system. Among the extracellular LRR proteins, these include epilepsy (*LGI1* (Kalachikov et al. 2002); *LGI2* (Seppala et al. 2011)), Tourette's syndrome (*SLITRK1 (Abelson et al. 2005, State 2011)*), congenital stationary night blindness (*Nyx* (Bech-Hansen et al. 2000, Lodha et al. 2012), congenital insensitivity to pain with anhidrosis (and mental retardation) (*TrkA* (Indo et al. 1996); (Mardy et al. 2001)), OCD-like behaviour (Shmelkov et al. 2010), Alzheimer's disease (*LRRTM3* (Majercak et al.

2006, Reitz et al. 2012), *TrkA* (Ginsberg et al. 2006)) and Parkinson's disease and essential tremors (*Lingo1* and *Lingo2* (Vilarino-Guell et al. 2010, Wu et al. 2011)). There has also been a number of LRR-containing proteins implicated in schizophrenia, such as *LRRTM1* (Francks et al. 2007), *Slitrk2* (Piton et al. 2011), *NgR* (Budel et al. 2008, Hsu et al. 2007), *LGR8* and *SALM5* (Xu et al. 2009) and *Ntrk-3 (Otnaess et al. 2009)*. Recently, *Ntrk-3* has also been associated with bipolar disorder (Athanasiu et al. 2011) while polymorphisms in two LRR-containing genes *LRRTM3* and *LRRN3* are associated with autism spectrum disorder (Sousa et al. 2010). As mentioned earlier, *Slitrk3* has been associated with increased seizure susceptibility. A list of these LRR proteins and the nature of their associations with common neurodevelopmental disorders is provided in table 1.2. A number of these associations have been made based on genetic mouse models displaying disorder-related phenotypes (Table 1.3).

LRR-containing proteins have also been indirectly linked to neurological disorders through their known binding partners. The slit receptor ROBO1 is implicated in dyslexia (Hannula-Jouppi et al. 2005, Bates et al. 2011). NGL1 and NGL2 binding partners, Netrin-G1 and Netrin-G2, have been linked with schizophrenia and bipolar disorder (Woo et al. 2009). Furthermore, Netrin-G1 has been implicated in Rett syndrome (Borg et al. 2005, Nectoux et al. 2007). Another NGL1 binding partner called Whirlin is the causative gene for Usher syndrome type IID which manifests as retinitis pigmentosa with hearing loss (Yang et al. 2010). Neurexin-1alpha, the LRRTM2 binding partner, has been linked to autism spectrum disorder and schizophrenia (Reichelt et al. 2012). The dysregulation of neurotrophins (bind Trks) has been identified in Alzheimer's disease (Schindowski et al. 2008) and *Latrophilin3*, which interacts with *Flrt3,* has been linked to attention deficit hyperactivity disorder (ADHD) (Arcos-Burgos et al. 2010) (Table 1.4).

The binding of NgR1 to the inhibitory myelin glycoproteins, NOGO, MAG and OMgp, contributes to the lack of axonal regeneration that occurs in the central nervous system (Abdesselem et al. 2009). NgR1 signals inhibition through the RhoGTPase pathway upon its interaction with p75 and the LRR-containing protein LINGO1 (Mi et al. 2004). Moreover, it has just been shown that another LRR-containing protein AMIGO3 can interact with NgR1-p75 complex in cultured cells

and the knockdown of AMIGO3 promoted axonal growth in retinal cultures (Ahmed et al. 2013). Current research for a potential therapeutic strategy for axonal regeneration after injury include *in vivo* knockdown of LINGO1 or AMIGO3 immediately after injury (Wu et al. 2013, Ahmed et al. 2013).

Proteins with intracellular LRRs have also been shown to produce deficits in CNS function, such as the Leucine-rich repeat kinase 2 protein (LRRK2) in Parkinson's disease. There has been huge interest in establishing how mutations in this gene cause Parkinson's disease (reviewed in (Kett and Dauer 2012)). Additionally, members of this superfamily have also been implicated in diseases affecting other tissues, such as cancer (FLRT3 (Whitman et al. 2001), AMIGO2 (Rabenau et al. 2004)), psoriasis (LRIGs (Karlsson et al. 2008)) and cardia bifidia (FLRT3 (Maretto et al. 2008)).

LRR proteins	Associated phenotype	Nature of evidence	Reference
SLITRK1	Tourette's syndrome	CGA, point mutations	Abelson *et al.*, 2005
SLITRK2	Schizophrenia	CGA, point mutations	Piton *et al.*, 2011
LRRTM1	Schizophrenia	GWAS, marker haplotype association	Francks *et al.*, 2007
LRRTM3	Alzheimer's disease	CGA, point mutations	Reitz *et al.*, 2012
LRRTM3	Autism spectrum disorder	CGA, point mutations	Sousa *et al.*, 2010
LRRN3	Autism spectrum disorder	CGA, point mutations	Sousa *et al.*, 2010
LINGO1 LINGO2	Parkinson's disease and essential tremors	CGA, point mutations	Vilariño-Güell *et al.*, 2010
NYX	Night blindness	CGA, point mutations	Bech-Hansen *et al.*, 2000
TRKA	CIPA	CGA, point mutations	Indo *et al.*, 1996
TRK receptors	Alzheimer's disease	Significant reduction of TRKs in AD brain tissue	Ginsberg *et al.*, 2006
NGR	Schizophrenia	CGA, point mutations	Hsu *et al.*, 2007
LGR8	Schizophrenia	GWAS, CNVs	Xu *et al.*, 2009
SALM5	Schizophrenia	GWAS, CNVs	Xu *et al.*, 2009
NTRK-3	Schizophrenia	CGA, marker haplotype association	Otnaess *et al.*, 2009
NTRK-3	Bipolar disorder	CGA, point mutations	Athanasiu *et al.*, 2011

Table 1.2 List of eLRR-containing proteins implicated in neurodevelopmental disorders. eLRR, extracellular leucines-rich repeat; CIPA, Congenital insensitivity to pain with anhidrosis; CGA, candidate gene association; GWAS, genome-wide association study; CNV, copy number variant.

LRR proteins	Associated phenotype in a mouse model	Reference
LGI1, LGI2	Epilepsy	Kalachikov *et al.*,2002 Seppälä *et al.*, 2011
SLITRK3	Increased seizure susceptibility	Takahashi *et al.*, 2012
SLITRK5	Obsessive compulsive disorder-like behaviour	Shmelkov, 2010
TRKA	CIPA-like behaviours	Indo *et al.*, 1996

Table 1.3 Genetic mouse models of common neurodevelopmental disorders. LRR proteins implicated in common neurodevelopmental disorders based on genetic mouse models displaying disorder-related phenotypes. CIPA, Congenital insensitivity to pain with anhidrosis

LRR proteins	Protein interactions	Associated phenotype	Reference
SLITs	ROBO1	Dyslexia	Hannula-Jouppi *et al.*, 2005
NGL-1 NGL-2	NETRIN-G1 NETRIN-G2	Schizophrenia, bipolar disorder	Woo *et al.*, 2009
NGL-1	Netrin-G1	Rett syndrome	Borg *et al.*, 2005
NGL-1	WHIRLIN	Usher syndrome	Yang *et al.*, 2010
LRRTM2	NEUREXIN-1α	Autism, Schizophrenia	Reichelt *et al.*, 2012
TRKs	NEUROTROPHINS	Alzheimer's disease	Schindowski *et al.*, 2008
FLRT3	LATROPHILIN3	ADHD	Arcos-Burgos *et al.*, 2010

Table 1.4 Neurological disorders associated with the binding partners of LRR-containing proteins. ADHD, attention-deficit/hyperactivity disorder.

1.3.5 eLRR proteins display differential patterns of expression in the brain

Many of the eLRR proteins functioning in the above mentioned aspects of neural connectivity exhibit region-specific patterns of expression in the brain further confirming a role in selective cell interactions that occur during neural connectivity. Furthermore, it has been noted that there is overlapping expression among members of subfamilies that may be working in combination to specify neural connectivity. For example, members of the Lrrtm family are involved in synaptogenesis and display both distinct and over-lapping expression patterns in specific regions of the mouse brain (Figure 1.5). Differential patterns are particularly observed in the olfactory bulb, thalamus, cerebellum, hippocampus and cortex. Additionally, overlapping patterns can also be observed among the four genes; for example, Lrrtm1 and Lrrtm2 are both expressed in neurons of the CA1-CA3 pyramidal layers and dentate gyrus granular cell layer of hippocampus where these two members are suggested to act redundantly to maintain excitatory synapses (Ko 2012).

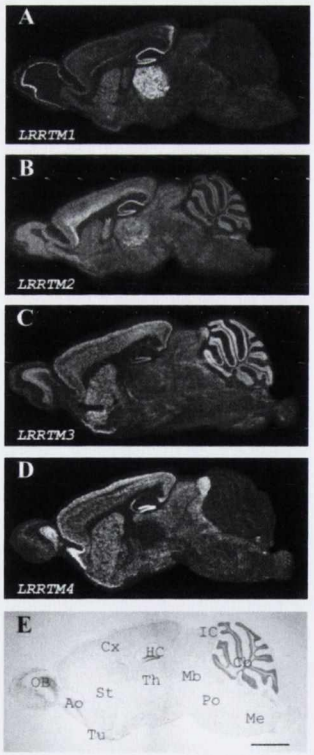

Figure 1.5 Differential expression patterns of LRRTM family members.
Messenger RNA *in situ* hybridisation patterns for (A) *Lrrtm1,* (B) *Lrrtm2,* (C) *Lrrtm3,* and (D) *Lrrtm4* in the adult mouse brain. (E) The bright-field image of (D). OB, olfactory bulb; Ao, anterior olfactory nucleus; Tu, olfactory tubercle; St, striatum; Cx, cerebral cortex; Th, thalamus; HC, hippocampus; IC, inferior colliculi; Mb, midbrain; Po, pons; Me, medulla; Cb, cerebellum. (Taken from Lauren et al. (2003).

The Slitrk family consists of six structurally related transmembrane proteins, with implicated functions in the modulation of neurite outgrowth and the regulation of both inhibitory and excitatory synapses. Members of this family exhibit both distinct and overlapping patterns of expression at E17 (Figure 1.6). Slitrk1 is expressed in mature neurons and has a role in promoting neurite outgrowth whereas Slitrk2 is mainly expressed in immature neurons in the ventricular layer, and has been shown to strongly inhibit neural outgrowth. The other members of this family have also been shown to inhibit neural outgrowth and with the exception of Slitrk6, exhibit a broader pattern of expression. Specific roles are therefore suggested for Slitrk1, 2 and 6 while it has been suggested the other members are functioning in combination to establish specificity in neural connectivity (Aruga and Mikoshiba 2003).

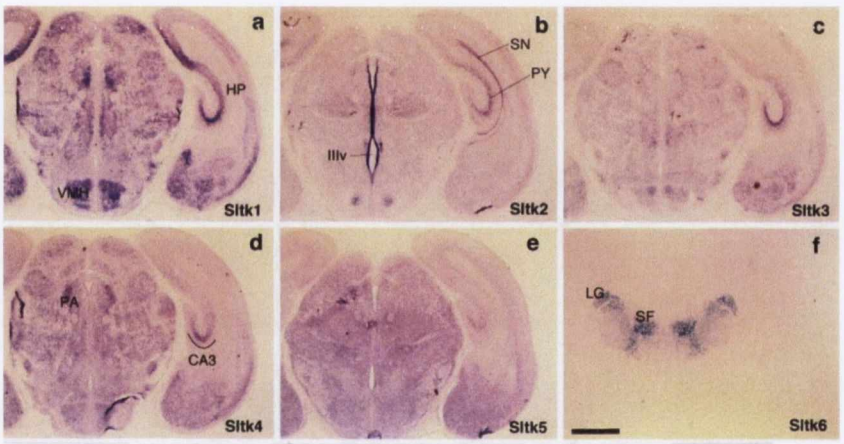

Figure 1.6 Differential expression patterns of the Slitrk family members. Messenger RNA in situ hybridisation results at E17 for (a) *Slitrk1* (b) *Slitrk2* (c) *Slitrk3* (d) *Slitrk4* (e) Slitrk5 and (f) Slitrk6. Sections through the diencephalon, hippocampus, and cerebral cortex. IIIv, third ventricle; CA3, CA3 region of the hippocampus; HP, hippocampus, LG, lateral geniculate nucleus; PA, periaqueductal gray matter; SF, suprafascicular nucleus; SN, subicular neurospithelium; VMH, ventromedial hypothalamus. (Taken from Aruga and Mikoshiba (2003).

Another example is the Salm/Lrfn family of eLRR proteins that have identified functions in synaptogenesis (Figure 1.7). Lrfn2 and Lrfn5 display very similar patterns of expression mainly restricted to mature neurons, whereas, a more widespread pattern of expression is observed for the other members of this family. Lrfn2 and Lrfn3 have been shown to form a coimmunopreciptatable complex. Additionally, Lrfn4 and Lrfn5 are in both pre- and postsynaptic membranes and are capable of binding homophilically. This family also demonstrates specific-binding abilities with only Salm1, Salm2 and Salm3 capable of interacting with PSD-95. The distinct and overlapping expression patterns, differential binding capacities to PSD-95 and pre-and post synaptic locations for these proteins suggest that these proteins may be functioning in combination to specify synaptic connectivity.

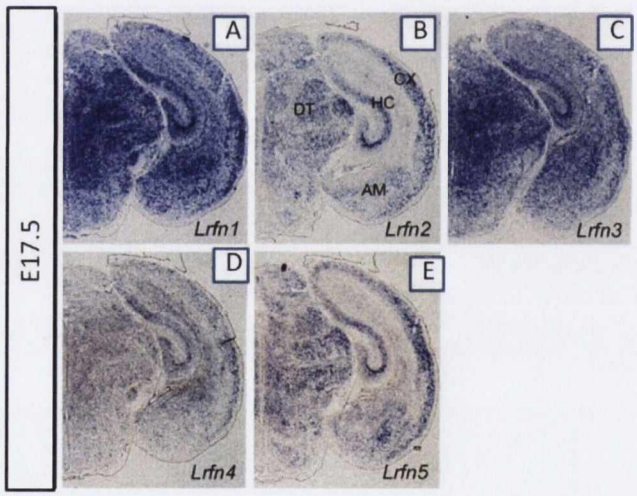

Figure 1.7 Differential expression patterns of the Lrfn/Salm genes. Messenger RNA in situ hybridisation results at E17 for (a) *Lrfn1* (b) *Lrfn2* (c) *Lrfn3* (d) *Lrfn4* (e) Lrfn5. AM, amygdala; CX, cerebral cortex; DT, dorsal thalamus; HC, hippocampus. (Taken from Morimura et al. (2006).

1.4 Aims of this thesis

It was apparent from the literature that leucine-rich repeat-containing proteins play crucial roles in the developing CNS with functions in axon guidance, regeneration, target selection and synaptogenesis. The astounding complexity of each of these processes cannot be fully explained by the number of molecules identified thus far, and the general consensus is that there are a great many more yet-unidentified molecules functioning in specifying neural connectivity.

In this study, we aimed to utilise a reverse genetics approach to search for candidate genes involved in neural connectivity. With particular focus on the leucine-rich repeat motif, our first objective was to complete a comprehensive survey of proteins in the human, mouse, fly and worm. Only proteins with the LRR domains located extracellularly were included to enrich for proteins involved in cell-cell interactions. The inclusion of the four species allowed for the examination of their evolutionary relationships and identified novel proteins and subfamilies that have arisen with the increasing complexity of the mammalian brain. Surprisingly, this family of proteins had received far less attention as a class than other better characterised families like the immunoglobulin (Vogel et al. 2003) and cadherin (Takeichi 2007) superfamilies. Due to this, the bioinformatics approach undertaken in this project resulted in the first comprehensive report of the eLRR superfamily (Dolan et al. 2007). A subsequent expression screen of the novel eLRR superfamily members led to the identification of a family of two novel and highly conserved transmembrane proteins that we name Elfn1 and Elfn2. Elfn1 displayed highly localised expression in particular regions of the brain and was chosen for further investigation. This work is presented in chapter 3.

In chapter 4, a comprehensive description of Elfn1 expression was accomplished with a knockout mouse line where expression of *Elfn1* is replaced with a β-galactosidase cell body marker. Protein localisation was detected using a pan-Elfn antibody. Elfn1 was detected in discrete subsets of cells in the hippocampus, cortex, habenula and many regions interconnected with the habenula. Expression was noted in GABAergic interneurons, and long-range-projecting GABAergic and glutamatergic neurons, where it has been found to localise to both the dendrites and axons.

In chapter 5, an interaction between Elfn1 and Robo3 in the mouse was confirmed both *in vivo* and *in vitro*. Analyses of the expression patterns of both genes identified the habenula as region of compatable spatiotemporal expression.

In chapter 6, we investigated for an anatomical phenotype in the Elfn$^{-/-}$ mouse. Comparative brain sections from *Elfn*$^{-/-}$ and *Elfn1*$^{+/-}$ brains were analysed for abnormalities with markers for the cell body and neuronal processes. No gross anatomical phenotype was detected. However, preliminary results have shown that there is a reduction in vGlut2 staining in the habenula of *Elfn*$^{-/-}$ mice which suggests decreased excitatory transmission to the habenula in the absence of Elfn1.

In chapter 7, we tested for behavioural abnormalities in *Elfn1*$^{-/-}$ mice. We discovered that the loss of Elfn1 resulted in motor abnormalities, reduced thigmotaxis and spontaneous seizures. Furthermore, *Elfn1*$^{-/-}$ mice exhibit increased locomotion that is paradoxically attenuated by amphetamine, suggestive of an ADHD-like phenotype.

The results presented in this thesis suggest that Elfn1 is specifying functional connectivity in various regions of the brain.

2 Chapter 2 Materials and Methods

2.1 Database pipeline

Protein sequences for all four species were retrieved from the Ensembl FTP site: Mouse release 36 NCBI m34 assembly (36471 sequences); Human release 36, NCBI 35 assembly (33869 sequences); Worm release 37, Wormbase 150 dataset (26032 sequences); Fly release 37, BDGP assembly release 4 (19369 sequences). In addition, 68627 mouse and 57366 human protein sequences were downloaded from the International Protein Index, version 3.14. A further 24273 human and 19258 mouse protein sequences were retrieved through the web interface (http://www.ncbi.nlm.nih.gov/FLC/getmgc.cgi) from the August 2006 version of the Mammalian Gene Collection. We also included a further 879 sequences comprising many from an older version of the Mammalian Gene Collection (February 2006) that were absent from the August 2006 release as well as several more added manually. All sequences were stored for easy access in a MySQL database.

The data set was reduced through use of a small Perl script that filters out duplicate copies of sequences for each species and keeps either the Ensembl version or an entry with a flag indicating its preference after manual curation. The non-redundant data sets for mouse, human, worm, and fly contained 85991, 74866, 22698, and 16857 sequences, respectively.

These sequences were subjected to an all-against-all Blast search (NCBI BlastP, version 2.2.12) carried out on a high-performance Linux cluster. An expectation cut-off of 0.1 was specified, and the top 200 hits for each search in tab-delimited format (-m8) were reported. The Blast results were parsed with the mcxdeblast tool using expectation cut-offs from e^{-10} to e^{-40} and formatted for clustering with the mcxassemble tool (options -q -r max --map -b), both part of the MCL package (version 1.005, 05-272). Each output was then subjected to Markov clustering with the MCL program using inflation parameters ranging from 1.2 to 5. The program Tribe-families was then run to produce the final clusters.

For proteins from the IPI and MGC set that did not have gene IDs assigned, we produced alignments using T-Coffee (version 3.93) with their best Blast hits. If sequences with matching protein names were found that are fully contained in another one or showed identity over at least 95% and sequence difference of maximal 15% we transferred Ensembl gene ID annotation where available. Through this, 2490 sequences from mouse and 1458 sequences from human were assigned Ensembl gene IDs. The gene information was used to remove isoforms from the clusters: only the protein with the longest sequence was kept for each gene. In some cases, where dubious excessive amino acids seem to have been added to a sequence, manual curation was necessary to overwrite this behaviour and select proteins that seemed biologically more plausible.

For prediction of architecture we used HMMpfam of the HMMER package (version 2.3.2) (Eddy 1998), together with the SMART (release 25 Nov. 2004) and Pfam (version 19.0) HMM libraries. Transmembrane predictions were produced by the programs TMHMM (version 2.0 (Krogh et al. 2001)), HMMTOP (version 2.1(Tusnady and Simon 2001)), and TMPred (Hofmann and Stoffel 1993). Signal Sequence analysis was carried out using SignalP (version 3.0 (Bendtsen et al. 2004)) and GPI-link results calculated by the BIG-PI program (Eisenhaber et al. 1999) were obtained for human (HumanGPI) and fly (FlyGPI). In addition, information about the genomic location and synonyms for a gene were retrieved from Ensembl, MGI, Wormbase and Flybase. Clustering and annotation information were combined into a large spreadsheet for the final output.

2.2 LRRscan

Based on a number of published studies (Kobe and Kajava 2001, Kajava 1998, Matsushima et al. 2005, Bell et al. 2003) and our own inspection of the sequences in our dataset we defined the minimal N-terminal part of a single extracellular-type LRR as: LxxLxLxxN. This is followed by a C-terminal part of each LRR of typically 10-21 amino acids that are quite variable. Consensus sequences for the LRR capping domains (LRR-NT at the N-terminus and LRR-CT at the C-terminus)

(Kajava 1998) have been defined by, including three different consensus sequences for the LRR-CT domain, derived from different classes of proteins. LRR-CT1 is the most common type, LRR-CT2 is found in small proteoglycans and LRR-CT3 in G-protein-coupled receptors:

LRR-CT1 domain: P(w/f)xCxCxoxWLxxw(9-24)oxC(9-18)CxxP

LRR-CT2domain: nl(s/t)xogxxdFCxoxxxxo(4-5)y(4)LxxNpo(6)PxxfxCo

LRR-CT3 domain: LxxAxL(s/t)YPSHCCAFxN(6-19)nosxCnxsxxR...

LRR-NT domain: (7-10)CP(2-5)CxC(4-17)oxC(2-4)oxxoPxxoP

"x" represents any residue and "o" a non-polar residue (Kajava 1998).

We derived a minimal consensus sequence from each of the above and designed a new program, LRRscan, to search for these sequences as well as the minimal LRR defined above. The search for LRR-NTs and LRR-CTs focuses exclusively on the cysteines, which are the most conserved amino acids in these motifs. The regular expressions applied are as follows:

LRR: L..L.L..N.{10,21}

LRR-NT: C.{2,8}C.C.{6,19}C.{11,15}

LRR-CT1: ...C.C.{19,34}C.{9,18}C.{3}

LRR-CT1_short: ...C.C.{19,34}C.{22}

LRR-CT2: .{10}C.{30,31}C.

LRR-CT3: ..CC.{14,27}C.{6}

(Each dot represents any single letter, numbers in curly brackets indicate a repeat frequency, either exact or as a range where two numbers are given. Dots at the beginning or end of a domain denote spacing from the start or end of other motifs, including LRRs).

LRRscan was written in Perl and has been especially designed for the detection of LRR motifs. Input consists of a sequence file in FASTA format as well as search parameters. Each sequence is scanned for patterns, specified as strings, and alternative amino acids for certain positions, specified as triplets comprising position, alternative amino acid and score. The LRR pattern used in our search was 'LxxLxLxxN', where a small 'x' acts as a placeholder for any amino acid. The alternative options were amino acids A, I, V, F, G, M, or W for any of the leucines and C, S, or T instead of the asparagine. Each exact match between an

amino acid and the search pattern produces a score of 1, whereas a match to an alternative letter only scores 0.4. The scores are summed up over the length of the pattern and a minimum score of 2 would lead to further consideration of the sequence region. To allow for maximum sensitivity an exhaustive search is carried out, i.e., all patterns that match the search criteria are initially captured even if they overlap.

In the next step the regions are grouped into stretches of LRRs located within a specific distance from each other, in our case allowing for a gap of 20 to 30 amino acids between starts of pattern. Within a sequence of LRRs the overlaps are removed by only keeping the highest scoring regions. However, overlaps between sets of LRRs are allowed in the LRRscan output. Such occurrences are indicated in the output by a backward shift in the sequence location, i.e. the end of one stretch of LRRs might be printed again at the beginning of the next one. This is usually interpreted in the manual curation process as an insertion in the LRR domain. Each sequence is also scanned for a minimal LRR-NT pattern in the upstream sequence and for a minimal LRR-CT pattern (one of three possible types) in the downstream sequence. These are allowed to overlap with predicted LRRs to maximise the detection rate. The presence of additional elements from the more complete consensus sequences defined by Kajava was considered as supportive evidence in the manual curation process. Two alternative types of LRR-NT have been proposed, with different numbers of cysteines (Gangloff et al. 2004). We found it difficult to ascertain whether these were really evolutionarily distinct or whether some cysteines were simply not well conserved and SMART and Pfam can detect both types. For these reasons we have not attempted to distinguish between these putative types of LRR-NT. Similarly, some LRR-CT domains could not be categorized definitively as CT1 or CT2 subtypes; these are denoted as LRR-CT in Table 1 and [see Additional File 3]

.

The output from LRRscan reports the sequence that was searched and the positions of the motifs found followed by the sequence of the motifs themselves. The LRRs are numbered sequentially (within a set of grouped LRRs) and spaced to easily distinguish the well-conserved N-terminal from the more variable C-

terminal part [see Additional File 2]. We ran LRRscan on a set of protein sequences for which HMMpfam had predicted LRR motifs already (using the PFAM and SMART databases). The high sensitivity might result in an excessive number of false positives if applied to other sequences, but our goal was to further increase the detection rate of LRRs in sequences that showed an initial sign of LRR occurrence. A summary graphical output was generated for the output of each program for each sequence and aligned for easy comparison [see Additional File 2]. Through extensive manual curation a consensus predicted architecture was produced. It was found during manual curation that the cysteine residues in the NT and CT domains were not always positioned strictly according to the above consensuses and some flexibility was allowed for in these cases. We counted the final half repeat before the CT domain as one and did not include putative LRRs that overlapped with well-defined LRR-NT or LRR-CT domains in the total number of repeats.

2.3 RNA *in situ* hybridization

2.3.1 RNA in situ hybridization of *Drosophila* embryos

Wildtype *Drosophila* embryos were collected for 12 hours at room temperature and then aged for an additional 3 hours to attain a range of stages from stage 5 to stage 17, all staging according to Campos-Ortega and Hartenstein (Campos-Ortega 1985). Digoxigenin labelled RNA probes were prepared according to the manufacturers instructions (Roche diagnostics). PCR products were amplified from a cDNA library created by M. Georgiou, a T7 RNA polymerase consensus site was added to the reverse primer. In situ hybridizations were performed according to the Berkley Drosophila Genome Project (BDGP) 96-well plate protocol (http://www.fruitfly.org/about/methods/RNAinsitu.html) (adapted from (Tautz and Pfeifle 1989)) with a few minor modifications. The embryos were post fixed in 4% paraformaldehyde, pre-hybridization was carried out at 54°C and the wash buffers contained 0.2% Tween 20. The embryos were cleared in 70% glycerol, mounted on slides and photographed at x200 magnification using a Zeiss

Axioscope microscope, Axiocam camera and the accompanying Axiovision software.

2.3.2 Mouse in situ hybridization

Digoxigenin-labelled antisense cRNA probes for in situ hybridization were designed to encompass a section of coding sequence and 3'UTR >500bp in length. Briefly this involved TA cloning of PCR products into the TOPO vector (Invitrogen) and simultaneous synthesis and Dig-labelling of RNA transcripts from linearised vector using T7- or Sp6- RNA polymerase. Detailed information on probes is available upon request.

In situ hybridization was carried out on vibratome-sectioned C57Bl6 mouse brains (Jackson Laboratories) as described (Riddle *et al* 1993) with modifications. To obtain brains at E15, timed pregnancy mice were killed by cervical dislocation and embryos were fixed and stored in 4% paraformaldehyde-PBS at 4°C until use. For P0, brains were dissected out prior to immersion in 4% paraformaldehyde-PBS (PFA) at 4°C. P9 brains were fixed by perfusion followed by immersion in 4% paraformaldehyde-PBS at 4°C. Fixed brains were embedded in 3% agarose and 70μm sections were obtained on a vibratome (VT1000S Leica). Sections were washed twice in PBST (PBS containing 0.1% Tween-20), permeabilised in RIPA buffer (150mM NaCl, 50mM Tris-HCl pH 8.0, 1mM EDTA, 1% Nonidet-P40, 0.5% sodium deoxycholate, 0.1% SDS) and postfixed in 4% PFA and 0.2% gluteraldehyde. Hybridisation was performed in a humidified environment overnight at 65°C with 1μg/ml labeled probe in hybridisation buffer (50% formamide, 5X SSC pH4.5, 1% SDS, 50μg/ml yeast tRNA, 50μg/ml heparin). Posthybridisation washes were completed at 65°C using solution I (50% formamide, 5X SSC pH4.5, 1% SDS) and solution III (50% formamide, 2X SSC pH4.5, 0.1% Tween-20) and at room temperature using TBST (TBS containing 1% Tween-20). Brain sections were incubated for >1hr in blocking buffer (TBST, 10% heat-inactivated sheep serum). Immunodetection was carried out in blocking buffer at 4°C overnight using a phosphatase conjugated anti-digoxigenin antibody (Roche) at a 1:2000 dilution. Following antibody incubation extensive TBST

washes were performed. Sections were equilibrated in NTMT (100mM Tris-HCl pH 9.5, 100mM NaCl, 50mM $MgCl_2$, 1% Tween-20) prior to colourimetric detection using 2µl/ml NBT/BCIP (Roche) in NTMT. Sections were mounted on Superfrost glass slides (VWR international) and analysed with an Olympus IX51 microscope.

2.4 Animal Husbandry

Mice were maintained and bred in a 12hr light/12hr dark cycle, in a specific pathogen free unit. All procedures were performed in accordance with Statutory Instrument No. 566 of 2002 (Amendment of Cruelty to Animals Act, 1876). Mice used for experiments was an inbred strain of C57BL/6JolaHsd (Harlan) and a strain of C57BL/6 mice with a complete deletion of the *Elfn1* coding region obtained from KnockOut Mouse Project (KOMP). Newborn (P0) mice were collected on day of birth and decapitated. Brains were collected and dissected in ice-cold PBS before fixation at 4°C for 4-24 hours in either 4% paraformaldehyde (PFA) or 2% PFA;0.2% Glutaraldehyde.

For embryonic brains at specific developmental time-points, animals were time-mated and plug visualisation taken as an indication of conception and regarded as embryonic day (E0).

2.5 Genotyping of mice

Approximately 3mm of fresh tail tissue was digested in 200µl Boston Buffer (50mM Tris pH 8.0, 50mM KCl, 2.5mM EDTA, 0.45% NP40, 0.45% Tween20) with 14-22mg/ml Proteinase K overnight at 56°C. 1µl was used as template for PCR. The PCRs were carried out with taq DNA polymerse and corresponding buffers from Invitrogen. Primer sequences were produced by Sigma-Genosys.

Primer	Sequence (5'-3')
Elfn1forward	TGCAGCAGAGAGTACTTCAG
Elfn1reverse	TCTCACACACCGAGAGCTTG
LacZreverse	GTCTGTCCTAGCTTCCTCACTG

Table 2.1 Primer sequences used for genotyping PCR reactions

Elfn1 genotyping programme
95 °C for 2 min
32 cycles of: Denaturing: 95 °C for 15 sec Annealing: 63 °C for 30 sec Extension: 72 °C for 1 min
72 °C for 10 min

Table 2.2 Description of the PCR genotyping programme

2.6 Immunohistochemistry

Fixed brains were embedded in agarose (Sigma), 4% w/v, in PBS. Free floating sections (50-70μm) were collected using a vibrating microtome (Leica VT1000S) and washed twice for 10 minutes each, in PBS containing 0.2% triton X-100. Sections were then incubated in blocking buffer (10% normal serum in PBS) for 1 hour at room temperature, with gentle agitation. Incubation in primary antibody was carried out in PBS at 4°C with gentle agitation, for 24-48 hours. A list of antibodies table 2.2. After removal of primary antibody, sections were washed three times for 10 minutes each in PBS at room temperature. Sections were then incubated for 2-4 hours in the dark with a fluorescently tagged secondary antibody, diluted in PBS. This was followed by two washes in PBS of 10 minutes each, and a 10 second incubation in 4',6-diamidino-2-phenylindole (DAPI) diluted 1:5000 in dH_2O. Sections were washed briefly in PBS and mounted onto slides with aqua polymount (Polysciences Inc.). Results were viewed with an epifluorescence

microscope (Zeiss Axioplan2, Carl Zeiss Ltd. UK) or a laser scanning confocal microscope (Leica, DMRE).

Primary antibody	**Dilution**
pan-Elfn (anti-Elfn2) (Sigma; HPA000781)	1:50
anti-Ctip2 (Rat; Abcam 25B6)	1:250
anti-neurofilament (Mouse;DSHB 3H2)	1:250
anti-vGlut2 (Mouse; Millipore MAB5504)	1:1000
anti-Robo3 (Goat; R&D AF3076)	1:300
anti-substance P (Rat; Chemicon MAB356)	1:125
anti-somatostatin (Rat; Millipore MAB354)	1:50
anti-βgalactosidase (Rabbit; MP Biomedicals 08559762)	1:10,000
anti-GAD67 (Mouse; Millipore MAB5406)	1:1000
anti-GABA (Mouse; Swant 3A12)	1:5000
Secondary antibody	**Dilution**
goat anti-rabbit Alexa Fluor555 (Jackson immune research)	1:500
goat anti-rat Alexa Fluor555 (Jackson immune research)	1:500
goat anti- mouse Alexa Fluor488 (Jackson immune research)	1:500
goat anti-rat Alexa Fluor488 (Jackson immune research)	1:500
Goat anti-rabbit Alexa Fluor488 (Jackson immune research)	1:500
Donkey anti-goat Alexa Fluor488 (Invitrogen)	1:500
Donkey anti-rabbit Alexa Fluor488 (Invitrogen)	1:500

Table 2.3 List of antibodies used in this study. All primary antibodies and fluorescent-conjugated secondary antibodies are listed here along with their dilutions of use.

2.7 Production of tagged proteins

Tagged Elfn plasmids were prepared using the pcDNA3.1 myc-His plasmid. The full-length and extracellular regions of the mouse *Elfn1* and *Elfn2* genes were

amplified by PCR using specifically designed primers containing restriction enzyme sites for directional cloning (Table 2.3). PCR was carried out using Phusion high-fidelity DNA polymerase (Finnzymes, as per manual). PCR products were run on a 1% TAE gel and the amplified bands were cut from the gel and purified using a Nucleospin gel extract kit (Macherey-Nagel, as per manual). Iμg of PCR product and Iμg of pcDNA3.1 were digested with *EcoRI* and *XhoI* (New England Biolabs, as per manual). Digested PCR products were run on a gel and purified as before. The digested plasmid was dephosphorylated using Bacterial Alkaline Phosphatase (Invitrogen). The PCR products were then ligated into the digested pcDNA3.1 using T4 DNA ligase (Roche, as per manual). The ligation product was transformed into Top 10F' competent cells (Invitrogen) and plated on LB agar plates containing ampicillin (100μg/ml). Plates were incubated overnight, inverted at 37°C. The following day, single colonies were cultured overnight in LB/AMP broth, and preparation of plasmid DNA was carried out using QIAprep Spin Miniprep kit (Qiagen, as per manual). Successful cloning was confirmed by DNA sequencing (Eurofins-MWG/Operon). Full-length Robo3-Myc/His plasmids and extracellular Robo3-AP plasmids (only the extracellular domain of Robo3) were obtained from the lab of Alain Chédotal.

Primer	**Primer sequence**
Elfn1forward (with EcoRI site)	5'-gatcgaattcgccaccatggctgggcacgggtgg-3'
Elfn1reverse (with XhoI site)	5'- gctactcgagtcggacttgtgctgggcagacacg-3'
Elfn2forward (with EcoRI site)	5'-gatcgaattcaaagcctggggccatgct-3'
Elfn2reverse (with XhoI site)	5'-gctactcgagtgcagcttctgctgggctga-3'

Table 2.4 Primers used to amplify Elfn1 and Elfn2 transcripts for directional cloning into pcDNA3.1. The *EcoRI and XhoI* cleavage sites were included in the primer design and are underlined.

AP proteins were produced in COS-7 cells cultured in DMEM high glucose growth medium (10% FBS, 25mM HEPES, 1x glutamine, 1x penstrep). Cells were cultured to approximately 60% confluency and transfected with plasmids using Effectene transfection reagent (Qiagen, as per protocol). Three days later, medium

was collected, centrifuged and filtered. NaN3 (0.05%) was added for long term storage. For an experimental control, medium was also collected after transfection with empty pAPtag-5 plasmid (Genhunter). The amount of AP activity of each lysate was determined spectrophotometrically at 405 nm using 9 mg/ml *p*-nitrophenylphosphate (Sigma) (in 1M diethanolamine, pH 9.8, 0.5 mM $MgCl_2$) as a colorimetric, water-soluble substrate. A fusion protein concentration of 0.6 nm was used for AP-binding assays.

2.8 AP in situ hybridization

Free floating sections (50µm) were collected in PBS and washed twice in HBAH buffer (HBSS, 0.5mg/ml BSA, 0.05% NaN3, 20mM HEPES pH7.4). Sections were then incubated in 0.6nm Robo3a-AP, Robo3b-AP (see appendix for sequences) and the supernatant produced from the pAPtag5 plasmid for 2 hours at room temperature. After removal of AP protein, sections were washed six times in HBAH, followed by 15 seconds in 8% formalin and two washes in HBS buffer (150mM NaCl, 20M HEPES pH7.4). Heat inactivation of endogenous phosphatases was carried out in HBS at 65°C for two hours. Sections were then incubated in AP staining buffer (100Mm NaCl, 100Mm Tris-HCL, 5Mm MgCl2, with NBT/BCIP (Roche applied science)) at 37°C in the dark until colour developed.

2.9 Behaviour analysis

All behavioural tests within an experiment were carried out at the same time of day (either 9am-1pm or 2-4pm). Only male mice were tested and were handled for 3 days prior to each behaviour test. Animals were brought to the test room 15 minutes before each experiment to allow habituation to the surroundings.

2.9.1 Wire-hang test

To evaluate muscle strength and co-ordination in *Elfn1*$^{-/-}$ and *Elfn1*$^{+/-}$ mice, front- and hind- paw strength was evaluated on the wire-hang test. The apparatus consisted of a horizontal steel wire (26 cm long, 0.2 cm diameter), suspended between 2 wooden poles (19.5cm high) above a padded surface. The test consisted of 3 one-minute trials. On each trial the mice were suspended from the wire by the front 2 paws only. The mice were released and any mouse that crossed the wire to the poles at either end was deemed successful. The length of time taken to reach a pole was recorded.

2.9.2 Open-field test

The first set of open field tests were conducted in 2 rectangular plastic boxes (30cm x 50cm x 18cm) and (34cm x 60cm x 20cm) with open tops and a grid marked out on the floor. The smaller box contained a grid consisting of 15 squares (10cm x 10 cm each) and was black in colour. The larger box contained 18 squares (9.5cm x 11cm each) and was cream in colour. Boxes were placed on a table and against a wall in the behaviour room, away from direct fluorescent lighting. Activity measurements involved manual observation of grid line crosses with a counter. Immediately after placement of a mouse in the field, the number of line crosses were noted over 3 minutes. 16 mice were tested, 8 heterozygous and 8 homozygous mutant at 4-5 months old. Testing was carried out on consecutive days in the same box to observe habituation. Further testing in the second open-field box was carried out to evaluate novelty induced behaviour.

A second cohort of mice were tested in a new open field area with video tracking equiptment and activity was analysed using EthoVision. The open field box was cream in colour, and placed within a white circular tank (60cm in height) above which the video camera was positioned. This environment was more exposed and more brightly lit than in the previous experiment. Ten mice of each genotype (-/- and +/-) were tested and distance travelled and zone preference (peripheral or centre) were recorded over 10 minutes in an open field box (34cm x

53cm x 18cm). Testing was carried out on consecutive days in the same box to observe habituation behaviours.

2.9.3 Drug Administration

Amphetamine was dissolved in saline and injected intraperitoneally. Two concentrations were used, 0.5mg/kg and 2mg/kg. Saline solutions were administered to control anmals. Animals were injected 15 minutes before testing in the open field (as detailed above).

2.9.4 Seizure observation

Mice were placed in an empty cage with clean litter and observed for seizure behaviour over a 3 minute time period (Papaleo et al. 2011). Two genotypes were assessed, *Elfn1*$^{-/-}$ mice and *Elfn1*$^{+/-}$ and mice were aged 6-7 months old. Length of time in seconds was noted for each seizure from the first clonus behaviour to when the mouse regained motor control.

Seizures were described using a modification of Racine's seizure scoring system (Racine 1972) by (Croll et al. 1999). In this paper, Croll and colleagues attribute scores from 1-8 with increasing severity of the seizure. A score of 1 represented freezing or staring, 2 represented nodding, gnawing, facial atomatisms, or mild tremors, 3 represented unilateral clonus, 4 represented bilateal forelimb clonus, 5 represented severe seizures with prolonged loss of postural control or prolonged tonus, 6 represented status epilepticus defined as 10 minutes or more of continous or closely spaced seizures with no return to normal behaviour, 7 represented status epilepticus which included a stage 5 seizure, and 8 represented seiure-induced death.

2.9.5 Data analysis

All values are means and comparisons were performed using Student's *t*-test to determine the significance of differences between the two groups using GraphPad. Results were considered significant is $p < 0.05$. Post-hoc analysis of

the motor strength and coordination results was carried out using Fisher's exact test.

3 Chapter 3 The extracellular Leucine-Rich Repeat superfamily

The extracellular Leucine-Rich Repeat superfamily; a comparative survey and analysis of evolutionary relationships and expression Patterns.

The following chapter is published work (Dolan et al. 2007).

3.1 Introduction

Leucine-rich repeats (LRRs) are protein-ligand interaction motifs found in a large number of proteins of diverse structure, localization and function in bacteria, fungi, plants and animals (Kobe and Kajava 2001). Many of these have well-known functions in the innate immune system (Nurnberger et al. 2004). Many others, especially those with extracellular LRRs (eLRRs), are involved in various aspects of nervous system development (Chen et al. 2006). In both cases, the nature of the LRR motifs is important for generating a diversity of interactions, with exogenous factors in the immune system and with the huge number of different cell types in the developing nervous system. The structure of LRR motifs and their arrangement in repetitive stretches of variable length generate a versatile and highly evolvable framework for the binding of diverse proteins and non-protein ligands.

Seven classes of LRR have been defined (Kobe and Kajava 2001); (these have been referred to as LRR "subfamilies" (Kajava 1998); we use the term subfamily here in the phylogenetic sense to refer to sets of closely-related genes). Within animals, four separate types are recognised, three typically intracellular and one extracellular. Whether all these different classes are evolutionarily related by descent or represent convergent evolution is open to debate (Kobe and Kajava 2001) but they all share a characteristic structure. Each repeat is typically 19-29 amino acids long and has a well-conserved N-terminal stretch of 9-12 amino acids that is characterized by precisely-positioned hydrophobic residues (usually leucines) and that forms a β-strand and a C-terminal stretch of 10-19 amino acids that is more variable in length, sequence and structure. The arrangement of

multiple repeats in tandem generates a horseshoe-shaped solenoidal structure, with the β-strands stacking to form the concave surface and the variable stretches forming the convex surface (Kobe and Kajava 2001, Bell et al. 2005, Mosyak et al. 2006, He et al. 2003). Most LRR regions typically also have both N-terminal and C-terminal cap regions, which shield the hydrophobic core of the LRR structure. In extracellular proteins these regions (LRR-NT and LRR-CT domains, of which several subtypes exist) are defined by precisely positioned cysteine residues (Kajava 1998).

LRR proteins, both intracellular and extracellular, have well-characterized functions in the innate immune system that are similar from plants to mammals (Nurnberger et al. 2004). The extracellular LRR (eLRR) proteins in animals include the Toll-like receptors (TLRs), a family of transmembrane proteins characterized by an LRR region, a transmembrane (TM) domain and a cytoplasmic Toll/IL-1 receptor (TIR) domain. This family has expanded in vertebrates to allow detection of a diverse set of antigens (West et al. 2006). In flies, the TLR family has also expanded, where, in addition to roles in immunity for some of these proteins (Lazzaro et al. 2006), many are required for various aspects of embryonic and nervous system development (Anderson et al. 1985, Halfon et al. 1995, Gangloff et al. 2003, Kambris et al. 2002). Tol-1 in worms is also important in development, possibly contributing to a code of molecules defining neuronal connectivity (Pujol et al. 2001, Kaufman et al. 2006). Recent reports indicate that some mammalian TLR genes may also be expressed and function in neurons (Wadachi and Hargreaves 2006, Afzal and Lightfoot 2007).

A large number of other eLRR proteins have been implicated in various aspects of neural development, genetically in flies (Van Vactor et al. 1988, Nose et al. 1994, Kidd et al. 1999) and in mammals in assays of neurite outgrowth (Tsuji et al. 2004, Aruga and Mikoshiba 2003, Lauren et al. 2003, Lin et al. 2003) fasciculation (Kuja-Panula et al. 2003) and/or synapse formation (Kim et al. 2006, Ko et al. 2006). Some of these contain, in addition to the extracellular LRR domain, immunoglobulin (Ig) or fibronectin type-3 (FN3) domains (for review see (Chen et al. 2006)). In some cases, the functions of eLRR proteins are mediated by homophilic interactions (Kuja-Panula et al. 2003, Karaulanov et al. 2006, Nose et al. 1997, Shinza-Kameda et al. 2006). In other cases they are mediated by the

binding of other proteins *in cis* (Park et al. 2005, Shao et al. 2005, Wang et al. 2002a) and *in trans* (Kim et al. 2006, Conover and Yancopoulos 1997, Wang et al. 2002b, Fukata et al. 2006). Several eLRR proteins have been found to modulate the signaling of various growth factor pathways (e.g., ((Ghiglione et al. 1999, Fukamachi et al. 2002, Bottcher et al. 2004, Fetchko et al. 2002, Ohta et al. 2004)).

Surprisingly, apart from the TLR genes (Beutler et al. 2006) and small secreted proteoglycans (Ameye and Young 2002), relatively few eLRR genes have been studied genetically in mice. Among the ones that have, examples of phenotypic effects in the nervous system include increased plasticity, sprouting and nerve regeneration (McGee et al. 2005), and defects in axon guidance and cell migration (Long et al. 2004), learning and memory (Bando et al. 2005), myelination (Mi et al. 2005, Bermingham et al. 2006) and neuronal survival (Conover and Yancopoulos 1997).

The importance of this class of proteins for nervous system development in humans is apparent from the large number of examples implicated in neurological or psychiatric disorders (reviewed in (Matsushima et al. 2005)). These include epilepsy (Kalachikov et al. 2002), Tourette's syndrome (Abelson et al. 2005), night blindness (Bech-Hansen et al. 2000), congenital insensitivity to pain (with mental retardation) (Indo et al. 1996), and possible links to Alzheimer's disease (Majercak et al. 2006).

Despite the growing number of eLRR proteins implicated in nervous system development or disease this family of proteins has received far less attention as a class than other better characterized families like the immunoglobulin (Rougon and Hobert 2003, Vogel et al. 2003) and cadherin (Takeichi 2007) superfamilies. In particular, there have been no systematic surveys of the genomic complement of these proteins or investigation of their evolutionary relationships. We therefore set out to catalogue the entire extracellular leucine-rich repeat proteome of four organisms: *Caenorhabditis elegans*, *Drosophila melanogaster*, *Mus musculus* and *Homo sapiens*. We used a hierarchical clustering system to analyse within and between-species relationships, revealing independent diversification and expansion of subfamilies in each species and rapid sequence divergence. These analyses highlight the large number of novel, uncharacterized eLRR proteins in

each of these genomes, including several novel subfamilies. A number of these show highly restricted expression in the nervous system in mouse or fly.

3.2 Results

3.2.1 Bioinformatics strategy

We began by obtaining whole proteome sets of known and predicted proteins from each of the four species, as described in Methods. Our initial approach was to filter the starting proteome datasets using transmembrane (TM) and signal peptide prediction programs (TMHMM (Krogh et al. 2001) and SignalP (Bendtsen et al. 2004) to identify transmembrane or secreted proteins and then to filter that set using a motif recognition program (Pfam (Bateman et al. 2004)) to identify the subset with motifs of interest. However, this approach using serial filters missed a number of known axon guidance molecules because TMHMM or SignalP misclassified them or Pfam did not detect specific motifs. We therefore included a number of other TM-prediction and motif-recognition programs, including a customised program to look for LRR domains (LRRscan, see below) in the pipeline. In addition, we first performed a clustering step using TribeMCL (Enright et al. 2002) on the entire proteome sets so as to identify related proteins even where these programs failed to detect specific motifs or architectures. Rather than using any of these programs or a combination of them as strict filters we generated a database containing all the results that could be browsed or searched using various criteria to extract particular gene families of interest (Figure 3.1).

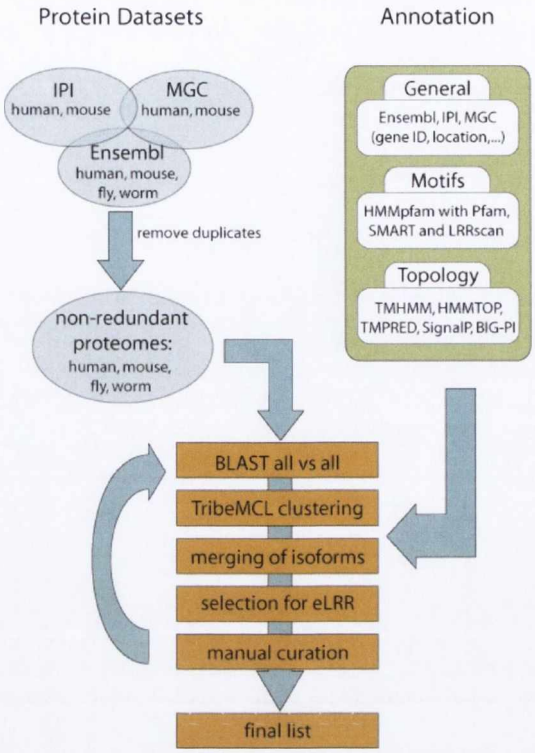

Figure 3.1 Bioinformatics pipeline. Figure shows starting datasets (blue), annotation programme (green) and clustering pipeline (orange) used to generate final dataset.

3.2.2 Clustering

TribeMCL is a program designed to cluster proteins into related families based on simultaneous examination of all pairwise BLAST similarity scores (Enright et al. 2002). This program uses a Markov cluster algorithm that is particularly well suited to cluster highly divergent proteins with repeated domains into separate subfamilies, a task for which multiple alignment programs are not appropriate. The Markov cluster algorithm is based on simulated 'flow' through a network or graph, where each node is a gene and each connection is weighted by the symmetric pairwise BLAST score. A random walk of a certain length from node to node through this network, which begins within a small cluster of interconnected genes will have a higher probability of ending up within that cluster than crossing to a gene that is only related to one of them. The results of many

simulated random walks thus define the clusters. Each time this process is reiterated the links within the clusters that emerge are given a higher weighting and the links that were not used are downgraded. Multiple rounds of this process eventually lead to completely separate clusters. There are two parameters that can be varied that affect the clustering; the first is the e-value cutoff of the BLAST scores that are used, which determines the initial set of connections considered. The second is the inflation parameter; this determines how strongly the links are upgraded with each iteration. A higher inflation parameter increases the 'granularity' of the output; i.e., it generates a larger number of smaller clusters. We used a number of e-value cutoffs (from e^{-10} to e^{-40}) and inflation parameters (1.2, 2, 3, 4 and 5) and compared the output produced.

The output from TribeMCL, for any given e-value cutoff and inflation parameter can be viewed as a list of genes organized into clusters with a number assigned to each cluster (lower numbers have more members). We reasoned that hierarchical sorting of genes across various inflation parameters should yield a tree-like structure, with larger clusters at low inflation parameters splitting into more discrete clusters at higher inflation parameters. At each e-value cutoff we therefore sorted the list of genes first at inflation parameter 1.2, then 2, then 3, 4 and 5. For the most part, increasing inflation parameter does lead to splitting of large clusters into smaller clusters and yields a tree-like arrangement of genes with relationships apparent across various levels (but see discussion on "LRR_Tollkin" group below).

3.2.3 Identification of LRR motifs

To identify LRR proteins, the database was searched for all genes containing at least one LRR, LRR-NT or LRR-CT predicted by either SMART or Pfam. The cutoff values used were based on analysis of the results for proteins with known architecture (see section 2.2 for details). This analysis yielded a total of 2,698 entries. These include both genes with intracellular LRRs and those with extracellular LRRs. It also contains isoforms for many genes. To screen out false positives we used the following criteria: if only one LRR was predicted in a gene

and only by one of the programs and it was not predicted in either the mouse or human orthologue (for mammalian genes), or in other members of a closely-related cluster then it was considered a false positive and discarded.

3.2.4 Identification of extracellular LRR proteins

Comparison of several TM-prediction programs suggests that TMHMM is the most reliable, although it is also the most selective (Kall and Sonnhammer 2002). A quick survey of some known TM receptors revealed that TMHMM failed to identify TM domains in several of them, including Robo2 in mammals and Kekkon2 and 3 in flies, for example. For that reason we also used two other programs, HMMTOP (Tusnady and Simon 2001) and TMPred (Hofmann and Stoffel 1993) to search for TM domains. At least one of these three programs successfully detected the TM domain in all the known TM receptors examined (while also increasing the number of false positives).

SignalP (Bendtsen et al. 2004) was used to detect signal peptides. This suffered from poor prediction of 5' exons for many mammalian genes, which was solved by manual curation (see below). The GPI-prediction program BIG-PI (Eisenhaber et al. 1999) identified a small number of GPI-linked proteins, including all the known GPI-linked proteins such as Connectin, NgRs and Nyx (the latter in human but not mouse, as reported (O'Connor et al. 2005). A number of other genes were tentatively assigned to the GPI-class by manual inspection based on the presence of a characteristic short C-terminal hydrophobic stretch (and a signal peptide).

In addition to examining the convergent evidence from these various programs to identify eLRR proteins we used three additional criteria. The first is the type of LRR predicted: extracellular proteins typically contain LRR types designated LRR_1, 2 or 3 by Pfam or LRR_typical by SMART, while the intracellular proteins have LRR_RI or LRR_sd22 (Kobe and Kajava 2001). Second, the prediction of an LRR-NT and/or LRR-CT domain was taken as evidence for extracellular localization. Third, especially at low e-value stringencies (e^{-10}), the majority of extracellular LRR proteins cluster together with TribeMCL in

one large group (and a few small ones), distinct from the intracellular proteins. Using these criteria in addition to the data from the prediction programs described above we collected what we believe is a comprehensive set of extracellular LRR proteins across worm, fly, mouse and human. We call these the eLRR proteome.

3.2.5 Manual curation of extracellular sequences

To reduce the complexity of the final data set a single protein isoform was chosen for each gene and all others were removed (see section 2.1 and 2.2). Many peptides that we expected to be extracellular because of orthology, clustering or domain structure did not have a predicted signal peptide. Upon manual inspection of the sequences it was discovered that many gene predictions in Ensembl, especially for mammalian genes, were missing the 5'-most exon encoding the signal peptide. For many such genes we identified the 5' exon and the full coding sequence in a sequence from another database and/or by searching with an orthologous gene from mouse or human using BLASTN programmes. In other cases the 5' predicted sequence extended past the apparent true methionine start codon, which could be recognised by conservation and the presence of the signal sequence.

We identified two fly genes that have been incorrectly annotated in Ensembl as two separate genes each. CG32637 and CG4187 represent the 5' and 3' ends of a cDNA encoded by AB134171, a new member of the Lgr3 family. Similarly, CG4054 and CG13487 represent the 5' and 3' ends of the fish-lips fili) gene, encoded by AAV36870 (Adachi-Yamada et al. 2005) which is related to tartan and capricious (Milan et al. 2005, Adachi-Yamada et al. 2005). We detected one similar mis-annotation in the worm database (pxn-1) and presume that this type of error may also have occurred for some mammalian sequences.

All the manually curated gene sequences are provided [see Additional File 1]. These curated sequences were fed back into the starting database and the BLAST and clustering analyses were re-performed to ensure that spurious results had not been generated by incorrect sequences.

3.2.6 Defining consensus architectures

In order to derive a consensus architecture for each gene we compared the results of SMART and Pfam and the TM-prediction programs. Even at very low stringency some LRRs in proteins with known numbers of such repeats were missed by HMMpfam using the SMART and Pfam databases. This includes a number of somewhat degenerate LRRs in Lrrc8 proteins (Smits and Kajava 2004), for example, as well as atypical LRR-CT domains in small proteoglycans and G-protein-coupled receptors (Kajava 1998). For this reason, using a similar strategy to Smits and colleagues (Smits and Kajava 2004), we wrote a customised program, LRRscan, to search for a more inclusive minimal consensus that defines LRRs as well as searching for consensus sequences derived from non-canonical LRR-CT domains (see Methods for details). LRRscan was successful in identifying all the predicted LRRs in Lrrc8 proteins, including atypical or degenerate ones (Smits and Kajava 2004), and additional LRRs in many other proteins that were not detected by HMMpfam with SMART or Pfam.

The output from LRRscan and HMMpfam was compared for all proteins [see Additional File 2] and a consensus architecture including number of LRRs and presence of LRR-NT and LRR-CT domains was derived by manual curation. The consensus matches the architecture of a number of eLRR proteins with published structures (Bell et al. 2005, Mosyak et al. 2006, Choe et al. 2005, Huizinga et al. 2002) allowing for semantic differences in how the LRRs are counted. The final LRR before the LRR-CT domain (CT1 subtype) often contains only the first subdomain of nine residues; following the convention of Matsushima and colleagues (Matsushima et al. 2005) count this as one repeat rather than part of the LRR-CT domain, which in some cases may cause an apparent discrepancy with published reports. We also do not count in the total number of repeats putative LRRs which overlap with LRR-NT or LRR-CT domains, as has been done in some published cases (Fan and Hendrickson 2005, McEwan et al. 2006).

A consensus topology for each protein was also derived by comparison of the signal peptide, GPI anchor and TM-prediction programs. A full list of all the eLRR proteins is provided [see Additional File 3] and a sample is shown in Figure 3.2. These are sorted hierarchically across inflation parameters at an e-value

cutoff of –40. Figure 3.2 includes information on synonyms, a consensus architecture, peptide length and several other features. Clustering results at e-10 and e-25 are also presented [see Additional Files 4 and 5]. Figures 3.3 and 3.4 provide an overview of the consensus protein architectures of most of the eLRR proteins, arranged in subfamilies. A large number of singleton LRR_Only proteins are not shown in this diagram (these are listed separately in Table 3.1).

3.2.7 The eLRR superfamily

We categorized the eLRR proteins into four classes, based on their architecture and clustering. These are LRR_Ig/Fn3 (containing an Ig or FN3 domain but no other extracellular domains except LRRs), LRR_Tollkin (containing a cytoplasmic TIR domain or clustering with the Toll proteins), LRR_Other (containing some other domain, such as EGF repeats or a G-protein-coupled receptor domain) and LRR_Only (containing no other recognizable domain). These categories are broadly supported by the clustering results, although the LRR_Other group is clearly arbitrary and contains a number of unrelated subfamilies. The number of eLRR proteins in each of these classes in each of the four organisms studied is shown in Table 2. These are broken down into several categories, based on predicted localization: secreted, GPI-linked, type I transmembrane and multi-membrane spanning (all multi-membrane spanning proteins were classified into the LRR_Other group). Almost all of the LRR_Ig/FN3 group are associated with the plasma membrane, either as type I TM or GPI-linked proteins. In contrast, the LRR_Tollkin and LRR_Only groups contain a far higher percentage of secreted proteins. It is clear from an examination of these data that the eLRR superfamily has greatly expanded in mammals (>135 genes) and to a lesser extent, flies (O'Connor et al. 2005), compared to worms (Nose et al. 1997).

3.2.8 Subfamily expansion and diversification

In order to assess the extent of expansion (new members of existing subfamilies) and diversification (new subfamilies) across different organisms, we analysed the membership of clusters across mouse and fly. For this purpose, we defined clusters in such a way as to distinguish those with species-specific expansion from those with diversification [see Additional File 6]. For each cluster we counted the number of fly and mouse members and then generated histograms of the number of clusters with x fly members and y mouse members (Figure 3.5). For example, in the LRR_Ig/FN3 group there is one cluster with one fly gene and three mouse genes (Lrigs) and there are six clusters with no fly genes and three mouse genes (Ntrk, Lrrn1-3, Lrrc4, Amigo, FLRT and Lrrc21 groups). These graphs illustrate the different rates of expansion and diversification across these groups.

For the LRR_Ig-FN3 family there is a large number of clusters that have multiple mouse genes and no fly genes. These represent the diversification of new architectures and gene families in the mammalian lineage. There is only one case of expansion in the mouse within a conserved subfamily (the Lrig family which has three members in mouse and one, lambik, in fly (as well as one in worm)). Conversely, the kekkon family shows a specific expansion in flies compared to mammals, where there is only a single apparent closest orthologue, Lrrc24.

In contrast, in the LRR_Tollkin group there has been independent expansion of subfamilies in both flies and mammals (and even comparing mouse and human). Similar expansions are observed in the subfamilies of Toll-like receptor genes themselves and in the subfamilies of gene encoding proteins that do not have TIR domains but that cluster within this group (see below).

In the LRR_Only group there has also been independent expansion, apparently followed by rapid divergence, resulting in a very large number of singletons in each species. These are genes with no recognizable orthologue in the other species (fly or mouse) and no recognizable paralogue in their own species. The encoded proteins do not cluster at high stringency (e-value and inflation parameter) but many cluster into a very large group at lower stringency.

This trend may reflect increased divergence rates of this class of proteins. There is only one case in this group of apparent orthology, between CG6959 in fly and Tpbg /5T4 (Imamura et al. 2006) and a novel gene in mouse.

The LRR_Other group shows the opposite pattern with the largest number of clear orthologues between mouse and fly (clusters on the diagonal). This group also contains the most clusters with a clear worm orthologue [see Additional File 3 and Figure 3.4]. The members of this group include the Slit proteins, peroxidasins, and a number of G-protein coupled hormone receptors, which are all conserved, as well as a number of mammal-specific families including the Lgi proteins.

External_Name	Synonyms	cl1_2	cl2	cl3	cl4	cl5	Location
Lrig1		156	1728	1685	1622	1591	6:95066418-95161799
Lrig2		156	1728	1685	1622	1591	3:103884357-103939517
Lrig3		156	1728	1685	1622	1591	10:125665573-125714974
lbk	Lambik	156	1728	1685	1622	1591	2R:11679210-11684383
T21D12.9		156	1728	1685	1622	1591	IV: 274570-287201
Lrrn6a	Lingo1	636	1937	1898	1838	1809	9:56731965-56798743
Lrrn6b	Lingo3	636	1937	1898	1838	1809	10:80964866-80976093
Lrrn6c	Lingo2	636	1937	1898	1838	1809	4:35846472-36195578
Lrrn6d	Lingo4	636	1937	1898	1838	1809	3:93887043-93892325
Lrrn1	Nlrr1	636	3698	3710	3680	3664	6:108031528-108072472
Lrrn2	Nlrr2	636	3698	3710	3680	3664	1:132741816-132801420
Lrrn3	Nlrr3	636	3698	3710	3680	3664	12:38061168-38095273
Lrrc4	Ngl-2	636	5118	5199	5214	5224	6:28876652-28878610
Lrrc4b	Ngl-3	636	5118	5199	5214	5224	7:38517725-38540037
Lrrc4c	Ngl-1	636	5118	5199	5214	5224	2:97172341-97336348
XP_485967	Garp/ Lrrc32	671	2804	5902	5974	5994	unmapped
Lrrc33	Garpl1	671	2804	7897	8069	8147	16:30952197-30974848
Lrrc15	Lib	671	3320	9586	9863	10054	16:29076635-29091261
Gp5	Glycoprotein 5/GPV	671	3320	10192	10520	10743	16:29115637-29118723
Cpn2	Carboxypeptidase N, polypeptide 2	671	3320	12102	12561	12887	16:29063712-29074853
Igfals	Als	671	7252	7532	7676	7734	17:24607540-24609348
1200009O22Rik	mKIAA0644	671	10234	10860	11238	11494	6:53745044-53750272.
CG7509-PA		671	25631	27360	28472	29304	3L:4783924-4786121
C56E6.6		1796	5143	8386	22037	22689	II:6540165-6544297
CG40500-PD		1796	5143	8386	11883	14994	Xh:214902-235557.
CG5195-PA		1796	5143	8386	27788	28588	3L:20388531-20398189
CG7896-PA		1796	5143	8386	11883	29432	3R:25809174-25816514
chp	Chaoptin	1796	5143	13751	25152	25868	3R:27029904-27036452
CG4168-PA		1796	5143	13751	27464	28254	2L:15158036-15174249
CG8561-PA		1796	5143	27662	28794	29638	2R:9786463-9789735
Tol-1		1796	7985	8352	8558	8674	I:444002-461590
Toll-7	dToll7	1796	7985	8352	8558	8674	2R:15341768-15346108
18w	18 Wheeler	1796	7985	8352	8558	8674	2R:15626374-15631795
Tollo	dToll8	1796	7985	8352	8558	8674	3L:15200900-15208091
Toll-6	dToll6	1796	7985	8352	8558	8674	3L:15301959-15307470
Tl	dToll1	1796	9274	9759	10055	12016	3R:22624765-22668125
MstProx	dToll3	1796	9274	9759	10055	12016	3R:3191661-3195027
Toll-4	dToll4	1796	9274	9759	10055	12016	2L:9084107-9089440
Tehao	dToll5	1796	9274	9759	10055	29162	2L:13435637-13440955
Chad	Chondroadherin	4838	5233	11926	12369	12678	11:94386155-94390215
XP_001001535		4838	5233	8540	8733	8858	15:81522436-81523284

Figure 3.2 Sample from list of all eLRR genes, hierarchically clustered at e^{-40} cutoff. Proteins have been sorted in this table based on the clustering output from TribeMCL. This has been done hierarchically across inflation parameters, starting at 1.2, then 2, 3, 4 and 5. For most proteins this yields a tree-like structure with cluster stringency increasing (and membership decreasing) from low inflation parameters to high. Numbers used to identify clusters are generated by TribeMCL with larger clusters having lower numbers. Proteins are colour-coded by species: black, mammalian; blue, fly; red, worm. For the mammalian proteins, only the mouse orthologue is listed. The table shows examples of clusters in the LRR_Ig/FN3 group with mouse, fly and worm orthologues (the Lrig subfamily) and

with mouse paralogues only (the Lrrn6, Lrrn1-3 and Lrrc4 subfamilies, which cluster together at level 1.2). It also shows many of the proteins in the LRR_Tollkin group, with the hierarchical clustering apparent across inflation parameters and indicated by shading. One subfamily containing a known and novel member is shown at the bottom. Proteins encoded by genes located in tandem in the genome are boxed in the right-hand column. A complete list of all eLRR proteins is provided [see Additional File 3]. Lists clustered at the e^{-25} and e^{-10} cutoff levels are given [see Additional Files 4 and 5].

LRR_Ig/FN3 group

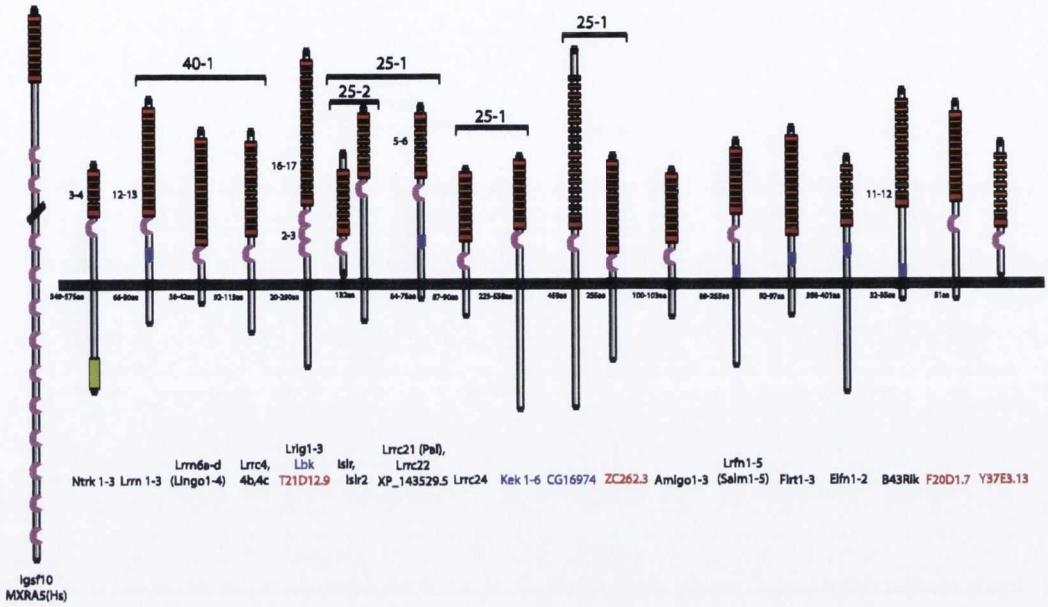

LRR_Only group
(subfamilies; for singletons see Table 2)

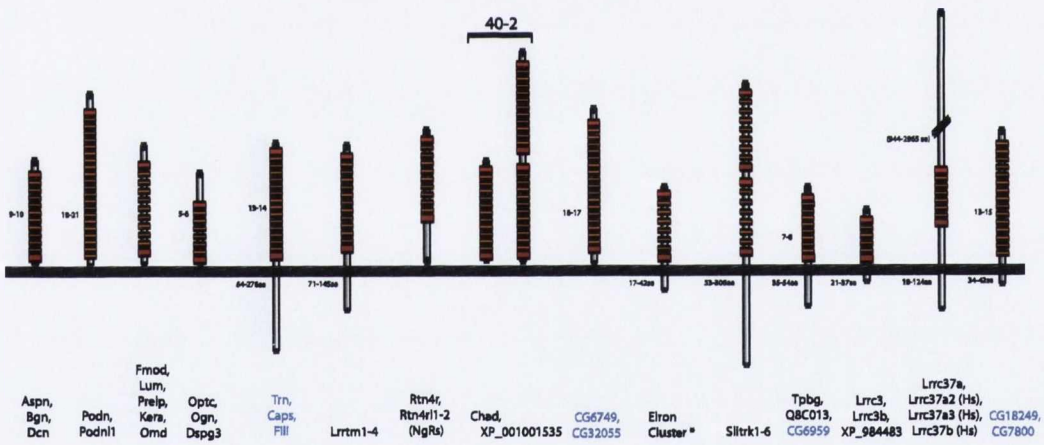

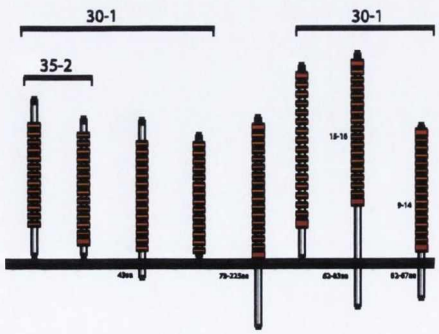

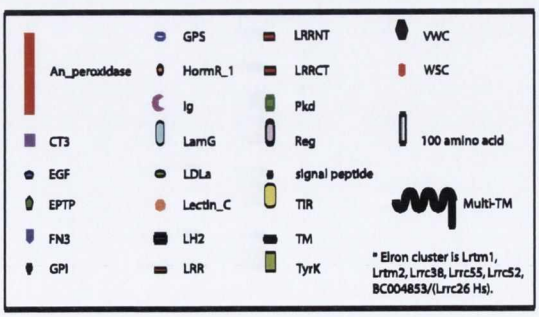

Figure 3.3 eLRR protein predicted architectures (part 1). Consensus architectures are shown for all proteins in the LRR_Ig/FN3 group and for all proteins in subfamilies in the LRR_Only group. An additional set of LRR_Only singletons is listed separately in Table 3.1. Protein names are shown below the corresponding structures (black, mammalian; blue, fly; red, worm). All figures are drawn to scale (see Key). Consensus architectures were derived for single proteins and across subfamilies from convergent evidence from motif and topology prediction programmes. Where there is a range in number of predicted LRRs or other domains across members of a subfamily, this is indicated next to the domain. A range in length of the cytoplasmic domain is similarly indicated, where it exceeds 20 amino acids. Tightly clustered subfamilies (e.g., Slits, Amigos) are listed under a single consensus architecture. Clusters with more structurally diverse proteins are indicated by the brackets; the numbers refer to e-value and inflation parameter at which the proteins cluster in the MCL programme. See Key for more information.

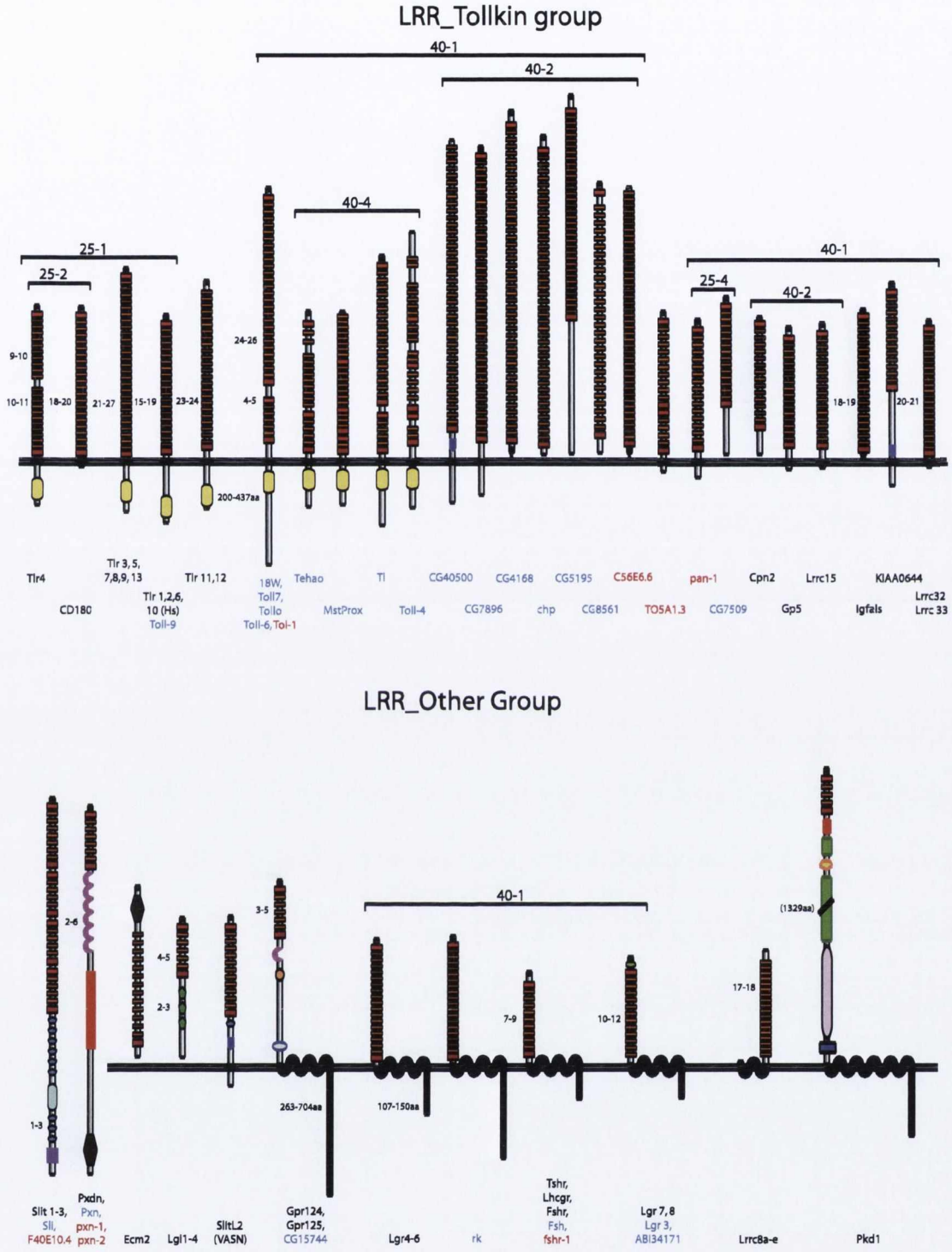

Figure 3.4 eLRR protein predicted architectures (part 2). Consensus architectures are shown for all proteins in the LRR_Tollkin and LRR_Other groups. See Figure 3.3 legend for details.

Symbol	Name/synonyms	Peptide length	Consensus architecture
Mammalian proteins			
BC031901	novel	872	SS, 7LRR, TM
Cd14		366	SS, LRRNT, 11LRR, GPI
Gp1ba	Glycoprotein 1b, alpha polypeptide	734	SS, LRRNT, 8LRR, LRRCT1, TM
Gp1bb	Glycoprotein 1b, beta polypeptide	214	SS, LRRNT, 2LRR, LRRCT1, TM
Gp9	Glycoprotein 9	177	SS, LRRNT, 2LRR, LRRCT1, TM
Lrg1	Leucine-rich alpha-2-glycoprotein 1	342	SS, LRRNT, 9LRR, LRRCT2
Lrrc17		443	SS, LRRNT, 4LRR, LRRCT1, LRRNT, 3LRR, LRRCT1
Lrrc19		364	SS, LRRNT, 6LRR, LRRCT1, TM
Lrrc25		297	SS, 2LRR, LRRCT1, TM
Nepn	Nephrocan / 5730521E12Rik	512	SS, LRRNT, 17LRR, LRRCT1
Nyx	Nyctalopin (mouse)	476	SS, LRRNT, 11LRR, LRRRCT1, TM
NYX	Nyctalopin (human)	481	SS, LRRNT, 12LRR, LRRRCT1, GPI
Omg	Oligodendrocyte myelin protein	440	SS, LRRNT, 7LRR, LRRCT2, GPI
Q7Z2Q7	Synleurin (human)	621	SS, LRRNT, 13LRR, LRRCT1, TM
Tsku	Tsukushi / Lrrc54	354	SS, LRRNT, 10LRR, LRRCT2
Fly proteins			
Con	Connectin	691	SS, LRRNT, 11LRR, LRRCT1, GPI
Gp150	Gp150	1051	SS, LRRNT, 15LRR, LRRCT2, TM
hfw	Halfway	611	SS, LRRNT, 4LRR, LRRNT, 2LRR, LRRCT1
wdp	windpipe	677	SS, LRRNT, 4LRR, LRRCT1, TM
CG1504		392	...11LRR, LRRCT1, TM
CG4781		469	SS, LRRNT, 11LRR, LRRCT1, TM
CG5096		491	SS, LRRNT, 12LRR, LRRCT, TM
CG5541		463	SS, LRRNT, 6LRR, TM
CG5819		915	SS, LRRNT, 17LRR, LRRCT1, TM
CG5888		455	SS, LRRNT, 8LRR
CG7702		537	SS, LRRNT, 11LRR, LRRCT1, TM
CG8852		663	SS, 10LRR, LRRCT, TM
CG10148		329	SS, 9LRR
CG11136		799	SS, LRRNT, 13LRR, LRRCT1, TM
CG14351		1316	SS, LRRNT, 12LRR, LRRCT1, TM
CG14662		550	SS, 6LRR, TM
CG14762		470	SS, LRRNT, 14LRR, LRRCT1
CG15658		343	SS, LRRNT, 7LRR, LRRCT1, TM
CG17667		458	SS, LRRNT, 7LRR, TM
CG18095		548	SS, 18LRR, TM
CG18480		550	SS, LRRNT, 7LRR, LRRCT, TM
CG32372		817	SS, 23LRR
Worm proteins			
C02C6.3		369	SS, LRRNT, 8LRR, LRRCT1, GPI
C41C4.3		630	SS, 8LRR
F10F2.4		656	SS, LRRNT, 18LRR, LRRCT1, TM
F37E3.2		568	SS, LRRNT, 11LRR, TM
K03A1.2		586	SS, LRRNT, 9LRR, LRRCT1, TM
T22E7.1a		341	SS, 8LRR, LRRCT1, TM
T23G11.6		653	SS, LRRNT, 15LRR, LRRCT, TM
Y39A1A.7		187	SS, LRRNT, 4LRR
Y71F9B.8		542	SS, LRRNT, 14LRR, LRRCT1, TM
Y75B8A.5		448	SS, LRRNT, 6LRR, LRRCT1
Y76A2B.2		782	SS, LRRNT, 6LRR, GPI

Table 3.1 List of LRR_Only singletons. List contains proteins not shown in figure 3.3. For the mammalian proteins, only the mouse orthologue is listed, with the following exceptions: both human and mouse Nyctalopin (Nyx) are listed as they have different topologies (GPI-linked and TM, respectively) and *synleurin* is a human gene that has been pseudogenised in mouse. Domains listed in parentheses are weakly predicted.

LRR_Ig/FN3					
	Type I TM	GPI	Secreted	Multi-TM	Total
Worm	3	0	1	0	4
Fly	8	0	0	0	8
Mouse	35	1	1	0	37
Human	35	1	2	0	38
Total	81	2	4	0	87
LRR_Tollkin					
Worm	3	1	0	0	4
Fly	11	1	4	0	16
Mouse	17	0	2	0	19
Human	17	0	2	0	19
Total	49	2	7	0	58
LRR_Other					
Worm	0	0	3	1	4
Fly	0	0	2	5	7
Mouse	1	0	9	16	26
Human	1	0	9	16	26
Total	2	0	23	38	63
LRR_Only					
Worm	11	2	4	0	17
Fly	23	1	10	0	35*
Mouse	28	5	19	0	52
Human	32	6	19	0	57
Total	94	14	52	0	161*

Table 3.2 Complement of eLRR proteins by group, localisation and species. The numbers of eLRR proteins in each of the four major groups is listed for each species, broken down by predicted protein localisation or topology: type I transmembrane, GPI-linked, secreted and multiple-membrane-spanning. *includes CG1504, unclassified localisation.

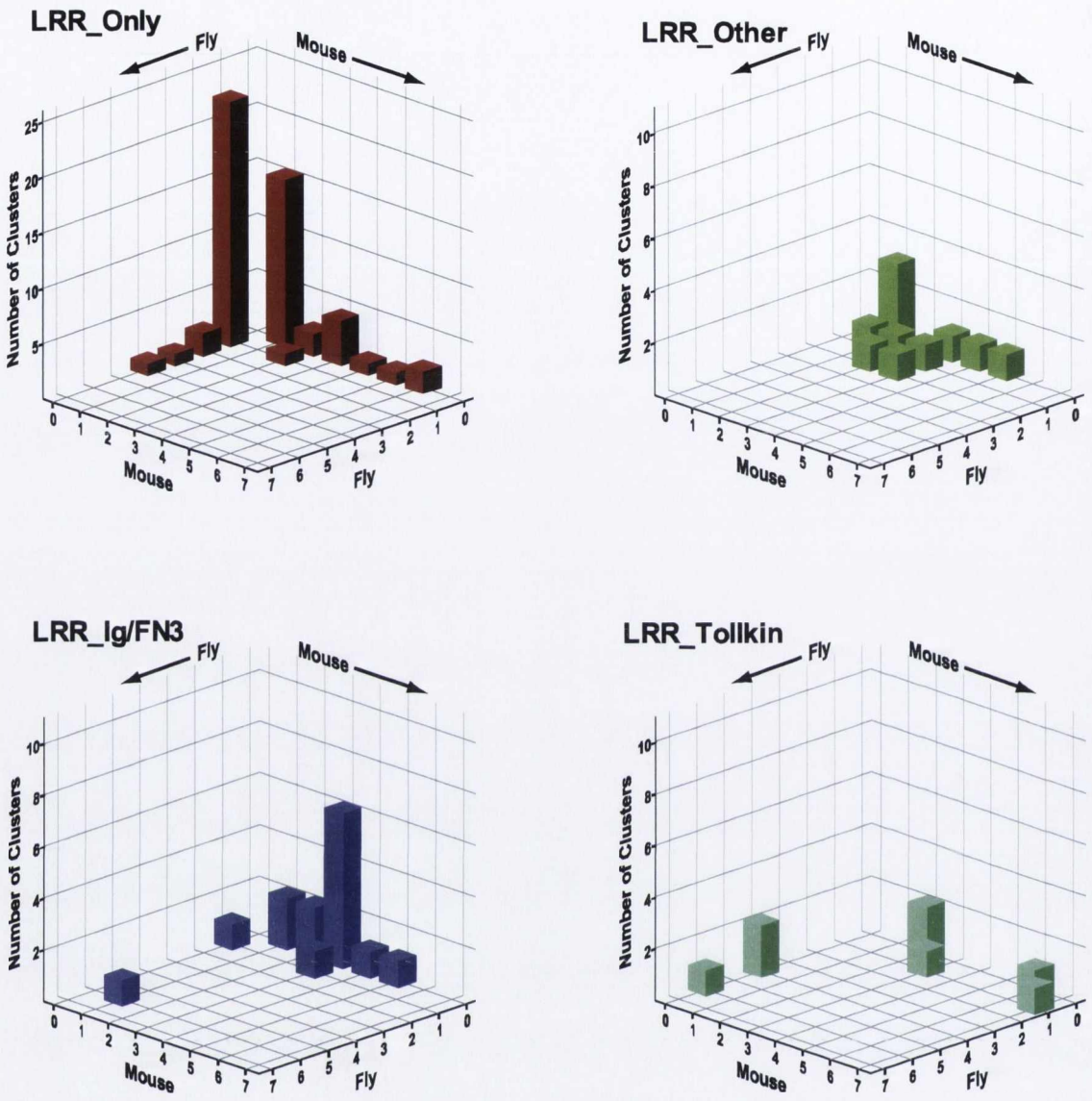

Figure 3.5 Group-specific patterns of expansion and diversification. The graphs depict three-dimensional histograms showing the number of clusters (on the *z* axis) having *x* members in the fly and *y* members in the mouse. The clusters used for this analysis are listed [see Additional File 6]. Different patterns of expansion (new members in one species of a conserved subfamily) and diversification (novel subfamilies in one species) are observed across the four major groups of eLRR proteins. Graphs were generated with the SPSS program.

3.2.9 Clustering of known proteins

These analyses provide an overview of relationships within the eLRR superfamily and highlight a number of previously unreported associations, allowing us to classify several novel proteins as paralogues of Lrrc21/Pal, Tpbg/5T4, Lrrc3 or Chad, for example. Conversely, it is clear that the recently named NLRR4 is not in fact a paralogue of the other NLRR proteins (-1, 2 and 3; also confusingly known as Lrrn1, 2 and 3). Also, the Lrig proteins in mammals are orthologous not to kekkon proteins in the fly, as has been suggested previously (Nilsson *et al.*, 2001), but to the lambik protein in flies (and T21D12.9 in worms). The mammalian protein Lrrc24 appears to be the closest orthologue of the kekkon proteins.

A particularly interesting finding is of a number of LRR proteins which cluster with the Toll-like receptors in both flies and mammals but which do not have a characteristic TIR domain. One of these: CD180, also known as RP105, clusters specifically with Tlr4. This protein lacks a TIR domain and has recently been found to act as a negative regulator of Tlr4 (Divanovic et al. 2005). Also in the LRR_Tollkin group in mammals is a subgroup of more distantly related proteins: carboxypeptidase N subunit 2 (Cpn2), glycoprotein V (Gp5) and leucine-rich repeat-containing protein 15 (Lrrc15, also known as Lib), (which form a sub-cluster), as well as insulin-growth factor acid labile subunit (Igfals) and KIAA0644 (which also has an FN3 domain). Lrrc32 (also known as GARP (Ollendorff et al. 1994)) and the related protein Lrrc33 also fall into this cluster, along with the novel fly protein CG7509. In the fly there is also another subcluster that clusters with the Tlrs. This subcluster includes chaoptin, which is known to function as an adhesion molecule in neural development (Van Vactor et al. 1988) and several other novel proteins, including one with an FN3 domain (CG40500-PD). The chaoptin cluster also contains the worm tol-1 protein and the novel worm protein C56E6.6. The large LRR_Tollkin group is one example where the expectation of hierarchical clustering does not hold; in many cases, individual proteins in this broad family cluster into different subfamilies at different e-values and inflation parameters [see Additional File 4 and discussion].

3.2.10 Novel protein families

These analyses have also catalogued a large number of novel proteins and subfamilies encoding eLRR proteins in worms, flies and mammals. Two novel clusters in mammals are of special interest due to their expression patterns in the nervous system (see below). One includes two closely related TM proteins currently identified as A930017N06Rik and Lrrc62 in the mouse. These proteins form a distinct subfamily at high stringency and are characterized by a signal peptide, 6 LRR repeats, an LRR-CT and an FN3 domain extracellularly, a TM domain and a long cytoplasmic tail (Figures 3.3, 3.6). The cytoplasmic tail contains a large number of tyrosines but no other detectable motifs. Both genes have two exons with the coding sequence entirely in the 3' exon. We propose to name these Elfn proteins, for extracellular-Leucine-rich repeat Fibronectin domain proteins. (A930017N06Rik is *Elfn1* and Lrrc62 is Elfn2).

Another cluster of related proteins comprises BC004853 (called LRRC26 in humans), Lrrc38, Lrrc52 and Lrrc55, Lrtm1 and Lrtm2 (names derived from sequencing projects (Okazaki et al. 2002). These are all LRR_Only proteins with a signal peptide, an LRR-NT, 6 LRR repeats, an LRR-CT, a TM domain and a short cytoplasmic tail containing a short stretch of acidic residues (Figures 3.3, 3.7). Lrtm1 and 2 also contain conserved predicted PDZ-binding sequences at their C-termini, suggestive of synaptic localisation. These proteins cluster in a group of six at low stringency (e^{-25}, level 1), but break into several subclusters at higher stringency (including Lrtm1 and 2 and Lrrc38 and 55). They are defined as paralogues in the Ensembl database but whether they represent a true "subfamily" is unclear. For convenience, we refer to this cluster as the "Elron" cluster, for extracellular-Leucine-Rich repeat-Only proteins, but have not renamed individual members.

In flies there are several subfamilies of novel proteins. These include CG7800 and CG18249, both LRR_Only TM proteins, CG32055 and CG6749, both secreted LRR_Only proteins and CG10824 and CG11910, which cluster as a pair at e^{-35}, level 2 and in a group of four with CG4950 and CG5810 at e^{-25}, level 1. CG4950 is a predicted TM protein while the others in this cluster are predicted secreted proteins.

In worms, a subfamily emerges comprising sym-1 (C44H4.3) and sym-5 (C44H4.2), both of which interact genetically with mec-8 (Davies et al. 1999), along with C44H4.1 and two other predicted proteins K07A12.2 and ZK682.5. There are also several cases of apparent one-to-one worm-fly orthology of novel proteins, including CG16974 and ZC262.3a, CG7509 and M88.6a, CG15151 and T01G9.3 and CG5819 and K07A12.2.

SS
LRR
LRR
LRR
LRR
LRR
LRR-CT
FN3
TM
Elfn1
Elfn2

Figure 3.6 Alignment of Elfn proteins. Predicted amino acid sequences from Elfn1 (A930017N06Rik) and Elfn2 (Lrrc62) from the mouse were aligned with CLUSTALW. Amino acids are colour-coded by chemical properties: blue: acidic; green: hydroxyl/amine/basic/Q; magenta: basic; red: small, hydrophobic (including aliphatic Y). Brackets indicate the extent of predicted motifs, including signal sequence (SS), six LRRs (the notch under the bracket indicates the end of the conserved N-terminal portion of each LRR), LRR-CT domain, fibronectin type-3 (FN3) domain and a transmembrane domain (TM). No recognizable LRR-NT domain was predicted. Note that the final LRR comprises the highly conserved N-terminal half-repeat only (consensus: LxxLxxLxLxxN). Identical residues are indicated by an asterisk, highly conservative substitutions by two dots and conservative substitutions by a single dot.

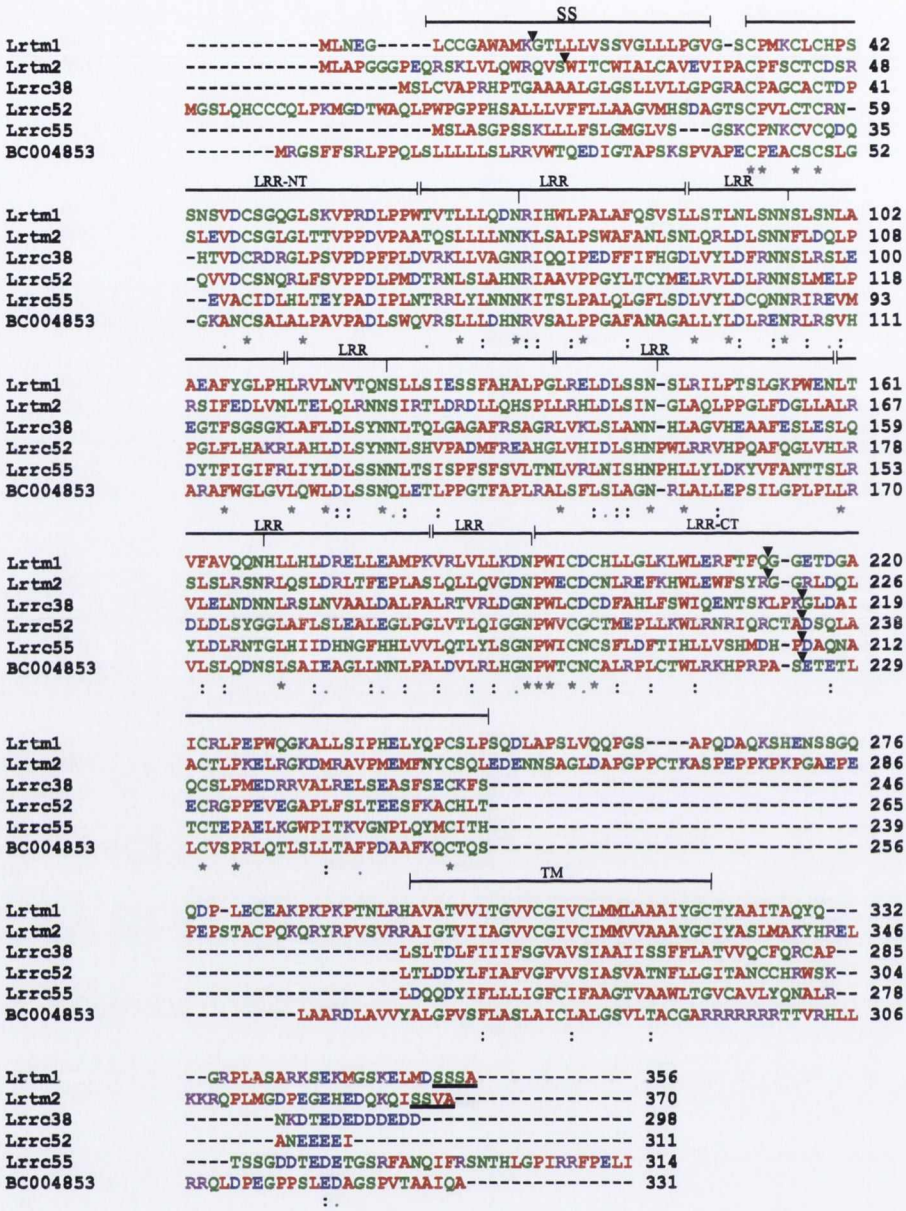

Figure 3.7 Alignment of proteins in Elron cluster. Predicted amino acid sequences from Lrtm1, Lrtm2, Lrrc38, Lrrc55, Lrrc52 and BC004853 from the mouse were aligned with CLUSTALW. Brackets indicate the extent of predicted motifs (consensus limits are shown); the notch under the bracket indicates the end of the conserved N-terminal portion of each LRR. Arrowheads denote exon-intron boundaries. The short cytoplasmic domain is poorly conserved, but does contain similarly positioned acidic residues (E/D) in all members. Lrtm1 and 2 end in consensus PDZ-binding domains (SSSA/SSVA), underlined. Abbreviations, amino acid colour-code and conservation symbols as in Figure 3.6.

3.2.11 Genomic clustering

To assess the possibility that some related genes might occur in clusters in the genome we examined genomic locations for all genes in our eLRR dataset [see Figure 3.2 and Additional File 3]. Not surprisingly, many closely related genes occur in tandem: five of the six *Slitrk* genes occur in two clusters in the mouse, one on the X chromosome and one on chromosome 14. Other genes occurring in tandem include *Tlr7* and *Tlr8*, *Islr1* and *Islr2*, *Lrrc21/Pal* and *Lrrc22*, *Lrrc8b*, *c* and *d* and *Fshr* and *Lhcgr*. We also found a number of examples where more distantly related genes occur in tandem in the genome, lending further support to the clustering results presented above, including *Cpn2*, *Gp5* and *Lrrc15/Lib*. In the fly, several Toll-related genes occur in adjacent pairs (*Tollo* with *Toll-6*, *Toll-7* with *18w* and *Toll-9* with *CG5195*, a novel non-TIR-containing member of the LRR_Tollkin group), as do *tartan* and *capricious*. Similarly, a number of the novel subfamilies identified above occur in tandem including *CG7800* with *CG18249*, *CG32055* with *CG6749* and *CG10824* with *CG5810*. In the worm genome, the C44H4 genes (.1, .2 (*sym-5*) and .3 (*sym-1*)) also occur in tandem.

We observed an interesting situation in the family of small secreted proteoglycans that includes decorin, biglycan, and related genes. Proteins in this family fall into several subclusters using TribeMCL, in agreement with previous analyses (Matsushima et al. 2000). Interestingly, many of them are also grouped in tandem in the genome in several different loci but each locus contains a representative of two or three subclusters. This suggests two early duplications in tandem and a subsequent triplication of the entire locus, with some additional gene losses and duplications (Tasheva et al. 2004). The *Ecm2* gene is also located in tandem in one of these loci (with *Aspn*, *Omd* and *Ogn*) but it is highly divergent from the other proteins and whether it should be considered a member of this family is debatable (McEwan et al. 2006).

3.2.12 Expression analyses

In order to begin to assess the possible involvement of these novel genes and families in neural development we analysed the expression of a subset of them by *in situ* hybridisation in the mouse or fly developing nervous system. *Elfn1* and *Elfn2* show rather complementary expression patterns in the embryonic and postnatal mouse brain (Figure 3.8). *Elfn1* is strongly expressed in interneurons in the hippocampus and cortex while *Elfn2* is expressed more broadly in the cortex in presumed glutamatergic neurons and in the hippocampus in pyramidal and granule cells. In the basal ganglia, *Elfn1* is expressed in the globus pallidus, while *Elfn2* is expressed more strongly in the other major division, the striatum. These patterns are maintained in adults, according to the Allen Brain Atlas (Lein et al. 2007). Based on abundance of cDNAs in the Unigene database, it appears that expression of *Elfn2* is quite restricted to the nervous system (Unigene reference: Mm.323188), while *Elfn1* is also expressed in endocrine and reproductive tissues (Unigene reference: Mm.237102).

Among the genes in the Elron cluster, three (*Lrtm1*, *Lrtm2* and *Lrrc55*) are expressed in discrete regions of the developing mouse brain, in particular marking different nuclei in the developing thalamus as well as a number of other areas (Figure 3.9). According to the Allen Brain Atlas, the expression of *Lrtm1* declines after development and is practically undetectable in adults. In contrast, *Lrtm2* is maintained at high levels in adults in a number of discrete regions including the granule cell layer in the olfactory bulb, the basal ganglia, dorsal thalamus, dentate gyrus, layers 2/3 and 5 in the cortex and Purkinje cells in the cerebellum. *Lrrc55* is also maintained at high levels in mitral cells in the olfactory bulb, in the habenula and in layers 4 and 6a in the cortex. *Lrrc38* is expressed at lower levels during development (data not shown) but is expressed in a specific pattern in the adult brain, including the CA3 region of the hippocampus and the zona incerta (Lein *et al.*, 2007). *BC004853* and *Lrrc52* do not appear to be expressed in the embryonic or postnatal brain. This result is confirmed by the absence of expression in the Allen Brain Atlas and by analysis of cDNA abundance in the Unigene database, which show that *Lrrc52* (Mm.159799) is specific to muscle and testis and that *BC004853* (Mm.275228) is almost exclusively expressed by the vesicular organ in

the male reproductive system. Similar cDNA abundance data for the other four genes show that *LRTM2* (in this case human, Hs.585579) is almost brain-specific, while *Lrtm1*(Mm.95780), *Lrrc38* (Mm.94020) and *Lrrc55* (Mm.291095) are also expressed in a small number of other tissues. The expression of the *Elfn* genes and of several genes in the Elron cluster is thus consistent with a possible role in specifying neuronal connectivity, especially thalamic and cortical connectivity.

The expression patterns of many of the *Drosophila* eLRR genes identified in the bioinformatic screen were also examined in the embryo by *in situ* hybridisation. A summary of the expression patterns we identified and those previously described is presented [see Additional File 7]. We describe here the expression patterns of those novel eLRR genes identified in our survey that include expression in the nervous system (Figure 3.10). *CG7702* is expressed dynamically in the peripheral nervous system (PNS), appearing at stage 11 and disappearing during stage 15. *CG40500* is exclusively expressed in the CNS and is restricted to a subset of cells at the ventral midline, beginning during stage 14 and remaining into stage 17. *CG11910* expression is restricted to the most dorsal layer of the CNS in a position consistent with the longitudinal glia. This expression begins at stage 12 and continues throughout embryonic development. *CG5888* is expressed from stage 5 throughout the embryo with exception of the anterior tip (data not shown). At stage 15 expression of *CG5888* is initiated in a subset of cells in the CNS. *CG11136* is expressed in an anteroposterior stripe within the neurogenic region and in the prospective brain lobes during stages 8-10 (data not shown) and in discrete cells at the midline of the CNS during stages 11 and 12. From stage 11 onwards *CG11136* expression is seen predominantly in the somatic musculature.

The additional files referred to in this chapter are located on the accompanying CD

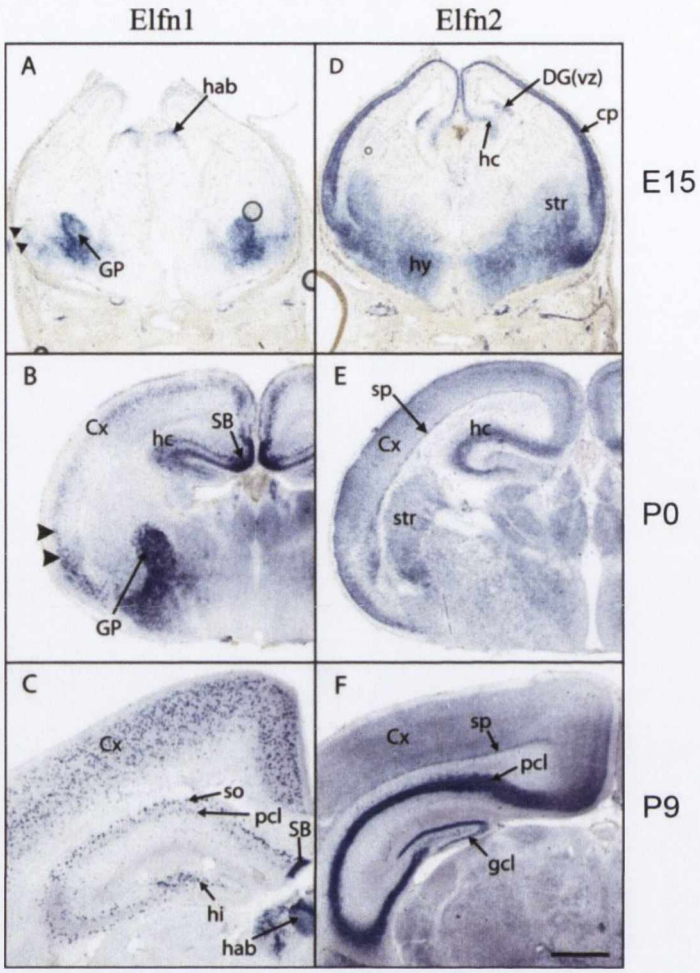

Figure 3.8 Expression of *Elfn* genes in developing mouse brain. Expression as defined by RNA *in situ* hybridisation is shown for *Elfn1* (A-C) and *Elfn2* (D-F) in coronal sections of mouse brain at three ages (embryonic day 15 (E15), A, D; postnatal day zero (P0), B, E; and postnatal day 9 (P9), C, F). *Elfn1* is strongly expressed in globus pallidus and interneurons in cortex and hippocampus, while *Elfn2* is expressed in striatum and in projection neurons in cortex and hippocampus. Arrowheads in A and B indicate presumed interneurons migrating towards cortex. Abbreviations: cp, cortical plate; Cx, cortex; DG(vz), ventricular zone of dentate gyrus; gcl, granule cell layer (of dentate gyrus); GP, globus pallidus; hab, habenula; hc, hippocampus; hi, hilus (of dentate gyrus); hy, hypothalamus; pcl; pyramidal cell layer (of hippocampus); SB, subiculum; sp, subplate; so, stratum oriens (of hippocampus), str, striatum. Scale bar: E15, 200 microns; P0 and P9, 500 microns.

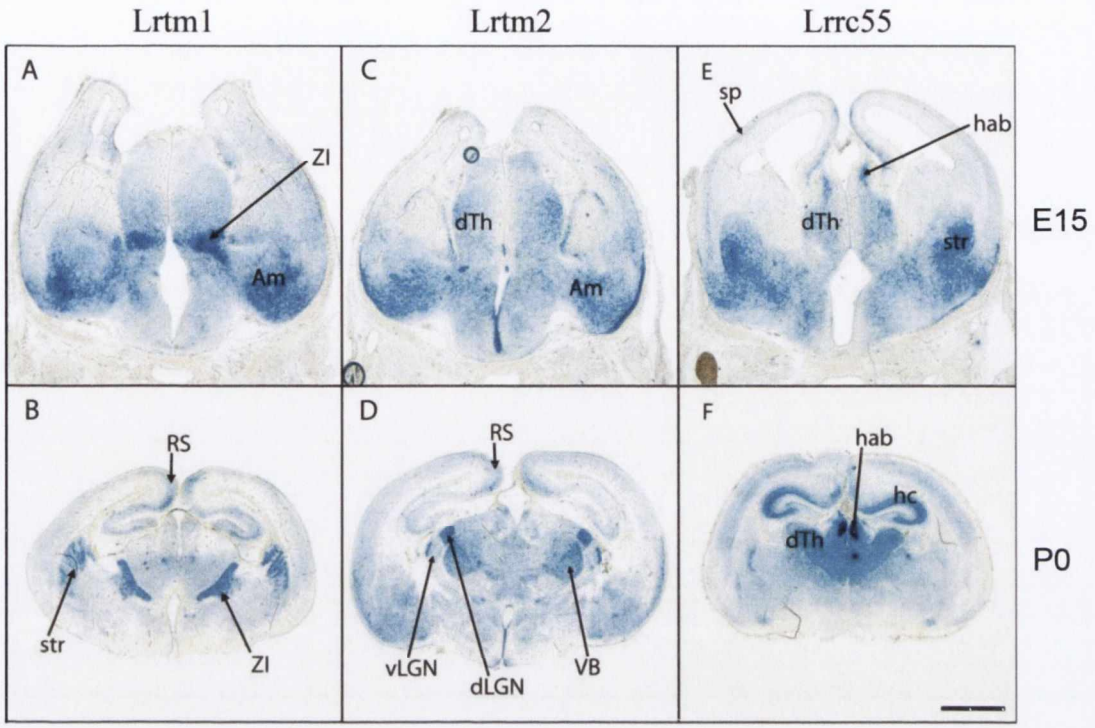

Figure 3.9 Expression of Elron cluster genes in developing mouse brain. Expression as defined by RNA *in situ* hybridisation is shown for *Lrtm1* (A, B), *Lrtm2* (C, D) and *Lrrc55* (E, F) in coronal sections of mouse brain at two ages (E15, A, C, E and P0, B, D, F). Differential staining in subsets of thalamic nuclei and across cortex is observed. Abbreviations: Am, amygdala; dLGN, dorsal lateral geniculate nucleus; dTh, dorsal thalamus; hab, habenula; hc, hippocampus; RS, retrosplenial cortex; sp, subplate; str, striatum; vLGN, ventral lateral geniculate nucleus; ZI, zona incerta. Scale bar: E15, 200 microns; P0, 500 microns.

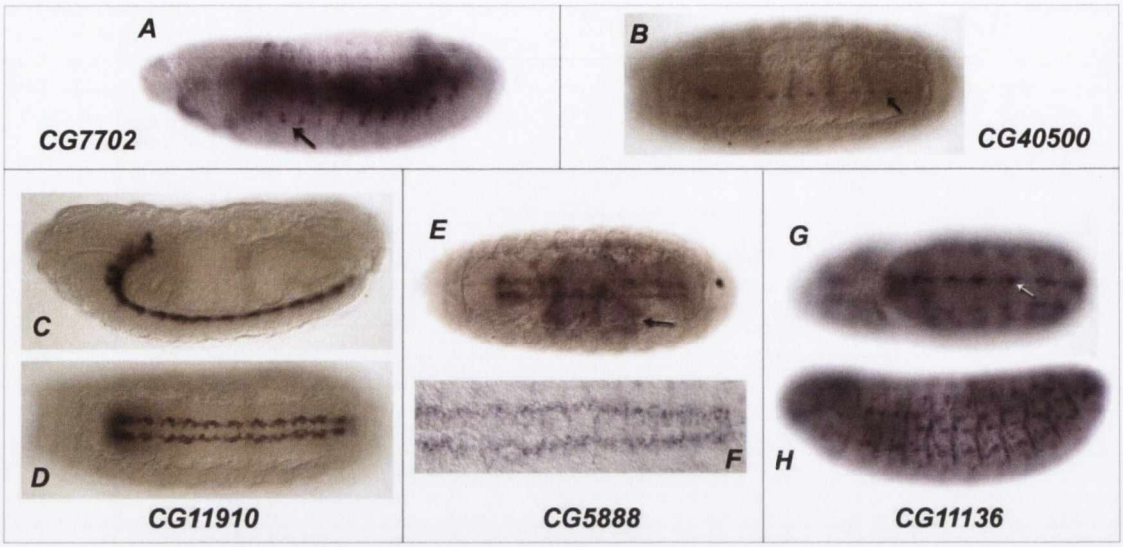

Figure 3.10 Expression of novel eLRR genes in the *Drosophila* embryo. (A) A lateral view of a stage 12 embryo showing expression of *CG7702* in the midgut and the peripheral nervous system, PNS expression is indicated by a black arrow. (B) *CG40500* expression in a stage 16 embryo, expression can be seen at the midline (indicated by a black arrow). (C and D) Lateral and ventral views, respectively, of a stage 15 embryo showing *CG11910* expression in the central nervous system. (E) A stage 16 embryo with *CG5888* expression in the CNS and midgut chamber, midgut chamber is indicated by a black arrow. (F) A dissected ventral nerve cord fillet with *CG5888* expression (shown at 400x magnification). (G) A stage 11 embryo showing *CG11136* expression at the midline, indicated by a white arrow and (H) a stage 15 embryo showing expression of *CG11136* in the somatic musculature. All whole embryos are shown at 200x magnification. In all views anterior is to the left, in all lateral views dorsal is at the top, B, D and E show ventral views and G shows a dorsal view (Work carried out in the lab of Guy Tear, King's College London.)

3.3 Discussion

This study aimed to catalogue the full repertoire of eLRR proteins in the proteomes of worms, flies, mice and humans, to examine their evolutionary

relationships and to identify novel proteins and subfamilies that may have important roles in nervous system development.

3.3.1 Methodological issues

Generating this dataset required identifying all LRR proteins, distinguishing eLRR proteins among this set (i.e., correctly predicting cellular localisation) and analyzing evolutionary relationships across a large set of highly divergent, multi-domain, repetitive proteins in four distantly related species. For all of these tasks we found the use of single programs only partly reliable. It was especially difficult to derive a single set of parameters for any program that would reliably predict the presence of a particular motif or correctly identify orthologues and paralogues for all proteins in the dataset. To overcome this problem we developed an approach of parallel annotation with many different programs, followed by manual curation to arrive at a consensus architecture for each gene, along with a hierarchical clustering method designed to reveal relationships at multiple levels. This is in contrast to the automated one-size-fits-all approaches currently used by some of the large genome databases.

3.3.2 A comprehensive, curated dataset

Our bioinformatics searches and exhaustive manual curation have yielded what we are confident should be an extremely comprehensive set of eLRR proteins across the four species examined. Rather than employing a series of strict filters we used the combined evidence from a variety of prediction programs and from clustering to distinguish eLRR proteins from intracellular LRR proteins. We think it is therefore unlikely that we have missed many true eLRR genes in any of the organisms. This obviously depends on the quality and comprehensiveness of the gene predictions in our starting datasets. There may in the first instance be cases of genes that have simply not been predicted at all yet. We also came across numerous cases of mispredicted genes where only a fragment was predicted or where a single ORF was split into two predicted genes, for example.

In most of these cases the fragments still clustered with other eLRR genes and a full-length sequence was often identifiable from one of the starting datasets. It is difficult to estimate how common such annotation errors are but it is reasonable to expect that they may have caused us to miss a small number of additional eLRR genes or to misclassify some as cytoplasmic.

The manual curation of these sequences has added substantially to the value of this dataset. An appreciable percentage of predicted protein sequences had to be amended in some way to yield what we consider to be the "correct" predicted full-length protein. These corrections were based on various factors including comparison of architectures across orthologues or paralogues, the absence of an expected signal peptide or the location of the predicted start codon with respect to the signal peptide.

Because degenerate or atypical LRRs have been described (Kajava 1998, Matsushima et al. 2005, Smits and Kajava 2004) that do not match the consensus motifs defined by SMART and Pfam we designed a customised program, LRRscan, to search for a minimal consensus that defines animal extracellular LRRs. We also searched for minimal consensus motifs that define LRR-NT and several varieties of LRR-CT domains found in different types of proteins, including small proteoglycans and G-protein-coupled receptors (Kajava 1998). These predictions were compared with the results of SMART and Pfam [see Additional File 2] and a consensus architecture was predicted by manual inspection, based on converging evidence. The results match those of proteins with known structures (Bell et al. 2005, Mosyak et al. 2006, He et al. 2003, Choe et al. 2005, Kim et al. 2005, Huizinga et al. 2002, Fan and Hendrickson 2005, Scott et al. 2004), significantly better than a combination of SMART and Pfam alone (allowing for semantic differences in whether the final half repeat is counted as one and whether putative LRRs overlapping with NT or CT domains are counted). The predicted transmembrane topologies are also based on converging evidence from multiple programs and have also been subject to expert evaluation. Nevertheless, the architectures presented should be viewed as predictions that will require experimental verification. In particular, the absence of a predicted LRR-NT or LRR-CT domain does not mean there is no domain present that is performing a capping function; there may be additional varieties of such domains that have not

yet been defined. In addition, we have chosen a representative isoform for each gene; the database thus contains no information on alternative splice forms or other isoforms that may have differing architectures.

3.3.3 Hierarchical clustering

The hierarchical clustering method we used gets around the problem of defining a unique set of parameters that is suitable to all proteins and levels of inter-relationship. In most cases, it generates a tree-like structure that reveals relationships across many different levels at once. This is a difficult problem for multiple alignment programs such as CLUSTALW or T-COFFEE, which work well for closely related proteins but which are not designed to compare highly divergent proteins with differing architectures. Previous attempts using multiple alignment programs to derive a phylogenetic tree across many eLRR subfamilies at once contain numerous differences from our results and from known relationships (Chen et al. 2006, Wang et al. 2003).

In some cases, the results of TribeMCL depart from the expected hierarchical relationship. This is the case for the extended LRR_Tollkin group of proteins, including many proteins characterized by an eLRR domain but lacking an obvious TIR domain. While the clustering of these proteins with the TLR group is quite convincing, based on direct inspection of the BLAST results, it is extremely difficult, indeed impossible with these data, to discern more discrete relationships within this large family. The reasons for the anomalous hierarchical clustering results with these genes may relate to the large number of LRRs present in these proteins and the very slight differences in pairwise similarities across the group. At different levels of stringency small differences in BLAST scores may be amplified by the TribeMCL algorithm to result in membership of different clusters that do not share the expected hierarchical relationship. Attempts to resolve the phylogeny of all the genes in this group using the T-COFFEE multiple alignment program were no more enlightening, resulting in a starburst pattern where the roots of each subfamily are too close to each other to resolve (data not shown). Despite these

limitations, the TribeMCL analysis has revealed a group of eLRR proteins that are clearly more related to the TLR proteins than to other LRR_Only proteins.

3.3.4 Nomenclature

The current nomenclature of eLRR proteins is very confusing, with multiple synonyms for many genes [see Additional File 3], many of which do not give accurate information on relationships. For example, there is a large number of proteins designated LrrcX, where X is a number. These names were apparently derived from large-scale genome projects and do not represent a specific subfamily of related proteins. For that reason we have proposed the names *Elfn1* and 2 for one novel subfamily. We also identify another discrete cluster of six "novel" proteins (which we refer to as the Elron cluster), although whether they represent a true subfamily is open to debate. In addition, some novel proteins that group into small subfamilies with Lrrc21/Pal, Chad, Lrrc3 and Tpbg/5T4 [see Additional File 3, Figures 3.3 and 3.4] could be given names to reflect that fact. Finally, while Lrrn1, 2 and 3 (also known as NLRR1, 5 and 3) form a subfamily, the recently named NLRR4 (Bando et al. 2005) is not in fact a member of this subfamily. It does not have the Ig domain present in these genes and does not cluster with those genes at any parameters.

3.3.5 Comparative analyses of major groups

For the purposes of some of the analyses we split the eLRR proteins into four groups, based on architecture and clustering results. The LRR_Ig/FN3 group includes the largest percentage of mammal-specific subfamilies, many with multiple members. Almost all of the proteins in this group are associated with the membrane, either type I TM or GPI-linked. The majority of these subfamilies (including Ntrks, Lrfns/Salms, Flrts, Lrigs, Netrin-G ligands, and Lingo proteins) show discrete expression in the nervous system and many of them have been shown to have functions in neural development (Chen et al. 2006) and/or have been implicated in neurological or psychiatric disease (Matsushima et al. 2005).

Expansion of this class of proteins is thus correlated with the evolution of the complex mammalian brain and plausibly contributed to it by providing the requisite specificity of cellular interactions to mediate a large number of selective connectivity decisions. We have identified a novel mammal-specific LRR_FN3 subfamily, the Elfn proteins, with discrete nervous system expression.

The LRR_Only group shows independent diversification in flies and mammals, with a large number of singletons (unclustered proteins), suggesting rapid sequence divergence. This group also contains a number of proteins implicated in nervous system development or function including the Nogo-receptor, Lrrtm and Slitrk families, and connectin, Gp150, Tpbg/5T4 and Nyx for example. We have identified six proteins in another novel mammal-specific cluster, the Elron cluster, several of which show highly suggestive expression patterns in the developing nervous system. We have also discovered a number of novel fly proteins in this class that are similarly discretely expressed in the embryonic nervous system.

The LRR_Tollkin group shows a different pattern of evolution, with parallel expansions in flies and mammals, of both the Toll-like receptor genes and of the genes that cluster with them. In mammals, the latter include Cpn2, Gp5 and Lrrc15 (Lib), which form a subcluster and which are also arrayed in tandem on chromosome 3 in humans (16 in mouse). These proteins have diverse binding partners and biochemical functions but are all involved in inflammation in some way: as a regulatory subunit of carboxypeptidase (Matthews et al. 2004), as a component of the platelet glycoprotein complex (which also contains the eLRR proteins GP1bα and GP1bβ (Li et al. 1995), and as a mediator of the glial response to β-amyloid (Satoh et al. 2005), respectively. They form a slightly larger cluster with Igfals, the acid-labile subunit of insulin growth factor, which regulates IGF signaling (Baxter 1994) and with the novel gene KIAA0644, which has an FN3 domain in addition to the LRR domain. Lrrc32/GARP (Roubin et al. 1996) and its paralogue Lrrc33 also cluster with this group at e^{-40}, level 1, but not at some lower levels. The novel fly gene CG7509 also clusters with this group at e^{-40}, level 1 and with other fly genes including chaoptin at some other levels. Whether it can be said to be directly orthologous to any (or all) of these mammalian proteins is hard to determine. The other fly genes in this group are mostly novel and include

CG40500-PD, which has an FN3 domain and which shows very discrete expression in the midline of the embryonic nervous system.

The LRR_Other group is an arbitrary default group as it contains many unrelated genes or subfamilies. Nevertheless, it is interesting to note that this group contains the highest percentage of genes with orthologues across all species, including worms (e.g., the slits and peroxidasins and some of the seven-transmembrane hormone receptors). This group also includes the mammalian Lgi subfamily, recently implicated in epilepsy and myelination.

3.3.6 Human-mouse differences

Only a small number of proteins are specific to either human or mouse. There are two cases where there are genes in humans that are not represented in mouse that both seem to be caused by specific loss in mice, rather than representing human-specific genes. The human gene synleurin appears to have been pseudogenised in rodents, although it is present in many other species besides humans (including dog, cow and chick, for example). Also, MXRA5 (or adlican), a paralogue of the large secreted protein Igsf10, is not detectable in the mouse genome (but is present in cow, dog and opossum, for example).

There is also a small number of examples where there has been independent expansion of subfamilies in either humans or mice. These include the Toll-like receptors TLR10 in humans and TLR11, 12 and 13 in the mouse. They also include the unusual subfamily of LRRC37 genes, which is represented by a single gene in the mouse (called Lrrc37a) but multiple, highly related genes in humans (LRRC37A, A2 and A3 and LRRC37B, as well as a number of other partial duplicates lacking LRRs). These are located in tandem on chromosome 17 and have arisen from multiple duplications of the BRCA1 region in primates (Jin et al. 2004). The extracellular domains of these TM proteins are characterised by six predicted LRRs but these make up only a small fraction of the overall protein, which is highly variable in length. The functions and expression patterns of these unusual proteins are unknown.

3.4 Conclusions

This survey presents a comprehensive overview of the repertoire of eLRR proteins in various species and their inter-relationships. As such, it provides the necessary foundation for a systematic analysis of the functions of this class of genes, which are likely to include prominently neural development, innate immunity and inflammation. In particular, expansion of the eLRR proteome is correlated with increasing complexity of the nervous system. Given the functions and discrete expression patterns of many known members, it seems likely that this superfamily, including the novel proteins identified here, could provide the requisite specificity of cellular interactions to mediate a large number of selective connectivity decisions.

4 Chapter 4 *Elfn1* expression in the mouse brain

4.1 Introduction

The analyses detailed in Chapter 3 resulted in a large number of novel proteins containing extracellular leucine-rich repeats (eLRRs). Accumulating evidence suggests that many members of the eLRR superfamily play vital roles in the developing nervous system with functions in axon guidance, regeneration, target selection and synaptogenesis (reviewed in Chapter 1). Due to this, it seems likely that the novel LRR superfamily proteins that were identified in the analyses have the potential to function in similar roles, specifying neuronal connectivity.

To identify a novel gene for further study, an *in situ* hybridisation screen was carried out to establish the temporal and spatial expression patterns of each gene. Interesting candidates for this study should display discrete patterns of expression necessary for a role in specifying cellular connectivity. From the screen, the *Elfn* genes (see Chapter 3; Figure 3.8) were chosen for further study based on their novelty and a specific pattern of expression that was restricted to a number of functionally interesting regions of the brain, for *Elfn1* in particular.

4.1.1 Elfn genes

The Elfn genes are characterised by a signal peptide, 6 LRR repeats, an LRR-CT and an FN3 domain extracellularly, a TM domain and a long cytoplasmic tail (Figure 4.1a). Both Elfn genes are very closely related, vertebrate-specific and do not cluster with any other members of the eLRR superfamily (Chapter 3, Figure 3.3). Their expression is not restricted to the nervous system, and Expressed Sequence Tagged (EST) data from mouse shows *Elfn1* is expressed most strongly in the thyroid followed by testis, eye and brain, whereas Elfn2 transcripts were more abundant in the brain but also found in the testis, lung and eye (http://www.ncbi.nlm.nih.gov/UniGene).

The long cytoplasmic tail (388aa's and 404aa's) of the Elfn proteins suggests a function in intracellular signalling and within this portion are three

highly conserved cytoplasmic regions (CCR1, CCR2 and CCR3, Figure 4.1b). There is only one identifiable sequence motif in the intracellular domain. It is located within the CCR3, and is a primary Protein Phosphatase 1 (PP1)-docking motif referred to as the RVxF, which constitutes a consensus sequence of K/R K/R V/I x F/W, where x is any residue other than Phe, Ile, Met, Tyr, Asp, or Pro (Hendrickx et al. 2009). An amino acid sequence alignment of *Elfn1* and Elfn2 across human, mouse and Zebrafish species within this region illustrates that it is highly conserved between the two genes and across these species (Figure 4.1c). Furthermore, the Elfn genes were confirmed biochemically to bind to PP1 with pull-down assays, and this binding was shown to inhibit the phosphatase activity (Hendrickx et al. 2009). PP1 is involved in dephosphorylation events that regulate cell-cycle progression, protein synthesis, muscle contraction, carbohydrate metabolism, transcription and, interestingly for this work, neuronal signalling (Cohen 2002). More specifically, PP1 has been implicated in synaptic function and plasticity (Blitzer et al. 1998) and is highly concentrated in post-synaptic density fractions (Strack et al. 1997).

a

Figure 4.1 Protein architecture and intracellular sequence alignment for Elfn1 and Elfn2.

(a) Consensus architecture for the Elfn proteins consists of a signal peptide (black), 6 LRR repeats (orange), an LRR-CT (red), FN3 domain (purple), a TM domain (black) and a long cytoplasmic tail with three conserved regions (blue). (b) Amino acid sequence alignment of the cytoplasmic region of the Elfn1 and Elfn2. Brackets indicate the extent of the transmembrane domain (TM) and three conserved cytoplasmic regions (CCR1, CCR2 and CCR3). (c) Amino acid sequence alignment of the Protein Phosphatase 1 (PP1)-docking motif (*) in Elfn1 and Elfn2 in mouse (Mm), human (Hs) and Zebrafish (Danio rerio (Dr)). This motif is located within the CCR3 of the Elfn proteins' cytoplasmic domain.

b
TM
Elfn1 QPQEEIRLTNLYTLTNYTYCVVSTSSGTHHNHTCLTICLPKPPSPPGPVPSPSTATHYIM
Elfn2 NKKEIVTLDKLRAHTEYTFCVTSLRNSRRFNHTCLTFTT-RDLVPGDLAPSTSTTTHYIM
Elfn1 TILGCLFGMVLVLGAVYYCLRKRRRQEEKHKKAVAAAAGSLKKTIIELKYGPEIEAPGLA
Elfn2 TILGCLFGMVIVLGAVYYCLRKRRMQEEKQK------SVNVKKTILEMRYGADVDAGSIV
CCR1
Elfn1 PLTQG----PLLGPEAVTRIPYLPAATSDVEQYKLVESSETPKATKGNYIEVRTGEPQE-
Elfn2 HAAQKLGEPPVLPVARMSSIPSMVGEKLPASKGLEAGLDTPKVATKGNYIEVRTGAAGDS
CCR2
Elfn1 --RRGCELSRPGEPQSSVAEISTIAKEVDRVNQIINNCIDALKSESTSFQGAKSGAVSAA
Elfn2 LARPEEELPEIENGQGSAAEISTIAKEVDKVNQIINNCIDALKLDSASFLGGGGGGGGGG
Elfn1 EPQLVLLSEPLAS----------KHSFLSPVYKDAFGHGGLQRHHSVEAAPGPPRA
Elfn2 DSDLAFECQSLPAAPAASSAATPGALERPSFLSPPYKESS-HHPLQRQLSADAAVSRKTC
Elfn1 STSSSGSARSPRTFRAEATGTHKAP---ATETKYIEKSSPVPETILTVTPAATVLRAEAD
Elfn2 SVSSSGSIKSAKVFSLDVPDHPTPTGLAKSDSKYIEKGSPL-NSPLDRLPLVPTGSSGSS
Elfn1 KSRQYGEHRHSYPGSHPAEPPAPPPPPPTHEGLG--GRKASILEPLTRPRPRDLVYSQLS
Elfn2 GGGGGIHHLEVKPAYHCSEHRHSFPALYYEEGADSLSQRVSFLKPLTRSK-RDSTYSQLS
CCR3
Elfn1 PQYHNLSYSSSPEYTCRASPSIWERLRLSRRRHKDDAEFMAAGHALRKKVQFAKDEDLHD
Elfn2 PRHYYSGYSSSPEYSSESTHKIWERFRPYKKHHR-EEVYMAAGHALRKKVQFAKDEDLHD
Elfn1 ILDYWKGVSAQHKS
Elfn2 ILDYWKGVSAQQKL
C
*
MmElfn2 SPEYSSESTHKIWERFRPYKKHHR-EEVYMAAGHALRKKVQFAKDEDLHDILDYWKGVSA
HsELFN2 SPEYSSESTHKIWERFRPYKKHHR-EEVYMAAGHALRKKVQFAKDEDLHDILDYWKGVSA
DrElfn2 SPEYSTESTLRIWERFRPHRKGPREESCYVTAGNALRKKVQFAKGEDLHDILDYWKGVSA
MmElfn1 -PEYTCRASPSIWERLRLSRRRHKDDAEFMAAGHALRKKVQFAKDEDLHDILDYWKGVSA
HsELFN1 -PEYTCRASQSIWERFRLSRRRHKEEEEFMAAGHALRKKVQFAKDEDLHDILDYWKGVSA
DrElfn1 -PEYSCRPSLSLWERFKLHRKRHRDEEEYIAAGHALRRKVQFAKDEDLHDILDYWKGVSA

4.1.2 *Elfn1*

The expression analyses of the Elfn genes identified *Elfn1*, in particular, as the best candidiate for this study. Unlike the widespread expression of *Elfn2*, *Elfn1* displayed highly localised expression in particular subregions of the brain, a prerequisite for a function in specifying connectivity. There were no commercial Elfn antibodies available for further study, however, a knockout mouse for *Elfn1* became available and was obtained from the KnockOut Mouse Project (KOMP) (Figure 4.2a). A null allele for *Elfn1* is created while the endogenous promotor drives a beta-galactosidase reporter. It is important to note that with this mouse line the reporter localises to cell bodies and reflects where gene expression is occuring but not necessarily protein localisation. However, one of the benefits of the knockout mouse line lay in the ability to perform double immunohistochemistry which provided a platform for simultaneous analysis of *Elfn1* expression with that of known genes. This can give vital clues for function, highlighting cell type, possible functional pathways and potential interacting molecules.

While carrying out this research, the first functional result for *Elfn1* was published (Sylwestrak and Ghosh 2012). They revealed that *Elfn1* is selectively expressed by somatostatin-containing oriens lacunosum-moleculare (OL-M) interneurons in the hippocampus and is involved in modulating synaptic transmission. Excitingly, they identified that *Elfn1* in the postsynaptic interneuron transsynaptically directs the specific synapse type from the innervating pyramidal cells, providing the first evidence of target-driven modulation of transmission. They established that the presence of *Elfn1* directed the formation of highly facilitating synapses, whereas, the absence of *Elfn1* with knockdown experiments, dramatically reduced short term facilitation.

The study carried out by Sylwestrak and Ghosh (2012) focused on a postsynaptic function of *Elfn1* in hippocampal interneurons, and knockdown and ectopic expression experiments were implemented postnatally. In this project, a knockout mouse model provides the opportunity to further investigate the function of *Elfn1* throughout the brain, and the effect that the absence of the gene has on development.

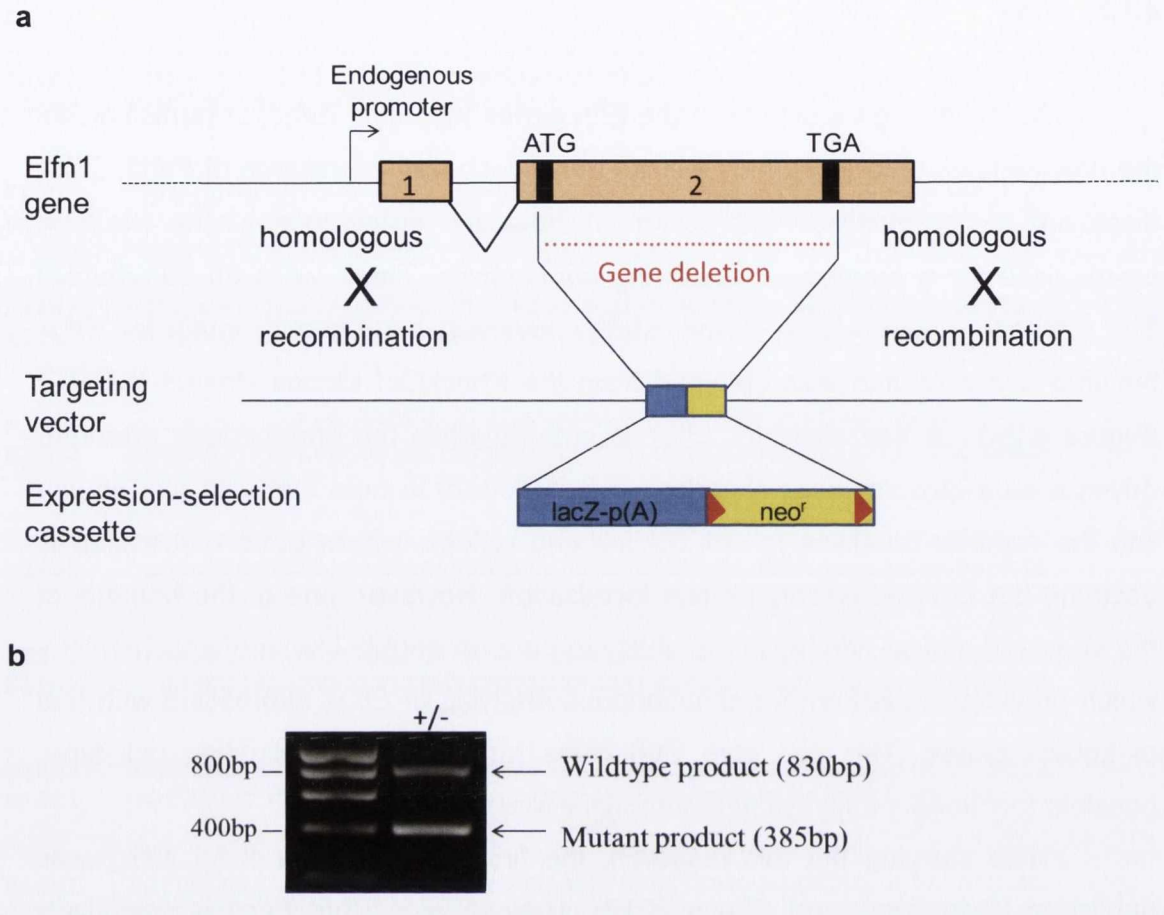

Figure 4.2 Targeted allele of Elfn1. (a) Schematic of the targeting vector and the Elfn1 locus (adapted from the Knockout Mouse Project (KOMP); null allele targeting strategy (www.velocigene.com/komp/detail/10112). The full coding sequence is contained in exon 2, and this region is replaced by the expression-selection cassette. LacZ, β-galactosidase coding sequence; Neo^r, neomycin phophotransferase; red triangles represent *loxP* sites. (b) PCR genotyping of genomic DNA from an $Elfn1^{+/-}$ mouse. A wildtype product of 830bp and 385bp Elfn1-targeting vector fragment.

4.1.3 Habenula Circuitry

The *in-situ* hybridisation results for *Elfn1* identified gene expression in many regions of the brain including the interneuron-free medial habenula (Dolan et al. 2007). Consequently, the investigation of *Elfn1* in the habenula and connected neural networks provides the opportunity to identify additional *Elfn1* functions.

The habenula is a relatively small brain structure located above the thalamus, bordering the third ventricle and is divided into two paired nuclei termed the medial and lateral habenula. The importance of this structure is emphasised by the fact that it is highly conserved in all vertebrates, including the lamprey, and therefore dating over 560 million years (Stephenson-Jones et al. 2012). Two of the main axon bundles of the brain, the stria medullaris (SM) and the fasciculus retroflexus (FR) are the input and output pathways of the habenula respectively and these three components have been named the dorsal diencephalic conduction (DDC) system. The function of the DDC is in the connection of the limbic forebrain and basal ganglia to monaminergic sites in the mid- and hindbrain. There are two major pathways in the brain with this role, the other more ventral pathway is the medial forebrain bundle (MFB) which interconnects the anterior olfactory regions, with the lateral preoptic, lateral hypothalamic, and ventral tegmental areas (Sutherland 1982). These two pathways most likely act in tandem with shared input and target regions (Bianco and Wilson 2009, Gallistel et al. 1985).

The DDC system is identifiable in all vertebrates with the distinction that in fish and amphibians, the habenular nuclei and the FR display substantial bilateral asymmetries. Left-right differences in size, chemoarchitecture and connectivity are displayed. Studies in zebrafish have uncovered differences in the time-course of neurogenesis between the two sides of the habenula (Bianco and Wilson 2009). Moreover, a major determinant of this laterality includes the nodal-signalling control of the migration of parapineal cells from the pineal organ to the vicinity of one side of the habenula (Beretta et al. 2012). Habenula asymmetries are very subtle in birds and mammals with only a 5% volume difference identified in the albino rat (Wree et al. 1981) which may in part be attributed to the loss of pineal eyes during evolution and therefore the lack of parapineal cells (Bianco and Wilson 2009).

4.1.3.1 Subcellular organisation of the habenula

The separation of the habenula into medial and lateral divisions was first established based on Nissl-stained sections that identified a cell-dense medial region and a lateral region containing cells more loosely dispersed. Subsequently, Andres and colleagues proposed additional subdivisions consisting of fifteen subnuclei within the habenula, five in the medial habenula (MHb) and ten in the lateral habenula (LHb) (Andres et al. 1999). This was based on regional morphological differences using light and electron microscopy. These seperate subdivisions in the LHb, were strengthened with immunohistochemical (Geisler et al. 2003, Aizawa et al. 2012) and electrophysiological studies (Kim and Chang 2005). The MHb can be seperated into two regions neurochemically with cells in the dorsal MHb expressing Substance P and the ventral cells express choline acetyltransferase (Lecourtier and Kelly 2007). Another interesting aspect of this structure is that there are no GABAergic cells in the MHb (Qin and Luo 2009).

The further elucidation of the cellular organisation of the habenula and their involvement in distinct neuronal circuits is essential to provide explanations for the large number of diverse biological functions and behaviours atributed to this system. Such behaviours include motor activity, sleep, stress, pain, anxiety, spatial learning, attention, reward-seeking (Klemm 2004, Lecourtier and Kelly 2007) and impulsivity (Lecourtier and Kelly 2005) while its dysfunction has been linked to psychological conditions such as depression, schizophrenia, anxiety, ADHD-like behaviour and drug addiction (Li et al. 2011, Shepard et al. 2006, Baldwin et al. 2011, Murphy et al. 1996, Lee and Goto 2011), reviewed in (Bianco and Wilson 2009).

4.1.3.2 DDC connectivity

The connectivity of the DDC was first established in 1977 with a horseradish peroxidase (HRP) tracing study by Herkenham and Nauta. They found that both the medial and lateral habenula have largely separate sub-circuits despite a small overlap in sources of afferent inputs and efferent targets (Herkenham and Nauta 1979) (Figure 4.3).

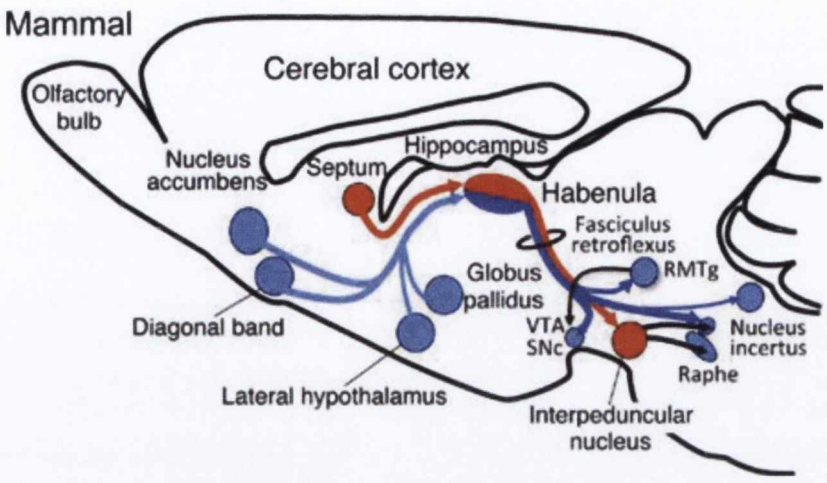

Figure 4.3 Schematic diagram of the dorsal diencephalic conduction (DDC) system. Sagittal section from a rat showing the medial (red) and lateral (blue) habenula circuitries. RMTg, rostromedial tegmental nucleus; SNc, substantia nigra pars compacta; VTA, ventral tegmental area. (Figure adapted from Aizawa et al. (2011).

The majority of input to the MHb arrives via the stria medullaris and originates in the septal nuclei, particularly the septofimbrial nucleus (Wang and Aghajanian 1977) and the triangular septal (TS) nucleus. Both have been shown to innervate in a target-specific manner with axons from the SFi projecting to the rostral MHb, while the TS axons project to the caudal MHb. Ascending monoaminergic inputs have also been shown to arise from the ventral tegmental area (VTA) (Phillipson and Pycock 1982) and locus coeruleus and the superior cervical ganglion (Gottesfeld 1983). Minor inputs to the MHb are also received from the nucleus of the diagonal band of Broca (DBB), the medial septum and the bed nucleus of the stria terminalis (Swanson and Cowan 1979). Output axons from MHb course through the core of fasciculus retroflexus to innervate their main target, the interpeduncular nucleus (IPN), in a topographical manner. The dorsal MHb cells innervate the lateral IPN, cells of the medial MHb innervate the ventral IPN and the lateral MHb target the dorsal IPN (Herkenham and Nauta 1979). The IPN in turn projects to the monoaminergic cell-containing median raphe, ventral tegmental area and dorsal tegmental area (Shibata and Suzuki 1984). Therefore, it has been proposed that the MHb functions to modulate midbrain monoaminergic

neurons indirectly through the IPN (Gioia et al. 1994). Furthermore, the majority of cells in the IPN have been identified as GABAergic (Kawaja et al. 1989) and the habenulointerpeduncular pathway has been shown to exhibit an inhibitory influence on the midbrain dopaminergic (Nishikawa et al. 1986) and serotonergic nuclei (Park 1987)

The Lateral habenula (LHb) is the site of convergence for inputs from the basal ganglia and the limbic forebrain, which travel along the stria medullaris to their point of innervation. The majority of inputs originate in the entopeduncular (EP) nucleus (also called internal globus pallidus (GPi)), with additional inputs from the lateral preoptic area, and lateral hypothalamus (Herkenham and Nauta 1979). A small number of inputs have been identified from septal areas, the DBB, nucleus accumbens and medial frontal cortex (Greatrex and Phillipson 1982). Ascending fibres most likely travel through the fasciculus retroflexus from median raphe and locus coeruleus which provide serotonergic and noradrenergic inputs (Gottesfeld 1983) and from the VTA which provides dopaminergic input (Phillipson and Pycock 1982). The LHb establishes connections with a wide range of targets including the substantia nigra pars compacta (SNc), the ventral tegmental area (VTA) and the median (MRN) and dorsal raphe nuclei (DRN) (reviewed in (Sutherland 1982);(Bianco and Wilson 2009). A recent study has shown that LHb also projects strongly to a cell group in the ventromedial mesopontine tegmentum (RMTg) situated behind the VTA and dorsolateral to the interpeduncular nucleus this small nucleus has been identified as GABAergic and projects to the midbrain dopaminergic system (Geisler and Trimble 2008, Jhou et al. 2009). The efferent fibres from the LHb travel along the mantle portion of the FR, but before reaching the IPN they split off to directly innervate the above-mentioned midbrain nuclei (Kim and Chang 2005). The lateral habenula exerts an inhibitory influence on midbrain dopaminergic cells in the VTA and substantia nigra. Specifically, glutamatergic neurons of the lateral habenula innervate GABAergic cells of the VTA, SNc and RMTg which in turn innervate the dopaminergic neurons (Balcita-Pedicino et al. 2011). Likewise, stimulation of the LHb invoked an inhibitory response in dorsal raphe serotonergic neurons indirectly through GABAergic neurons (Park 1987).

Connectivity within the habenula has received little investigation thus far. A tracing and electrophysiology study carried out in live rat brain slices found evidence of two populations of medial habenula cells based on their intrinsic connectivity. Tracings of 35 medial habenula cells showed that approximately a third of these cells projected to the LHb, and the other two-thirds project towards the FR. MHb axons also exhibited en passant boutons within the medial habenula, indicating intrinsic connectivity within the cells of the MHb. Cells of the LHb that were traced did not project to the MHb, therefore there is medial to lateral connectivity but not vice versa (Kim and Chang 2005).

4.1.4 Aims of this chapter

The main aim of this chapter was to establish a comprehensive description of *Elfn1* expression in the newborn mouse brain. This was achieved using the KOMP *Elfn1* knockout line and the β-Galactosidase (βgal) reporter. The identification of specific regions, circuits and cell types containing *Elfn1* helps to elucidate its possible roles in the development of the mouse brain. Particular focus was placed on the expression of Elfn1 in the habenula and its extended circuitry due to the accumulation of evidence identifying the importance of this structure in the brain, and the enrichment of *Elfn1* in this region.

4.2 Results

4.2.1 Investigation of the *Elfn1* knockout model

The successful deletion of *Elfn1* and replacement with the reporter was examined in the mouse line with the genotyping protocol outlined in section 2.2.5 using primers provided by the the Knockout Mouse Project (KOMP, appendix 9.1). Polymerase chain reaction (PCR) of genomc DNA from a heterozygous animal resulted in the amplification of the wildtype band of 830 basepairs (bp), and the mutant band of 385bp as expected (Figure 4.2b). The reliability of the *Elfn1*

knockout mouse was further investigated by comparing the expression of the LacZ gene in *Elfn1* heterozygous mice with *in situ* hybridisation results obtained from wildtype mice, both at P0. The results demonstrated that the LacZ expression showed the same overall patterns as those obtained by *in situ* hybridisation with strong expression observed in the globus pallidus, ventral pallidus, septal nuclei and in discrete nuclei within the habenula. Immunoreactivity was also evident in a subset of cells in the hippocampus and the cortex, as well as the Diagonal band of Broca, Islands of Calleja and amygdala (Figure 4.4 and 4.5). The ISH results did not indicate expression in the lateral hypothalamus as was identified by immunohistochemistry, but this may be due to the difference in sensitivity of these two methods and the low number of cells which appear to be positive for *Elfn1*.

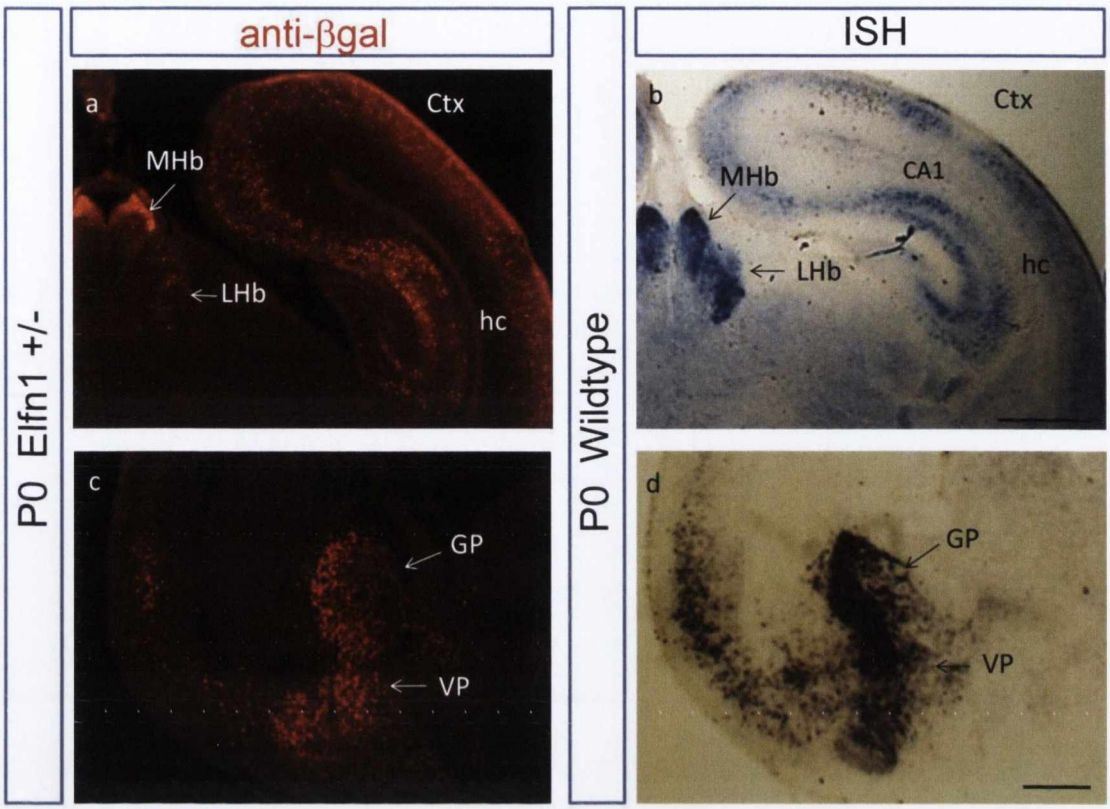

Figure 4.4 βgal immunohistochemistry replicates *Elfn1 in-situ* hybridisation staining patterns (part 1). Comparative coronal sections of βgal immunoreactivity in an Elfn1$^{+/-}$ mouse brain and *in situ* hybridisation staining using an *Elfn1* probe in a wildtype brain, both at P0. (a,b) Strong staining is evident in the dorsal MHb and the central region of the LHb. Scattered cells in the cortex, and layer specific expression the hippocampus is displayed, with particularly strong staining in the CA1 region of the hc. (c,d) Strong staining of Elfn1 positive cells are identified with both methods in the globus pallidus and ventral pallidum, with intense staining specifically in the lateral cells of the GP. MHb, medial habenula; LHb, lateral habenula; hc, hippocampus; ctx, cortex; CA1, CA1 region of the hippocampus; GP, globus pallidus; VP, ventral palidum. Scale bar: 300 microns

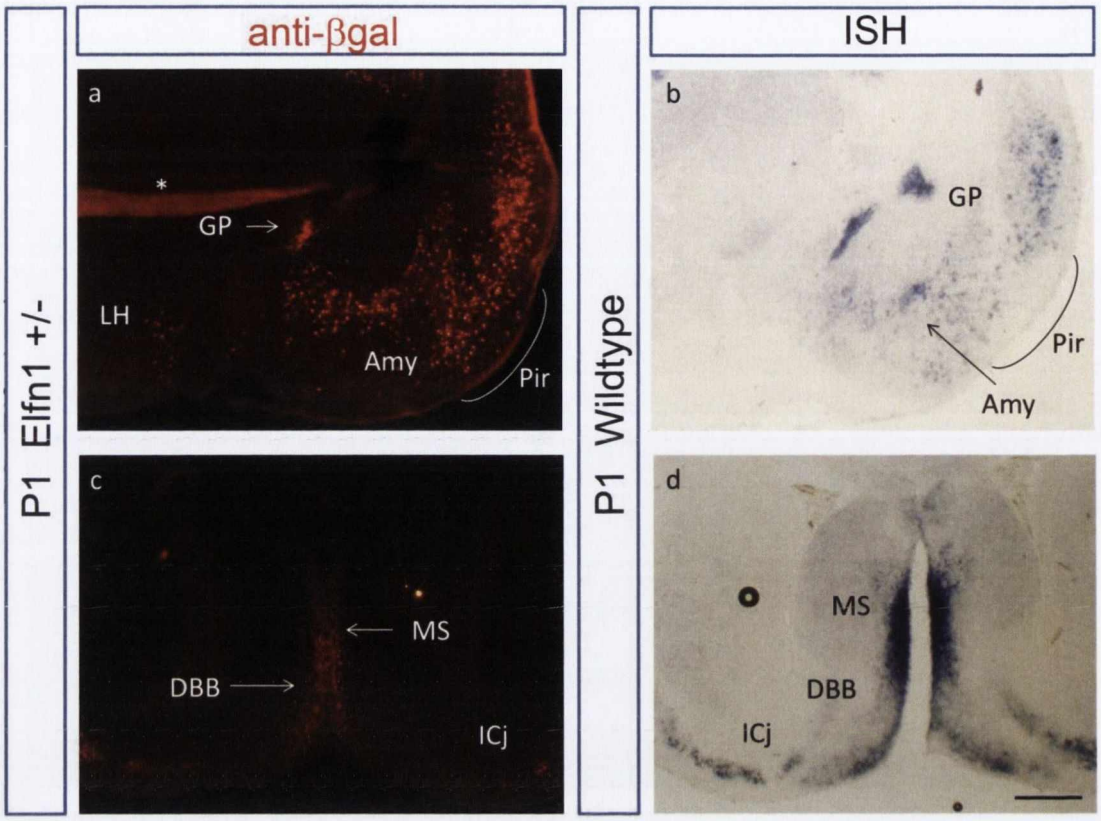

Figure 4.5 βgal immunohistochemistry replicates *Elfn1 in-situ* hybridisation staining patterns (part 2). Comparative coronal sections of βgal immunoreactivity in an Elfn1$^{+/-}$ mouse brain and *in situ* hybridisation staining using an *Elfn1* probe in a wildtype brain, both at P1. (a,b) The amygdala, piriform cortex, and the caudal region of the globus pallidus exhibit comparative staining. The lateral hypothalamus shows immunoreactivity for βgal but no positive staining is visible in this region with the *Elfn1* RNA probe.(c,d) Intense staining in the medial septum, and to a lesser extent in the DBB, is evident. The forming Islands of Calleja also show staining with both methods of Elfn1 detection. A fold in the tissue in (a) is labelled with an asterix. GP, globus pallidus; amy, amygdala; LH, lateral hypothalamus; Pir, pirform cortex; DBB, diagonal band of Broca; MS, medial septum; ICj; islands of Caleja. Scale bar: 300 microns.

4.2.2 *Elfn1* is expressed in interneurons of the hippocampus and cortex

Strong βgal staining was detected throughout the cerebral cortex, scattered in all layers in presumed interneurons. Double immunohistochemistry with the anti-Ctip2 and anti-βgal antibodies at posnatal day (P0) reveal that *Elfn1* is not expressed in Ctip2-positive cells in the cortex (Figure 4.6a,b). Ctip2 is known to be expressed in subcerebral projection neurons (Arlotta et al. 2005) in layers V and VI, where staining is weak in layers Va and VI but strong in Vb (Molyneaux et al. 2007). From this we can see that *Elfn1* expression is highest in layers IV and V, with less expression in layers II and III and present in a discrete number of cells of layers I and VI. In the 3-layer piriform cortex, Ctip2 is expressed in layer II and again shows no overlap with *Elfn1* positive cells which appear mainly resticted to layer III and the endopiriform. A small number of positive cells could also be seen in layer 1, and the pyramidal cell-rich layer 2 (Figure 4.6c,d).

In the hippocampus at P0, *Elfn1* expression is located in the stratum oriens and the stratum radiatum layers and in scattered cells in the hilus of the dentate gyrus. The most intense immunoreactivity was observed in the subiculum and CA1 regions (Figure 4.4). A recent study of *Elfn1* expression in the hippocampus found colocalisation with somatostatin (SST)-positive interneurons, where 96% of *Elfn1* containing cells also contained SST. The other 4% stained positive for parvalbumin (Sylwestrak and Ghosh 2012). To establish if *Elfn1* is expressed in interneurons of the cortex, double staining for somatostatin (SST) and βgal was performed. Somatostatin-positive cells are found across every layer of the neocortex, in layer III of the piriform cortex and in the endopiriform nucleus (Cummings 1997, Rudy et al. 2011). Throughout the neocortex, all *Elfn1* positive cells appear to contain SST (Figure 4.7a). Furthermore, a small number of positive cells for somatostatin and *Elfn1* were found in the fibre-rich layers 1a and 1b (Figure 4.7c,d). It is important to note however, that not all somatostatin-containing cells in the neocortex or pirform cortex are positive for *Elfn1* (Figure 4.7, arrowheads). Therefore, in these regions, *Elfn1* is expressed in a subset of somatostatin positive interneurons.

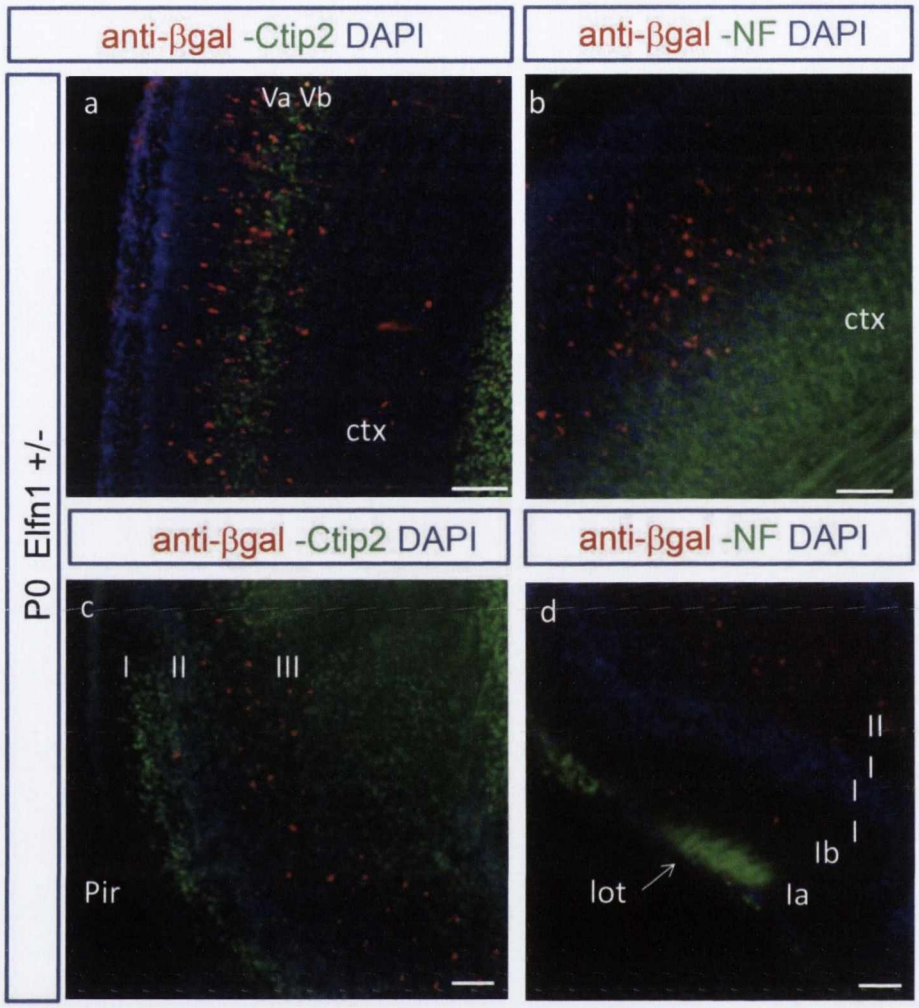

Figure 4.6 βgal expression in scattered cells throughout the neocortex and piriform cortex. (a,c) Double immunofluorescence staining on coronal sections at P0 with anti-ctip2 identifies that Elfn1 is not expressed in ctip2 positive projection neurons. Ctip2 is highly expressed in layers V and VI, with strongest staining found in layer Vb. Elfn1 positive cells are most intense in layers IV and V, but there are also a low number of scattered cells throughout the other layers. In the piriform cortex, ctip2 expression is restricted to layer II. Elfn1 is expressed in layer III and the endopiriform cortex. (b,d) The strongest immunoreactivity for neurofilament is found in the deep cortical layers where there are few positive cells for βgal (b). Elfn1 is expressed by a small number of cells surrounding the neurofilament-positive lot in layers Ia and Ib. ctx, cortex; Pir, piriform cortex; lot, lateral olfactory tract. Scale bar: 30 microns.

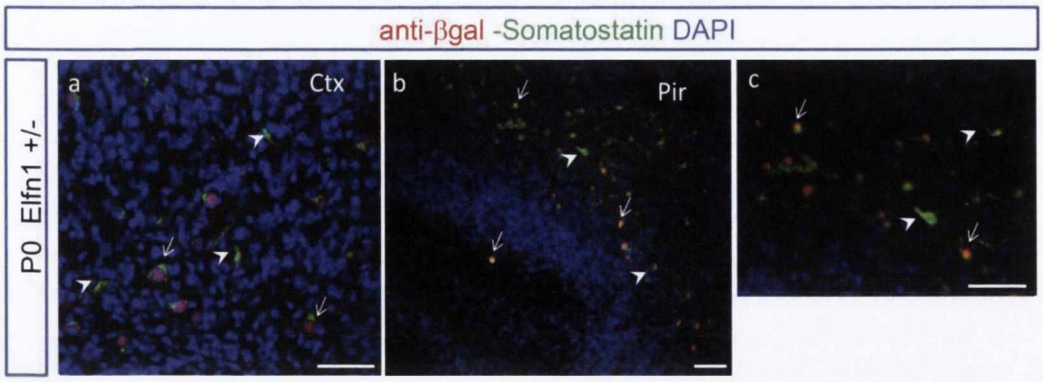

Figure 4.7 βgal is expressed in a subset of somatostatin-positive cells in the cortex. (a) In the neocortex, all βgal-positive cells contain SST immunoreactivity (arrows). (b,c) In the piriform cortex, βgal-positive cells also contain SST. Double staining in Layer III is shown in c. In both the neocortex and piriform cortex, not all SST-positive cells contained βgal (arrowheads). Ctx cortex; Pir, piriform cortex. Scale bar: 30 microns.

4.2.3 *Elfn1* is expressed in GABAergic cells of the Globus pallidus

The globus pallidus (GP) exhibits a very high expression of *Elfn1*, during develpment at E15 and at P0 (Chapter 3, Figure 3.8). βgal-positive cells can be seen throughout the the rostro-caudal extent of this structure (Figure 4.8a,b). In rostral sections, the lateral-most part displays the strongest signal of βgal, complementary to Substance P-positive fibres that are localised in the medial region of the GP, where βgal expression is less evident (Figure 4.8c). The entopeduncular nucleus contains intense substance P staining, but as we can see from the lack of LacZ expression, the cells in this region do not express *Elfn1* (figure 4.8d). A small corridor of cells bordering this region display weak βgal staining, likely to be the caudal-most part of the globus pallidus.

Double staining for somatostatin (SST) and βgal established that in the globus pallidus, unlike in the cortex and hippocampus, *Elfn1* is not expressed in Somatostatin-positive interneurons (Figure 4.9a). However, *Elfn1*-expressing cells were identified as GABAergic with colocalisation of βgal and GAD67 immunoreactivities (Figure 4.9b,c). Approximately two-thirds of GP neurons are

parvalbumin positive and most of the remaining cells contain calbindin and enkephalin (Kita 1994). It is therefore likely that, based on the abundance of cells immunopositive for βgal, *Elfn1* is expressed in a parvalbumin-positive neurons in the globus pallidus. These two main cell types are intermingled throughout the GP and cells expressing parvalbumin have recently been shown to innervate downstream basal ganglia nuclei such as the subthalamic nucleus (STN), the substantia nigra (SN) and the entopeduncular (EP) nucleus, whereas cells exhibiting preproenkephaln (PPE) immunoreactivity exhibited local or striatal connectivity (Mallet et al. 2012). GP neurons have been divided into two populations designated "outer" and "inner" neurons where the former are located beside the striatopallidal border, and the later are approximately 100 μm or more from this border in rats. These two populations were characterised based on the qualitative and quantitative differences in connectivity (Sadek et al. 2007). The more intense Elfn1 staining appears to coinside with these "outer" globus pallidus neurons.

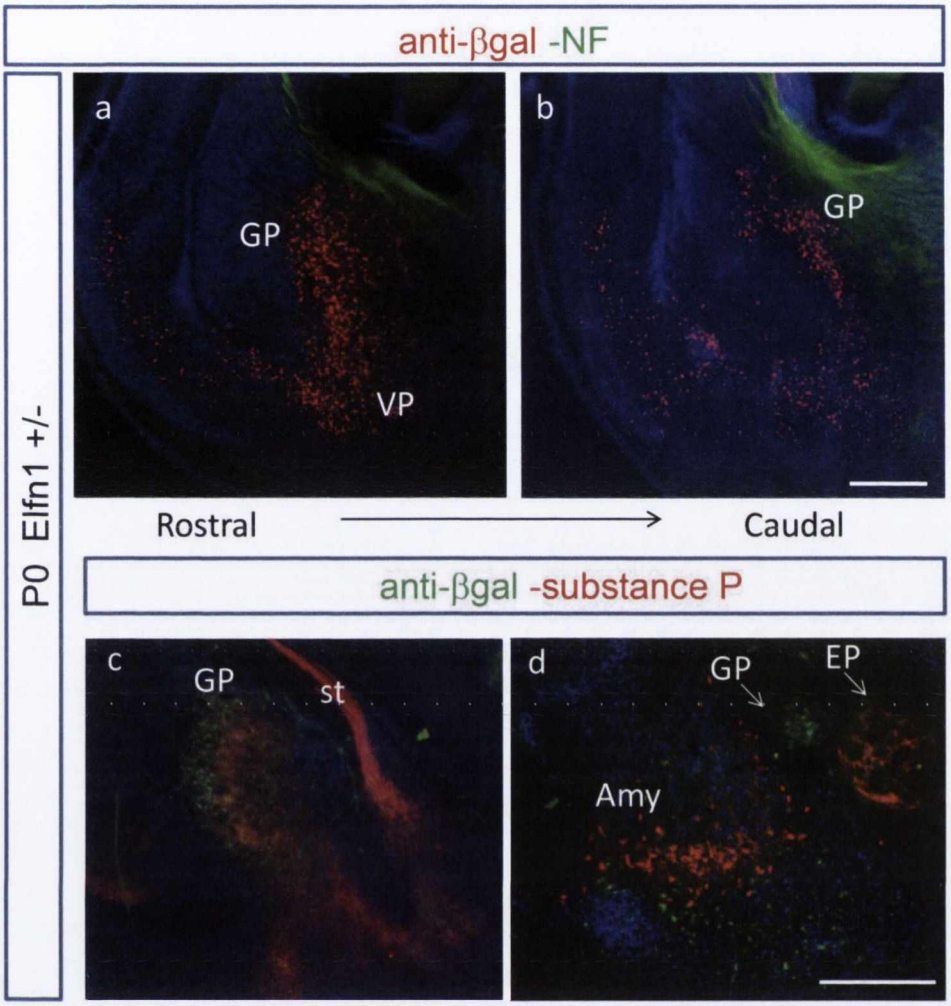

Figure 4.8 Elfn1 is expressed throughout the rostrocaudal extent of the globus pallidus. (a,b) Staining for βgal can be seen in a coronal section of the rostral portion of the GP, with a strong lateral to medial gradient (a) and thoughout the more elongated structure in caudal sections (b). (c) Substance P immunoreactivity in the GP appears complementary to the more intense βgal staining in the lateral cells. (d) βgal staining is not observed in the entopeduncular nucleus which in highly immunopositive for Subsance P. GP, globus pallidus; st, stria terminals; Amy, amygdala; EP, entopeduncular nuleus; VP, ventral pallidum. Scale bar: 300 microns.

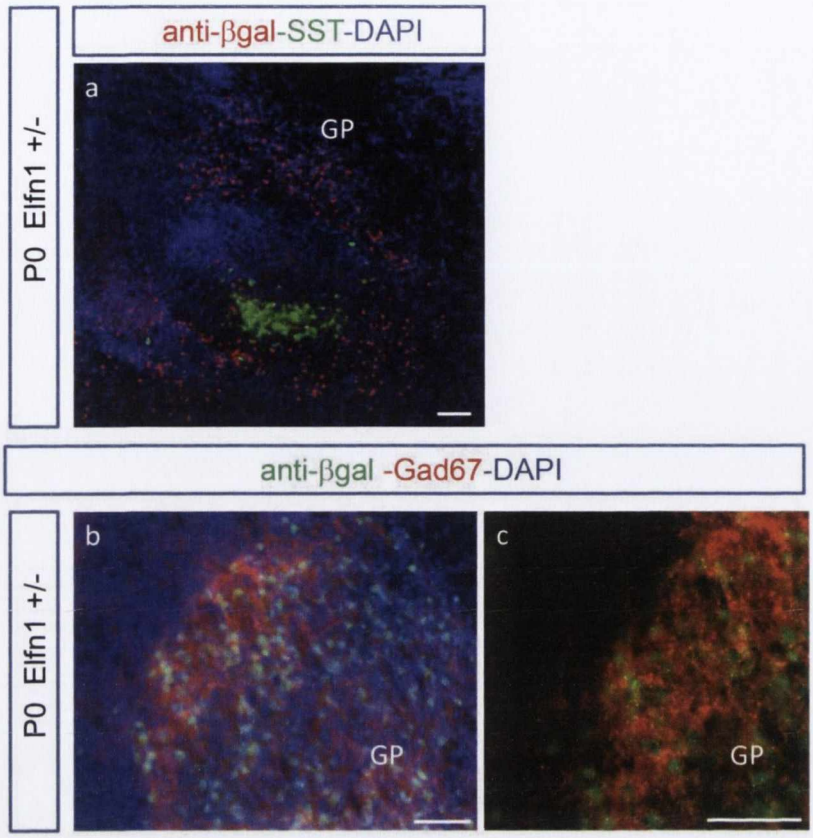

Figure 4.9 Elfn1 expressing cells in the globus pallidus are GABAergic. (a) Cells positive for βgal and SST do not colocalise in the globus pallidus. (b, c) βgal-positive cells contain GAD67 immunoreactivity, with particularly strong staining for both antbodies in the lateral cells of the globus pallidus. Sections are coronal mouse brain at P0. GP; globus pallidus. Scale bar: 100 microns (a) and 50 microns (b and c).

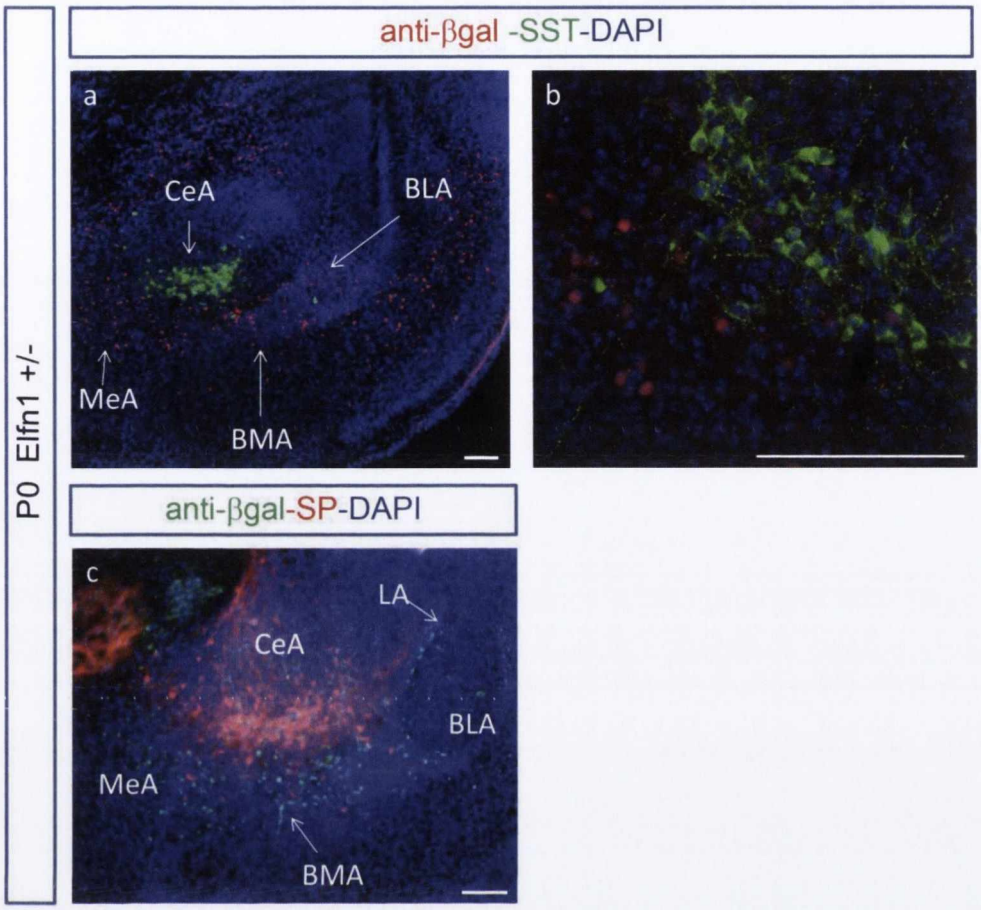

Figure 4.10 Elfn1 expression in the amygdala. (a) βgal expression is evident in the medial (MeA), basomedial (BMA) and basolateral amygdala (BLA). Scattered cells in the central (CeA) and lateral amygdala (LA) are also positive for βgal. Double immunoreactivity with βgal and SST antibodies identify that expression of these two proteins are largely in separate regions of the amygdala (b) A magnified confocal image of (a) shows that βgal-positive cells do not contain SST. (c) Substance P (SP) immunoreactivity is largely restricted to the central amygdala (CeA) where there are a few βgal-positive cells. βgal staining is further identied in the MeA, BMA, and BLA. CeA, central amygdala; BLA, basolateral amygdala; BMA, basomedial amygdala; MeA, medial amygdala. Scale bar: 100 microns.

4.2.4 Elfn1 expression in the Amygdala

βgal immunoreactivity was detected in cells throughout the amygdala, especially in the medial (MeA) and basolateral (BLA) nuclei and in a small number of cells in the central amygdaloid nucleus (Figure 4.10a). Somatostatin-containing cells have been identified in the central amygdala (CeA) (Batten et al. 2002) aswell as the basolateral (BLA) nucleus (Muller et al. 2007) and as we confirmed in Figure 4.10a, somatostatin staining is strong in the CeA and in much fewer cells of the BLA where neither nuclei showed overlapping immunoreactivity with βgal (Figure 4.10b). Therefore *Elfn1* is not expressed in somatostatin-containing interneurons in the amygdala. Substance P is expressed by neurons in the central and medial amygdala, and a subset of neurons positive for both Substance P and somatostatin have been identified in the medial division of the central amygdaloid nucleus (Shimada et al. 1989). Elfn1 does not appear to be expressed in substance P containing cells in the majority of the amygdala, however there may be a small overlap in staining in the CeA (Figure 4.10c).

4.2.5 Elfn1 expression in the Septal Nuclei and islands of Calleja

In the medial septal nucleus, there is a high concentration of cells positive for βgal. The expression continues ventrally into the diagonal band of Broca (DBB) to include both the vertical and horizontal limbs (Figure 4.11a). Scattered cells of the septofimbrial nucleus are βgal immunopositive, however, the lateral septum (LS) and the Triangular septal nucleus (TS) appear to be absent of staining (Figure 4.11c). Double immunohistochemistry with GAD67 and βgal antibodies identify Elfn1 positive interneurons in the medial septum, however, it appears that Elfn1 is expressed in non-GABAergic cells in the SFi (Figure 4.12).

The investigation of Elfn1 in the Islands of Calleja (ICj) was carried out at postnatal day 2 (P2) as these structures appear and develop during the first postnatal week (Hsieh and Puche 2013). They consist of seven complex aggregations of granule cells in the ventral striatum, and one large group located between the septum, nucleus accumbens and nucleus of the diagonal band

(Fallon et al. 1978). These areas have been shown to be highly GABAergic, exhibiting discrete and dense staining patterns (Richards et al. 1987) which aid in the identification of these structures and helped to confirm that Elfn1 is expressed in the newly-forming Islands of Calleja at P2, but not in the large island group (Figure 4.11a,b). Co-localisation analysis of βgal and GAD67 stainings, however, appeared to show overlap in only a subset of cells. GAD67 immunoreactivity is found in the dorsal region of the ICj while βgal staining is located more ventrally. Cells in the central region showed overlapping stainings (Figure 4.13b,c) This may be explained by the differential pattern of expression of GAD67 and GAD65 in the islands of Calleja (Turner et al. 2010, Hsieh and Puche 2013) where it has recently been shown that the majority of cells express GAD65, and GAD67 appears to be restricted to the more dorsal aspect of these structures (Turner et al. 2010). Interestingly, the study by Turner and colleagues identified a similar staining pattern of parvalbumin-GAD67 to the βgal-GAD67 shown here. Due to this, we hypothesise that Elfn1 expressing neurons in the islands of Calleja are parvalbumin containing interneurons.

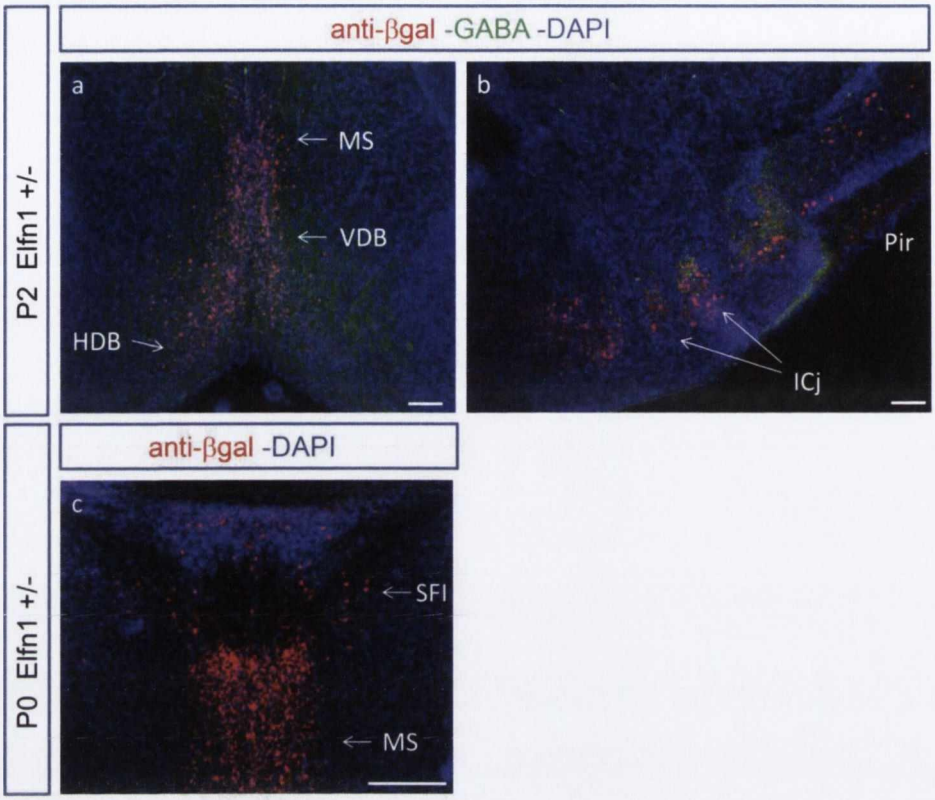

Figure 4.11 Elfn1 is expressed in the septal nuclei and the islands of Calleja. (a) βgal staining is identified in the medial septum, and continues down into the vertical and horizontal arms of the diagonal band of Broca. These structures are highly GABAergic (b) The postnatally forming islands of Calleja are identified as GABAergic cell clusters and are also positive for βgal staining at P2 (c) At the dorsal end of the MS, scattered cells of the Sfi are βgal-positive. MS, medial septum; VDB; vertical limb of the diagonal band of Broca; HDB; horizontal limb of the diagonal band of Broca; Pir, piriform cortex; ICj; islands of Calleja; SFi; septofimbrial nucleus.Scale bar: 100 microns.

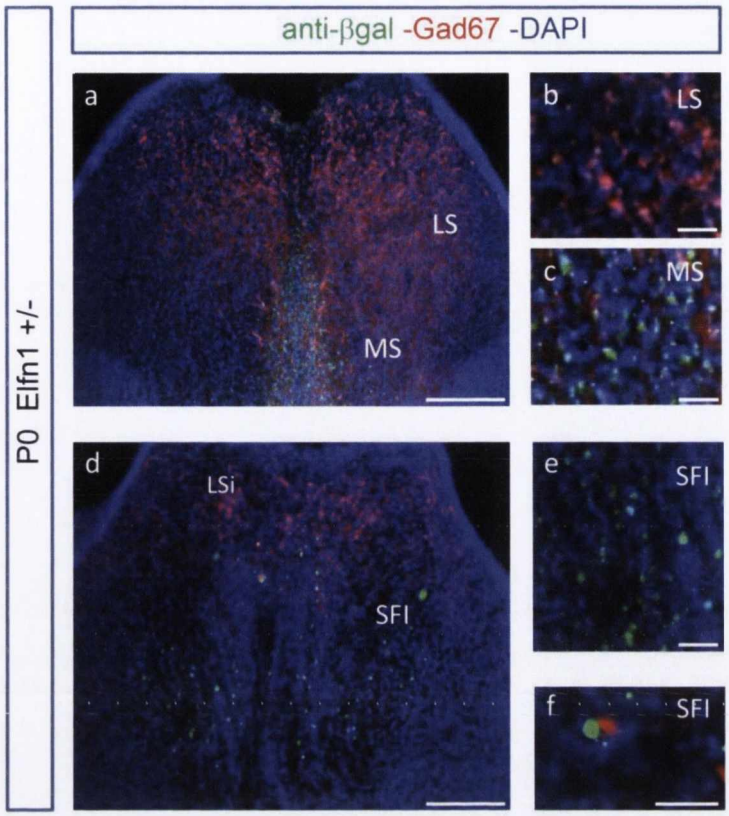

Figure 4.12 Elfn1 is expressed in interneurons of the medial septum. (a-c) The lateral septum exhibits high GAD67 immunoreactivity but no βgal-positive cells. Conversely, the medial septum contains cells with both GAD67 and βgal staining.(d-f) The septofimbrial nucleus shows scattered βgal-positive cells that do not contain GAD67 immunoreactivity. MS, medial septm; LS, lateral septum; LSi, intermediate part of the lateral septal nucleus; septofimbrial nucleus. Scale bar: 100 microns (a and d), 200 microns (b, c, e, f).

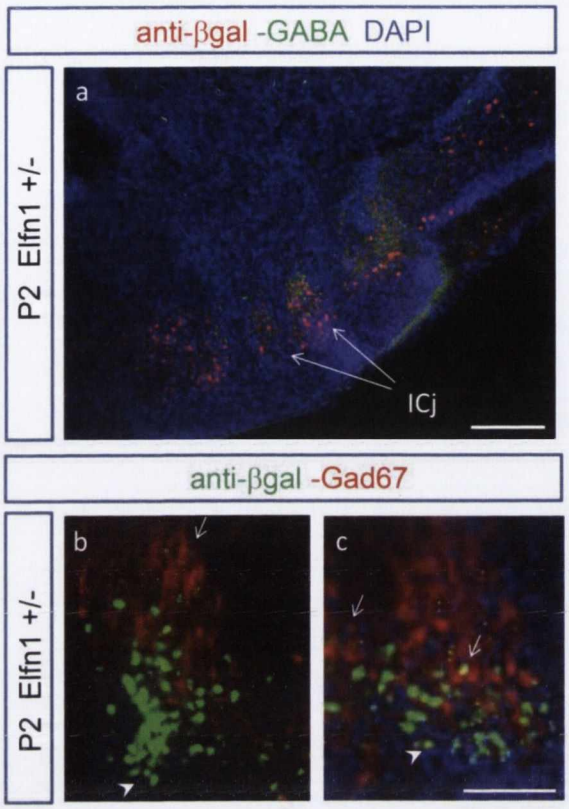

Figure 4.13 A subset of Elfn1 containing cells are positive for GAD67 in the islands of Calleja. (a-c) The islands begin to show distinct clusters of GABAergic cells.The majority of βgal-positive cells appear to locate to the ventral region of these clusters, whereas GAD67 staining is most intense in the dorsal region. Cells exhibiting both immunoreactivities can be seen in the central and dorsal region of the islands (arrows) whereas cells positive for βgal and negative for GAD67 are located ventrally (b)(c) (arrowheads). ICj, islands of Calleja.Scale bar: 100 microns (a) and 25 microns (b,c).

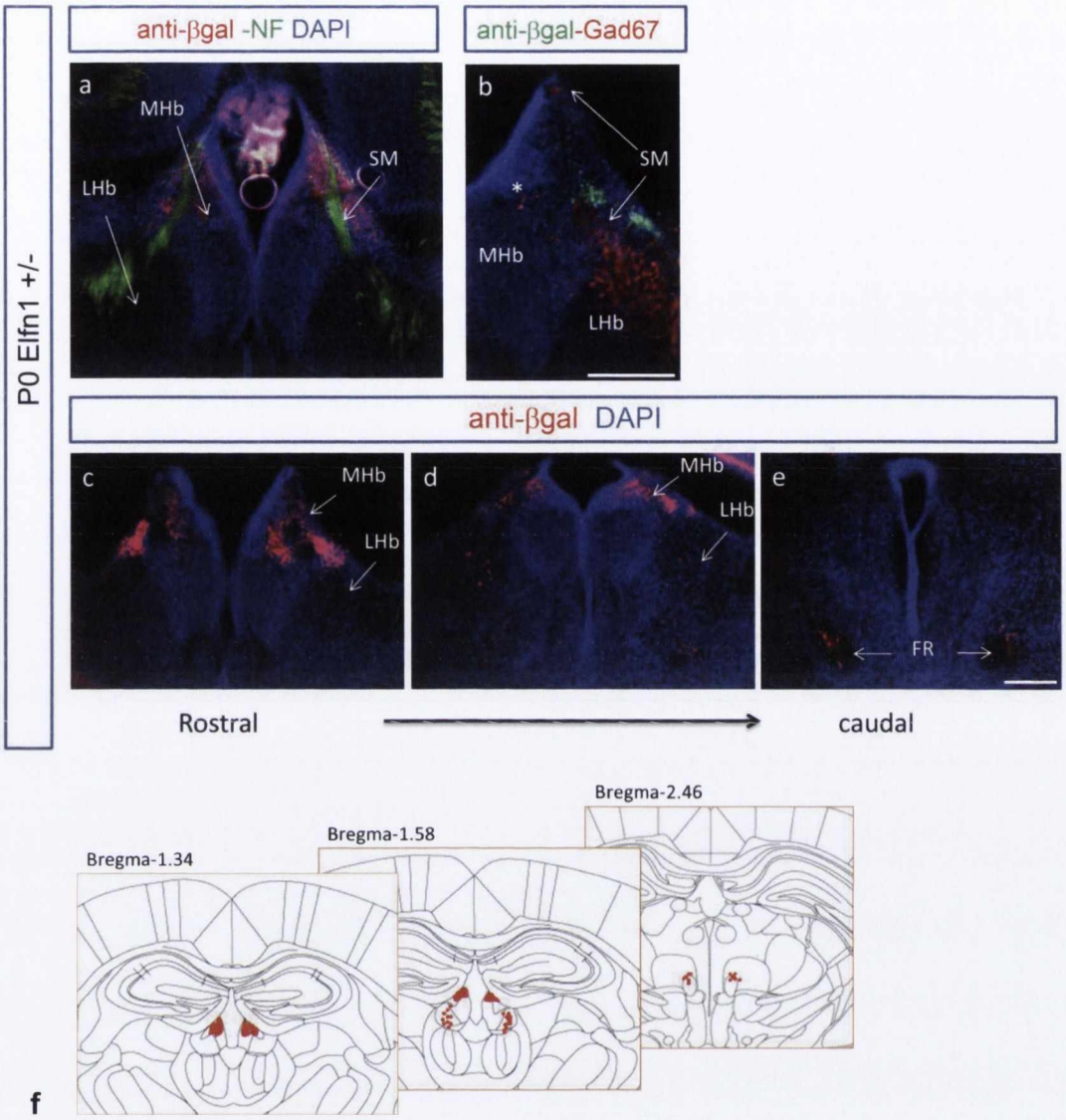

Figure 4.14 Elfn1 expression in a subset of cells in the medial and lateral habenula. (a) βgal staining is identified in a subset of cells restricted to the dorsal MHb, either side of the stria medullaris. (b) GAD67 staining is localised to the stria medullaris, and the lateral habenula. * indicates GAD67 immunoreactivity in a blood vessel. There is no overlap in βgal and GAD67 staining in the MHb. (c-e) βgal staining is evident throughout the rostrocaudal extent of the habenula. In a rostral coronal section (c), staining is limited to the dorsolateral MHb, and absent from the LHb. Further caudally (d), staining is restricted to a smaller subset of cells in the dorsolateral MHb, and in scattered cells of the central LHb. (e) In the caudal-most section, βgal staning is absent from the MHb, and a few positive cells are located in the ventral LHb, dorsal to the fasciculus retroflexus. (f) Coronal sections

of the habenula showing the distribution of βgal staining (diagrams made by modifying templates the from Paxinos and Franklin (2001) mouse atlas. MHb, medial habenula; LHB, lateral habenula; SM, stria medullaris; FR; fasciculus retroflexus. Scale bar:100 microns.

4.2.6 Elfn1 in the Habenula

Immunolabelling for βal was evident throughout the rostrocaudal extent of the habenula, where it was restricted to the dorsal part of the medial habenula and in scattered cells of the lateral habenula (Figure 4.14a). In the rostral portion of this structure, labelled cells are found in the dorsolateral medial habenula, and are absent from the LHb. As you move caudally through the Hb, expression of βgal is further restricted to a discrete subset of cells in the dorsal-most region of the MHb, while a small number of scattered positive cells become evident in the central part of the LHb. Further caudally, there are no labelled cells in the MHb and expression appears to be localised only to the ventral region of the LHb, surrounding the fasciculus retroflexus (Figure 4.14c-e) .

Substance P expression is restricted to cells of the dorsal medial habenula, with a highly similar pattern of expression as the LacZ gene in the Elfn1$^{+/-}$ mouse. This can be seen at the mRNA level with *in situ* hybridisation (Quina et al. 2009) as substance P immunoreactivity displays the axonal localisation of this protein. It had previously been noted that there are no GABAergic cells in the MHb (Qin and Luo 2009) and in this study, double staining for GAD67 and βgal showed no cellular overlap (Figure 4.14b). Therefore, in the MHb Elfn1 is not expressed in interneurons.

4.2.7 Elfn1 localises to axons of the fasciculus retroflexus, the IPL and the substantia nigra pars compacta

A pan-Elfn antibody became available that recognises both Elfn1 and Elfn2, but cannot differentiate between the two. Unfortunately, widespread expression of Elfn2 in the mouse brain prohibits the identification of Elfn1 protein localisation. However, the Elfn1 knockout mouse allows for the comparison of pan-Elfn immunoreactivity in Elfn1$^{-/-}$ and Elfn1$^{+/-}$ mice. Loss of staining in the Elfn1$^{-/-}$ mouse identifies regions of Elfn1 localisation.

In Figures 4.15 and 4.16, Elfn1+/- coronal brain sections exhibit strong pan-Elfn immunoreactivity in the fasciculus retroflexus, the lateral IPN and the

substantia nigra pars compacta that is absent in Elfn1$^{-/-}$ mice. There was no βgal staining in any of these regions and therefore we can conclude that Elfn1 is localised to axons of the fasciculus retroflexus, the lateral subnucleus of the IPN and in axons innervating the SNc. Furthermore, substance P and Robo3 are expressed in the medial habenula and are localised to the output axons which travel through the core of the FR (Figure 4.15) similar to the pan-Elfn staining identified.

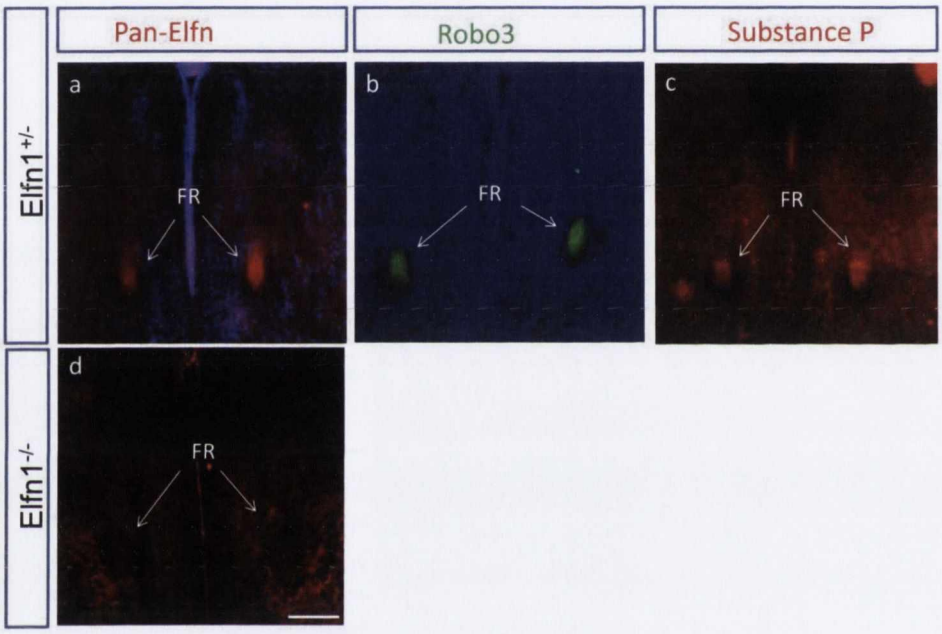

Figure 4.15 Elfn1 localises to axons of the fasciculus retroflexus. (a-c) In the Elfn1$^{+/-}$ brain at P0, the pan-Elfn antibody exhibits strong axonal-like staining in the core of the fasciculus retroflexus (FR). Robo3 and Substance P are known to localise to axons of the FR (Quina et al. 2009). This is confirmed in (b) and (c). (d) pan-Elfn antibody staining is absent from the FR in the Elfn1$^{-/-}$ brain. Scale bar: 100 microns.

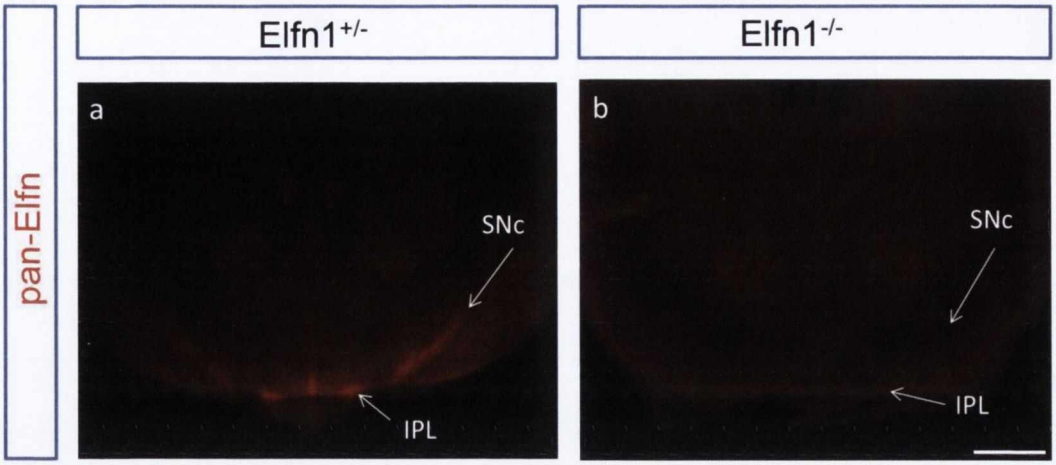

Figure 4.16 Elfn1 expression in the lateral IPN and the SNc. (a,b) Pan-Elfn positive staining is visible in the IPL of the Elfn1+/- (a) but this staining pattern is missing in the Elfn1-/- (b). The SNc also shows immunoreactivity for pan-Elfn in Elfn1+/- (a) but not in Elfn1-/- (b). Elfn1 is present in axons terminating in the IPL, and also in the SNc. IPL, lateral subnucleus of the interpeducular nucleus; SNc; substantia nigra pars compacta. Scale bar: 300 microns.

4.3 Discussion

The aim of this study was to define the expression of *Elfn1* in newborn mice, identifyng *Elfn1*-positive cell types and circuits and thereby providing clues to potential functions of this gene. We established that *Elfn1* is expressed in a number of brain regions including the globus pallidus, ventral pallidus, septal nuclei, diagonal band of Broca (DBB), amygdala, islands of Calleja, lateral hypothalamus and subsets of cells in medial and lateral habenula, the hippocampus and the cortex. Sylwestrak and Ghosh (2012) discovered that in the hippocampus, Elfn1 localises to dendrites in SST-containing interneurons and functions post-synaptically in the determination of synapse type from CA1 pyramidal neurons. Here, we confirmed that Elfn1 is expressed in two different cells types, both SST and parvalbumin containing interneurons, but also in non-GABAergic cells. Furthermore, Elfn1 immunoreactivity was localised to axons of excitatory neurons of the MHb and in axons innervating the SNc. Therefore, Elfn1

may have additional functions in non-inhibitory cells and in the presynaptic axon. It is reasonable to consider an axon guidance or synaptic target selection function due to the localisation of Elfn1 in long-range projecting axons. With these analyses, we have also discovered that Elfn1 is expressed in a number of regions that interconnect to form the dorsal diencephalic conduction (DDC) system. These include the habenula, globus pallidus, septal nuclei and DBB. From this result, we speculate that Elfn1 is functioning in specifying connectivity in this system, and the absense of which could cause dysfunction in the neural network resulting in psychopathology.

4.3.1 Elfn1 in the cortex and hippocampus

In the hippocampus, Elfn1 functions transynaptically in the development of highly facilitating synapses from CA1 pyramidal cells onto O-LM interneurons (Sylwestrak and Ghosh 2012). In Elfn1 knockdown experiments, short term facilitation was dramatically reduced in neurons expressing shRNA's. Furthermore, a stronger reduction in excitatory postsynaptic current (EPSC) amplitude was detected when knockdown was instigated at P1 than at P6. The implications of this in the knockout Elfn1 mouse is that the absense of the gene throughout development may result in abnormalities of hippocampus-dependent behaviours such as learning, memory, anxiety and stress regulation (reviewed in (Leuner and Gould 2010). In particular, loss of Elfn1 in these interneurons may produce an acute or chronic effect on the function of the inhibitory circuit, producing an increase in overall excitability of the hippocampus. Disruptions in the delicate balance of inhibition-excitation are known to be a cause of seizure activity (Stringer 1993). Specifically, enhanced CA1 excitability has been shown to cause seizures in a chronic model of temporal lobe epilepsy (Mangan and Bertram Iii 1997).

We have shown that Elfn1 is also expressed in SST-containing interneurons of the neocortex and the piriform cortex. The fine balance of inhibition and excitation is the basis for normal functioning in these regions which includes cognition and olfaction. While only 20-30% of cortical neurons are interneurons,

they play a critical role in the regulation of pyramidal cell excitability, and dysfunction of these cells have been linked to seizure disorders (Avoli et al. 1997) reviewed in (Milton 2012), and the piriform cortex has been established as epileptic-prone (Panuccio et al. 2012).

4.3.2 Elfn1 in the habenula circuitry

Elfn1 is expressed in many of the regions that connect to form the dorsal diencephalic conduction system. Furthermore, we have identified Elfn1 in regions with direct connectivity to the components of the DDC. These results would suggest a specific involvement of Elfn1 in specifying the connectivity of this neural network; the function of which could be in anatomical connectivity or functional connectivity, or indeed both. The discrete expression of Elfn1 in the MHb is suggestive of its involvement in a microcircuit within the habenula system. To identify possible Elfn1-positive subcircuits, the expression results from this study and known connectivity data were analysed. In addition to the published data relating to DDC connectivity, we utilised the connectivity resource from the Allen Brain Atlas that consists of a large brain dataset of neural connections in the adult mouse brain (www.connectivity.brain-map.org).

In the medial habenula, Elfn1 is expressed in a subset of cells restricted to the dorsolateral region in rostral sections and further caudally it is restricted to a smaller number of dorsally located cells. As mentioned in section 4.2.3, cells in the dorsal aspect of the MHb contain Substance P (an excitatory neurotransmitter (Chen et al. 2009) and are also glutamatergic (Aizawa et al. 2011). The cells in this region of the MHb project to the lateral region of the IPN (Herkenham and Nauta 1979) and anterograde tracing has shown that the dorsal tegmental (DTg) area receives its main contribution of projections from the lateral IPN (Groenewegen et al., 1986). Subsequently, cholinergic cells of the DTg modulate dopaminergic cells of the VTA (Shabani et al, 2010). However, the lateral IPN may also project to the VTA, RMTg and the raphe nuclei (Aizawa et al., 2011). The lateral IPN, therefore, may exert inhibitory influence on the serotonergic-positive raphe nuclei but it appears to have a direct and indirect modulatory effect on

dopaminergic cells of the VTA. In addition to projecting to the IPN, there is evidence that cells in the dorsal MHb project to the LHb. It was discovered that sectioning of Substance P efferents from the MHb reduced Substance P immunoreactivity in the LHb (Sutherland 1982).

Scattered expression of βgal in the LHb identifies the location of Elfn1 containing cells to the magnocellular part of the lateral division of LHb (LHbLMc) which contains more loosely arranged neurons than the surrounding LHb areas (Geisler et al. 2003, Aizawa et al. 2012). This region shows strong immunoreactivity for neurofilament, and a small number of cells express Gaba-B receptors (Geisler et al. 2003). Interestingly for this study, the administration of amphetamine causes neurons localised in the LHbLMc to become activated (Wirtshafter et al. 1994, Rajakumar et al. 1994) (see Chapter 7). Furthermore, this subnucleus was shown to recieve GABAergic inputs from the entopeduncular nucleus (Parent et al. 1981) and may therefore play a role in the basal ganglia circuitry.

Within the basal ganglia, the entopeduncular (EP) nucleus receives GABAergic innervation from the globus pallidus and the ventral pallidum (Clarke et al. 1996, Bolam and Smith 1992); both structures display intense Elfn1 expression (Figure 4.4c). The substantia nigra pars compacta has been described as an extension of the EP, also receiving inputs from the GP (Tepper and Lee 2007). We have shown that axons positive for Elfn1 innervate the SNc and it is most likely that these inputs originate in the GABAergic long-range cells of the GP as the other major input to the SNc, the striatum, lacks βgal staining. Therefore, we suggest a presynaptic role for Elfn1 in GP axons that are functioning in exerting an inhibitory influence on the SNc and EP. However, in order to establish potential functions for the Elfn1-positive circuits, the cell-types that Elfn1-positive axons are projecting to need to be identified. The SNc contains both dopaminergic and GABAergic cells and it is unknown onto which cell type Elfn1 positive axons innervate. The substantia nigra pars compacta is implicated in functions including motor control and reward-based learning and it is established that a complicated system of balance between excitation and inhibition underlies normal behaviour (Reviewed in (Tepper and Lee 2007). How Elfn1 specifically functions in this system requires further investigation, however, we speculate that the absence of

Elfn1 may disrupt connectivity in this system that could manifest as a motor function abnormality.

The medial septum and the DBB contain a high concentration of Elfn1-expressing cells, and neurons from these areas project to both the MHb and LHb (Bianco and Wilson 2009). Available connectivity results from the Allen Brain Atlas confirm that the medial septum and DBB produce widespread innervation across the MHb and LHb, excluding the dorsal tip of the MHb (Figure 4.17f). This innervation has been identified as inhibitory (Qin and Luo 2009). Injection of tracer into the SFi, TS and LS regions shows innervation in a subset of cells located in the central MHb, dorsolateral MHb as well as the dorsal LHb as indicated in the rostrally-located section of the Hb (Figure 4.17i). TS cells are known to project to the caudal region of the MHb, axons from the SFi project to the rostral MHb while the LS does not directly innervate the habenula (Herkenham and Nauta 1979). Consequently, it is likely that the SFi projections to the habenula converge on the Elfn1 positive region in the dorsolateral MHb. Further evidence suggests that these projections are excitatory as backlabelling from the MHb combined with GAD67 immunohistochemistry did not reveal overlapping staining in the SFi (Qin and Luo 2009). The SFi region itself also contains Elfn1 positive cells and double labelling of βgal and GAD67 in this region did not show overlapping expression patterns (Figure 4.12). These analyses would suggest that Elfn1 containing SFi cells may be exerting excitatory influence onto a specific subset of cells in the medal habenula, and that these cells in the MHb could potentially be Elfn1 positive as well. In summary, innervation onto Elfn1 positive cells in the dorsolateral MHb may originate in the SFi, and be excitatory in function. Furthermore, Elfn1 is expressed in a subset of cells in the SFi. The localisation of Elfn1 to both dendrites and axons raises a possibility that Elfn1 could bind homophilically, and the expression and connectivity patterns in the MHb further suggest this possibility.

Further investigation of regions projecting to the habenula with the Allen brain atlas uncovered a pattern of neural input to cells that appears very similar to the βgal staining pattern in this study (Figure 4.17). The input originates from the bed nucleus of the stria terminals (BNST), and is known to project to the MHb. Moreover, the pattern of innervation onto these cells broadly follows the rostrocaudal pattern of Elfn1 expression – strong dorsolateral MHb staining which

reduces to a smaller dorsal subset in more rostral portions of the habenula. However, minor innervation to the LHb does not quite follow the Elfn1 pattern of expression. This could be due to innervation onto Elfn1 positive cells by only a subset of axons from the bed nucleus of the stria terminalis. Also, injection of tracer may unintentionally include surrounding structures, particularly for small target regions.

The bed nucleus of the stria terminalis receives extensive input from the amygdala, and is sometimes referred to as the extended amygdala. The structures have been identified as vital components of circuitry involved in fear-related responses, dysfunction of which has been linked to various anxiety disorders. Other functions attributed to this system are learning and memory, and emotional processing (SAH et al. 2003). Elfn1 is expressed in medial (MeA) and basolateral (BLA) nuclei and in a small number of cells in the central amygdaloid nucleus. The amygdaloid complex displays a vast number of intercellular and intracellular connections however, data on how information passes through this structure is limited. The role of Elfn1 in this complex and its function in the extended circuitry requires further analysis and identification of the specific subsets of cells in which it is expressed. If Elfn1 is functioning in specifying connectivity as we have suggested, the disruption in connectivity in mutant mice could cause abnormalities in fear and anxiety-related behaviours.

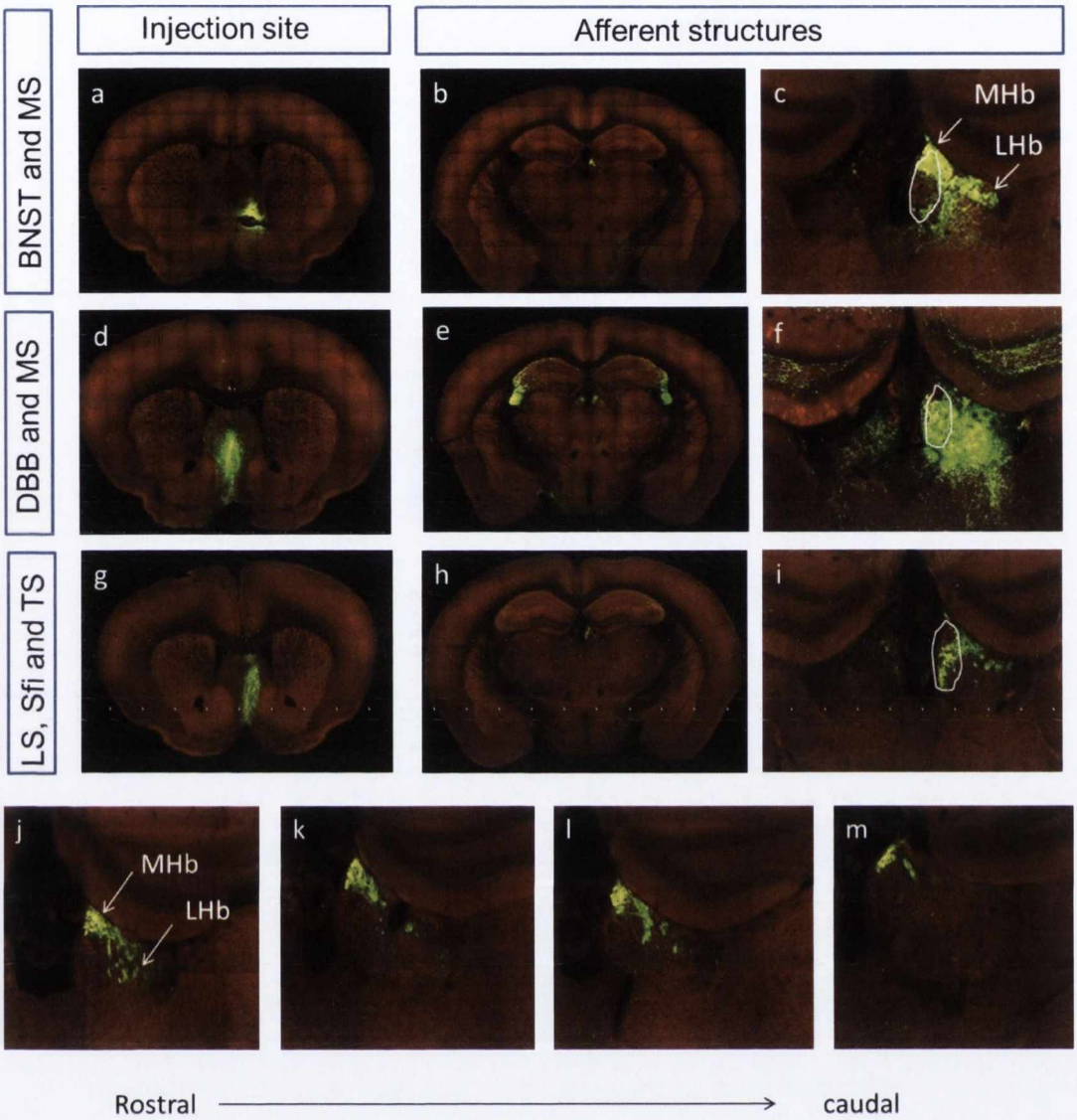

Figure 4.17 Allen brain atlas habenula connectivity in adult. (a-c) Tracer injection in the BNST and MS (a) identifies projections to the dorsal MHb, and the dorsal and medial LHb (b,c). (d-f) The DBB and MS project to all regions of the MHb and LHb except for the dorsal tip of the MHb. (g-i) Injection into the region of the LS, Sfi and TS identifies neural input to the central and medioventral MHb, and the dorsal LHb. (j-m) Afferent input to sections of the habenula (rostral to caudal) from the BNST. The pattern of tracer staining in the MHb is similar to the βgal staining for Elfn1 (see Figure 4.14) MS, medial septum; BNST; bed nucleus of the stria terminalis; DBB, diagonal band of Broca; LS, lateral septum; SFi, septofimbrial nucleus; TS, triangular septal nucleus.

4.3.3 Elfn1 and the islands of Calleja

The islands of Calleja (ICj) are located in the olfactory tubercle, innervated by dopamine neurons of the mesencephalon and interconnected with olfactory and non-olfactory components of the basal forebrain. Interestingly, neurons in these islands express high concentrations of dopamine D3 receptors, and are innervated by dopaminergic cells of the ventral tegmental area and substantia nigra (Fallon et al. 1978). A study producing a 27% decrease in D3 receptors in the islands of Calleja produced an increased locomotor phenotype in rats (Menalled et al. 1999, Diaz et al. 1995). Furthermore, D3 knockout mice exhibit increased basal locomotion (Viggiano et al. 2003). To identify the specific cell type within which Elfn1 is expressed necessitates further double labelling with parvalbumin and GAD65 antibodies. However, if Elfn1 is functioning in interneurons of the ICj as a synaptic modulator, we speculate that the loss of Elfn1 could produce abnormal dopaminergic innervation of this region. Another aspect to consider in Elfn1$^{-/-}$ mice is that dopaminergic innervation to this region from the VTA and SN is altered due to dysfunction in the habenula and basal ganglia circuitries.

4.3.4 Conclusion

Elfn1 localises to the dendrites of specific interneuron populations, and axons of glutamatergic and long range GABAergic cells. It is apparent from the literature, and the Allen brain atlas connectivity study that the DDC system contains multiple neural circuits and it has not yet been established how each is involved in all the behaviours attributed to this system. Further identification of the specific cell types and circuits in which Elfn1 is expressed, and whether it is functioning pre-synaptically or post-synaptically is needed before a complete understanding of the role of this gene in each region of expression can be realised. The expression results in this chapter will guide functional analyses and the interpretation of the mutant phenotypes.

5 Chapter 5 Investigation of an interaction between Elfn1 and Robo3

5.1 Introduction

All cellular processes are determined by protein interactions and therefore the identification and characterisation of Elfn1 interacting proteins is essential to the understanding of the role Elfn1 plays in the developing brain. As proteins do not work alone, it is unknown what the absence of a single gene may have on complex molecular pathways and compensatory processes may take over the function of the protein. Due to this, it can be hugely beneficial to investigate for altered expression or function of related genes or genes that might interact with Elfn1.

5.1.1 Elfn1 interacts with Robo3 in zebrafish

A large *in vitro* screen in the zebrafish identified Robo3 as a binding partner for *Elfn1*, and Boc, Sid4 and Igsf21 for Elfn2 (Sollner and Wright 2009); and a database for the continuing screen is available online (www.sanger.ac.uk/cgi-bin/teams/team30/arnie). The study specifically set out to identify novel extracellular protein interactions using neural LRR and immunoglobulin (IG) superfamily members. The methodology included an assay developed by the researchers called AVEXIS (Avidity-based Extracellular Interaction Screen) which involved testing for interactions among 150 receptor ectodomains and maintains the detection of weak protein interactions with a low false positive rate. Moreover, positive and negative controls were included in the screens and identified interactions were re-verified with new protein samples. The researchers analysed expression patterns of the discovered interactions and found that Elfn1 and Robo3 are both expressed in the zebrafish dorsal habenular nuclei, which is equivalent to the medial habenula in mammals (Concha and Wilson 2001). The AVEXIS methodology biases towards the identification of *in trans* interactions, and

therefore, the interaction between Robo3 and Elfn1 is not restricted to the region of expression but could also be involved in neuronal connectivity. Robo3 is expressed symmetrically in both habenular nuclei while Elfn1 showed higher expression levels in the left nucleus (Sollner and Wright 2009). Left-right asymmetry in gene expression and axonal projections onto subnuclei of the IPN have been found in the Zebrafish (Roussigne et al. 2009) where the left habenula innervates the dorsal and ventral IPN, and the right habenula only innervates the ventral IPN (Gamse et al. 2005). In mammals, the IPN consists of seven subnuclei and a diverse repertoire of afferent and efferent projections (Bianco and Wilson 2009). It is regarded as a major integrative structure and the correct topographical targeting of this region from the habenula is vital for normal function in mid- and hindbrain monoaminergic nuclei.

Further investigation after the initial AVEXIS screen identified that only one specific robo3 isoform (Robo3a) binds Elfn1. Two isoforms have been identified that differ in the N-terminal domain and it is Robo3a (which contains an extra 26 conserved amino acids) that is expressed in the zebrafish habenula, with a function in dorsoventral cell fate specification (Challa et al. 2005).

5.1.2 Robo3 in the mouse developing nervous system

Robo3 (also known as Rig1) is one of four members in the Robo family and contains five Ig domains, three FN3 motifs, a transmembrane domain and cytoplasmic tail containing three conserved regions, that are suggested to interact with downstream signalling molecules (Li et al. 2006, Bashaw et al. 2000). Gene expression analysis has revealed that it functions mainly during development and in axon guidance and cell migration (Camurri et al. 2004). During this time, it is involved in the regulation of axon guidance at the vertebrate midline within the spinal cord (Sabatier et al. 2004) and hindbrain (Marillat et al. 2004). More specifically, Robo3 is strongly expressed in precrossing axons, and downregulated after midline crossing, and therefore suggested to play a role in superseding Robo1-Slit mediated chemorepulsion at the midline. Robo3 has been shown to bind homophilically, and also to interact with Robo1, Ncam and Slit. Conversely,

Camurri *et al* (2005) has suggested the existance of two Robo3 isoforms that differ at the N-terminal portion of the protein, one of which does not bind Slit. Messenger RNA transcripts for both isoforms have been identified in human and mouse (Camurri et al. 2005), but there is no evidence of functional proteins being produced from both transcripts. Beyond this, the N-terminal Robo3 isoforms have not recieved much attention in the literature outside of the zebrafish. Moreover, only the longer form (Robo3a) shows amino acid conservation across multiple species. Amino acid sequence alignment of the mouse Robo3 isoforms is displayed in appendix 9.2.

Two different splice isoforms of Robo3 (Robo3.1 and Robo3.2) that encode different C-terminal cytoplasmic domains were identified in commissural axons. Robo3.1 is highly expressed in the ipsilateral side and allows midline crossing and upregulation of robo3.2 on the contralateral side prohibits recrossing. It is not yet fully understood the exact mechanisms by which the sequential expression of these two isoforms contribute to normal midline crossing (Chen et al. 2008). A further role for Robo3 was also identified in migrating interneurons. Here, it was found to be expressed in an early population of migrating interneurons and involved in regulating cellular morphology where the removal of Robo3 resulted in increased process length, branching, and a greater number of processes at E13.5 (Barber et al. 2009).

5.1.3 Aims of this chapter

The investigation of the Elfn1-Robo3 interaction in mouse was accomplished both *in vitro* and *in vivo*. Upon confirmation of this interaction, we aimed to establish possible sites of interaction for these genes in the mouse brain. This involved the comparison of *in silico* gene expression data for Robo3 with Elfn1 in situ hybridisation results to identify comparable spatiotemporal regions of expression. We speculate that analysis of Robo3 in the Elfn1$^{-/-}$ brain may uncover abnormalities where a direct interaction to Elfn1 is lost. Preliminary analyses have begun with the investigation of Robo3 expression patterns in the Elfn1 knockout mouse.

5.2 Results

5.2.1 *In silico* expression analysis of Robo3 and Elfn1

The postnatal expression of Robo3 has been little studied in mouse, however, in the later stages of development the majority of expression is restricted to the medial habenula (Shimogori et al. 2010) (Figure 5.1). Strong *Robo3 in situ* hybridisation (ISH) staining is evident throughout the MHb at E14.5, and overlaps with the restricted ISH staining pattern we identified for *Elfn1* in the dorsal region of the MHb at E15. Furthermore, gene expression data from the Allen Brain Atlas in adult mouse shows an enrichment of Robo3 transcripts in the ventral MHb, thus producing a complementary expression pattern to that of Elfn1 in the dorsal MHb (Figure 5.2). Therefore, it is possible that these two proteins are interacting *in trans* in the MHb. Indeed, interaction could also be occuring between axons within the FR, or at the IPN since Elfn1 localises to these axons (see section 4.2.7) as does Robo3 (Quina et al. 2009).

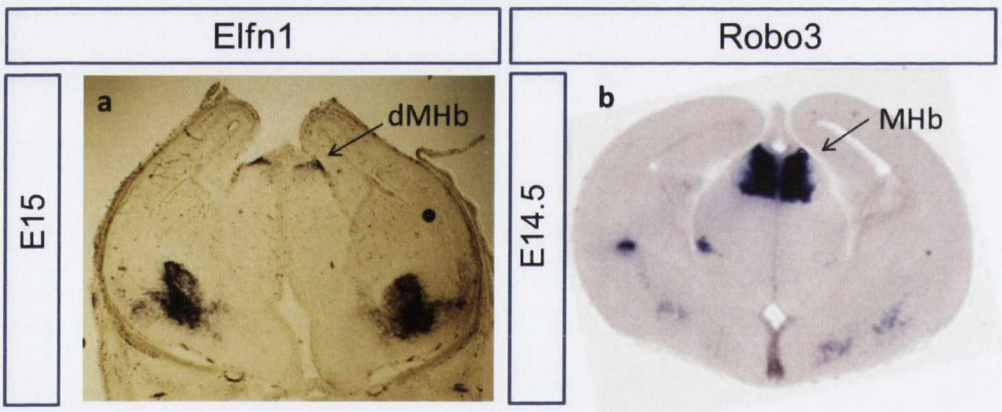

Figure 5.1 Expression of Efn1 and Robo3 in the developing mouse brain. Messenger RNA levels revealed by *in situ* hybridisation with probes for Elfn1 (a) and Robo3 (b). Both genes are expressed in the MHb, with Elfn1 in the dorsal-most part of the MHb at E15 and Robo3 displaying intense staining throughout the MHb at E14.5. The Robo3 figure was taken from Shimogori et al. (2010). MHb, medial habenula; dMHB, dorsal medial habenula

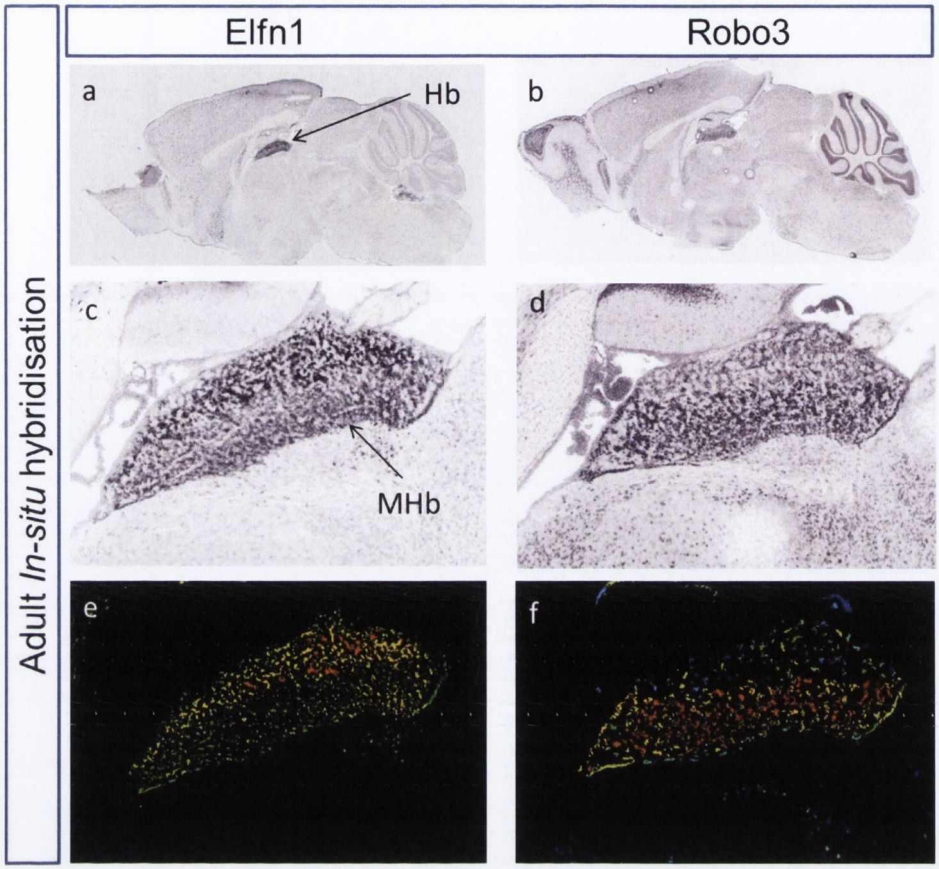

Figure 5.2 Elfn1 and Robo3 expression in the habenula. Adult brain sagital sections from the Allen Brain Atlas show normal expression of Elfn1 (a,c and e) and Robo3 (b,d and f). (c-f) Elfn1 displays strong expression in the dorsal region of the MHb (c,d) while Robo3 shows strong expression in the ventral region of the medial habenula (d,f). Images e and f show the heat expression mask generated from the images in c and d. Hb, habenula; MHb; medial habenula.

5.2.2 Robo3a binds Elfn1 in mouse

To assess whether an interaction between Elfn1 and Robo3 occurs in mouse, a co-immunoprecipitation experiment was carried out in the lab of Alain Chédotal with expression vectors for myc-tagged Robo3 (Robo3A1, Robo3A2 and Robo3B2; see appendix 9.2) and full-length myc-tagged Elfn1 and Elfn2 plasmids (see section 2.7). These constructs were co-expressed in HEK293T cells, and lysates were immuprecipitated with a Robo3 antibody and immunobotted with anti-myc. While both the Robo3 and Elfn constructs contained myc tags, the size difference between them allowed for differentiation on the blot (Robo3 is 250kDa, and Elfn1 and Elfn2 appear as a doublet at approximately 130kDa). Three different Robo3 constructs were tested, representing the isoform differences at both the N-terminal and C-terminal ends of Robo3. The results show that Elfn1 precipitated with the Robo3 proteins (Figure 5.3a) whereas Elfn2 appeared not to pulldown with Robo3 (Figure 5.3b). All isoforms of Robo3 pulled down Elfn1 but the significance of this result is unknown without evidence of translation *in vivo*. However, we can conclude from this result that Elfn1 is interacting with the shared region of the isoforms in the extracellular domain, either with the IGs or FN3 domain.

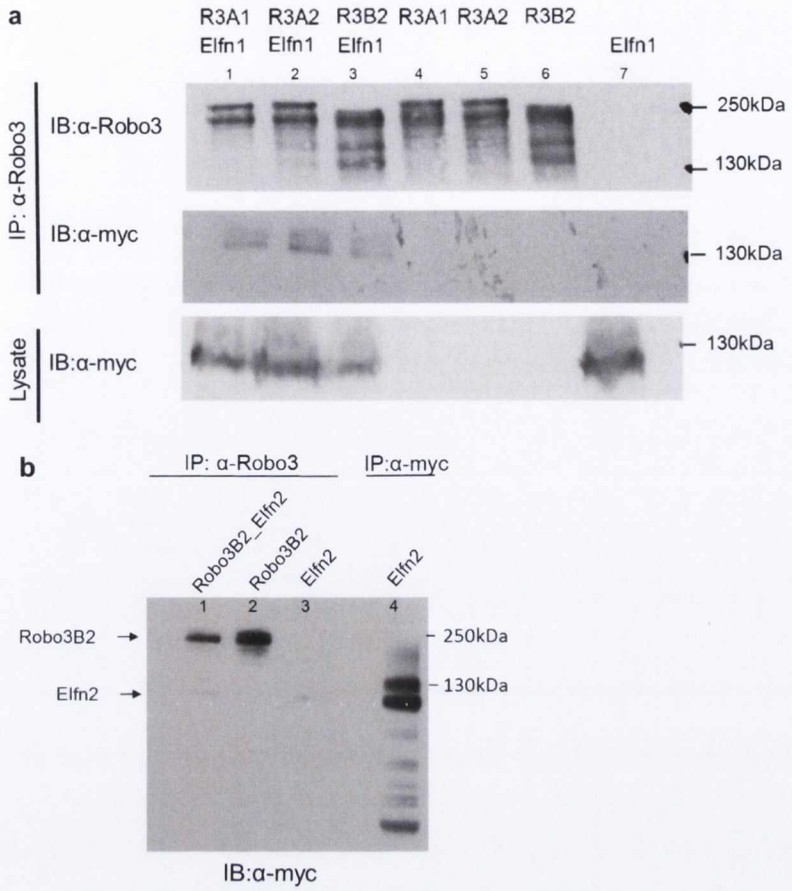

Figure 5.3 In vitro co-imunoprecipitation of Robo3 and Elfn1 proteins. HEK293T cells were transfected with the indicated constructs (three different myc-tagged Robo3 vectors and myc-tagged Elfn1 and Elfn2 vectors). Lysates were tested for expression and co-immunoprecipitation by immunoblotting. (a) Expression of Elfn1 was confirmed in the lysate using an anti-myc antibody which detected a doublet band at approximately 130kDa. Anti-Robo3 antibody was able to precipitate Elfn1 in the presence of all 3 Robo3 vectors (lanes 1-3). In cells transfected with Robo3 only, no Elfn1 was detected (lanes 4-6). Elfn1 was not imunoprecipitated from cells expressing Elfn1 only (lane 7). (b) Elfn2 expression was confirmed with anti-myc and produced a doublet band at approx. 130kDa (lane 4). Immunoprecipitation with anti-Robo3 followed by blotting with anti-myc did not detect co-immunoprecipitation of Elfn2 (lane 1). In cells transfected with Robo3 only, no Elfn2 was detected (lane 2). Elfn2 was not imunoprecipitated from cells expressing Elfn2 only (lane 3). Work carried out by Yvrick Zagar in the lab of Alain Chédotal.

An investigation into the interaction between Robo3 and Elfn1 *in vivo* was facilitated by the hybridisation of the Robo3-alkaline phosphatase(AP) tagged protein to wildtype and Elfn1$^{-/-}$ brain sections. The extracellular Robo3a-AP plasmid (provided by the lab of Alain Chédotal) was transfected into COS-7 cells to produce a Robo3a-AP fusion protein (the longer and conserved N-terminal Robo3 isoform). This investigation also included AP protein lysate produced by the empty pAPtag-5 (Genhunter) plasmid as a negative control.

Robo3-AP bound to P0 wildtype brain sections in a widespread manner with strong binding evident in the cortex, hippocampus and thalamus. This is not unexpected due to the number of Robo3 binding partners that have been identified. However, comparison of wildtype binding patterns to those in Elfn1$^{-/-}$ brain sections show a substantial reduction in binding of Robo3a-AP to the globus pallidus and the striatum in absence of Elfn1 (Figure 5.4). The globus pallidus contains strong Elfn1 expression, and cells in this region project to the striatum further lending weight to the results of this experiment that Robo3-AP protein is binding to Elfn1 in the globus pallidus and the striatum. To investigate if binding is occuring in regions of Elfn1 and Robo3 co-localisation (see section 5.1.3), sections through the habenula and fasciculus retroflexus were analysed. Robo3a-AP binding in wildtype and Elfn1$^{-/-}$ habenula show largely comparable staining patterns, indicating that a strong interaction between Robo3 and another protein is occuring in this region. However, there does appear to be slightly stronger staining in the lateral habenula of the Elfn1$^{-/-}$ mutant (Figure 5.5a,b; n = 2). Results show that Robo3-AP does not bind to fibres in the fasciculus retroflexus in either wildtype or Elfn1$^{-/-}$ sections (Figure 5.8c,d). One possible explanation for the lack of binding is that this methodology, unlike in the immunohistochemistry protocol, does not allow for the probe to penetrate into the cell. Therefore, for binding to occur, the receptor must be present on the cell surface and available in a sufficient concentration in the target tissue.

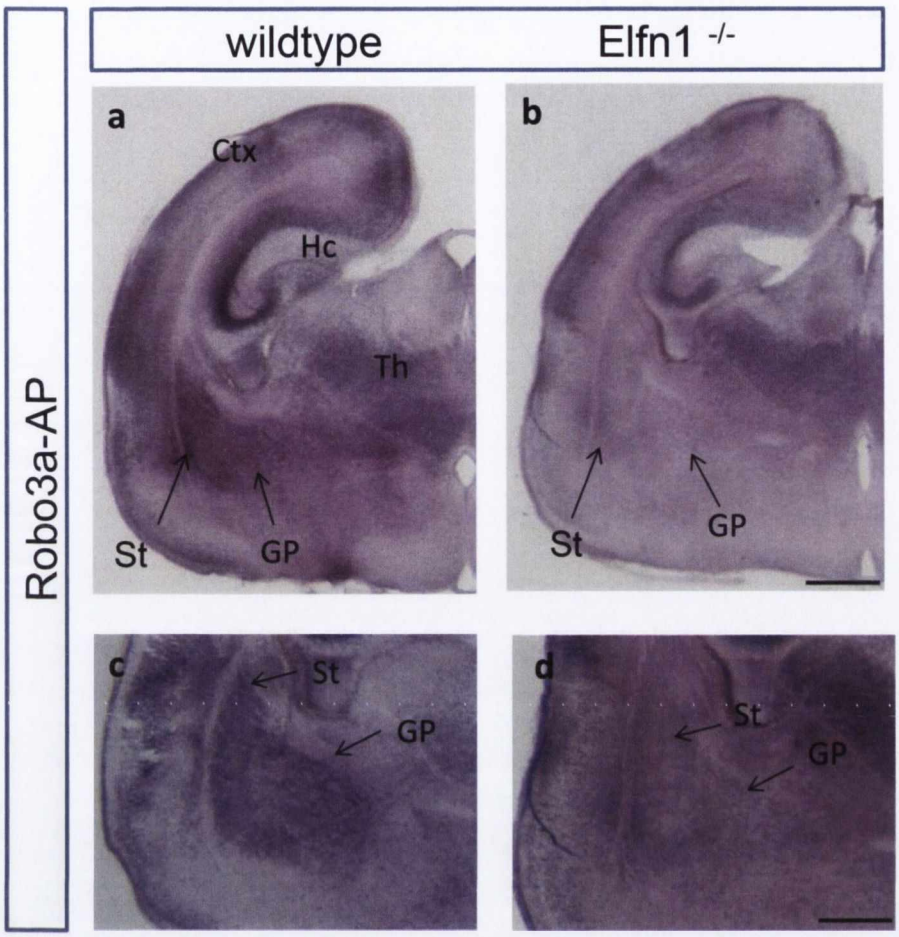

Figure 5.4 Robo3-AP *in situ* hybridisation indentifies robo3-Elfn1 interaction *in vivo*. (a-d) Robo3-AP bound to P0 brain sections in a widespread manner with binding evident in the cortex, hippocampus and thalamus. Comparison of staining pattern in wildtype and Elfn1$^{-/-}$ brain sections show a huge reduction in binding of Robo3a-AP to the globus pallidus and the striatum in the absence of Elfn1 (b and d; n = 2). Ctx, cortex; Hc, hippocampus; Th, thalamus; St, striatum; GP, globus pallidus. Scale bar: 500 microns (a,b), 800 microns (c,d).

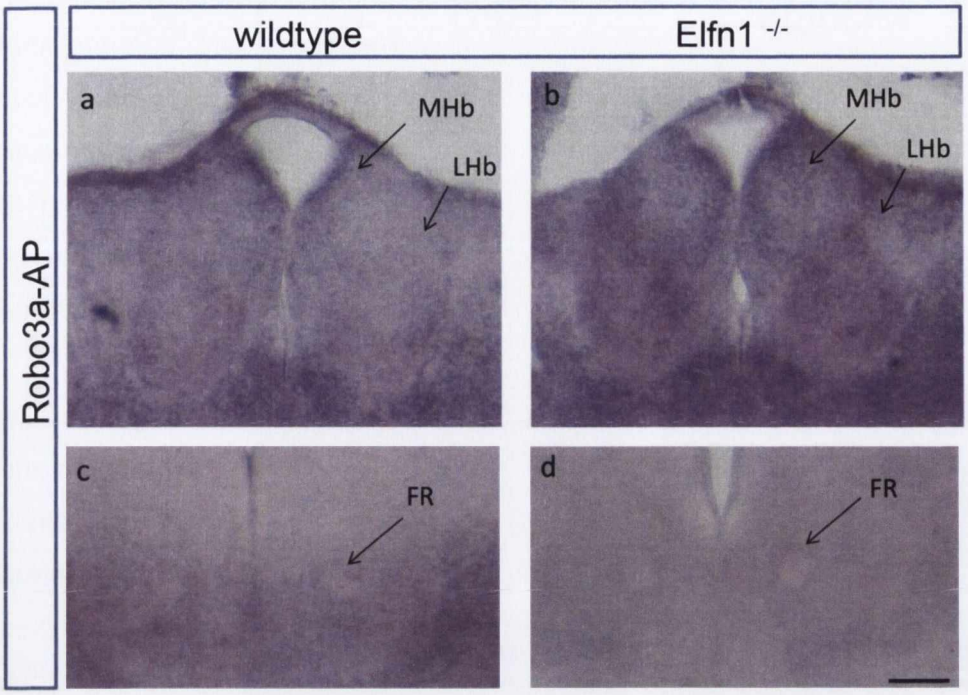

Figure 5.5 Robo3a-AP staining in the habenula and fasciculus retroflexus. (a,b) Staining patterns appear largely the same in P0 wildtype and Elfn1$^{-/-}$ mice with the exception of slightly higher staining in the LHb of Elfn1$^{-/-}$ sections. (c,d) Robo3a-AP does not bind to fibres within the FR in wildtype or Elfn1-/- brain sections. MHb, medial habenula; LHb, lateral habenula; FR, fasciculus retroflexus. Scale bar: 100 microns.

5.2.3 Preliminary analysis reveals normal innervation of the IPN by Robo3-expressing axons

While only at the initial stage of investigation, the innervation of Robo3-positive fibres to the IPN appears grossly normal. Figure 5.6 shows the innervation at the IPN of Elfn1- and Robo3-positive fibres and the crossing pattern of these fibres as they travel towards the IPN in Elfn1$^{+/-}$ and Elfn1$^{-/-}$ brain sections (n = 1).

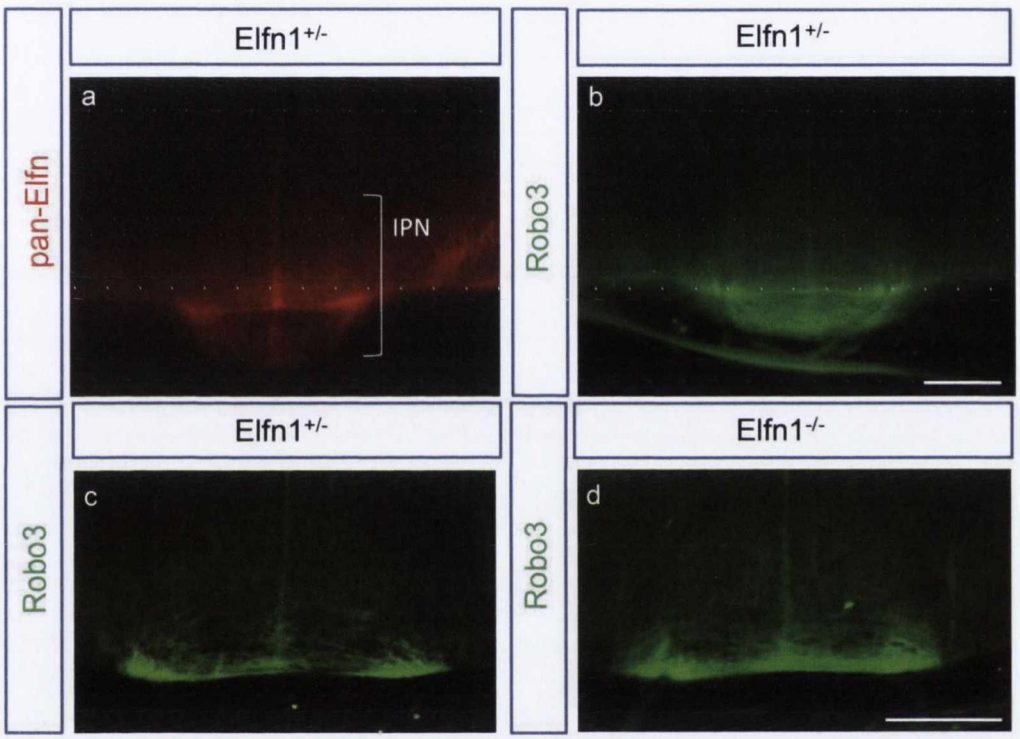

Figure 5.6 Normal innervation of Robo3-containing fibres at the IPN. (a,b) Elfn1-containing axons (a) and robo3-containing axons (b) display an intricate crossing pattern of innervation at the IPN in Elfn1$^{+/-}$ coronal sections at P0. (c,d) Comparable coronal sections showing innervation of Robo3-containing axons at the IPN of Elfn1$^{+/-}$ and Elfn$^{-/-}$ mice, with no obvious difference in connectivity (n = 1). IPN, interpeduncular nucleus. Scale bar: 600 microns.

5.3 Discussion

5.3.1 Confirmation of Robo3 as a binding partner for Elfn1

In this study, we have shown evidence for an interaction between Elfn1 and Robo3 *in vitro* and *in vivo*. Co-immunoprecipitation results confirm that in the mouse, Robo3 binds Elfn1 but not Elfn2. Further investigation of this interaction with Robo3-AP *in situ* hybridisation identified binding of the extracellular region of Robo3 to Elfn1 in the globus pallidus and striatum. This confirms that the interaction has physiological significance, however, we did not specifically identify binding of Robo3 to Elfn1 in the habenula or the fasciculus retroflexus, where expression of these genes and the localisation of the proteins coincide. This could be due to the sensitivity of the protocol, and binding only occuring where Elfn1 is abundantly available on the cell surface.

The identification of an Elfn1 interacting protein provides additional possibilities for the investigation of Elfn1 function. Robo3 has been extensively studied in axon guidance and there are many resources available to analyse Robo3 in the Elfn1 mutant mouse including antibodies, expression data in silico, constructs and knockout mouse lines. The main region of overlapping expression is in the habenula during late developmental stages (Figure 5.1) and postnatally (Figure 5.2), however, functional interaction may be occuring earlier in embyonic development. Moreover, low levels of Robo3 staining may persist as late as E18.5 in the medial septum, the hippocampus and piriform and lateral cortices (Barber et al. 2009). Further analysis of Elfn1 during embryonic stages may shed light on additional regions and time-points for potential interactions.

The AVEXIS screen identified the longer N-terminal Robo3 isoform (Robo3a) as a binding partner for Elfn1. In this study Robo3a interacted with Elfn1 expressing cells in the globus palidus and to Elfn1 localised in the striatum. In zebrafish, Robo3a is highly expressed in the MHb and was shown to function in dorsoventral patterning (Challa et al. 2005). If Robo3 is performing a similar function in the mammalian habenula then we would speculate that Robo3, and possibly Elfn1, function in specifying subnuclei of the habenula and in turn, specific

DDC subcircuits that are governing distinct monoaminergic nuclei. The complementary expression patterns of these genes in the habenula could be a consequence of this function and the localisation of Robo3-positive cells in the habenula of Elfn1 knockout mice may be abnormal. This potential phenotype should be investigated by comparing mRNA *in situ* hybridisation patterns in Elfn1$^{-/-}$ and Elfn1$^{+/-}$ brain sections.

5.3.2 Possible role in axon guidance

Robo3 is a known axon guidance molecule, and mouse mutants have shown severe pathfinding phenotypes, with major axonal tracts failing to cross the midline in the hindbrain (Marillat et al. 2004). This phenotype is similar to the human condition of horizontal gaze palsy and progressive scoliosis, where the corticospinal and dorso column-medial lemnicus tracts fail to cross the midline, and is caused by homozygous mutations in the extracellular domain of Robo3 (Jen et al. 2004). Due to the confirmed interaction of Elfn1 with Robo3 and the colocalisation of Elfn1 and Robo3 in the axons of the FR, we speculate that there may be inter-neuronal communication between the co-extending axons. The normal topographical targeting of the IPN may require this interaction. Preliminary analysis of Robo-3 expressing axons of the FR and their innervation at the IPN have not identified any abnormalities in Elfn1$^{-/-}$ mice thus far. However, more detailed analysis of the habenulo-interpeduncular pathway in Elfn1 knockout mice is required. The location of the IPN and the crossing pattern of innervating fibres necessitate analysis on each plane of section, particularly the horizontal plane. Furthermore, gene expression analysis of *Elfn1* in the spinal cord and hindbrain should be performed to identify if an interaction could be occuring in these regions, where Robo3 has a well-described function in axon guidance.

The role of Robo3 in the mouse habenula has not been established and a parallell investigation of its normal function is essential. The huge amount of resources available for the study of Robo3, as mentioned earlier, include antibodies, constructs and knockout mouse lines. While homozygous mutant mice die within a few hours of birth (Sabatier et al. 2004), a transheterozygote with Elfn1

may display an obvious phenotype providing evidence that these genes work in the same pathway. Likewise, knockdown of Robo3 transcripts in the habenula of Efn1$^{-/-}$ mice may produce a detectable phenotype that would confirm an interaction in this region and be revealing of function.

5.3.3 Conclusion

The results in this chapter confirm that Robo3 and Elfn1 interact in vivo, and this interaction is likely to occur in the habenula; a region of compatable spatiotemporal expression of both genes. Furthermore, both Elfn1 and Robo3 are localised to axons of the fasciculus retroflexus where inter-neuronal communication could be occuring. Robo3 is a well-known axon guidance molecule leading to the hypothesis that Elfn1 may be functioning in this process also. Preliminary results have not uncovered any gross connectivity defects in Robo3-containing FR axons in the Elfn1$^{-/-}$ brain, but requires further extensive analysis. In the zebrafish habenula Robo3 has been implicated in dorsoventral cell fate specification, but there have been no published studies investigating the functional role of Robo3 in the mammalian habenula.

6 Chapter 6 Phenotypic investigation of the *Elfn1* mutant mouse

6.1 Introduction

The *Elfn1* knockout mice are viable and fertile and appear to develop normally up to adulthood. At the initial stages of this study with no function known for *Elfn1*, preliminary analysis focused on the investigation of the neuroanatomical consequences owing to the lack of Elfn1. The βgal staining patterns in the heterozygote can be compared with the homozygous mutant to find cell proliferation, migration or organisation defects. Neuronal connectivity defects in cells lacking *Elfn1* could not be analysed since the insertion cassette contains a cell body marker only, and there are no Elfn1-specific antibodies available. However, gross connectivity can be analysed for abnormalities with a neurofilament marker, which labels neuronal processes.

6.1.1 Elfn1 functions in synaptic transmission

During the course of this research, a function for Elfn1 in synaptic transmission was identified. It was discovered that in the hippocampus, Elfn1 is expressed in the CA1 pyramidal cell targets, the OL-M interneurons, and is involved in the modulation of presynaptic excitatory transmission (Sylwestrak and Ghosh 2012) (see section 4.1.2). Due to this, we decided to investigate for this function in other Elfn1-positive regions of the brain. The release of L-glutamate from excitatory synapses is dependent on vesicular glutamate transporters (vGluts). In the rodent brain, the distribution of the two main glutamate transporters are complementary, with vGlut1 expression high in limbic regions and vGlut2 is localised to the diencephalic and lower brainstem regions. In particular, the MHb and LHb exhibit high levels of vGlut2 immunoreactivity at P0, whereas vGlut1 levels were weak in this region (Nakamura et al. 2005). Due to this, impaired or altered glutamatergic transmission to the habenula can be investigated by comparing vGlut2 expression patterns in Elfn1$^{+/-}$ and Elfn1$^{-/-}$ brain sections.

6.1.2 Aims of this chapter

One of the main aims of this chapter was the investigation for gross anatomical or connectivity abnormalities in the Elfn1$^{-/-}$ brain. This was achieved using βgal and neurofilament antibody stainings in comparable brain sections of Elfn1$^{+/-}$ and Elfn1$^{-/-}$ mice. The preliminary investigation for altered synaptic transmission in the habenula of the Elfn1 knockout mouse was carried out with vGlut2 immunohistochemistry.

6.2 Results

6.2.1 No anatomical abnormality detected in the Elfn1$^{-/-}$ mice

The βgal staining patterns in Elfn1$^{+/-}$ and Elfn1$^{-/-}$ mice were compared in coronal sections of mouse brain at P0, and no gross morphological differences were detected. A limitation of this investigation became apparent with the difference in βgal protein levels between the two genotypes. The homozygous mutant mice contain two copies of the LacZ gene and therefore exhibit stronger βgal immunoreactivity. Nevertheless, in all regions of Elfn1 expression, the pattern and abundance of immunoreactive cells appeared normal in the homozygous mutant (Figure 6.1 and 6.2; n = 4/genotype).

6.2.2 Gross connectivity in Elfn1$^{-/-}$ mice is normal

Neuronal processes were immunostained with a neurofilament antibody and comparable sections in Elfn1$^{+/-}$ and Elfn1$^{-/-}$ mice were analysed. No gross connectivity abnormality was identified with this experiment (Figure 6.3, n = 4). Particular focus on the SM and FR revealed normal innervation patterns in the habenula and the IPN (Figure 5.4).

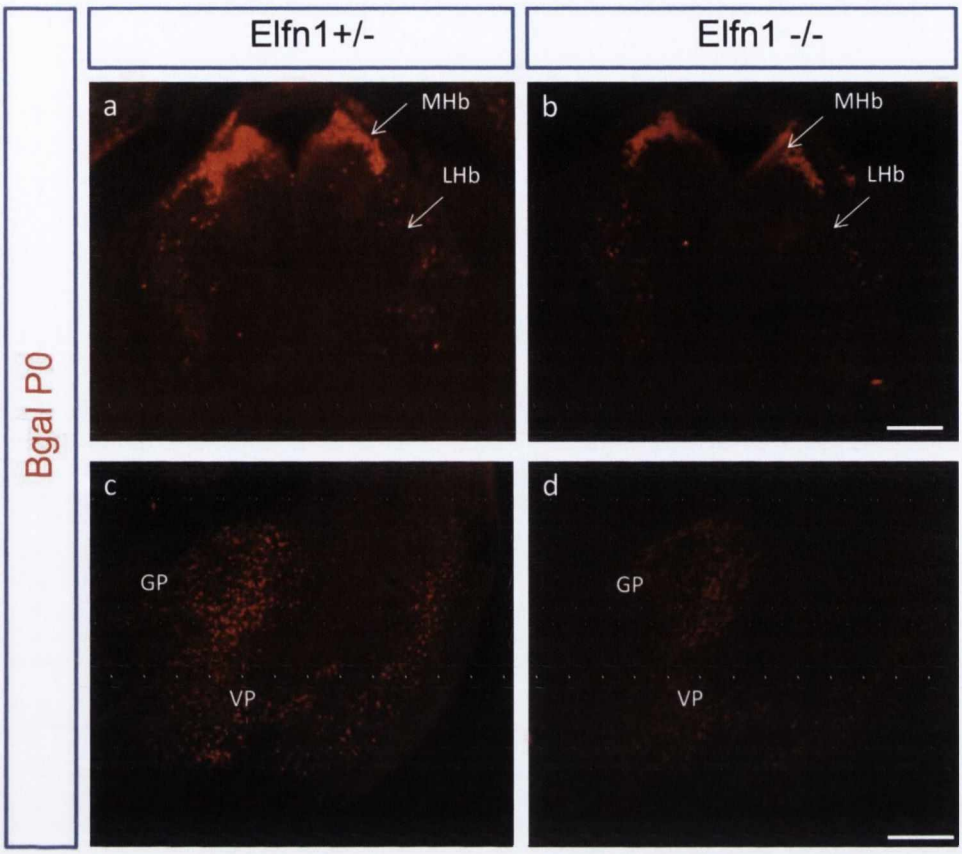

Figure 6.1 Anatomical analyses of the Elfn1$^{-/-}$ mouse brain at P0 (part 1). (a,b) Representative habenula staining patterns in coronal sections of the Elfn1$^{+/-}$ (a) and Elfn1$^{-/-}$ (b), both showing comparable patterns with strong dorsolateral MHb staining, and in scattered cells of the central LHb. (c,d) Staining in the globus pallidus and ventral pallidus exhibit similar patterns in the Elfn1$^{+/-}$ (c) and Elfn1$^{-/-}$ (d), with intense staining in the lateral region of the GP. MHb, medial habenula; LHb, lateral habenula; GP, globus pallidus; VP, ventral pallidus. Scale bar: 100 microns (a,b), 300 microns (c,d).

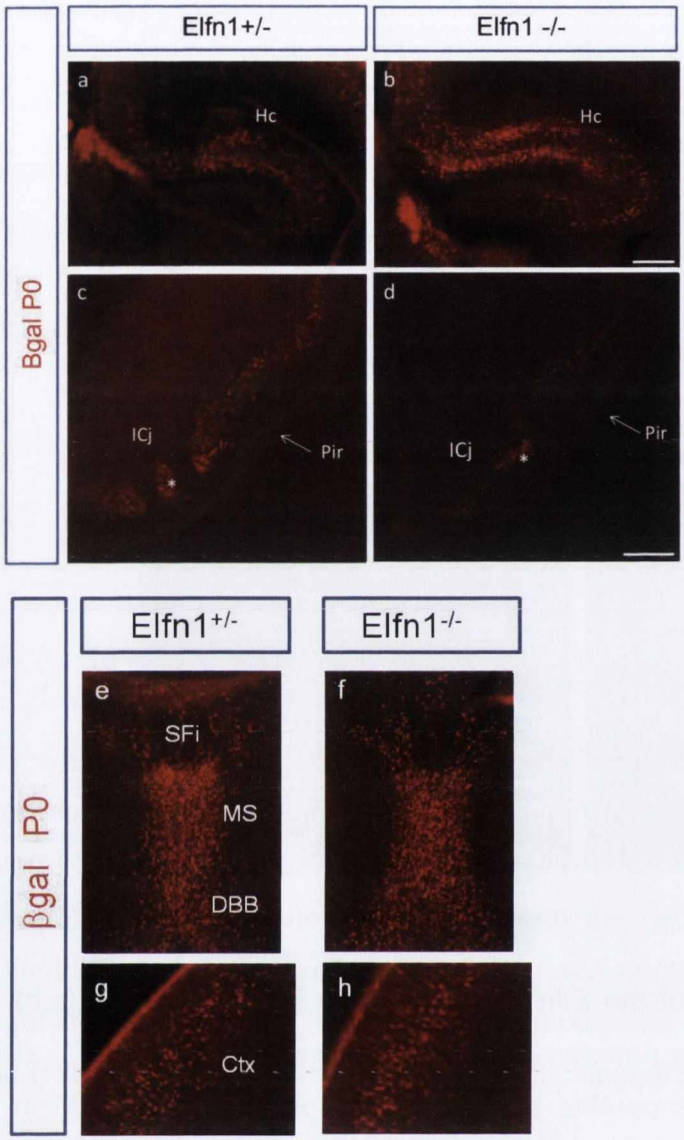

Figure 6.2 Anatomical analyses of the Elfn1$^{-/-}$ mouse brain at P0 (part 2). (a-d) The hippocampus of Elfn1$^{+/-}$ (a) and Elfn1$^{-/-}$ (b) exhibit a similar pattern of βgal staining, as does the piriform cortex (c,d). At P0, the islands of Calleja are only beginning to form but an asterix marks the aggregation of Elfn1-positive granule cells in both the Elfn1$^{+/-}$ (c) and Elfn1$^{-/-}$ (d). (e-h) The MS and Sfi show comparable staining patterns in Elfn1$^{+/-}$ (e) and Elfn1$^{-/-}$ (f) brain sections, as does the cortex at P0 (g,h). Scale bar Hc, hippocampus; Pir, piriform cortex, Icj, islands of Calleja; Sfi, septofimbrial nucleus; MS, medial septum; DBB; diagonal band of Broca; Ctx, cortex. . Scale bar: 100 microns (a,b, e, f ,g and h), 300 microns (c,d).

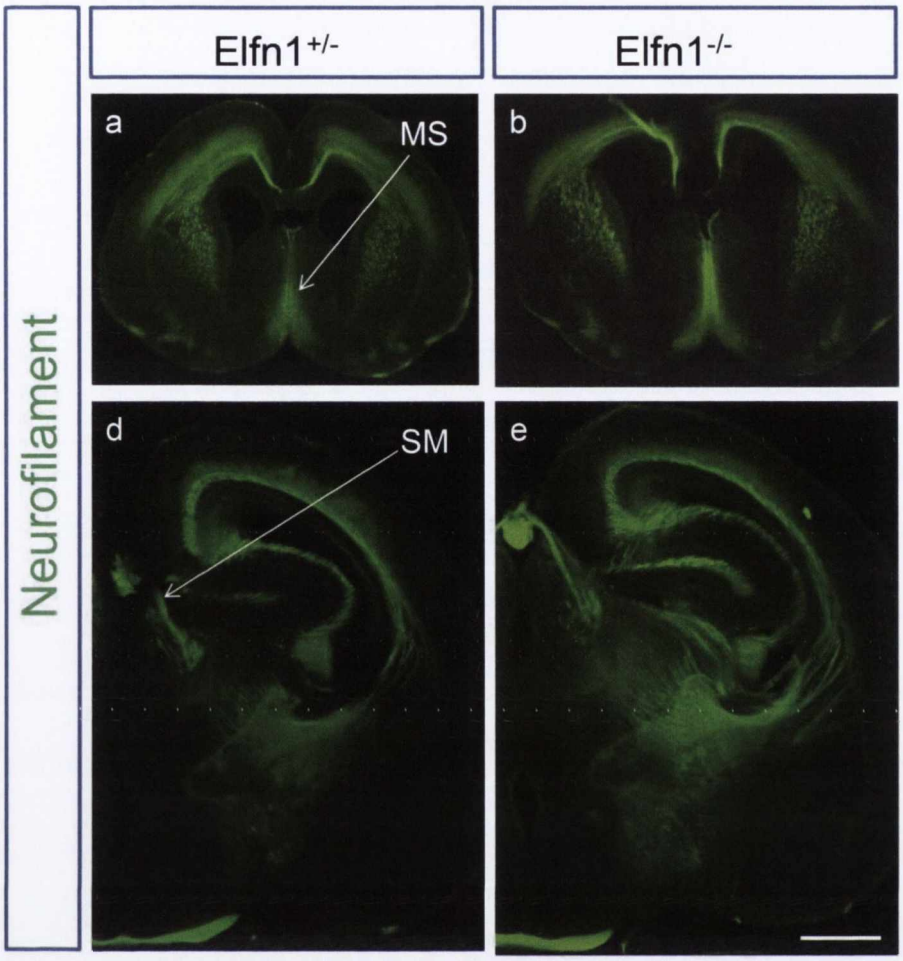

Figure 6.3 Phenotypic analysis of neuronal connectivity in Elfn$^{-/-}$ brain. This figure shows coronal sections through the brain of Elfn1+/- and Elfn1+/- mice at P0. Neurofilament staining patterns in the regions of the septal nuclei, habenula and globus pallidus are displayed with no apparent abnormality in connectivity (n = 4). MS, medial septum; SM, stria medullaris; GP, globus pallidus.Scale bar: 500 microns.

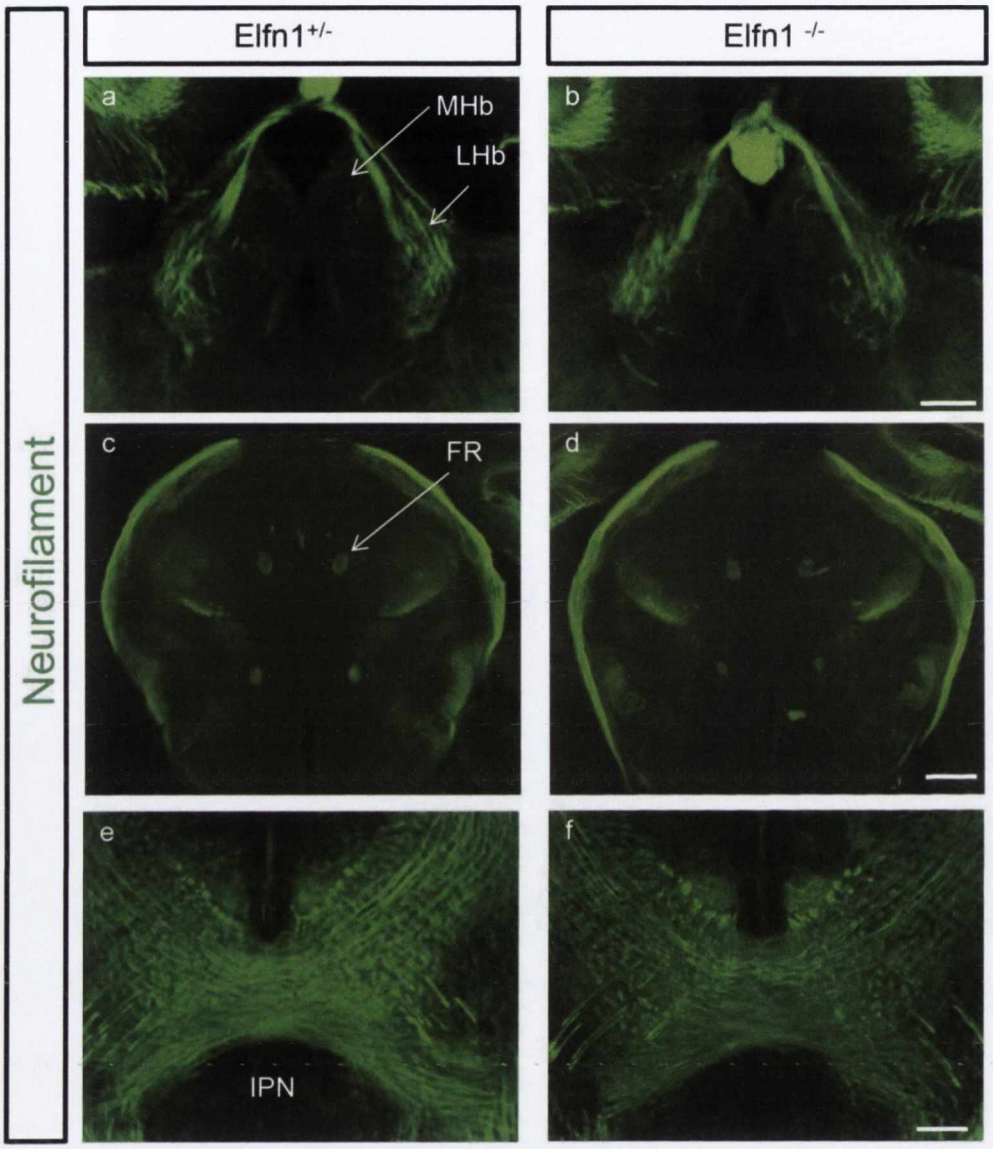

Figure 6.4 Phenotypic analysis of habenulopeduncular connectivity in the Elfn1$^{-/-}$ brain. Neurofilament staining patterns of the stria medullaris (SM) and fasiculus retroflexus (FR) show the innervation of the habenula and the interpeduncular nucleus (IPN) respectively. No gross connectivity phenotype is evident in these regions. Scale bar: 100 microns (a,b,e,f) and 300 microns (c,d).

6.2.3 Reduced vGlut2 immunoreactivity in the habenula of Elfn1$^{-/-}$ mice

A reduction in the levels of the excitatory presynaptic marker, vGlut2, was found in the habenula of Elfn1$^{-/-}$ mice, particularly at the level of the dorsolateral MHb, and the dorsal LHb through the rostrocaudal extent of the habenula (Figure 6.5a-f; n=2). Moreover, in the wildtype, vGlut2-positive fibre boutons can be detected around the somata of cells in the region of the dorsolateral MHb that are absent in the Elfn1$^{-/-}$ habenula (Figure 6.5 g,h). This region also contains cells positive for Elfn1 (Figure 6.5i), although further investigation with double labelling for βgal and vGlut2 is needed to identify if the innervation is occuring directly onto the cell bodies of Elfn1-expressing cells.

6.3 Discussion

6.3.1 Elfn1$^{-/-}$ mice lack obvious anatomical or connectivity defects

The investigation of the *Elfn1* knockout mice for an anatomical phenotype was carried out to reveal possible *Elfn1* functions in the brain. However, we found no apparent morphological or connectivity abnormalities in the brains of Elfn1$^{-/-}$ mice. It is not uncommon for single-gene mutants to result in no observable phenotype and there are a number of possibilities for this outcome. The first possibility is that in actual fact, there is no phenotype due to the lack of Elfn1. This point refers to the genetic robustness of the mammalian brain and the existence of alternative pathways resulting in the same process, a type of functional back-up. Additionally, the gene itself may be redundant to some extent. An example of which was identified in the Dishevelled (Dvl) gene family and their function in cell patterning and proliferation (Etheridge et al. 2008). In this case, an obvious phenotype emerged with the combined knockout of partially redundant family members. Elfn1 and Elfn2 are highly similar, sharing regions of nucleotide sequences and displaying overlapping patterns of expression. Consequently, further investigation of the expression of Elfn2 under normal conditions and in the Elfn1$^{-/-}$ mutant may reveal if there is any redundancy in the Elfn family. If this is the

case, over expression or ectopic expression of Elfn1 may be more revealing of function than loss-of-function analyses.

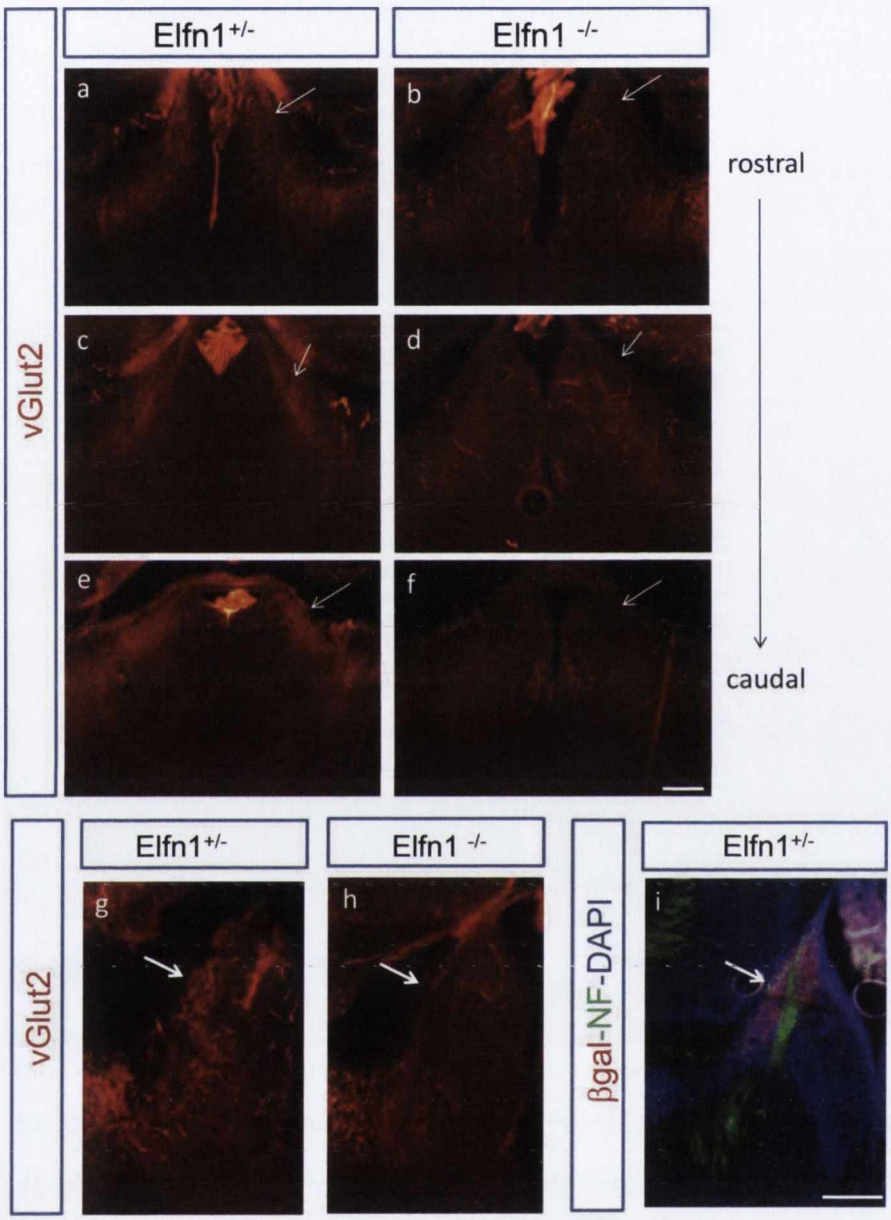

Figure 6.5 Reduced vGlut2 immunoreactivity in the habenula of Elfn1$^{-/-}$ mice. (a-f) vGlut2 stainings in sections through the habenula show a decreased intensity in the Elfn1$^{-/-}$ brain, particularly in the dorsolateral MHb and the dorsal LHb (arrows). (h-i) vGlut2 positive boutons on somata in wildtype habenula are absent in the Elfn1-/- mouse (n=1). This region of innervation coincides with cells expressing Elfn1.Scale bar: 100 microns

Another possibility is that there is a subtle phenotype that we have not discovered yet and would require a more detailed investigation of *Elfn1* expressing cells at a higher magnification. The morphology of axonal and dendritic processes is highly important for establishing functional synaptic circuits, and would necessitate confocal laser imaging or alternatively, an *in vitro* investigation of Elfn1-expressing neuronal cells in culture. Thirdly, a phenotype may not present at the particular time-point of analysis. The investigation in this study occured at post-natal day (P0) and the absense of Elfn1 throughout the development of the brain provided the opportunity for possible compensatory mechanisms to mask a phenotype. Due to this, analysis at earlier time-points may reveal transient abnormalities.

The investigation for a phenotype would benefit greatly from the use of an Elfn1-specific antibody, the lack of which has hindered progress on the comprehensive analysis of the *Elfn1* knockout mouse. The βgal marker identifies the cell bodies expressing Elfn1, however, the localisation of the Elfn1 protein to the specific region of the cell in which it is functioning, and the cells to which Elfn1 is interacting would isolate regions for higher magnification analysis.

6.3.2 Altered synaptic transmission in the habenula

Initial investigation suggests that the absence of Elfn1 in the habenula reduces excitatory transmission onto this region. Sylwestrak and Ghosh (2012) found that when Elfn1 was knocked down in the hippocampus, short-term facilitation was dramatically reduced. Taken together, we speculate that Elfn1 is functioning in a similar role in the habenula in the modulation of presynaptic glutamatergic release.

Both the medial and lateral habenula exert an inhibitory influence on the mid- and hindbrain monoaminergic nuclei. The MHb functions indirectly through the inhibitory cells of the IPN, and the lateral habenula directly innervates mostly GABAergic cells in the ventral tegmental area, substantia nigra and raphe nuclei. In these regions, the delicate balance of inhibition and excitation underlies normal

functioning in many different brain areas and in many different behaviours (see section 4.1.2). We speculate that in the Elfn1$^{-/-}$ mutant, a decrease in excitiatory transmission to the habenula, leads to a decrease in transmission from the habenula which in turn would manifest as a decrease in inhibition of dopaminergic nuclei of the ventral tegmental area and substantia nigra and serotonergic nuclei of the dorsal and medial raphe. Decreased transmission from the habenula has resulted in alterations in behaviours in relation to pain, stress, anxiety, sleep, reward, as well as cognitive and motor dysfunctions (reviewed in (Lecourtier and Kelly 2007). Therefore, this preliminary result provides the physiological basis for for a behavioural phenotype in the Elfn1 knockout mice.

If the lack of Elfn1 is causing a defect at the synaptic level and producing alterations in neuronal transmission, this can lead to a refinement of dendritic spines with altered shapes, densities and branching (He et al. 2012). This lends weight to the one of the possibilities mentioned earlier that a morphological phenotype may not yet be discovered. The dendrites of Elfn1 expressing cells in the habenula, and axonal arbors of contacting cells should be analysed for a phenotype in Elfn1$^{-/-}$ mice.

6.3.3 Conclusion

The results in this chapter show that cell morphology and neuronal connectivity in the Elfn1 knockout mouse appear normal. However, analyses thus far have involved comparing heterozygous and homozygous mutant mice at a gross level and lack more detailed and focused investigations. Indeed, the function of *Elfn1* in synaptic transmission, and the decrease in vGlut2 observed in Elfn1$^{-/-}$ mice leads to the hypothesis that there may be alterations in neuronal process morphology in *Elfn1* expressing regions. The reduction in vGlut2 immunoreactivity indicates a decrease in excitatory transmission onto the habenula in the absense of Elfn1. Excitingly, this result suggests that there is a reduction in transmission from the habenula, decreasing its inhibitory influence on monoaminergic nuclei, which would potentially result in behavioural abnormalities.

7 Chapter 7 Behavioural analyses of the *Elfn1* mutant mouse

7.1 Introduction

Elfn1 is expressed in a subset of cells in the hippocampus and cortex, and in distinct regions that are interconnected to form the basal ganglia and habenula circuitries. These results have led to our hypothesis that Elfn1 is involved in neural connectivity in various brain regions. Due to this, we speculate that removing the function of Elfn1 may have behavioural consequences. Anatomical analyses have not revealed a morphological phenotype and a behavioural phenotype would support a role for Elfn1 in the function of particular neural networks.

Mutations affecting neurodevelopment can result in neurological or psychiatric disorders and defects in cell migration, axon guidance and synaptogenesis have been shown to result in disorders such as schizophrenia, autism spectrum disorder, Tourette's syndrome and epilepsy (Mitchell 2011, Gatto and Broadie 2010, Engle 2010, Valiente and Marin 2010). Furthermore, mutations in LRR-containing proteins have been linked with neurological and psychiatric disorders (see section 1.3.4). The Elfn1 mutant mice were observed in their home cage and during handling to detect any major and obvious behavioural phenotypes. However, further behavioural tests were chosen based on the specificity of Elfn1 expression in the habenula circuitry and all the behaviours attributed to this system.

The habenula connects neuronal networks of the limbic forebrain and basal ganglia to midbrain areas that are involved in the release of dopamine (ventral tegmental area and substantia nigra) and serotonin (median and dorsal raphe nuclei) (Bianco and Wilson 2009). More specifically, the habenula has been shown to exhibit an inhibitory influence on both dopaminergic and serotonergic nuclei (Nishikawa et al. 1986, Park 1987). Studies have identified that stimulation of the lateral habenula results in the inhibition of midbrain dopamine-containing neurons and serotonergic neurons (Christoph et al. 1986, Wang and Aghajanian 1977). Conversely, lesions of the lateral habenula have been shown to increase the activation of dopaminergic and serotonergic neurons (Lecourtier and Kelly 2005,

Yang et al. 2008). While the majority of cells in the lateral habenula are glutamatergic, they are proposed to exert an inhibitory influence as a result of the activation of GABAergic interneurons which in turn inhibit the dopaminergic and serotonergic neurons (Ji and Shepard 2007, Wang and Aghajanian 1977). Additionally, the LHb also projects strongly to the ventromedial mesopontine tegmentum (RMTg) which has been identified as GABAergic and projects to the midbrain dopaminergic system (Geisler and Trimble 2008, Jhou et al. 2009). The MHb axons innervate the IPN, and the dorsal tegmental region and raphe nuclei are the major efferent targets of the IPN. Transmission from the MHb is entirely excitatory (Qin and Luo 2009). However, the majority of cells in the IPN are GABAergic (Kawaja et al. 1989) and therefore it is suggested that the MHb also exerts an inhibitory influence on these systems indirectly through the IPN (Gioia et al. 1994). The importance of this structure is fast becoming recognised due to this vital role in regulating dopaminergic and serotonergic transmission in the brain, and consequently the influence it exerts on many different behaviours such as motor activity, sleep, stress, pain, anxiety, spatial learning and attention (Klemm 2004, Lecourtier and Kelly 2007) while its dysfunction has been linked to psychological conditions such as depression, schizophrenia, anxiety and drug addiction (Li et al. 2011, Shepard et al. 2006, Baldwin et al. 2011, Murphy et al. 1996) and reviewed in Bianco and Wilson (2009).

The role of the habenula in the above mentioned motor and cognitive behaviours has derived from studies involving lesions, electrical and chemical stimulation, pharmacological inactivation, electrophysiology and *in vivo* microdialysis (Nair et al. 2012). There have been many investigations involving lesions of the habenula, and in particular, the LHb. Subsequent phenotypes have included reduced award seeking behaviour (Morissette and Boye 2008), disturbances in attention (Lecourtier and Kelly 2005), improvement in rat models of depression (Yang et al. 2008) and increased exploratory behaviour and locomotor activity (Lee and Huang 1988). Furthermore, lesions of the fasciculus retroflexus caused disruption in REM and non-REM sleep (Haun et al. 1992), and increased locomotion and anxiety (Murphy et al. 1996). Due to the small size of the habenular nuclei, particularly the MHb, many lesions studies include both the MHb and LHb, one of which resulted in impairments in spatial learning and memory

(Lecourtier et al. 2004). The electrical stimulation of the habenula has been shown to produce analgesia (Cohen and Melzack 1993). However, there are many inconsistencies across studies of habenula function. In contrast to the results from lesions studies, electrical stimulation of the habenula has also been shown to reduce award seeking behaviour (Friedman et al. 2011) and produce improvements in rat models of depression (Meng et al. 2011). The inconsistencies are in-part attributable to the fact that the monoamine systems are continually maturing up until early adulthood (Andersen 2003) and, therefore, the timing of an interruption in circuitry can produce different outcomes. One particular study identified that lesions in the fasciculus retroflexus performed at P3 produced a heightened anxiety phenotype, whereas rats lesioned at P70 did not show this phenotype (Murphy et al. 1996). The timing of the behavioural tests after habenula circuitry has been impaired is also crucially important. A neonatal lesion in both the MHb and LHb resulted in hyper-locomotion in juvenile rats, but this phenotype had disappeared when the rats had reached adulthood (Lee and Goto, 2011). This is suggestive of compensatory mechanisms being utilised and the age of the animal may correlate with differential abilities to compensate for deficits in function.

The emerging concept in studies of the habenula is that the paired nuclei of the MHb and LHb are comprised of multiple subnuclei (Aizawa et al. 2012). Furthermore, inputs from the limbic brain regions and the basal ganglia converge on distinct subnuclei (see chapter 4). Likewise, descending projections from the MHb and the LHb have shown topographically organised innervation of their targets (Kim 2009) which further supports the idea that there are subcircuits functioning in the habenula (reviewed in chapter 4). This suggests that distinct microcircuits produce parallel pathways of information flow to the midbrain monoaminergic nuclei and that there is microcircuit-specific control of functions. Due to this, deciphering functions and behaviours attributed to the habenula will necessitate microcircuit-specific analyses. In light of this, a recent study employed an optogenetic strategy to selectively stimulate LHb-RMTg fibres which resulted in active, passive and conditioned behavioural avoidance, and disrupted positive reinforcement (Stamatakis and Stuber 2012).

Most research to date has involved the investigation of the LHb, whereas studies involving the MHb alone are rare due to its relatively small size. One such

study achieved a MHb-specific lesion by taking advantage of the high concentration of nicotinic receptors in this region which are absent from LHb (Carlson et al. 2001). The technique involved the microinfusion of nicotine directly into the MHb and the resultant lesion produced hyperlocomotion, impulsivity and attention deficit phenotypes. Interestingly, an attenuation of the hyperlocomotion phenotype was achieved after amphetamine administration (Lee and Goto 2011). Very recently, a mouse containing a MHb lesion was generated by genetic ablation of the Gpr151-expressing MHb cells, located in the ventral part of the MHb. Increased locomotion was detected in these mice in addition to failure to habituate, impulsivity and a slight increase in anxiety-like behaviour (Kobayashi et al. 2013). These lesions occur postnatally at the onset of Gpr151 expression. This particular study establishes a habenula cell-type specific role. The complete understanding of the function of the habenula and how it modulates behaviour will necessitate further microcircuit-specific investigation.

The expression of *Elfn1* in the habenula circuitry is highly localised and we speculate that it is involved in the connectivity of specific subcircuits. Due to the highly localised expression of Elfn1 in the MHb, the first test of behaviour proposed for the *Elfn1*$^{-/-}$ mice was for locomotion abnormalities due to the hyperactivity phenotype that was produced in rats that received a MHb-specific lesion (Lee and Goto 2011). One of the most commonly used tests of mouse behaviour is the open field test (Walsh and Cummins 1976) which involves removing the mouse from its home cage, and placing into a walled open field for observation. It allows for the testing of unconditioned behaviour, and is useful for the study of locomotor and exploratory behaviour but can also be used to investigate anxiety-like behaviour (Carola et al. 2002), and the effects of pharmacological agents (van den Buuse and de Jong 1989, Menard and Treit 1996, Choleris et al. 2001).

The other area of interest in the extended habenula circuit is the globus pallidus owing to the high expression of *Elfn1* in this structure. The globus pallidus consists of an external segment and an internal segment called the entopeduncular necleus (EP) and it is from here that the LHb receives the majority of its input. The habenula, therefore, functions in intergrating the basal ganglia and the monoaminergic systems. The globus pallidus itself is a component of the basal

ganglia which includes the striatum, substantia nigra and subthalamic nucleus and collectively they are involved in the control of voluntary movement. Disturbances in function of the basal ganglia can give rise to various motor disorders (DeLong 1990, Vitek and Giroux 2000, Albin et al. 1989), many of which have been attributed to changes in dopaminergic activity (Mehler-Wex et al. 2006). To test for motor coordination and/or strength deficits in the Elfn1 knockout mice, the wire hang test (Rafael et al. 2000) was completed.

Elfn1 is expressed in somatostatin (SST)-containing interneurons of the hippocampus where it functions in the determination of synapse-type from the presynaptic pyramidal cell. The knockdown of Elfn1 in the hippocampus produced a reduction in synaptic strength (Sylwestrak and Ghosh 2012). With this in mind, we speculate that the complete loss of Elfn1 during development may affect the normal and delicate balance of excitation and inhibition which can result in seizure activity. This study has also determined that Elfn1 is expressed in SST-containing cells in the neocortex and piriform cortex, and both are regions known to exhibit epileptogenic activity (Milton 2012, Panuccio et al. 2012). Due to this, mice were observed over the course of several months under normal conditions, during handling and during cage changes in order to detect any possible seizure-like behaviour.

7.1.1 Aims of this chapter

The primary aim of this study was the investigation for possible behavioural phenotypes in the *Elfn1* mutant mouse. Expression analyses of Elfn1 has also led us to investigate general locomotion and movement abilities in the mutant mice, with the hypothesis that normal functioning of the habenula and basal ganglia are disrupted in the absense of *Elfn1*. Additonally, the identified function for *Elfn1* at CA1-interneuron synapses may result in disruption to excitation-inhibition balance in the *Elfn1* mutant mouse that could manifest in seizure-like activity. Behavioural tests included the the open field test which allows for the investigation of general locomotor activity and anxiety in the mice, while the wire-hang test was used to assess motor strength and/or coordination in the Elfn1 mutant mice. Mice were

observed in their home cages and during the mildly stressful circumstances of cage changes to detect any gross abnormalities in behaviour.

7.2 Results

7.2.1 Seizures in *Elfn1*$^{-/-}$ mice

A total of six seizures have been witnessed during routine cage changes in *Elfn1*$^{-/-}$ mice. These animals have been aged between 4 and 9 months old and included both males and females. Seizures described by the animal facility technicians have ranged from a score of 2 to a score 5 of the modified Racine's seizure scoring system (see section 2.11.4) with one animal losing postural control during the seizure, and another displaying rapid running and jumping. It is important to note that with the exception of an Adam23 knockout mouse line, known to exhibit severe temors (Leighton et al. 2001), seizures have never been observed in any of our mice lines in the facility over the last ten years.

In a three minute observation test (Papaleo et al. 2011), two out of eight *Elfn1*$^{-/-}$ mice and zero out of eight Elfn$^{+/-}$ mice displayed seizures when placed in a clean and empty cage. One seizure represented a score of 4 in the modified Racine's seizure scoring system with freezing immediately upon placement in the new cage, followed by bilateral forelimb clonus that lasted 33 seconds before motor control was regained. The second observed seizure also began with motor arrest, followed by head bobbing and mild shaking for 22 seconds. This seizure corresponds to a score of 2 in the modified Racine's seizure scoring system.

7.2.2 Reduced performance of *Elfn1*$^{-/-}$ mice in motor coordination and strength testing

In the wire-hang test, *Elfn1*$^{-/-}$ mice were less successful than the *Elfn1*$^{+/-}$ mice at completing the task (62.5% vs 91.67%, n = 8 mice/genotype; 3 trials per animal; p = 0.0363) (Figure 7.1a). Moreover, when successful trials were

compared across the 2 groups of mice, the time taken to reach a pole was significantly longer for the *Elfn1*$^{-/-}$ mice (18.47s ± 3.13, n = 15) than the *Elfn1*$^{+/-}$ mice (10.0s ± 1.02, n = 22; $p = 0.0054$) (Figure 7.1b).

Post hoc analysis revealed that all successful trials in heterozygous animals were completed with the use of 4 limbs. However, in 4 of the 15 successful trials carried out by *Elfn1*$^{-/-}$ mice, only the forelimbs were used to reach the poles after initial attempts to raise the hindlimbs onto the wire failed. In the 9 failed trials carried out by *Elfn1*$^{-/-}$ mice, the animals did not manage to raise their hindlimbs onto the wire, and subsequently fell off. These findings collectively indicate that *Elfn1*$^{-/-}$ mice exhibit reduced motor strength and/or coordination.

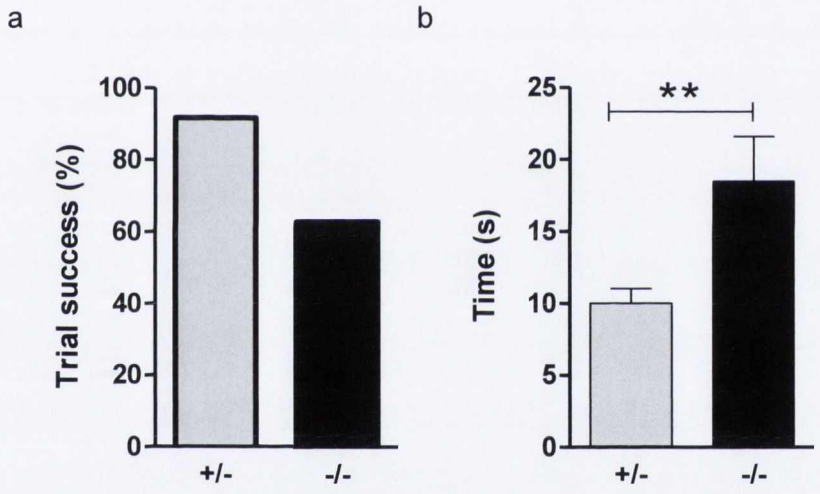

Figure 7.1 Motor performance of *Elfn1*$^{+/-}$ and *Elfn1*$^{-/-}$ mice in the wire-hang test. **(a)** *Elfn1*$^{+/-}$ mice completed the trial with a success rate of 91.67%, *Elfn1*$^{-/-}$ mice were only successful in 62.5% of the trials (n = 8/genotype; 3 trials per mouse; $p = 0.0363$). **(b)** The time taken to complete a successful trial was analysed, and *Elfn1*$^{-/-}$ mice took considerably longer to reach a pole ($p = 0.0054$). Data expressed as mean ± SEM (n = 22 for *Elfn1*$^{+/-}$ and n = 15 for *Elfn1*$^{-/-}$ *mice*). Student's t test was used to compare the means.

7.2.3 Elfn$^{-/-}$ mice exhibit hyperlocomotion

Activity behaviour was examined in two cohorts of male mice. The first cohort contained eight mice of each genotype (homozyous mutant and heterozygous), aged 3-4 months and the second contained ten mice of each genotype, aged 2-3 months (Appendix 9.1).

For the first trial of open field testing (Experiment 1), mice from cohort number 1 were placed in a rectangular box with a grid marked out on the floor. The dimensions of this box were (30cm x 50cm x 18cm) with an internal grid consisting of 15 squares (10cm x 10 cm each). The number of line crosses were noted over 3 minutes, and taken as an indication of activity. Student's t test was used to determine the significance of differences between the two groups, and demonstrated increased locomotion in *Elfn1*$^{-/-}$ mice (132.5 $\pm$ 10.11, n = 8) compared with the *Elfn1*$^{+/-}$ mice (97.88 ± 5.75, n = 8; p = 0.01) (Figure 7.2a). The following day, locomotor activity was measured again in the same field to analyse activity after habituation. The student's t test analysis showed that while activity levels decreased across both genotypes, the mean level of activity remained higher in *Elfn1*$^{-/-}$ mice (90.13 $\pm$ 13.32, n = 8) compared with the *Elfn1*$^{+/-}$ mice (67.38 ± 5.62, n = 8; Figure 7.2b) but did not reach statistical difference (p = 0.138). Confirmation of the increased actiivity in a new open field environment again revealed significantly higher activity in *Elfn1*$^{-/-}$ mice (120.1 $\pm$ 12.55 vs 71.13 $\pm$ 4.53, n = 8; p = 0.0025) (Figure 7.2c). The second testing box was bigger in size (34cm x 60cm x 20cm) with a grid consisting of 18 squares (9.5cm x 11cm each).

When the activity trials from the three experiments are accumulated, providing 24 activity values for each genotype, a student's t test for genotype differences confirms that *Elfn1*$^{-/-}$ mice have substantially higher activity levels (114.3 $\pm$ 7.62 vs 78.79 $\pm$ 4.08, n = 24; p = 0.0002).

The second cohort of mice were tested for differences in activity using EthoVision software (Experiment 2). The set-up for this experiment consisted of an open field box (34cm x 53cm x 18cm) placed within a white circular tank (60cm in height) in the centre of a brightly lit room. Video tracking equiptment was fixed on the ceiling above the open field. On day 1, evaluation of the distance travelled over a 10 minute duration using student's t test did not show statistical difference (5701

± 278.8 for *Elfn1*$^{-/-}$ and 5108 ± 222.4 for *Elfn1*$^{+/-}$, n = 10/genotype; p = 0.1141) (Figure 7.3a). However, as noted with cohort number 1, the mean activity levels of *Elfn1*$^{-/-}$ mice are higher than for *Elfn1*$^{+/-}$ mice. On the second day of testing, the activity levels of both genotype groups had decreased (6% for *Elfn1*$^{-/-}$ mice and 7.79% for *Elfn1*$^{+/-}$ mice). However, there was also a significant difference in distance travelled by *Elfn1*$^{-/-}$ mice (5360 ± 149.4, n = 10) when compared with *Elfn1*$^{+/-}$ mice (4710 ± 248.6, n = 10; p = 0.0381) (Figure 7.3b).

Post-hoc analysis of day 1 revealed that when the distance was binned into 2 minute intervals, a significant difference is evident over the final 2 minutes when activity levels in *Elfn1*$^{+/-}$ mice have decreased considerably (1128.24 ± 52.69 for *Elfn1*$^{-/-}$ and 889.42 ± 40.36, n = 10; p = 0.0021) (Figure 7.4a). Likewise on day 2, post-hoc time-intervel analysis revealed a significant difference at 4-6 minutes (p = 0.0024) and again over the final 2 minutes (p = 0.0067) (Figure 7.4b).

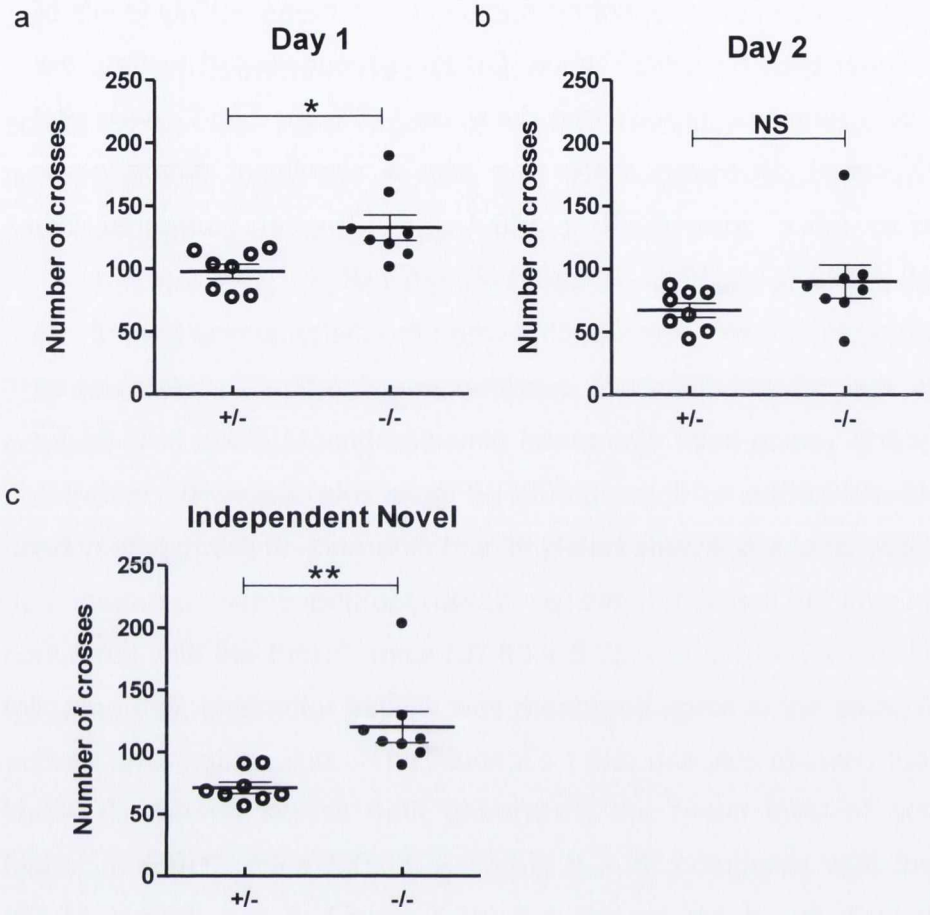

Figure 7.2 Hyperlocomotion of *Elfn1*$^{-/-}$ mice in experiment 1.

(a) The number of crosses on day 1 of open field testing was significantly higher for *Elfn1*$^{-/-}$ mice than in *Elfn1*$^{+/-}$ mice (p = 0.01; n = 8/genotype). **(b)** On day 2, in the same open field, there was no significant difference between the groups (p = 0.138) but the mean number of crosses remained higher for *Elfn1*$^{-/-}$ mice (90.13 ± 13.32) versus *Elfn1*$^{+/-}$ mice (67.38 ± 5.62; n = 8/genotype). **(c)** Introduction to a novel environment again confirmed a higher number of crosses in *Elfn1*$^{-/-}$ mice versus *Elfn1*$^{+/-}$ mice (p = 0.0025; n = 8/genotype). Student's t test was used to compare the means.

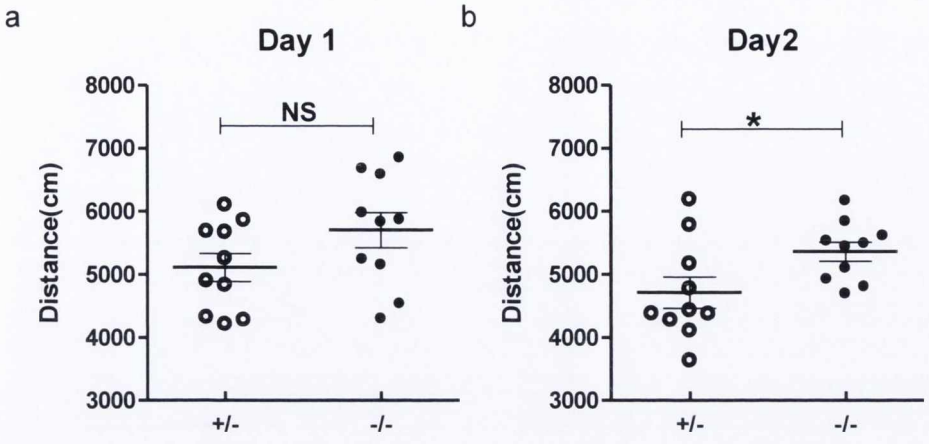

Figure 7.3 Increased locomotion in *Elfn1*$^{-/-}$ mice in experiment 2.

(a) Statistical analysis revealed no significant difference between the groups however, the mean distance travelled by *Elfn1*$^{-/-}$ mice was greater than by *Elfn1*$^{+/-}$ mice (5701 $\pm$ 278.8 for *Elfn1*$^{-/-}$ and 5108 $\pm$ 222.4 for *Elfn1*$^{+/-}$, n = 10/genotype; *p* = 0.1141). **(b)** On day 2, in the same open field, *Elfn1*$^{-/-}$ mice travelled a significantly greater distance than *Elfn1*$^{+/-}$ mice (p = 0.0381; n = 10/genotype).

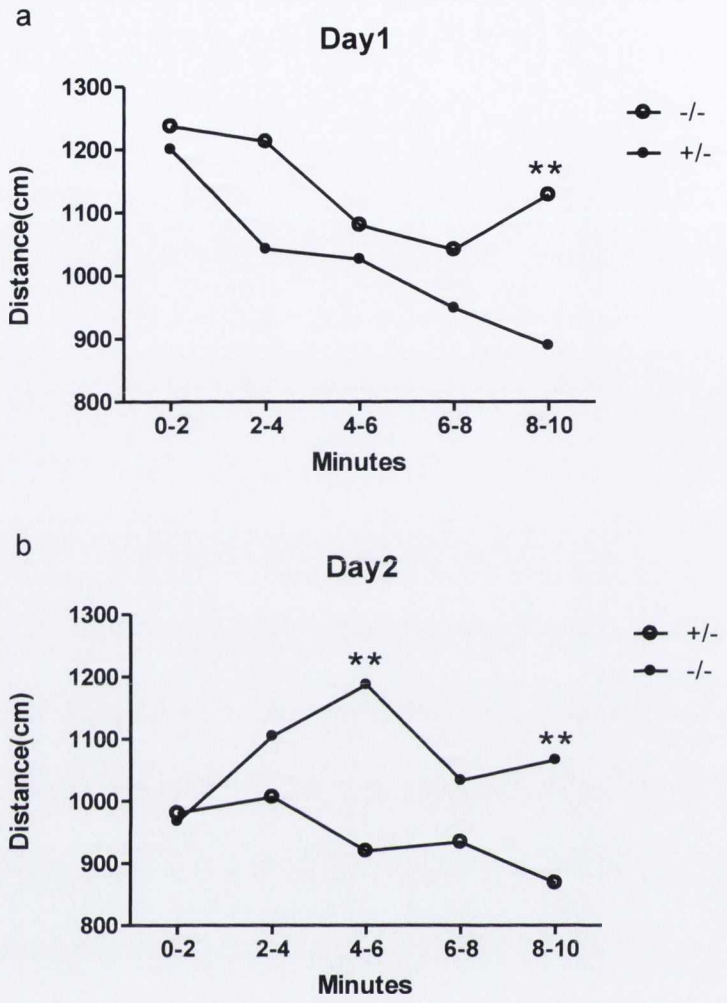

Figure 7.4 Locomotion of *Elfn1*$^{-/-}$ and *Elfn1*$^{+/-}$ mice over time in experiment 2.
(a) On day 1, the mean distance travelled by *Elfn1*$^{-/-}$ mice remained higher over the 10 minutes, and a significant difference between the genotypes is evident in the final 2 minute bin (p= 0.0021; n=10/genotype). **(b)** On day 2, a significant difference between groups in the mean distance travelled is identified at the 4-6 minute and 8-10 minute time bins (p = 0.0024 and p = 0.0067 respectively). All data expressed as means, and student's t test used to analyse statistical difference betwen the groups. Post-hoc analysis is not corrected for multiple testing.

7.2.4 Reduced thigmotaxis in *Elfn1*$^{-/-}$ mice

During open field behavioural testing, ethovision analysis revealed that *Elfn1*$^{-/-}$ mice exhibited a reduction in wall-hugging behaviour or thigmotaxis. The percentage of total time spent in the centre of the open field was significantly higher in *Elfn1*$^{-/-}$ mice (25.34 $\pm$ 1.88, n = 10) compared with the *Elfn1*$^{+/-}$ mice (16.12 ± 1.95, n = 10; p = 0.0031) (Figure 7.5a). The percentage of total distance travelled in centre of the open field was also significantly higher for *Elfn1*$^{-/-}$ mice (28.15 $\pm$ 1.60, n = 10) than for *Elfn1*$^{+/-}$ mice (21.82 ± 1.99, n = 10) (p = 0.023; Figure 7.5c). This behavioural phenotype was observed again on day 2 of testing with *Elfn1*$^{-/-}$ spending more time in the centre zone (21.86 $\pm$ 1.35 vs 15.13 ± 2.90 n= 10/genotype; p = 0.0496) (Figure 7.5b). Locomotion in the centre zone also remained significantly higher in *Elfn1*$^{-/-}$ mice (28.12 $\pm$ 1.30 vs 20.11 ± 2.33, n = 10/genotype; p = 0.0076) (Figure 6.5d). While thigmotaxic behaviour in *Elfn1*$^{+/-}$ mice remained relatively unchanged on day 2, *Elfn1*$^{-/-}$ mice displayed a slight increase in time spent in the periphery of the field.

Within each analysis of time spent and distance moved in the centre zone, an *Elfn1*$^{+/-}$ outlier was identified. One *Elfn1*$^{+/-}$ mouse displayed a value >2 standard deviations above the group mean for time spent in the centre zone, and repeated this behaviour on day 2. Likewise, another mouse travelled further in the centre zone with a distance >2 standard deviations above the group mean, with a similar value on day 2 (Figure 7.5). When both outliers are removed from statistcal analysis for differences between the two genotypes, a p value of 0.0001 is achieved for both time spent in the centre zone and distance travelled in the centre zone.

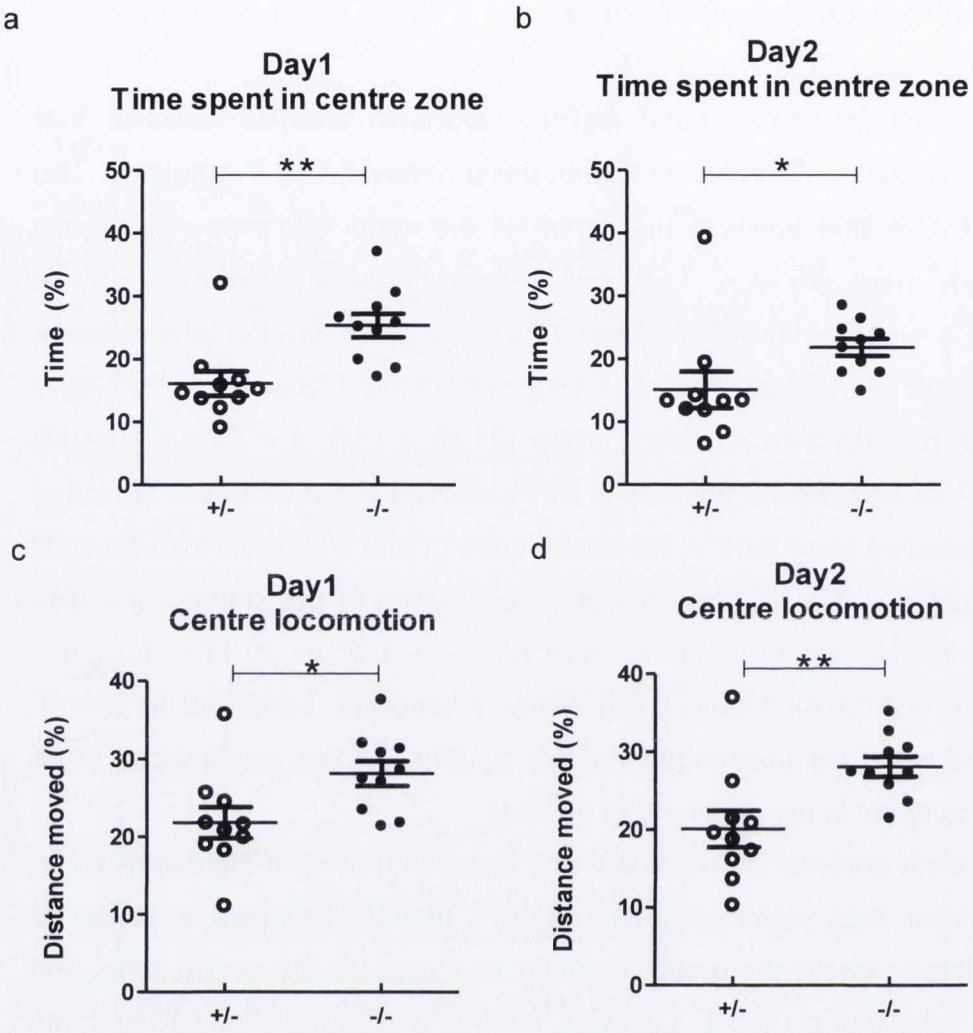

Figure 7.5 Reduced thigmotaxis in *Elfn1*$^{-/-}$ mice.

(a,b) Percentage of total time spent in the centre zone on day 1 (a) and day 2 (b). *Elfn1*$^{-/-}$ mice spent more time in the centre zone than *Elfn1*$^{+/-}$ mice on both days (p = 0.0031 for day 1, and p = 0.0496 for day 2; n = 10/genotype). **(c,d)** Percentage of total distance travelled in the centre zone on day 1 (c) and day 2 (d). *Elfn1*$^{-/-}$ mice travelled further than *Elfn1*$^{+/-}$ mice in the centre zone on both days (p = 0.023 for day 1 and p = 0.0076 for day 2). Student's t test used to identify statistical diference between the groups.

7.2.5 Attenuation of hyperlocomotion with amphetamine

Amphetamine (AMPH) has been shown to increase extracellular dopamine levels (Sulzer 2011). The resultant increase in dopamine levels induces hyperactivity in normal subjects (Costall et al. 1984) and exacerbates psychotic-like hyperactivity (van den Buuse and de Jong 1989, Drevets et al. 2001, Laruelle et al. 1996). Conversely, stimulant medication attenuates hyperactivity in children with attention-deficit/hyperactivity disorder (ADHD) (Butte et al. 1999, Brown et al. 2005). Due to this, the effects of amphetamine treatments were examined in the Elfn1 knockout mice. As there are dose-dependent effects of amphetamine on activity (bell shaped curve) we started with a low dose of 0.5mg/kg on all mice in cohort 1 (Lee and Goto 2011). The number of crosses for each mouse before and after amphetamine were compared. A time delay of one week between testing in the same open field has been shown to restore novelty-induced behaviours (Kalueff et al. 2006).

The percentage increase or decrease in the number of line crosses per animal after 0.5mg/kg AMPH was evaluated in a student's t test for genotype differences and results revealed a paradoxical attenuation of hyperactivity in *Elfn1*$^{-/-}$ mice with a mean decrease in locomotion (91.13% $\pm$ 10.17 n = 8) and a mean increase in locomotion, as expected, in *Elfn1*$^{+/-}$ mice (138.3% ± 13.87 n= 8; p = 0.0159) (Figure 7.6c).

The effect of a higher dose of amphetamine (2.0mg/kg) was tested with the second cohort of mice. Experimental design was altered for this test. All animals recieved both a saline injection (control) and an injection of amphetamine (1 week apart) and tested in the open field 15 minutes after administraton. On the first day, 5 *Elfn1*$^{-/-}$ and 5 *Elfn1*$^{+/-}$ mice received amphetamine, while the other 5 *Elfn1*$^{-/-}$ and 5 *Elfn1*$^{+/-}$ mice recieved saline. The following week, administrations of saline and amphetamine were swapped. The higher dose of amphetamine produced a significant decrease in locomotion in the *Elfn1*$^{-/-}$ mice (48.83 $\pm$ 9.363, n = 9; p = 0.0029), however, the expected increase in activity of *Elfn1*$^{+/-}$ mice did not occur (99.46 ± 10.97, n = 10) (Figure 7.6d). Post-hoc analysis revealed a considerable *Elfn1*$^{+/-}$ outlier >2 standard deviations below the group mean (Figure 7.6b) and

when removed from statistical analysis, the percentage increase in activity of *Elfn1*$^{+/-}$ mice rises to 108.14%, producing a *p* value of 0.0001.

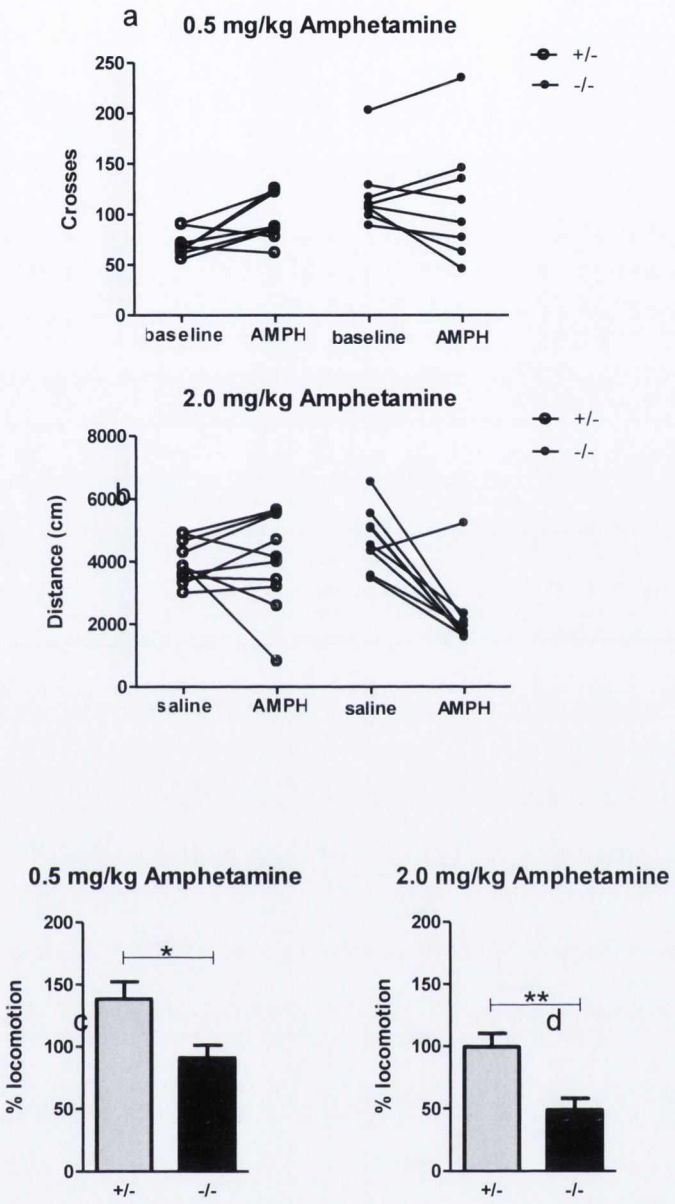

Figure 7.6 Reduced locomotion in *Elfn1*$^{-/-}$ mice with Amphetamine.

(a) Graph shows number of crosses before and after 0.5mg/kg AMPH for each mouse in experiment 1 (n = 8/genotype). *Elfn1*$^{+/-}$ (white circles), *Elfn1*$^{-/-}$ (black circles). **(b)** Graph depicts differences in distance travelled by each mouse when administered saline and 2.0mg/kg AMPH in experiment 2 (n = 10 *Elfn1*$^{+/-}$, 9 *Elfn1*$^{-/-}$). **(c,d)** The mean percentage distance travelled by *Elfn1*$^{+/-}$ and *Elfn1*$^{-/-}$ mice after 0.5mg/kg (c) and 2.0mg/kg (d) of AMPH. Student's *t* test *p* value = 0.0159 for 0.5mg/kg and *p* = 0.0029 for 2.0mg/kg (n = 10 *Elfn1*$^{+/-}$, 9 *Elfn1*$^{-/-}$).

7.3 Discussion

7.3.1 Behavioural abnormalities in *Elfn1*$^{-/-}$ mice

Preliminary observations suggest that *Elfn1*$^{-/-}$ mice can experience seizures precipitated by cage transfer that ranged in severity and are analogous to clinical partial seizures. With the exception of an Adam23 knockout mouse line, known to exhibit severe tremors (Leighton et al. 2001), seizures have never been observed in any of our mice lines in the facility over the last ten years (>3000 mice). However, seizures were not observed in all of the *Elfn1*$^{-/-}$ mice. There are two explanations for this, the first being that all of the *Elfn1*$^{-/-}$ mice are indeed having seizures but just not while being observed. On the other hand, there may be incomplete penetrance of the phenotype which would suggest that seizure activity is not directly caused by the loss of Elfn1. Furthermore, the seizures were all identified in mice older than 4 months old and therefore age could be a contributing factor in lowered seizure threshold.

A function for *Elfn1* was identified in specifying target-specific differential transmission in the hippocampus where the loss of *Elfn1* in knockdown experiments reduces short term facilitation (see section 4.1.2). This provides a potential explanation for the seizure activity in *Elfn1*$^{-/-}$ mice as abnormal alterations in the regulation of synaptic transmission is known to be a cause of seizure activity (Casillas-Espinosa et al. 2012, Fukata et al. 2010, Kalachikov et al. 2002). However, it might be expected that if the loss of Elfn1 produced an acute effect resulting in seizures that the penetrance would be higher, and occur at an earlier age. A more likely explanation is that abnormalities at the synapse due to the lack of Elfn1 may set into motion long-term progressive effects that eventually lead to a seizure-prone brain. The lack of observed seizure activity in young mice would support this theory. Therefore, we suggest that lack of Elfn1 causes epileptogenesis in the brain that may be precipitated by altered synaptic transmission to inhibitory interneurons. This may in turn lead to compensatory mechanisms further altering the delicate balance of inhibition and excitation which eventually lead to the seizure-susceptible brain (Walker et al. 2002).

Epileptogenesis has been shown to be induced over time after initial acute brain insults such as brain injury, neurodegenerative diseases and stroke (Loscher and Brandt 2010). Further investigation is needed to elucidate why the Elfn1 mice display spontaneous seizures, and where seizure activity is occurring. Elfn1 is expressed in SST-containing interneurons in the hippocampus, neocortex and piriform cortex, all regions known to exhibit epileptogenic activity (Milton 2012, Panuccio et al. 2012). Characterisation of the seizure susceptibility of these animals with electroencephalogram (EEG) monitoring, followed by c-fos immunohistochemistry would identify the cells and neural networks involved. These neural networks could then be investigation for secondary adaptations in synaptic properties.

The substandard performance of *Elfn1*$^{-/-}$ mice in the hang wire test suggests a deficit in motor circuitry. Voluntary movements are initiated in the cells of the cerebral motor cortex which innervate the spinal motor neurons that in turn project to the muscles. The projections pass via numerous subcortical circuits such as the basal ganglia which can alter the descending signal (Groenewegen et al. 1986). The importance of the basal ganglia in coordinated control of movement is apparent in Parkinson's disease where there is degeneration in the dopamine-containing cells of the substantia nigra pars compacta and in Huntington's disease which involves damage to the striatum (Stocco et al. 2010). Elfn1 is highly expressed in the globus pallidus and localised to axons innervating the substantia nigra pars compacta. However, the wire-hang test is a very simple and inexpensive means for preliminary investigation of a motor-associated phenotype however it is not possible to relate the outcome to a specific deficit such as motor strength, coordination or fatigue. Due to this, the role *Elfn1* plays in normal motor function will need further investigation.

7.3.2 *Elfn1* mice exhibit increased locomotion

Elfn1$^{-/-}$ mice repeatedly exhibit increased locomotion when compared to *Elfn1*$^{+/-}$ mice in 5 open field trials, three different open field boxes and with two cohorts of animals.

In experiment 1, a significant difference in locomotion between the genotypes was idenified (p = 0.01; figure 7.1a). The following day, as a part of experiment number 1, locomotion was measured again in the same open field to evaluate behaviour after habituation. It is expected that habituation to the environment would manifest as a decrease in spontaneous activity in normal mice. This was the case with the *Elfn1*$^{+/-}$ mice with a mean decrease of 31.16%, and the *Elfn1*$^{-/-}$ mice equally reduced their locomotion (decrease of 31.98%). Statistical analysis did not show a significant genotype difference on day 2 (p = 0.138), however, the mean value of locomotion remained considerably higher for *Elfn1*$^{-/-}$ mice (90.13 $\pm$ 13.32) versus *Elfn1*$^{+/-}$ mice (67.38 $\pm$ 5.62) (figure 7.1b). These results demonstrate that *Elfn1*$^{-/-}$ mice decrease spontaneous activity upon habituation to an environment but the baseline level of locomotion remains higher than normal. The increased locomotion phenotype was confirmed again with a third trial in a new open field arena (p = 0.0025), a greater difference in activity between the genotypes most likely attributed to the larger open field arena.

In experiment 2, using ethovision analysis software, we found that *Elfn1*$^{-/-}$ mice travelled a greater mean distance in 10 minutes compared with *Elfn1*$^{+/-}$ mice (5701cm $\pm$ 278.8 versus 5108cm $\pm$ 222.4). We confirmed that this difference in locomotion is not novelty dependent (p = 0.0381 on day 2) unlike the hyperactivity phenotype in the DAT$^{-/-}$ mouse (Giros et al. 1996) and the $GABA_{B1}^{-/-}$ mouse (Vacher et al. 2006). Post hoc analysis of two minute time bins verified this conclusion. If the increased behaviour was novelty dependent, the first 2 minutes would be expected to show the highest difference in locomotion which is not the case with the *Elfn1*$^{-/-}$ mice (Figure 7.4). Analysis of the final 2 minutes found an increase in activity of *Elfn1*$^{-/-}$ mice which is opposed to the decrease in activity over time (habituation) displayed by *Elfn1*$^{+/-}$ mice (figure 7.4). This would indicate a lack of habituation within 10 minutes of open field testing. However, In contrast to this, *Elfn1*$^{-/-}$ mice displayed a decrease in overall locomotion equivalent to that of Elfn$^{+/-}$ mice on day 2 of both experiments, which may indicate a delayed habituation process. The results of these analyses, taken together, suggest that it is unlikely that this phenotype is novelty dependent or due to a deficit in habituation and more likely a general hyperactivity phenotype. Hyperactivity in a familiar environment is

a symptom of Attention Deficit Hyperactivity Disorder (ADHD) and has been linked to impaired modulation of the dopaminergic system (Sagvolden et al. 2005a).

7.3.3 Reduced thigmotaxis in *Elfn1*$^{-/-}$ mice

Mice are a prey species and remain at the periphery of a new environment (thigmotaxis), avoiding open spaces to evade danger. In the open field test, a reduction in thigmotaxis observed in the *Elfn1*$^{-/-}$ mice is considered a reduced anxiety phenotype (Figure 7.5). This behavioural phenotype of hyperactivity with reduced anxiety have included Girk2$^{-/-}$ mice, which lack postsynaptic responses to several neurotransmitters (Blednov et al. 2001), A53T mutant of alpha-synuclein (shown to interact with the dopaminergic system)(Graham and Sidhu 2010). Increased locomotor activity has been found in D3 dopamine receptor mutant mice (Accili et al. 1996) as well as reduced anxiety-like behaviour (Steiner et al. 1997).

It has been shown that suppressing activity in the lateral septum causes a decrease in anxiety (Menard and Treit 1996), and the bed nucleus of the stria terminalis (BNST) may mediate behavioural responses to perceived threats (Walker et al. 2003). Interestingly, the medial habenula receives inputs from the septal nuclei and the BNST (Figure 4.17). Although purely speculative, a decrease in excitatory transmission from these regions to the habenula (Figure 7.5) may underlie the anxiolytic effect seen in *Elfn1*$^{-/-}$ mice. In contrast to this, however, a number of studies have shown that habenula lesions give rise to increased anxiety-like behaviours (Murphy et al. 1996, Kobayashi et al. 2013). In the lesion models, disrupted transmission from the habenula are implemented postnatally and behavioural differences may be a consequence of the timing of compensatory methods to correct deficits. Moreover, as mentioned earlier in section 7.1, lesions are crude methods of disrupting transmission and it is likely that in the *Elfn1*$^{-/-}$ mouse a more subtle and microcircuit specific disruption is occurring. It is important to note that hyperlocomotor behaviour can be a result of decreased anxiety, however, further tests would be needed so that motor circuit abnormalities or cognitive function can be dissociated. Therefore, further investigation of the

mechanisms involved in the decreased anxiety-like phenotype in *Elfn1*$^{-/-}$ mice is needed.

7.3.4 Psychostimulant-induced attenuation of hyperlocomotion

A number of studies have shown that changes in the dopaminergic system correlate with changes in locomotor activity (Lecourtier et al. 2008, Beninger 1983, Kelly 1998). Amphetmaine causes an increase in dopamine levels producing hyperactivity in normal subjects (Costall et al. 1984) and enhances psychotic-like hyperactivity (van den Buuse and de Jong 1989, Drevets et al. 2001, Laruelle et al. 1996). However, stimulants have been shown to have a paradoxical effect on hyperactivity in children with attention-deficit/hyperactivity disorder (ADHD) (Butte et al. 1999, Brown et al. 2005). We tested the effects of amphetamine on the *Elfn1*$^{-/-}$ mice to establish if the hyperlocomotion phenotype was due to a deficit in the dopamine pathway. In addition, this trial facilitated testing for the amphetamine-induced paradoxical attenuation of hyperlocomotion seen in ADHD-like animal models and the MHb lesioned rat generated by Lee and Goto (2011).

Two different concentrations of amphetamine were tested on both Elfn$^{-/-}$ and *Elfn1*$^{+/-}$ mice. The lower dose of 0.5mg/kg produced a slight decrease in the mean level of locomotion of the *Elfn1*$^{-/-}$ and an increase as expected in the *Elfn1*$^{+/-}$ mice (Figure 7.6a,c). The higher dose of 2mg/kg produced a very significant attenuation of locomotion, reducing the mean distance travelled by 48.83%. Surprisingly, there appears to be no effect on locomotion in the *Elfn1*$^{+/-}$ mice (Figure 7.6b,d). There may be a dose-dependent intermediate phenotype in *Elfn1*$^{+/-}$ mice, and therefore, a repeat of this experiment with wildtype littermates should be performed.

Due to the hyperactivity phenotype and the paradoxical effect of amphetamine on locomotion in the *Elfn1*$^{-/-}$ mice, they are potentially an animal model of ADHD. However, more behavioural analyses are required to test for impulsivity and attention deficits in order to fit the criteria for an optimal animal model of ADHD (Sagvolden et al. 2005b). It is interesting to note that developmental coordination disorder (DCD) occurs in up to 50% of children with

ADHD (Flapper et al. 2006), and therefore additional characterisation of motor abnormalities in the *Elfn*$^{-/-}$ mice should be performed. Furthermore, the prevalence of ADHD has been shown to be between 3-7% in children, whereas at least 20% of children with epilepsy also have ADHD (Kaufmann et al. 2009). The association is not fully understood however one of the suggested reasons is a common genetic defect. The human relevance of these findings is that the Elfn1 mutant mouse could provide a model for the continued research on ADHD-associated behaviours and the underlying cause of specific aspects of this disorder. Furthermore, this research would be directly relevant for people that may have rare mutations in the Elfn1 gene.

8 Chapter 8 Conclusions and future directions

8.1 Final conclusions

8.1.1 eLRR superfamily

The main aim of this project was to identify novel proteins containing extracellular leucine-rich repeats (eLRRs) with a potential function in specifying neural connectivity in the developing brain. For this, we compiled a comprehensive list of eLRR proteins in human, mouse, fly and worm, and the resultant eLRR superfamily was classified into related families and sub-families. While this part of the project identified novel candidate genes for further study, it is also a valuable resource in itself. The full number of eLRR genes and the evolution of this superfamily had been previously unknown. Our evolutionary investigation of the superfamily and its members has identified diversification of new protein families and specific family expansions that correlate with the increasing complexity of the mammalian brain. We suggest that these proteins could provide the necessary specificity of cellular interactions to mediate a large number of connectivity decisions. Indeed, the importance of this superfamily is becoming increasingly apparent with functions in neural development identified for many individual subfamilies, and many more have been shown to exhibit specific patterns of expression in the brain. Furthermore, many members of the eLRR superfamily have been implicated in neurological or psychiatric disorders.

8.1.2 The Elfn family

The bioinformatics survey led to the identification of a novel gene family consisting of two highly conserved proteins that we named Elfn1 and Elfn2. They are vertebrate-specific and the diversification of this family occurred during evolution, most likely as a manifestation of increased central nervous system complexity. Expression analysis of Elfn1 identified cell-type specific and region-specific expression patterns in the mouse brain. In the hippocampus and cortex,

Elfn1 localises to a subset of somatostatin (SST)-containing interneurons. More specifically, Sylwestrak and Ghosh (2012) have shown that Elfn1 localises to the dendrites of SST-containing interneurons in the hippocampus. Expression is also evident in a subset of cells in the MHb and LHb. In the MHb, Elfn1 is found in excitatory cells where it exhibits a highly restricted pattern of expression in the dorsal and dorsolateral MHb. Interestingly, Elfn1 is also expressed in several regions interconnecting with the habenula including the septal nuclei, globus pallidus, lateral hypothalamus and diagonal band of Broca. Due to this, we suggest a role for Elfn1 in the connectivity of the habenula circuit. We have found that Elfn1 can also be localised to the axons of cells in which it is expressed. In the MHb, Elfn1 protein was identified in the output axons of the FR that innervate the IPN. In the globus pallidus, Elfn1 localises to the axons of long-range GABAergic projection neurons that innervate the substantia nigra pars compacta (SNc).

In summary, the detailed investigation of Elfn1 expression identified that Elfn1 is not only expressed in GABAergic interneurons, but also in long-range-projecting GABAergic and glutamatergic neurons. It localises to both axons and dendrites and is therefore functioning in both presynaptic and postsynaptic mechanisms.

8.1.3 Interaction of Elfn1 and Robo3

We present both *in vitro* and *in vivo* evidence in this study of an interaction between Robo3 and Elfn1 in the mouse. Robo3 is a known axon guidance molecule, and gross connectivity defects have been identified in Robo3$^{-/-}$ mice. *In situ* hybridisation and *in silico* analyses of the expression of these two genes highlighted a strong and complementary pattern of expression in the MHb where we speculate that an interaction is occurring. Robo3 is expressed in the ventral MHb, and localises to axons of the FR. Elfn1 is expressed in the dorsal MHb, and also localises to axons of the FR. We know that differing regions of the habenula innervate particular subregions of the interpeduncular nucleus, thereby forming functionally distinct microcircuits. Therefore, we suggest that the interaction

between Robo3 and Elfn1 may contribute to the formation and/or regulation of this microcircuitry.

8.1.4 Anatomical investigation of Elfn1$^{-/-}$ mice

Anatomical analyses of the *Elfn1*$^{-/-}$ mice did not reveal any gross abnormalities in cell migration or connectivity. This suggests that Elfn1 may not be needed for axon guidance or cell-autonomous cell migration. However, it is possible that subtle phenotypes are present at the level of the neuronal processes. Indeed, changes in synaptic plasticity produce alterations in dendritic spine morphology (Yuste and Bonhoeffer 2001) and a function for Elfn1 in the regulation of synaptic properties has already been determined in SST-containing interneurons of the hippocampus (Sylwestrak and Ghosh 2012). Interestingly, our initial investigations have shown that there may be a reduction in glutamatergic innervation to the habenula in Elfn1$^{-/-}$ mice. We would suggest from this result that Elfn1 is functioning in the dendrites of cells in the habenula and is involved transneuronally in the formation of presynaptic glutamatergic synapses. The alteration in synaptic plasticity may cause dendritic spine alterations in the cells of the habenula.

8.1.5 Behavioural analyses of Elfn1$^{-/-}$ mice

Behavioural analyses have revealed very interesting phenotypes in *Elfn1*$^{-/-}$ mice that include spontaneous seizures, motor strength and/or coordination abnormalities, decreased anxiety and hyperactivity. Elfn1 is expressed by SST-containing interneurons in the neocortex, piriform cortex and hippocampus. The inhibitory circuit in these regions is highly important in preventing enhanced excitation which can lead to seizures, and interneuron dysfunctions have been shown to contribute to epileptogenesis (Sebe and Baraban 2011). More specifically, dysfunctions in SST-containing interneurons have been shown to cause seizure activity (Cossart et al. 2001). Knockdown of Elfn1 in hippocampal interneurons results in a dramatic reduction in synaptic strength in CA1 pyramidal

cells (Sylwestrak and Ghosh 2012). We suggest that the spontaneous seizures are a result of an alteration in the glutamatergic synapses at SST-containing interneurons in the absence of Elfn1. This acute effect may directly cause seizures. However, initial studies have shown that not all *Elfn1*$^{-/-}$ mice exhibit seizures and the onset of seizure activity appears to be in adult mice. Due to this, we hypothesise that an initial abnormality at the synapse due to the lack of Elfn1 may initiate compensatory mechanisms that progressively cause a disruption in the balance of excitation and inhibition leading to seizures. The spontaneous seizures observed in Elfn1$^{-/-}$ mice are analogous to clinical partial seizures. However, the specific regions and circuits of the brain where the seizures are occurring have yet to be identified.

Elfn1$^{-/-}$ mice also exhibit deficits in the control of voluntary movement, suggestive of a dysfunction in the basal ganglia. Elfn1 is strongly expressed in the globus pallidus, and also localises to the axons that innervate the substantia nigra, both structures of the basal ganglia. Motor disorders caused by disturbances in the function of the basal ganglia have been attributed to changes in dopaminergic activity (Mehler-Wex et al. 2006). Indeed, the habenula links the basal ganglia to these dopaminergic cells and therefore the role of Elfn1 in voluntary movement could involve both the basal ganglia and habenula circuitries.

The hyperactivity, reduced anxiety and ADHD-like behaviour observed in Elfn1 knockout mice are consistent with a dysfunction in habenula circuitry. Habenula lesion models exhibit hyperactivity that is attributed to a reduction in excitatory transmission from the habenula, which in turn reduces the inhibition of mid- and hindbrain dopaminergic nuclei (Nishikawa et al. 1986, Hikosaka 2010). We suggest, therefore, that the loss of Elfn1 in cells of the habenula causes reduced excitatory transmission to the IPN, which in turn reduces the inhibitory influence of the IPN on dopaminergic neurons. Indeed, preliminary results have shown that there is reduced vGlut2 expression in the habenula of *Elfn1*$^{-/-}$ mice. Attenuation of hyperactivity with stimulants is a very specific ADHD-like phenotype, and differs from psychotic-like hyperactivity which shows an increase in activity with amphetamine. The exact mechanisms at play are not fully established but it is suggested that when dopamine levels are high, stimulants exert a calming effect by increasing serotonin levels in the brain. This restores the

delicate balance between dopamine and serotonin and reduces hyperactivity (Gainetdinov et al. 1999).

8.2 Future directions

It is apparent from the literature and the Allen brain atlas connectivity study that the dorsal diencephalic conduction system (DDC) consists of multiple neural circuits. However, the precise connectivity of these circuits and how they function in relation to the behaviours attributed to this system have yet to be established. Manipulations of distinct circuits in this system with optogenetics will provide huge progress in this area. However, the next step for this study should include anterograde and retrograde tracings from Elfn1-positive regions to identify the specific cells and regions that are interconnected and therefore the microcircuit within which Elfn1 is functioning.

Whether Elfn1 is involved in axon guidance should be investigated through detailed analyses of the innervation topography of Robo3- and Elfn1-positive axons at the IPN. This can be achieved for Robo3 using immunohistochemistry with a Robo3 antibody. However, the study would greatly benefit from an Elfn1-specific antibody. Likewise, a morphological phenotype owing to altered synaptogenesis in the absense of Elfn1 would be more easily investigated with an Elfn1-specific antibody. This antibody would facilitate *in vitro* analyses to identify the exact localisation of the Elfn1 protein in different Elfn1-positive cell populations, while also providing a system for functional investigation. Due to this, the generation of this antibody would be invaluable for continued research

We have suggested that *Elfn1*$^{-/-}$ mice could potentially be an animal model for ADHD-like behaviour. Further behavioural experiments for impulsivity and attention deficit should be performed to establish if *Elfn*$^{-/-}$ mice fit the criteria for an optimal animal model of ADHD. The behavioural results have shown differences between heterozygous and homozygous mutant mice; however, it is important to further investigate these phenotypes in wildtype littermates. The higher concentration of amphetamine failed to raise the activity of *Elfn1*$^{+/-}$ mice, the expected outcome after administration of a stimulant. Due to this, it is important to

establish if *Elfn1*$^{+/-}$ have intermediate behavioural changes. We have speculated that reduced inhibition of mid- and hindbrain dopaminergic neurons is causing hyperactivity and therefore future experiments should include the investigation of dopamine and the dopamine transporter (DAT) levels in wildtype, *Elfn1*$^{+/-}$ and *Elfn1*$^{-/-}$ mice.

There are many possibilites for experiments with *in utero* electroporation, a prodedure carried out successfully in the habenula (Quina et al. 2009). We have proposed that the lack of *Elfn1* in the habenula produces the behavoural phenotypes we have identified in this study. This can be tested with the reintroduction of a functional gene copy into the habenula to see if a phenotype reverts to normal. Knockdown of Robo3 in the habenula may provide a phenotype that would confirm the interaction in the habenula, and provide information about the function of this interaction. The lack of an obvious phenotype in the Elfn1 mutant mice indicates that ectopic expression Elfn1 which could provide the key to establishing function, particulary if there is any redundancy of function within the Elfn family.

Future investigation of the seizure phenotype in *Elfn*$^{-/-}$ mice should include electroencephalography (EEG) recordings of spontaneous seizures and analysis of the seizure susceptibility of *Elfn1*$^{-/-}$ mice to chemoconvulsants. Subsequent c-fos immunoreactivity would identify the cells and neural networks involved in the seizure activity. Moreover, the identification of the Elfn1 transsynaptic binding partner would help elucidate the mechanisms and pathways in which Elfn1 is functioning.

This thesis has identified a novel protein that functions in the formation of neural circuitry in the brain. The *Elfn1*$^{-/-}$ mouse provides a potential animal model for the study of abnormalities in human behaviour such as movement disorders, seizures, anxiety and ADHD-like behaviour.

9 Chapter 9 Appendix

a

.....tactctcttctcttttctcttgcagGCAGAGAGTACTTCAGGCAGAGGAACCG
GGCGAAGCCACCAGGATACACAGGCCCATGGGAAAACAGGCTGT
GGCCACCTTGGGACCGGGGAGGACGACAAAGGGCGGCGGGCAG
TGAGGGAGCCATTCTCCCTCCCGACACCTGCGTCATGCAGCTTGG
GACAGGACATCTCTGACAGTGCAGGCAGTGATCCATCCCACCCCT
AAGTCCCCTGGGGGGGCCCACTGCCCAGCCCTCCCCCCATCCCCA
CAGGCAGTGTCCCGAGATGGCTGGGCACGGGTGGGGTACAGCGT
GGGTACTTGTGGCAGCCGCCACGTTACTGCACGCGGGTGGGCTG
GCCCAAGGTGACTGCTGGCTGATTGAGGGTGACAAAGGCTTCGT
GTGGTTGGCCATCTGCAGCCAGAACCAGCCACCCTATGAGGCCAT
CCCCCAACAGATCAACAACACCATCGTGGACCTGCGGCTTAACGA
GAACCGTATCCGCAGCGTGCAGTACGCCTCCCTGAGCCGCTTCGG
AAACCTCACATACCTCAACCTCACCAAGAACGAGATCGGCTACAT
CGAGGACGGGGCCTTCTCCGGCCAGTTCAACCTCCAGGTGCTGC
AGCTGGGCTACAACCGGCTGCGCAACCTCACGGAGGGCATGCTG
CGGGGCCTGAGCAAGCTCGAGTACCTGTACCTACAGGCCAACCTC
ATCGAGGTGGTGATGGCCAGCGCCTTCTGGGAGTGTCCCAACATC
GTCAACATAGATCTCTCCATGAATCGCATCCAGCAGCTGGGCAGC
GGCACCTTCGCAGGCCTGACCAAGCTCTCGGTGTGTGAGATCTAC
AGCAACCCTTTCTACTGCTCCTGTGAGCTGCTGGGTTTCCTGCGCT
GGCTGGCTGCCTTCACCAACGCCACACAGACC.....

b

.....tactctcttctcttttctcttgcagGCAGAGAGTACTTCAGGCAGAGGAACCG
GGCGAAGCCACCAGGATACACAGGCCCATGGGAAAACAGGCTGT
GGCCACCTTGGGACCGGGGAGGACGACAAAGGGCGGCGGGCAG
TGAGGGAGCCATTCTCCCTCCCGACACCTGCGTCATGCAGCTTGG
GACAGGACATCTCTGACAGTGCAGGCAGTGATCCATCCCACCCCT
AAGTCCCCTGGGGGGGCCCACTGCCCAGCCCTCCCCCCATCCCCA
CAGGCAGTGTCCCGAGGGTACCGATTTAAATGATCCAGTGGTCCTGCAGAG
GAGAGATTGGGAGAATCCCGGTGTGACACAGCTGAACAGACTAGCCGCCCACCC
CCCTTTGCTTCTTGGAGAAACAGTGAGGAAGCTAGGACAGACAGACCAAGCCAG
CAACTCAGATCTTTGAACGGGGAGTGGAGATTTGCCTGGTTTCCGG
CACCAGAAGC GGTGCCGGAA AGCTGGCTG.....

Figure 9.1 Nucleotide sequence of Elfn1 showing vector insertion site. (a) Wildtype Elfn1 sequence (Intron, blue; non-coding exon, red; coding exon, black; underlined font, forward and reverse Elfn1 primers. (b) Elfn1 allele with vector insertion (Intron, blue; non-coding exon, red; targeting vector, green; underlined font, forward and reverse primers.

```
Robo3A1     MLRYLLKTLLQMNLFADSLARDISNSSELLFGFNSSLAALNPSLLP--PGDPSLNGSRVG
Robo3A2     MLRYLLKTLLQMNLFADSLARDISNSSELLFGFNSSLAALNPSLLP--PGDPSLNGSRVG
Robo3B2     ----------------------MSEAEG-SLTLQ-SKPGLPPVALPGYLELPSSPGSRVG
                                  :*::.   : :: *  .* *  **     **  *****

Robo3A1     PEDAMPRIVEQPPDLVVSRGEPATLPCRAEGRPRPNIEWYKNGARVATAREDPRAHRLLL
Robo3A2     PEDAMPRIVEQPPDLVVSRGEPATLPCRAEGRPRPNIEWYKNGARVATAREDPRAHRLLL
Robo3B2     PEDAMPRIVEQPPDLVVSRGEPATLPCRAEGRPRPNIEWYKNGARVATAREDPRAHRLLL
            ************************************************************

Robo3A1     PSGALFFPRIVHGRRSRPDEGVYTCVARNYLGAAASRNASLEVAVLRDDFRQSPGNVVVA
Robo3A2     PSGALFFPRIVHGRRSRPDEGVYTCVARNYLGAAASRNASLEVAVLRDDFRQSPGNVVVA
Robo3B2     PSGALFFPRIVHGRRSRPDEGVYTCVARNYLGAAASRNASLEVAVLRDDFRQSPGNVVVA
            ************************************************************

Robo3A1     VGEPAVMECVPPKGHPEPLVTWKKGKIKLKEEEGRITIRGGKLMMSHTFKSDAGMYMCVA
Robo3A2     VGEPAVMECVPPKGHPEPLVTWKKGKIKLKEEEGRITIRGGKLMMSHTFKSDAGMYMCVA
Robo3B2     VGEPAVMECVPPKGHPEPLVTWKKGKIKLKEEEGRITIRGGKLMMSHTFKSDAGMYMCVA
            ************************************************************

Robo3A1     SNMAGERESGAAELVVLERPSFLRRPINQVVLADAPVNFLCEVQGDPQPNLHWRKDDGEL
Robo3A2     SNMAGERESGAAELVVLERPSFLRRPINQVVLADAPVNFLCEVQGDPQPNLHWRKDDGEL
Robo3B2     SNMAGERESGAAELVVLERPSFLRRPINQVVLADAPVNFLCEVQGDPQPNLHWRKDDGEL
            ************************************************************

Robo3A1     PAGRYEIRSDHSLWIDQVSSEDEGTYTCVAENSVGRAEASGSLSVHVPPQFVTKPQNQTV
Robo3A2     PAGRYEIRSDHSLWIDQVSSEDEGTYTCVAENSVGRAEASGSLSVHVPPQFVTKPQNQTV
Robo3B2     PAGRYEIRSDHSLWIDQVSSEDEGTYTCVAENSVGRAEASGSLSVHVPPQFVTKPQNQTV
            ************************************************************

Robo3A1     APGANVSFQCETKGNPPPAIFWQKEGSQVLLFPSQSLQPMGRLLVSPRGQLNITEVKIGD
Robo3A2     APGANVSFQCETKGNPPPAIFWQKEGSQVLLFPSQSLQPMGRLLVSPRGQLNITEVKIGD
Robo3B2     APGANVSFQCETKGNPPPAIFWQKEGSQVLLFPSQSLQPMGRLLVSPRGQLNITEVKIGD
            ************************************************************

Robo3A1     GGYYVCQAVSVAGSILAKALLEIKGASIDGLPPIILQGPANQTLVLGSSVWLPCRVIGNP
Robo3A2     GGYYVCQAVSVAGSILAKALLEIKGASIDGLPPIILQGPANQTLVLGSSVWLPCRVIGNP
Robo3B2     GGYYVCQAVSVAGSILAKALLEIKGASIDGLPPIILQGPANQTLVLGSSVWLPCRVIGNP
            ************************************************************

Robo3A1     QPNIQWKKDERWLQGDDSQFNLMDNGTLHIASIQEMDMGFYSCVAKSSIGEATWNSWLRK
Robo3A2     QPNIQWKKDERWLQGDDSQFNLMDNGTLHIASIQEMDMGFYSCVAKSSIGEATWNSWLRK
Robo3B2     QPNIQWKKDERWLQGDDSQFNLMDNGTLHIASIQEMDMGFYSCVAKSSIGEATWNSWLRK
            ************************************************************

Robo3A1     QEDWGASPGPATGPSNPPGPPSQPIVTEVTANSITLTWKPNPQSGATATSYVIEAFSQAA
Robo3A2     QEDWGASPGPATGPSNPPGPPSQPIVTEVTANSITLTWKPNPQSGATATSYVIEAFSQAA
Robo3B2     QEDWGASPGPATGPSNPPGPPSQPIVTEVTANSITLTWKPNPQSGATATSYVIEAFSQAA
            ************************************************************

Robo3A1     GNTWRTVADGVQLETYTISGLQPNTIYLFLVRAVGAWGLSEPSPVSEPVQTQDSSLSRPA
Robo3A2     GNTWRTVADGVQLETYTISGLQPNTIYLFLVRAVGAWGLSEPSPVSEPVQTQDSSLSRPA
Robo3B2     GNTWRTVADGVQLETYTISGLQPNTIYLFLVRAVGAWGLSEPSPVSEPVQTQDSSLSRPA
            ************************************************************

Robo3A1     EDPWKGQRGLAEVAVRMQEPTVLGPRTLQVSWTVDGPVQLVQGFRVSWRIAGLDQGSWTM
Robo3A2     EDPWKGQRGLAEVAVRMQEPTVLGPRTLQVSWTVDGPVQLVQGFRVSWRIAGLDQGSWTM
Robo3B2     EDPWKGQRGLAEVAVRMQEPTVLGPRTLQVSWTVDGPVQLVQGFRVSWRIAGLDQGSWTM
            ************************************************************

Robo3A1     LDLQSPHKQSTVLRGLPPGAQIQIKVQVQGQEGLGAESPFVTRSIPEEAPSGPPQGVAVA
Robo3A2     LDLQSPHKQSTVLRGLPPGAQIQIKVQVQGQEGLGAESPFVTRSIPEEAPSGPPQGVAVA
Robo3B2     LDLQSPHKQSTVLRGLPPGAQIQIKVQVQGQEGLGAESPFVTRSIPEEAPSGPPQGVAVA
            ************************************************************
```

Figure 9.2 Amino acid sequence alignment of Robo3 isoforms. Robo3a1 contains a longer N-terminal sequence than Robo3b2. Robo3A2 and Robo3B2 differ from Robo3A1 at the C-terminal region.

a Mouse cohort in experiment 1

Heterozygous	Weight(g)	Homozygous	Weight(g)
J183	33.2	J157	29
J190	31.2	J169	26.9
J194	27.9	J170	24.6
J200	29	J171	27.9
J201	29.5	J184	26.6
J202	26	J192	25.3
J210	24.1	J193	25.1
J211	24.8	J208	22.9

b Mouse cohort in experiment 2

Heterozygous	Weight(g)	Homozygous	Weight(g)
J289	28.9	J306	23.4
J290	23.1	J312	23.2
J311	25.8	J308	24.6
J307	26.3	J309	21.2
J315	26.6	J310	25.4
J320	30.7	J314	22.3
J321	25.4	J316	24.6
J322	22.7	J319	27.7
J330	17.9	J323	22.8
J331	22.4	J329	19.4

Table 9.1Elfn1 knockout mice used in the behavioural analyses. (a) The first cohort of mice consisted of eight homozygous mutant and eight heterozygous male mice. All aged 3-4 months old, and the weight of each mouse is indicated. (b) The second cohort consisted of ten male mice of each genotype, aged 2-3 months old. The weight of each mouse is indicated. Each mouse is given a unique identifier consisting of the letter J and a number.

10 Chapter 10 References

Abdesselem, H., Shypitsyna, A., Solis, G. P., Bodrikov, V. and Stuermer, C. A. O. (2009) 'No Nogo66- and NgR-Mediated Inhibition of Regenerating Axons in the Zebrafish Optic Nerve', *The Journal of Neuroscience,* 29(49), 15489-15498.

Abelson, J., Kwan, K., O'Roak, B., Baek, D., Stillman, A., Morgan, T., Mathews, C., Pauls, D., Rasin, M. and Gunel, M. (2005) 'Sequence variants in SLITRK1 are associated with Tourette's syndrome', *Science,* 310, 317 - 20.

Accili, D., Fishburn, C. S., Drago, J., Steiner, H., Lachowicz, J. E., Park, B. H., Gauda, E. B., Lee, E. J., Cool, M. H., Sibley, D. R., Gerfen, C. R., Westphal, H. and Fuchs, S. (1996) 'A targeted mutation of the D3 dopamine receptor gene is associated with hyperactivity in mice', *Proc Natl Acad Sci U S A,* 93(5), 1945-9.

Adachi-Yamada, T., Harumoto, T., Sakurai, K., Ueda, R., Saigo, K., O'Connor, M. B. and Nakato, H. (2005) 'Wing-to-Leg homeosis by spineless causes apoptosis regulated by Fish-lips, a novel leucine-rich repeat transmembrane protein', *Mol Cell Biol,* 25(8), 3140-50.

Afzal, A. J. and Lightfoot, D. A. (2007) 'Soybean disease resistance protein RHG1-LRR domain expressed, purified and refolded from Escherichia coli inclusion bodies: preparation for a functional analysis', *Protein Expr Purif,* 53(2), 346-55.

Ahmed, Z., Douglas, M. R., John, G., Berry, M. and Logan, A. (2013) 'AMIGO3 Is an NgR1/p75 Co-Receptor Signalling Axon Growth Inhibition in the Acute Phase of Adult Central Nervous System Injury', *PLoS One,* 8(4), e61878.

Aizawa, H., Amo, R. and Okamoto, H. (2011) 'Phylogeny and ontogeny of the habenular structure', *Front Neurosci,* 5, 138.

Aizawa, H., Kobayashi, M., Tanaka, S., Fukai, T. and Okamoto, H. (2012) 'Molecular characterization of the subnuclei in rat habenula', *J Comp Neurol,* 520(18), 4051-66.

Albin, R. L., Young, A. B. and Penney, J. B. (1989) 'The functional anatomy of basal ganglia disorders', *Trends Neurosci,* 12(10), 366-75.

Ameye, L. and Young, M. (2002) 'Mice deficient in small leucine-rich proteoglycans: novel in vivo models for osteoporosis, osteoarthritis, Ehlers-Danlos syndrome, muscular dystrophy, and corneal diseases', *Glycobiology,* 12, 107R - 16R.

Andersen, S. L. (2003) 'Trajectories of brain development: point of vulnerability or window of opportunity?', *Neurosci Biobehav Rev,* 27(1-2), 3-18.

Anderson, K., Bokla, L. and Nusslein-Volhard, C. (1985) 'Establishment of dorsal-ventral polarity in the Drosophila embryo: the induction of polarity by the Toll gene product', *Cell,* 42, 791 - 8.

Andres, K. H., von During, M. and Veh, R. W. (1999) 'Subnuclear organization of the rat habenular complexes', *J Comp Neurol,* 407(1), 130-50.

Arcos-Burgos, M., Jain, M., Acosta, M. T., Shively, S., Stanescu, H., Wallis, D., Domene, S., Velez, J. I., Karkera, J. D., Balog, J., Berg, K., Kleta, R., Gahl, W. A., Roessler, E., Long, R., Lie, J., Pineda, D., Londono, A. C., Palacio, J. D., Arbelaez, A., Lopera, F., Elia, J., Hakonarson, H., Johansson, S., Knappskog, P. M., Haavik, J., Ribases, M., Cormand, B., Bayes, M., Casas, M., Ramos-Quiroga, J. A., Hervas, A., Maher, B. S., Faraone, S. V., Seitz, C., Freitag, C. M., Palmason, H., Meyer, J., Romanos, M., Walitza, S., Hemminger, U., Warnke, A., Romanos, J., Renner, T., Jacob, C., Lesch, K. P., Swanson, J., Vortmeyer, A., Bailey-Wilson, J. E., Castellanos, F. X. and Muenke, M. (2010) 'A common variant of the latrophilin 3 gene, LPHN3, confers susceptibility to ADHD and predicts effectiveness of stimulant medication', *Mol Psychiatry,* 15(11), 1053-1066.

Arlotta, P., Molyneaux, B. J., Chen, J., Inoue, J., Kominami, R. and Macklis, J. D. (2005) 'Neuronal subtype-specific genes that control corticospinal motor neuron development in vivo', *Neuron,* 45(2), 207-21.

Aruga, J. and Mikoshiba, K. (2003) 'Identification and characterization of Slitrk, a novel neuronal transmembrane protein family controlling neurite outgrowth', *Mol Cell Neurosci,* 24(1), 117-29.

Athanasiu, L., Mattingsdal, M., Melle, I., Inderhaug, E., Lien, T., Agartz, I., Lorentzen, S., Morken, G., Andreassen, O. A. and Djurovic, S. (2011) 'Intron 12 in NTRK3 is associated with bipolar disorder', *Psychiatry Research,* 185(3), 358-362.

Avoli, M., Hwa, G., Louvel, J., Kurcewicz, I., Pumain, R. and Lacaille, J. C. (1997) 'Functional and pharmacological properties of GABA-mediated inhibition in the human neocortex', *Can J Physiol Pharmacol,* 75(5), 526-34.

Bahadori, R., Biehlmaier, O., Zeitz, C., Labhart, T., Makhankov, Y. V., Forster, U., Gesemann, M., Berger, W. and Neuhauss, S. C. (2006) 'Nyctalopin is essential for synaptic transmission in the cone dominated zebrafish retina', *Eur J Neurosci,* 24(6), 1664-74.

Balcita-Pedicino, J. J., Omelchenko, N., Bell, R. and Sesack, S. R. (2011) 'The inhibitory influence of the lateral habenula on midbrain dopamine cells: ultrastructural evidence for indirect mediation via the rostromedial mesopontine tegmental nucleus', *J Comp Neurol,* 519(6), 1143-64.

Baldwin, P. R., Alanis, R. and Salas, R. (2011) 'The Role of the Habenula in Nicotine Addiction', *J Addict Res Ther,* S1(2).

Bando, T., Sekine, K., Kobayashi, S., Watabe, A., Rump, A., Tanaka, M., Suda, Y., Kato, S., Morikawa, Y. and Manabe, T. (2005) 'Neuronal leucine-rich

repeat protein 4 functions in hippocampus-dependent long-lasting memory', *Mol Cell Biol,* 25, 4166 - 75.

Barber, M., Di Meglio, T., Andrews, W. D., Hernandez-Miranda, L. R., Murakami, F., Chedotal, A. and Parnavelas, J. G. (2009) 'The role of Robo3 in the development of cortical interneurons', *Cereb Cortex,* 19 Suppl 1, i22-31.

Barton, W. A., Liu, B. P., Tzvetkova, D., Jeffrey, P. D., Fournier, A. E., Sah, D., Cate, R., Strittmatter, S. M. and Nikolov, D. B. (2003) 'Structure and axon outgrowth inhibitor binding of the Nogo-66 receptor and related proteins', *EMBO J,* 22(13), 3291-302.

Bashaw, G. J., Kidd, T., Murray, D., Pawson, T. and Goodman, C. S. (2000) 'Repulsive axon guidance: Abelson and Enabled play opposing roles downstream of the roundabout receptor', *Cell,* 101(7), 703-15.

Bateman, A., Coin, L., Durbin, R., Finn, R., Hollich, V., Griffiths-Jones, S., Khanna, A., Marshall, M., Moxon, S. and Sonnhammer, E. (2004) 'The Pfam protein families database', *Nucleic Acids Res,* 32, D138 - 41.

Bates, T. C., Luciano, M., Medland, S. E., Montgomery, G. W., Wright, M. J. and Martin, N. G. (2011) 'Genetic variance in a component of the language acquisition device: ROBO1 polymorphisms associated with phonological buffer deficits', *Behav Genet,* 41(1), 50-7.

Batten, T. F. C., Gamboa-Esteves, F. O. and Saha, S. (2002) 'Evidence for peptide co-transmission in retrograde- and anterograde-labelled central nucleus of amygdala neurones projecting to NTS', *Autonomic neuroscience : basic & clinical,* 98(1), 28-32.

Baxter, R. (1994) 'Insulin-like growth factor binding proteins in the human circulation: a review', *Horm Res,* 42, 140 - 4.

Bech-Hansen, N., Naylor, M., Maybaum, T., Sparkes, R., Koop, B., Birch, D., Bergen, A., Prinsen, C., Polomeno, R. and Gal, A. (2000) 'Mutations in NYX, encoding the leucine-rich proteoglycan nyctalopin, cause X-linked complete congenital stationary night blindness', *Nat Genet,* 26, 319 - 23.

Bell, J., Botos, I., Hall, P., Askins, J., Shiloach, J., Segal, D. and Davies, D. (2005) 'The molecular structure of the Toll-like receptor 3 ligand-binding domain', *Proc Natl Acad Sci USA,* 102, 10976 - 80.

Bell, J. K., Mullen, G. E., Leifer, C. A., Mazzoni, A., Davies, D. R. and Segal, D. M. (2003) 'Leucine-rich repeats and pathogen recognition in Toll-like receptors', *Trends Immunol,* 24(10), 528-33.

Bella, J., Hindle, K. L., McEwan, P. A. and Lovell, S. C. (2008) 'The leucine-rich repeat structure', *Cell Mol Life Sci,* 65(15), 2307-33.

Bendtsen, J., Nielsen, H., von Heijne, G. and Brunak, S. (2004) 'Improved prediction of signal peptides: SignalP 3.0', *J Mol Biol,* 340, 783 - 95.

Beninger, R. J. (1983) 'The role of dopamine in locomotor activity and learning', *Brain Res,* 287(2), 173-96.

Bennett, M. K., Kulaga, H. M. and Reed, R. R. (2010) 'Odor-evoked gene regulation and visualization in olfactory receptor neurons', *Mol Cell Neurosci,* 43(4), 353-62.

Beretta, C. A., Dross, N., Guiterrez-Triana, J. A., Ryu, S. and Carl, M. (2012) 'Habenula circuit development: past, present, and future', *Front Neurosci,* 6, 51.

Bermingham, J., Shearin, H., Pennington, J., O'Moore, J., Jaegle, M., Driegen, S., van Zon, A., Darbas, A., Ozkaynak, E. and Ryu, E. (2006) 'The claw

paw mutation reveals a role for Lgi4 in peripheral nerve development', *Nat Neurosci,* 9, 76 - 84.

Beutler, B., Jiang, Z., Georgel, P., Crozat, K., Croker, B., Rutschmann, S., Du, X. and Hoebe, K. (2006) 'Genetic analysis of host resistance: Toll-like receptor signaling and immunity at large', *Annu Rev Immunol,* 24, 353-89.

Bianco, I. H. and Wilson, S. W. (2009) 'The habenular nuclei: a conserved asymmetric relay station in the vertebrate brain', *Philos Trans R Soc Lond B Biol Sci,* 364(1519), 1005-20.

Blednov, Y. A., Stoffel, M., Chang, S. R. and Harris, R. A. (2001) 'GIRK2 deficient mice. Evidence for hyperactivity and reduced anxiety', *Physiol Behav,* 74(1-2), 109-17.

Blitzer, R. D., Connor, J. H., Brown, G. P., Wong, T., Shenolikar, S., Iyengar, R. and Landau, E. M. (1998) 'Gating of CaMKII by cAMP-Regulated Protein Phosphatase Activity During LTP', *Science,* 280(5371), 1940-1943.

Bolam, J. P. and Smith, Y. (1992) 'The striatum and the globus pallidus send convergent synaptic inputs onto single cells in the entopeduncular nucleus of the rat: A double anterograde labelling study combined with postembedding immunocytochemistry for GABA', *J Comp Neurol,* 321(3), 456-476.

Borg, I., Freude, K., Kubart, S., Hoffmann, K., Menzel, C., Laccone, F., Firth, H., Ferguson-Smith, M. A., Tommerup, N., Ropers, H. H., Sargan, D. and Kalscheuer, V. M. (2005) 'Disruption of Netrin G1 by a balanced chromosome translocation in a girl with Rett syndrome', *Eur J Hum Genet,* 13(8), 921-7.

Botos, I., Segal, D. M. and Davies, D. R. (2011) 'The structural biology of Toll-like receptors', *Structure,* 19(4), 447-59.

Bottcher, R., Pollet, N., Delius, H. and Niehrs, C. (2004) 'The transmembrane protein XFLRT3 forms a complex with FGF receptors and promotes FGF signalling', *Nat Cell Biol,* 6, 38 - 44.

Brown, R. T., Amler, R. W., Freeman, W. S., Perrin, J. M., Stein, M. T., Feldman, H. M., Pierce, K. and Wolraich, M. L. (2005) 'Treatment of attention-deficit/hyperactivity disorder: overview of the evidence', *Pediatrics,* 115(6), e749-57.

Budel, S., Padukkavidana, T., Liu, B. P., Feng, Z., Hu, F., Johnson, S., Lauren, J., Park, J. H., McGee, A. W., Liao, J., Stillman, A., Kim, J. E., Yang, B. Z., Sodi, S., Gelernter, J., Zhao, H., Hisama, F., Arnsten, A. F. and Strittmatter, S. M. (2008) 'Genetic variants of Nogo-66 receptor with possible association to schizophrenia block myelin inhibition of axon growth', *J Neurosci,* 28(49), 13161-72.

Butte, N. F., Treuth, M. S., Voigt, R. G., Llorente, A. M. and Heird, W. C. (1999) 'Stimulant medications decrease energy expenditure and physical activity in children with attention-deficit/hyperactivity disorder', *J Pediatr,* 135(2 Pt 1), 203-7.

Campos-Ortega, J. A. a. H., V (1985) *The embryonic development of Drosophila melanogaster,* Berlin/Heidelberg/New-York/Tokyo.

Camurri, L., Mambetisaeva, E., Davies, D., Parnavelas, J., Sundaresan, V. and Andrews, W. (2005) 'Evidence for the existence of two Robo3 isoforms with divergent biochemical properties', *Mol Cell Neurosci,* 30(4), 485-93.

Camurri, L., Mambetisaeva, E. and Sundaresan, V. (2004) 'Rig-1 a new member of Robo family genes exhibits distinct pattern of expression during mouse development', *Gene Expr Patterns,* 4(1), 99-103.

Carlson, J., Noguchi, K. and Ellison, G. (2001) 'Nicotine produces selective degeneration in the medial habenula and fasciculus retroflexus', *Brain Res,* 906(1–2), 127-134.

Carola, V., D'Olimpio, F., Brunamonti, E., Mangia, F. and Renzi, P. (2002) 'Evaluation of the elevated plus-maze and open-field tests for the assessment of anxiety-related behaviour in inbred mice', *Behav Brain Res,* 134(1-2), 49-57.

Casillas-Espinosa, P. M., Powell, K. L. and O'Brien, T. J. (2012) 'Regulators of synaptic transmission: Roles in the pathogenesis and treatment of epilepsy', *Epilepsia,* 53, 41-58.

Challa, A. K., McWhorter, M. L., Wang, C., Seeger, M. A. and Beattie, C. E. (2005) 'Robo3 isoforms have distinct roles during zebrafish development', *Mech Dev,* 122(10), 1073-86.

Chang, K., Seabold, G. K., Wang, C. Y. and Wenthold, R. J. (2010) 'Reticulon 3 is an interacting partner of the SALM family of adhesion molecules', *J Neurosci Res,* 88(2), 266-74.

Chao, M. V. (2003) 'Neurotrophins and their receptors: a convergence point for many signalling pathways', *Nat Rev Neurosci,* 4(4), 299-309.

Chen, L., Cui, Q. L. and Yung, W. H. (2009) 'Neurokinin-1 receptor activation in globus pallidus', *Front Neurosci,* 3, 58.

Chen, Y., Aulia, S., Li, L. and Tang, B. (2006) 'AMIGO and friends: An emerging family of brain-enriched, neuronal growth modulating, type I transmembrane proteins with leucine-rich repeats (LRR) and cell adhesion molecule motifs', *Brain Res Brain Res Rev,* 51, 265 - 74.

Chen, Z., Gore, B. B., Long, H., Ma, L. and Tessier-Lavigne, M. (2008) 'Alternative splicing of the Robo3 axon guidance receptor governs the midline switch from attraction to repulsion', *Neuron,* 58(3), 325-32.

Cho, J. H., Prince, J. E. and Cloutier, J. F. (2009) 'Axon guidance events in the wiring of the mammalian olfactory system', *Mol Neurobiol,* 39(1), 1-9.

Choe, J., Kelker, M. and Wilson, I. (2005) 'Crystal structure of human toll-like receptor 3 (TLR3) ectodomain', *Science,* 309, 581 - 5.

Choleris, E., Thomas, A. W., Kavaliers, M. and Prato, F. S. (2001) 'A detailed ethological analysis of the mouse open field test: effects of diazepam, chlordiazepoxide and an extremely low frequency pulsed magnetic field', *Neurosci Biobehav Rev,* 25(3), 235-60.

Christoph, G. R., Leonzio, R. J. and Wilcox, K. S. (1986) 'Stimulation of the lateral habenula inhibits dopamine-containing neurons in the substantia nigra and ventral tegmental area of the rat', *J Neurosci,* 6(3), 613-9.

Clarke, N. P., Bolam, J. P. and Bevan, M. D. (1996) 'Glutamate-enriched inputs from the mesopontine tegmentum to the entopeduncular nucleus in the rat', *Eur J Neurosci,* 8(7), 1363-76.

Cohen, P. T. W. (2002) 'Protein phosphatase 1 – targeted in many directions', *Journal of Cell Science,* 115(2), 241-256.

Cohen, S. R. and Melzack, R. (1993) 'The habenula and pain: repeated electrical stimulation produces prolonged analgesia but lesions have no effect on formalin pain or morphine analgesia', *Behav Brain Res,* 54(2), 171-8.

Concha, M. L. and Wilson, S. W. (2001) 'Asymmetry in the epithalamus of vertebrates', *J Anat,* 199(Pt 1-2), 63-84.

Conover, J. and Yancopoulos, G. (1997) 'Neurotrophin regulation of the developing nervous system: analyses of knockout mice', *Rev Neurosci,* 8, 13 - 27.

Cossart, R., Dinocourt, C., Hirsch, J. C., Merchan-Perez, A., De Felipe, J., Ben-Ari, Y., Esclapez, M. and Bernard, C. (2001) 'Dendritic but not somatic GABAergic inhibition is decreased in experimental epilepsy', *Nat Neurosci,* 4(1), 52-62.

Costall, B., Domeney, A. M. and Naylor, R. J. (1984) 'Locomotor hyperactivity caused by dopamine infusion into the nucleus accumbens of rat brain: specificity of action', *Psychopharmacology (Berl),* 82(3), 174-80.

Croll, S. D., Suri, C., Compton, D. L., Simmons, M. V., Yancopoulos, G. D., Lindsay, R. M., Wiegand, S. J., Rudge, J. S. and Scharfman, H. E. (1999) 'Brain-derived neurotrophic factor transgenic mice exhibit passive avoidance deficits, increased seizure severity and in vitro hyperexcitability in the hippocampus and entorhinal cortex', *Neuroscience,* 93(4), 1491-1506.

Cummings, S. L. (1997) 'Neuropeptide Y, somatostatin, and cholecystokinin of the anterior piriform cortex', *Cell and Tissue Research,* 289(1), 39-51.

Davies, A., Spike, C., Shaw, J. and Herman, R. (1999) 'Functional overlap between the mec-8 gene and five sym genes in Caenorhabditis elegans', *Genetics,* 153, 117 - 34.

de Wit, J., Hong, W., Luo, L. and Ghosh, A. (2011) 'Role of leucine-rich repeat proteins in the development and function of neural circuits', *Annu Rev Cell Dev Biol,* 27, 697-729.

de Wit, J., Sylwestrak, E., O'Sullivan, M. L., Otto, S., Tiglio, K., Savas, J. N., Yates, J. R., 3rd, Comoletti, D., Taylor, P. and Ghosh, A. (2009) 'LRRTM2 interacts with Neurexin1 and regulates excitatory synapse formation', *Neuron,* 64(6), 799-806.

Dean, C. and Dresbach, T. (2006) 'Neuroligins and neurexins: linking cell adhesion, synapse formation and cognitive function', *Trends Neurosci,* 29(1), 21-9.

DeLong, M. R. (1990) 'Primate models of movement disorders of basal ganglia origin', *Trends Neurosci,* 13(7), 281-5.

Delprat, B., Michel, V., Goodyear, R., Yamasaki, Y., Michalski, N., El-Amraoui, A., Perfettini, I., Legrain, P., Richardson, G., Hardelin, J. P. and Petit, C. (2005) 'Myosin XVa and whirlin, two deafness gene products required for hair bundle growth, are located at the stereocilia tips and interact directly', *Hum Mol Genet,* 14(3), 401-10.

DeNardo, L. A., de Wit, J., Otto-Hitt, S. and Ghosh, A. (2012) 'NGL-2 regulates input-specific synapse development in CA1 pyramidal neurons', *Neuron,* 76(4), 762-75.

Dent, E. W., Gupton, S. L. and Gertler, F. B. (2011) 'The growth cone cytoskeleton in axon outgrowth and guidance', *Cold Spring Harb Perspect Biol,* 3(3).

Diaz, J., Lévesque, D., Lammers, C. H., Griffon, N., Martres, M. P., Schwartz, J. C. and Sokoloff, P. (1995) 'Phenotypical characterization of neurons expressing the dopamine D3 receptor in the rat brain', *Neuroscience,* 65(3), 731-745.

Dickson, B. J. and Gilestro, G. F. (2006) 'Regulation of commissural axon pathfinding by slit and its Robo receptors', *Annu Rev Cell Dev Biol,* 22, 651-75.

Divanovic, S., Trompette, A., Atabani, S., Madan, R., Golenbock, D., Visintin, A., Finberg, R., Tarakhovsky, A., Vogel, S. and Belkaid, Y. (2005) 'Negative regulation of Toll-like receptor 4 signaling by the Toll-like receptor homolog RP105', *Nat Immunol,* 6, 571 - 8.

Dolan, J., Walshe, K., Alsbury, S., Hokamp, K., O'Keeffe, S., Okafuji, T., Miller, S., Tear, G. and Mitchell, K. (2007) 'The extracellular Leucine-Rich Repeat superfamily; a comparative survey and analysis of evolutionary relationships and expression patterns', *BMC Genomics,* 8(1), 320.

Drevets, W. C., Gautier, C., Price, J. C., Kupfer, D. J., Kinahan, P. E., Grace, A. A., Price, J. L. and Mathis, C. A. (2001) 'Amphetamine-induced dopamine release in human ventral striatum correlates with euphoria', *Biol Psychiatry,* 49(2), 81-96.

Eddy, S. (1998) 'Profile hidden Markov models', *Bioinformatics,* 14, 755 - 63.

Eisenhaber, B., Bork, P. and Eisenhaber, F. (1999) 'Prediction of potential GPI-modification sites in proprotein sequences', *J Mol Biol,* 292(3), 741-58.

Engle, E. C. (2010) 'Human genetic disorders of axon guidance', *Cold Spring Harb Perspect Biol,* 2(3), a001784.

Enright, A., Van Dongen, S. and Ouzounis, C. (2002) 'An efficient algorithm for large-scale detection of protein families', *Nucleic Acids Res,* 30, 1575 - 84.

Etheridge, S. L., Ray, S., Li, S., Hamblet, N. S., Lijam, N., Tsang, M., Greer, J., Kardos, N., Wang, J., Sussman, D. J., Chen, P. and Wynshaw-Boris, A. (2008) 'Murine dishevelled 3 functions in redundant pathways with dishevelled 1 and 2 in normal cardiac outflow tract, cochlea, and neural tube development', *PLoS Genet,* 4(11), e1000259.

Fallon, J. H., Riley, J. N., Sipe, J. C. and Moore, R. Y. (1978) 'The islands of calleja: Organization and connections', *J Comp Neurol,* 181(2), 375-395.

Fan, Q. and Hendrickson, W. (2005) 'Structure of human follicle-stimulating hormone in complex with its receptor', *Nature,* 433, 269 - 77.

Fetchko, M., Huang, W., Li, Y. and Lai, Z. (2002) 'Drosophila Gp150 is required for early ommatidial development through modulation of Notch signaling', *Embo j,* 21, 1074 - 83.

Flapper, B. C., Houwen, S. and Schoemaker, M. M. (2006) 'Fine motor skills and effects of methylphenidate in children with attention-deficit-hyperactivity disorder and developmental coordination disorder', *Dev Med Child Neurol,* 48(3), 165-9.

FlyGPI.

Francks, C., Maegawa, S., Lauren, J., Abrahams, B. S., Velayos-Baeza, A., Medland, S. E., Colella, S., Groszer, M., McAuley, E. Z., Caffrey, T. M., Timmusk, T., Pruunsild, P., Koppel, I., Lind, P. A., Matsumoto-Itaba, N., Nicod, J., Xiong, L., Joober, R., Enard, W., Krinsky, B., Nanba, E., Richardson, A. J., Riley, B. P., Martin, N. G., Strittmatter, S. M., Moller, H. J., Rujescu, D., St Clair, D., Muglia, P., Roos, J. L., Fisher, S. E., Wade-Martins, R., Rouleau, G. A., Stein, J. F., Karayiorgou, M., Geschwind, D. H., Ragoussis, J., Kendler, K. S., Airaksinen, M. S., Oshimura, M., DeLisi, L. E. and Monaco, A. P. (2007) 'LRRTM1 on chromosome 2p12 is a maternally suppressed gene that is associated paternally with handedness and schizophrenia', *Mol Psychiatry,* 12(12), 1129-39, 1057.

Friedman, A., Lax, E., Dikshtein, Y., Abraham, L., Flaumenhaft, Y., Sudai, E., Ben-Tzion, M. and Yadid, G. (2011) 'Electrical stimulation of the lateral habenula produces an inhibitory effect on sucrose self-administration', *Neuropharmacology,* 60(2-3), 381-7.

Fukamachi, K., Matsuoka, Y., Ohno, H., Hamaguchi, T. and Tsuda, H. (2002) 'Neuronal leucine-rich repeat protein-3 amplifies MAPK activation by

epidermal growth factor through a carboxyl-terminal region containing endocytosis motifs', *J Biol Chem,* 277(46), 43549-52.

Fukata, Y., Adesnik, H., Iwanaga, T., Bredt, D., Nicoll, R. and Fukata, M. (2006) 'Epilepsy-related ligand/receptor complex LGI1 and ADAM22 regulate synaptic transmission', *Science,* 313, 1792 - 5.

Fukata, Y., Lovero, K. L., Iwanaga, T., Watanabe, A., Yokoi, N., Tabuchi, K., Shigemoto, R., Nicoll, R. A. and Fukata, M. (2010) 'Disruption of LGI1–linked synaptic complex causes abnormal synaptic transmission and epilepsy', *Proceedings of the National Academy of Sciences.*

Gainetdinov, R. R., Wetsel, W. C., Jones, S. R., Levin, E. D., Jaber, M. and Caron, M. G. (1999) 'Role of serotonin in the paradoxical calming effect of psychostimulants on hyperactivity', *Science,* 283(5400), 397-401.

Gallistel, C. R., Gomita, Y., Yadin, E. and Campbell, K. A. (1985) 'Forebrain origins and terminations of the medial forebrain bundle metabolically activated by rewarding stimulation or by reward-blocking doses of pimozide', *J Neurosci,* 5(5), 1246-61.

Gamse, J. T., Kuan, Y. S., Macurak, M., Brosamle, C., Thisse, B., Thisse, C. and Halpern, M. E. (2005) 'Directional asymmetry of the zebrafish epithalamus guides dorsoventral innervation of the midbrain target', *Development,* 132(21), 4869-81.

Gangloff, M., Ludidi, P. and Gay, N. (2004) 'Structures and motifs involved in Toll signaling', *Toll receptors.*

Gangloff, M., Weber, A., Gibbard, R. and Gay, N. (2003) 'Evolutionary relationships, but functional differences, between the Drosophila and human Toll-like receptor families', *Biochem Soc Trans,* 31, 659 - 63.

Gatto, C. L. and Broadie, K. (2010) 'Genetic controls balancing excitatory and inhibitory synaptogenesis in neurodevelopmental disorder models', *Front Synaptic Neurosci,* 2, 4.

Geisler, S., Andres, K. H. and Veh, R. W. (2003) 'Morphologic and cytochemical criteria for the identification and delineation of individual subnuclei within the lateral habenular complex of the rat', *J Comp Neurol,* 458(1), 78-97.

Geisler, S. and Trimble, M. (2008) 'The lateral habenula: no longer neglected', *CNS Spectr,* 13(6), 484-9.

Ghiglione, C., Carraway, K., Amundadottir, L., Boswell, R., Perrimon, N. and Duffy, J. (1999) 'The transmembrane molecule kekkon 1 acts in a feedback loop to negatively regulate the activity of the Drosophila EGF receptor during oogenesis', *Cell,* 96, 847 - 56.

Ginsberg, S. D., Che, S., Wuu, J., Counts, S. E. and Mufson, E. J. (2006) 'Down regulation of trk but not p75NTR gene expression in single cholinergic basal forebrain neurons mark the progression of Alzheimer's disease', *J Neurochem,* 97(2), 475-87.

Gioia, M., Vizzotto, L. and Bianchi, R. (1994) 'A cluster analysis of the neurons of the rat interpeduncular nucleus', *J Anat,* 185 (Pt 3), 459-64.

Giros, B., Jaber, M., Jones, S. R., Wightman, R. M. and Caron, M. G. (1996) 'Hyperlocomotion and indifference to cocaine and amphetamine in mice lacking the dopamine transporter', *Nature,* 379(6566), 606-612.

Gottesfeld, Z. (1983) 'Central and peripheral contributions of deafferentation-induced norepinephrine increase in the habenula', *Brain Res,* 268(2), 359-61.

Graham, D. R. and Sidhu, A. (2010) 'Mice expressing the A53T mutant form of human alpha-synuclein exhibit hyperactivity and reduced anxiety-like behavior', *J Neurosci Res,* 88(8), 1777-83.

Greatrex, R. M. and Phillipson, O. T. (1982) 'Demonstration of synaptic input from prefrontal cortex to the habenula i the rat', *Brain Res,* 238(1), 192-7.

Groenewegen, H. J., Ahlenius, S., Haber, S. N., Kowall, N. W. and Nauta, W. J. (1986) 'Cytoarchitecture, fiber connections, and some histochemical aspects of the interpeduncular nucleus in the rat', *J Comp Neurol,* 249(1), 65-102.

Halfon, M., Hashimoto, C. and Keshishian, H. (1995) 'The Drosophila toll gene functions zygotically and is necessary for proper motoneuron and muscle development', *Dev Biol,* 169, 151 - 67.

Hannula-Jouppi, K., Kaminen-Ahola, N., Taipale, M., Eklund, R., Nopola-Hemmi, J., Kaariainen, H. and Kere, J. (2005) 'The axon guidance receptor gene ROBO1 is a candidate gene for developmental dyslexia', *PLoS Genet,* 1(4), e50.

Haun, F., Eckenrode, T. C. and Murray, M. (1992) 'Habenula and thalamus cell transplants restore normal sleep behaviors disrupted by denervation of the interpeduncular nucleus', *J Neurosci,* 12(8), 3282-90.

He, H., Mahnke, A. H., Doyle, S., Fan, N., Wang, C.-C., Hall, B. J., Tang, Y.-P., Inglis, F. M., Chen, C. and Erickson, J. D. (2012) 'Neurodevelopmental Role for VGLUT2 in Pyramidal Neuron Plasticity, Dendritic Refinement, and in Spatial Learning', *The Journal of Neuroscience,* 32(45), 15886-15901.

He, X., Bazan, J., McDermott, G., Park, J., Wang, K., Tessier-Lavigne, M., He, Z. and Garcia, K. (2003) 'Structure of the Nogo receptor ectodomain: a recognition module implicated in myelin inhibition', *Neuron,* 38, 177 - 85.

Hendrickx, A., Beullens, M., Ceulemans, H., Den Abt, T., Van Eynde, A., Nicolaescu, E., Lesage, B. and Bollen, M. (2009) 'Docking Motif-Guided Mapping of the Interactome of Protein Phosphatase-1', *Chemistry & Biology,* 16(4), 365-371.

Herkenham, M. and Nauta, W. J. (1979) 'Efferent connections of the habenular nuclei in the rat', *J Comp Neurol,* 187(1), 19-47.

Hikosaka, O. (2010) 'The habenula: from stress evasion to value-based decision-making', *Nat Rev Neurosci,* 11(7), 503-13.

Hofmann, K. and Stoffel, W. (1993) 'TMbase - A database of membrane spanning proteins segments', *Biol Chem Hoppe-Seyler,* 374, 166.

Homma, S., Shimada, T., Hikake, T. and Yaginuma, H. (2009) 'Expression pattern of LRR and Ig domain-containing protein (LRRIG protein) in the early mouse embryo', *Gene Expr Patterns,* 9(1), 1-26.

Hong, W., Zhu, H., Potter, C. J., Barsh, G., Kurusu, M., Zinn, K. and Luo, L. (2009) 'Leucine-rich repeat transmembrane proteins instruct discrete dendrite targeting in an olfactory map', *Nat Neurosci,* 12(12), 1542-50.

Hsieh, Y.-C. and Puche, A. C. (2013) 'Development of the Islands of Calleja', *Brain Res,* 1490(0), 52-60.

Hsu, R., Woodroffe, A., Lai, W. S., Cook, M. N., Mukai, J., Dunning, J. P., Swanson, D. J., Roos, J. L., Abecasis, G. R., Karayiorgou, M. and Gogos, J. A. (2007) 'Nogo Receptor 1 (RTN4R) as a candidate gene for schizophrenia: analysis using human and mouse genetic approaches', *PLoS One,* 2(11), e1234.

http://www.ncbi.nlm.nih.gov/FLC/getmgc.cgi.

Huang, E. J. and Reichardt, L. F. (2003) 'Trk receptors: roles in neuronal signal transduction', *Annu Rev Biochem,* 72, 609-42.

Huizinga, E., Tsuji, S., Romijn, R., Schiphorst, M., de Groot, P., Sixma, J. and Gros, P. (2002) 'Structures of glycoprotein Ibalpha and its complex with von Willebrand factor A1 domain', *Science,* 297, 1176 - 9.

HumanGPI.

Imamura, F., Nagao, H., Naritsuka, H., Murata, Y., Taniguchi, H. and Mori, K. (2006) 'A leucine-rich repeat membrane protein, 5T4, is expressed by a subtype of granule cells with dendritic arbors in specific strata of the mouse olfactory bulb', *J Comp Neurol,* 495(6), 754-68.

Inaki, M., Shinza-Kameda, M., Ismat, A., Frasch, M. and Nose, A. (2010) 'Drosophila Tey represses transcription of the repulsive cue Toll and generates neuromuscular target specificity', *Development,* 137(13), 2139-46.

Indo, Y., Tsuruta, M., Hayashida, Y., Karim, M., Ohta, K., Kawano, T., Mitsubuchi, H., Tonoki, H., Awaya, Y. and Matsuda, I. (1996) 'Mutations in the TRKA/NGF receptor gene in patients with congenital insensitivity to pain with anhidrosis', *Nat Genet,* 13, 485 - 8.

Irani, N. G., Di Rubbo, S., Mylle, E., Van den Begin, J., Schneider-Pizon, J., Hnilikova, J., Sisa, M., Buyst, D., Vilarrasa-Blasi, J., Szatmari, A. M., Van Damme, D., Mishev, K., Codreanu, M. C., Kohout, L., Strnad, M., Cano-Delgado, A. I., Friml, J., Madder, A. and Russinova, E. (2012) 'Fluorescent castasterone reveals BRI1 signaling from the plasma membrane', *Nat Chem Biol,* 8(6), 583-9.

Jen, J. C., Chan, W. M., Bosley, T. M., Wan, J., Carr, J. R., Rub, U., Shattuck, D., Salamon, G., Kudo, L. C., Ou, J., Lin, D. D., Salih, M. A., Kansu, T., Al Dhalaan, H., Al Zayed, Z., MacDonald, D. B., Stigsby, B., Plaitakis, A., Dretakis, E. K., Gottlob, I., Pieh, C., Traboulsi, E. I., Wang, Q., Wang, L., Andrews, C.,

Yamada, K., Demer, J. L., Karim, S., Alger, J. R., Geschwind, D. H., Deller, T., Sicotte, N. L., Nelson, S. F., Baloh, R. W. and Engle, E. C. (2004) 'Mutations in a human ROBO gene disrupt hindbrain axon pathway crossing and morphogenesis', *Science,* 304(5676), 1509-13.

Jepson, S., Vought, B., Gross, C. H., Gan, L., Austen, D., Frantz, J. D., Zwahlen, J., Lowe, D., Markland, W. and Krauss, R. (2012) 'LINGO-1, a transmembrane signaling protein, inhibits oligodendrocyte differentiation and myelination through intercellular self-interactions', *J Biol Chem,* 287(26), 22184-95.

Jessell, T. M. and Sanes, J. R. (2000) 'Development. The decade of the developing brain', *Curr Opin Neurobiol,* 10(5), 599-611.

Jhou, T. C., Fields, H. L., Baxter, M. G., Saper, C. B. and Holland, P. C. (2009) 'The rostromedial tegmental nucleus (RMTg), a GABAergic afferent to midbrain dopamine neurons, encodes aversive stimuli and inhibits motor responses', *Neuron,* 61(5), 786-800.

Ji, H. and Shepard, P. D. (2007) 'Lateral habenula stimulation inhibits rat midbrain dopamine neurons through a GABA(A) receptor-mediated mechanism', *J Neurosci,* 27(26), 6923-30.

Jin, H., Selfe, J., Whitehouse, C., Morris, J., Solomon, E. and Roberts, R. (2004) 'Structural evolution of the BRCA1 genomic region in primates', *Genomics,* 84, 1071 - 82.

Kajava, A. (1998) 'Structural diversity of leucine-rich repeat proteins', *J Mol Biol,* 277, 519 - 27.

Kalachikov, S., Evgrafov, O., Ross, B., Winawer, M., Barker-Cummings, C., Martinelli Boneschi, F., Choi, C., Morozov, P., Das, K. and Teplitskaya, E. (2002) 'Mutations in LGI1 cause autosomal-dominant partial epilepsy with auditory features', *Nat Genet,* 30, 335 - 41.

Kall, L. and Sonnhammer, E. (2002) 'Reliability of transmembrane predictions in whole-genome data', *FEBS Lett,* 532, 415 - 8.

Kalueff, A. V., Keisala, T., Minasyan, A., Kuuslahti, M. and Tuohimaa, P. (2006) 'Temporal stability of novelty exploration in mice exposed to different open field tests', *Behav Processes,* 72(1), 104-12.

Kambris, Z., Hoffmann, J., Imler, J. and Capovilla, M. (2002) 'Tissue and stage-specific expression of the Tolls in Drosophila embryos', *Gene Expr Patterns,* 2, 311 - 7.

Karaulanov, E., Bottcher, R. and Niehrs, C. (2006) 'A role for fibronectin-leucine-rich transmembrane cell-surface proteins in homotypic cell adhesion', *EMBO Rep,* 7, 283 - 90.

Karaulanov, E., Bottcher, R. T., Stannek, P., Wu, W., Rau, M., Ogata, S., Cho, K. W. and Niehrs, C. (2009) 'Unc5B interacts with FLRT3 and Rnd1 to modulate cell adhesion in Xenopus embryos', *PLoS One,* 4(5), e5742.

Karlsson, T., Mark, E. B., Henriksson, R. and Hedman, H. (2008) 'Redistribution of LRIG proteins in psoriasis', *J Invest Dermatol,* 128(5), 1192-5.

Kaufman, A., Dror, G., Meilijson, I. and Ruppin, E. (2006) 'Gene expression of Caenorhabditis elegans neurons carries information on their synaptic connectivity', *PLoS Comput Biol,* 2(12), e167.

Kaufmann, R., Goldberg-Stern, H. and Shuper, A. (2009) 'Attention-deficit disorders and epilepsy in childhood: incidence, causative relations and treatment possibilities', *J Child Neurol,* 24(6), 727-33.

Kawaja, M. D., Flumerfelt, B. A. and Hrycyshyn, A. W. (1989) 'Glutamate decarboxylase immunoreactivity in the rat interpeduncular nucleus: a light and electron microscope investigation', *Neuroscience,* 30(3), 741-53.

Keleman, K. and Dickson, B. J. (2001) 'Short- and long-range repulsion by the Drosophila Unc5 netrin receptor', *Neuron,* 32(4), 605-17.

Kelly, P. H. (1998) 'Defective inhibition of dream event memory formation: a hypothesized mechanism in the onset and progression of symptoms of schizophrenia', *Brain Res Bull,* 46(3), 189-97.

Kett, L. R. and Dauer, W. T. (2012) 'Leucine-rich repeat kinase 2 for beginners: six key questions', *Cold Spring Harb Perspect Med,* 2(3), a009407.

Kidd, T., Bland, K. and Goodman, C. (1999) 'Slit is the midline repellent for the robo receptor in Drosophila', *Cell,* 96, 785 - 94.

Kim, J., Lee, C., Jin, M., Lee, C., Paik, S., Lee, H. and Lee, J. (2005) 'Crystal structure of CD14 and its implications for lipopolysaccharide signaling', *J Biol Chem,* 280, 11347 - 51.

Kim, S., Burette, A., Chung, H., Kwon, S., Woo, J., Lee, H., Kim, K., Kim, H., Weinberg, R. and Kim, E. (2006) 'NGL family PSD-95-interacting adhesion molecules regulate excitatory synapse formation', *Nat Neurosci,* 9, 1294 - 301.

Kim, U. (2009) 'Topographic commissural and descending projections of the habenula in the rat', *J Comp Neurol,* 513(2), 173-187.

Kim, U. and Chang, S. Y. (2005) 'Dendritic morphology, local circuitry, and intrinsic electrophysiology of neurons in the rat medial and lateral habenular nuclei of the epithalamus', *J Comp Neurol,* 483(2), 236-50.

Kita, H. (1994) 'Parvalbumin-immunopositive neurons in rat globus pallidus: a light and electron microscopic study', *Brain Res,* 657(1–2), 31-41.

Klemm, W. R. (2004) 'Habenular and interpeduncularis nuclei: shared components in multiple-function networks', *Med Sci Monit,* 10(11), Ra261-73.

Ko, J. (2012) 'The leucine-rich repeat superfamily of synaptic adhesion molecules: LRRTMs and slitrks', *Mol Cells.*

Ko, J., Fuccillo, M. V., Malenka, R. C. and Südhof, T. C. (2009) 'LRRTM2 Functions as a Neurexin Ligand in Promoting Excitatory Synapse Formation', *Neuron,* 64(6), 791-798.

Ko, J., Kim, S., Chung, H., Kim, K., Han, K., Kim, H., Jun, H., Kaang, B. and Kim, E. (2006) 'SALM synaptic cell adhesion-like molecules regulate the differentiation of excitatory synapses', *Neuron,* 50, 233 - 45.

Kobayashi, Y., Sano, Y., Vannoni, E., Goto, H., Suzuki, H., Oba, A., Kawasaki, H., Kanba, S., Lipp, H. P., Murphy, N. P., Wolfer, D. P. and Itohara, S. (2013) 'Genetic dissection of medial habenula-interpeduncular nucleus pathway function in mice', *Front Behav Neurosci,* 7, 17.

Kobe, B. and Deisenhofer, J. (1995) 'A structural basis of the interactions between leucine-rich repeats and protein ligands', *Nature,* 374(6518), 183-6.

Kobe, B. and Kajava, A. (2001) 'The leucine-rich repeat as a protein recognition motif', *Curr Opin Struct Biol,* 11, 725 - 32.

Kohsaka, H. and Nose, A. (2009) 'Target recognition at the tips of postsynaptic filopodia: accumulation and function of Capricious', *Development,* 136(7), 1127-35.

Kolodkin, A. L. and Tessier-Lavigne, M. (2011) 'Mechanisms and molecules of neuronal wiring: a primer', *Cold Spring Harb Perspect Biol,* 3(6).

Krogh, A., Larsson, B., von Heijne, G. and Sonnhammer, E. (2001) 'Predicting transmembrane protein topology with a hidden Markov model: application to complete genomes', *J Mol Biol,* 305, 567 - 80.

Kuja-Panula, J., Kiiltomaki, M., Yamashiro, T., Rouhiainen, A. and Rauvala, H. (2003) 'AMIGO, a transmembrane protein implicated in axon tract development, defines a novel protein family with leucine-rich repeats', *J Cell Biol,* 160(6), 963-73.

Kurusu, M., Cording, A., Taniguchi, M., Menon, K., Suzuki, E. and Zinn, K. (2008) 'A screen of cell-surface molecules identifies leucine-rich repeat proteins as key mediators of synaptic target selection', *Neuron,* 59(6), 972-85.

Kwon, S. K., Woo, J., Kim, S. Y., Kim, H. and Kim, E. (2010) 'Trans-synaptic adhesions between netrin-G ligand-3 (NGL-3) and receptor tyrosine phosphatases LAR, protein-tyrosine phosphatase delta (PTPdelta), and PTPsigma via specific domains regulate excitatory synapse formation', *J Biol Chem,* 285(18), 13966-78.

Laruelle, M., Abi-Dargham, A., van Dyck, C. H., Gil, R., D'Souza, C. D., Erdos, J., McCance, E., Rosenblatt, W., Fingado, C., Zoghbi, S. S., Baldwin, R. M., Seibyl, J. P., Krystal, J. H., Charney, D. S. and Innis, R. B. (1996) 'Single photon emission computerized tomography imaging of amphetamine-induced dopamine release in drug-free schizophrenic subjects', *Proceedings of the National Academy of Sciences,* 93(17), 9235-9240.

Lauren, J., Airaksinen, M., Saarma, M. and Timmusk, T. (2003) 'A novel gene family encoding leucine-rich repeat transmembrane proteins differentially expressed in the nervous system', *Genomics,* 81, 411 - 21.

Lazzaro, B., Sackton, T. and Clark, A. (2006) 'Genetic Variation inDrosophila melanogaster Resistance to Infection: A Comparison Across Bacteria', *Genetics,* 174, 1539 - 54.

Lecourtier, L., Defrancesco, A. and Moghaddam, B. (2008) 'Differential tonic influence of lateral habenula on prefrontal cortex and nucleus accumbens dopamine release', *Eur J Neurosci,* 27(7), 1755-62.

Lecourtier, L. and Kelly, P. H. (2005) 'Bilateral lesions of the habenula induce attentional disturbances in rats', *Neuropsychopharmacology,* 30(3), 484-96.

Lecourtier, L. and Kelly, P. H. (2007) 'A conductor hidden in the orchestra? Role of the habenular complex in monoamine transmission and cognition', *Neurosci Biobehav Rev,* 31(5), 658-72.

Lecourtier, L., Neijt, H. C. and Kelly, P. H. (2004) 'Habenula lesions cause impaired cognitive performance in rats: implications for schizophrenia', *Eur J Neurosci,* 19(9), 2551-60.

Lee, E. H. and Huang, S. L. (1988) 'Role of lateral habenula in the regulation of exploratory behavior and its relationship to stress in rats', *Behav Brain Res,* 30(3), 265-71.

Lee, Y. A. and Goto, Y. (2011) 'Neurodevelopmental disruption of cortico-striatal function caused by degeneration of habenula neurons', *PLoS One,* 6(4), e19450.

Leighton, P. A., Mitchell, K. J., Goodrich, L. V., Lu, X., Pinson, K., Scherz, P., Skarnes, W. C. and Tessier-Lavigne, M. (2001) 'Defining brain wiring patterns and mechanisms through gene trapping in mice', *Nature,* 410(6825), 174-9.

Lein, E., Hawrylycz, M., Ao, N., Ayres, M., Bensinger, A., Bernard, A., Boe, A., Boguski, M., Brockway, K. and Byrnes, E. (2007) 'Genome-wide atlas of gene expression in the adult mouse brain', *Nature,* 445, 168 - 76.

Leuner, B. and Gould, E. (2010) 'Structural plasticity and hippocampal function', *Annu Rev Psychol,* 61, 111-40, C1-3.

Li, B., Piriz, J., Mirrione, M., Chung, C., Proulx, C. D., Schulz, D., Henn, F. and Malinow, R. (2011) 'Synaptic potentiation onto habenula neurons in the learned helplessness model of depression', *Nature,* 470(7335), 535-9.

Li, C., Dong, J., Lanza, F., Sanan, D., Sae-Tung, G. and Lopez, J. (1995) 'Expression of platelet glycoprotein (GP) V in heterologous cells and evidence for its association with GP Ib alpha in forming a GP Ib-IX-V complex on the cell surface', *J Biol Chem,* 270, 16302 - 7.

Li, X., Chen, Y., Liu, Y., Gao, J., Gao, F., Bartlam, M., Wu, J. Y. and Rao, Z. (2006) 'Structural basis of Robo proline-rich motif recognition by the srGAP1 Src homology 3 domain in the Slit-Robo signaling pathway', *J Biol Chem,* 281(38), 28430-7.

Lin, J., Ho, W., Gurney, A. and Rosenthal, A. (2003) 'The netrin-G1 ligand NGL-1 promotes the outgrowth of thalamocortical axons', *Nat Neurosci,* 6, 1270 - 6.

Linhoff, M. W., Lauren, J., Cassidy, R. M., Dobie, F. A., Takahashi, H., Nygaard, H. B., Airaksinen, M. S., Strittmatter, S. M. and Craig, A. M. (2009) 'An unbiased expression screen for synaptogenic proteins identifies the LRRTM protein family as synaptic organizers', *Neuron,* 61(5), 734-49.

Lodha, N., Loucks, C. M., Beaulieu, C., Parboosingh, J. S. and Bech-Hansen, N. T. (2012) 'Congenital stationary night blindness: mutation update and clinical variability', *Adv Exp Med Biol,* 723, 371-9.

Long, H., Sabatier, C., Le, M., Plump, A., Yuan, W., Ornitz, D. M., Tamada, A., Murakami, F., Goodman, C. S. and Tessier-Lavigne, M. (2004) 'Conserved Roles for Slit and Robo Proteins in Midline Commissural Axon Guidance', *Neuron,* 42(2), 213-223.

Loscher, W. and Brandt, C. (2010) 'Prevention or modification of epileptogenesis after brain insults: experimental approaches and translational research', *Pharmacol Rev,* 62(4), 668-700.

Lykissas, M. G., Batistatou, A. K., Charalabopoulos, K. A. and Beris, A. E. (2007) 'The role of neurotrophins in axonal growth, guidance, and regeneration', *Curr Neurovasc Res,* 4(2), 143-51.

Ma, Y., Li, J., Chiu, I., Wang, Y., Sloane, J., Lu, J., Kosaras, B., Sidman, R., Volpe, J. and Vartanian, T. (2006) 'Toll-like receptor 8 functions as a negative regulator of neurite outgrowth and inducer of neuronal apoptosis', *Journal of Cell Biology,* 175, 209 - 215.

Mah, W., Ko, J., Nam, J., Han, K., Chung, W. S. and Kim, E. (2010) 'Selected SALM (synaptic adhesion-like molecule) family proteins regulate synapse formation', *J Neurosci,* 30(16), 5559-68.

Majercak, J., Ray, W., Espeseth, A., Simon, A., Shi, X., Wolffe, C., Getty, K., Marine, S., Stec, E. and Ferrer, M. (2006) 'LRRTM3 promotes processing of amyloid-precursor protein by BACE1 and is a positional candidate gene for late-onset Alzheimer's disease', *Proc Natl Acad Sci USA,* 103, 17967 - 72.

Mallet, N., Micklem, B. R., Henny, P., Brown, M. T., Williams, C., Bolam, J. P., Nakamura, K. C. and Magill, P. J. (2012) 'Dichotomous organization of the external globus pallidus', *Neuron,* 74(6), 1075-86.

Mandai, K., Guo, T., St Hillaire, C., Meabon, J. S., Kanning, K. C., Bothwell, M. and Ginty, D. D. (2009) 'LIG family receptor tyrosine kinase-associated proteins modulate growth factor signals during neural development', *Neuron,* 63(5), 614-27.

Mangan, P. S. and Bertram Iii, E. H. (1997) 'Shortened-duration GABAA receptor-mediated synaptic potentials underlie enhanced CA1 excitability in a chronic model of temporal lobe epilepsy', *Neuroscience,* 80(4), 1101-1111.

Mardy, S., Miura, Y., Endo, F., Matsuda, I. and Indo, Y. (2001) 'Congenital insensitivity to pain with anhidrosis (CIPA): effect of TRKA (NTRK1) missense mutations on autophosphorylation of the receptor tyrosine kinase for nerve growth factor', *Hum Mol Genet,* 10(3), 179-188.

Maretto, S., Müller, P.-S., Aricescu, A. R., Cho, K. W. Y., Bikoff, E. K. and Robertson, E. J. (2008) 'Ventral closure, headfold fusion and definitive endoderm migration defects in mouse embryos lacking the fibronectin leucine-rich transmembrane protein FLRT3', *Developmental Biology,* 318(1), 184-193.

Marillat, V., Sabatier, C., Failli, V., Matsunaga, E., Sotelo, C., Tessier-Lavigne, M. and Chedotal, A. (2004) 'The slit receptor Rig-1/Robo3 controls midline crossing by hindbrain precerebellar neurons and axons', *Neuron,* 43(1), 69-79.

Matsushima, N., Ohyanagi, T., Tanaka, T. and Kretsinger, R. (2000) 'Super-motifs and evolution of tandem leucine-rich repeats within the small proteoglycans-biglycan, decorin, lumican, fibromodulin, PRELP, keratocan, osteoadherin, epiphycan, and osteoglycin', *Proteins,* 38, 210 - 25.

Matsushima, N., Tachi, N., Kuroki, Y., Enkhbayar, P., Osaki, M., Kamiya, M. and Kretsinger, R. (2005) 'Structural analysis of leucine-rich-repeat variants in proteins associated with human diseases', *Cell Mol Life Sci,* 62, 2771 - 91.

Matthews, K., Mueller-Ortiz, S. and Wetsel, R. (2004) 'Carboxypeptidase N: a pleiotropic regulator of inflammation', *Mol Immunol,* 40, 785 - 93.

McEwan, P., Scott, P., Bishop, P. and Bella, J. (2006) 'Structural correlations in the family of small leucine-rich repeat proteins and proteoglycans', *J Struct Biol,* 155, 294 - 305.

McGee, A., Yang, Y., Fischer, Q., Daw, N. and Strittmatter, S. (2005) 'Experience-driven plasticity of visual cortex limited by myelin and Nogo receptor', *Science,* 309, 2222 - 6.

Mehler-Wex, C., Riederer, P. and Gerlach, M. (2006) 'Dopaminergic dysbalance in distinct basal ganglia neurocircuits: implications for the pathophysiology of Parkinson's disease, schizophrenia and attention deficit hyperactivity disorder', *Neurotox Res,* 10(3-4), 167-79.

Menalled, L. B., Dziewczapolski, G., Garcia, M. C., Rubinstein, M. and Gershanik, O. S. (1999) 'D3 receptor knockdown through antisense oligonucleotide administration supports its inhibitory role in locomotion', *Neuroreport,* 10(15), 3131-6.

Menard, J. and Treit, D. (1996) 'Lateral and medial septal lesions reduce anxiety in the plus-maze and probe-burying tests', *Physiol Behav,* 60(3), 845-53.

Meng, H., Wang, Y., Huang, M., Lin, W., Wang, S. and Zhang, B. (2011) 'Chronic deep brain stimulation of the lateral habenula nucleus in a rat model of depression', *Brain Res,* 1422, 32-8.

Mi, S., Lee, X., Shao, Z., Thill, G., Ji, B., Relton, J., Levesque, M., Allaire, N., Perrin, S., Sands, B., Crowell, T., Cate, R. L., McCoy, J. M. and Pepinsky, R. B. (2004) 'LINGO-1 is a component of the Nogo-66 receptor/p75 signaling complex', *Nat Neurosci,* 7(3), 221-8.

Mi, S., Miller, R., Lee, X., Scott, M., Shulag-Morskaya, S., Shao, Z., Chang, J., Thill, G., Levesque, M. and Zhang, M. (2005) 'LINGO-1 negatively regulates myelination by oligodendrocytes', *Nat Neurosci,* 8, 745 - 51.

Milan, M., Perez, L. and Cohen, S. M. (2005) 'Boundary formation in the Drosophila wing: functional dissection of Capricious and Tartan', *Dev Dyn,* 233(3), 804-10.

Milton, J. G. (2012) 'Neuronal avalanches, epileptic quakes and other transient forms of neurodynamics', *Eur J Neurosci,* 36(2), 2156-63.

Mitchell, K. J. (2011) 'The miswired brain: making connections from neurodevelopment to psychopathology', *BMC Biol,* 9, 23.

Molyneaux, B. J., Arlotta, P., Menezes, J. R. and Macklis, J. D. (2007) 'Neuronal subtype specification in the cerebral cortex', *Nat Rev Neurosci,* 8(6), 427-37.

Morimura, N., Inoue, T., Katayama, K. and Aruga, J. (2006) 'Comparative analysis of structure, expression and PSD95-binding capacity of Lrfn, a novel family of neuronal transmembrane proteins', *Gene,* 380(2), 72-83.

Morissette, M. C. and Boye, S. M. (2008) 'Electrolytic lesions of the habenula attenuate brain stimulation reward', *Behav Brain Res,* 187(1), 17-26.

Mosyak, L., Wood, A., Dwyer, B., Buddha, M., Johnson, M., Aulabaugh, A., Zhong, X., Presman, E., Benard, S. and Kelleher, K. (2006) 'The structure of the LINGO-1 ectodomain, a module implicated in CNS repair inhibition', *Journal of Cell Biology,* 281, 36378 - 90.

Muller, J. F., Mascagni, F. and McDonald, A. J. (2007) 'Postsynaptic targets of somatostatin-containing interneurons in the rat basolateral amygdala', *J Comp Neurol,* 500(3), 513-529.

Murphy, C. A., DiCamillo, A. M., Haun, F. and Murray, M. (1996) 'Lesion of the habenular efferent pathway produces anxiety and locomotor hyperactivity in rats: a comparison of the effects of neonatal and adult lesions', *Behav Brain Res,* 81(1-2), 43-52.

Nair, S. G., Strand, N. S. and Neumaier, J. F. (2012) 'DREADDing the lateral habenula: A review of methodological approaches for studying lateral habenula function', *Brain Res.*

Nakamura, K., Hioki, H., Fujiyama, F. and Kaneko, T. (2005) 'Postnatal changes of vesicular glutamate transporter (VGluT)1 and VGluT2 immunoreactivities and their colocalization in the mouse forebrain', *J Comp Neurol,* 492(3), 263-288.

Nam, J., Mah, W. and Kim, E. (2011) 'The SALM/Lrfn family of leucine-rich repeat-containing cell adhesion molecules', *Semin Cell Dev Biol,* 22(5), 492-8.

Nectoux, J., Girard, B., Bahi-Buisson, N., Prieur, F., Afenjar, A., Rosas-Vargas, H., Chelly, J. and Bienvenu, T. (2007) 'Netrin G1 mutations are an uncommon cause of atypical Rett syndrome with or without epilepsy', *Pediatr Neurol,* 37(4), 270-4.

Nguyen-Ba-Charvet, K. T. and Chedotal, A. (2002) 'Role of Slit proteins in the vertebrate brain', *J Physiol Paris,* 96(1-2), 91-8.

Nishikawa, T., Fage, D. and Scatton, B. (1986) 'Evidence for, and nature of, the tonic inhibitory influence of habenulointerpeduncular pathways upon cerebral dopaminergic transmission in the rat', *Brain Res,* 373(1-2), 324-36.

Nishimura-Akiyoshi, S., Niimi, K., Nakashiba, T. and Itohara, S. (2007) 'Axonal netrin-Gs transneuronally determine lamina-specific subdendritic segments', *Proc Natl Acad Sci U S A,* 104(37), 14801-6.

Nose, A. (2012) 'Generation of neuromuscular specificity in Drosophila: novel mechanisms revealed by new technologies', *Front Mol Neurosci,* 5, 62.

Nose, A., Takeichi, M. and Goodman, C. (1994) 'Ectopic expression of connectin reveals a repulsive function during growth cone guidance and synapse formation', *Neuron,* 13, 525 - 39.

Nose, A., Umeda, T. and Takeichi, M. (1997) 'Neuromuscular target recognition by a homophilic interaction of connectin cell adhesion molecules in Drosophila', *Development,* 124(8), 1433-41.

Nurnberger, T., Brunner, F., Kemmerling, B. and Piater, L. (2004) 'Innate immunity in plants and animals: striking similarities and obvious differences', *Immunol Rev,* 198, 249-66.

O'Connor, E., Eisenhaber, B., Dalley, J., Wang, T., Missen, C., Bulleid, N., Bishop, P. and Trump, D. (2005) 'Species specific membrane anchoring of nyctalopin, a small leucine-rich repeat protein', *Hum Mol Genet,* 14, 1877 - 87.

O'Sullivan, M. L., de Wit, J., Savas, J. N., Comoletti, D., Otto-Hitt, S., Yates, J. R., 3rd and Ghosh, A. (2012) 'FLRT proteins are endogenous latrophilin ligands and regulate excitatory synapse development', *Neuron,* 73(5), 903-10.

Ohta, K., Lupo, G., Kuriyama, S., Keynes, R., Holt, C., Harris, W., Tanaka, H. and Ohnuma, S. (2004) 'Tsukushi functions as an organizer inducer by inhibition of BMP activity in cooperation with chordin', *Dev Cell,* 7, 347 - 58.

Okazaki, Y., Furuno, M., Kasukawa, T., Adachi, J., Bono, H., Kondo, S., Nikaido, I., Osato, N., Saito, R. and Suzuki, H. (2002) 'Analysis of the mouse transcriptome based on functional annotation of 60,770 full-length cDNAs', *Nature,* 420, 563 - 73.

Ollendorff, V., Noguchi, T., deLapeyriere, O. and Birnbaum, D. (1994) 'The GARP gene encodes a new member of the family of leucine-rich repeat-containing proteins', *Cell Growth Differ,* 5(2), 213-9.

Otnaess, M. K., Djurovic, S., Rimol, L. M., Kulle, B., Kahler, A. K., Jonsson, E. G., Agartz, I., Sundet, K., Hall, H., Timm, S., Hansen, T., Callicott, J. H., Melle, I., Werge, T. and Andreassen, O. A. (2009) 'Evidence for a possible association of neurotrophin receptor (NTRK-3) gene polymorphisms with hippocampal function and schizophrenia', *Neurobiol Dis,* 34(3), 518-24.

Panuccio, G., Sanchez, G., Levesque, M., Salami, P., de Curtis, M. and Avoli, M. (2012) 'On the ictogenic properties of the piriform cortex in vitro', *Epilepsia,* 53(3), 459-68.

Papaleo, F., Silverman, J. L., Aney, J., Tian, Q., Barkan, C. L., Chadman, K. K. and Crawley, J. N. (2011) 'Working memory deficits, increased anxiety-like traits, and seizure susceptibility in BDNF overexpressing mice', *Learning & Memory,* 18(8), 534-544.

Parent, A., Gravel, S. and Boucher, R. (1981) 'The origin of forebrain afferents to the habenula in rat, cat and monkey', *Brain Res Bull,* 6(1), 23-38.

Park, J., Yiu, G., Kaneko, S., Wang, J., Chang, J., He, X., Garcia, K. and He, Z. (2005) 'A TNF receptor family member, TROY, is a coreceptor with Nogo receptor in mediating the inhibitory activity of myelin inhibitors', *Neuron,* 45, 345 - 51.

Park, M. R. (1987) 'Monosynaptic inhibitory postsynaptic potentials from lateral habenula recorded in dorsal raphe neurons', *Brain Res Bull,* 19(5), 581-6.

Phillipson, O. T. and Pycock, C. J. (1982) 'Dopamine neurones of the ventral tegmentum project to both medial and lateral habenula. Some implications for habenular function', *Exp Brain Res,* 45(1-2), 89-94.

Piton, A., Gauthier, J., Hamdan, F. F., Lafreniere, R. G., Yang, Y., Henrion, E., Laurent, S., Noreau, A., Thibodeau, P., Karemera, L., Spiegelman, D., Kuku, F., Duguay, J., Destroismaisons, L., Jolivet, P., Cote, M., Lachapelle, K., Diallo, O., Raymond, A., Marineau, C., Champagne, N., Xiong, L., Gaspar, C., Riviere, J. B., Tarabeux, J., Cossette, P., Krebs, M. O., Rapoport, J. L., Addington, A., Delisi, L. E., Mottron, L., Joober, R., Fombonne, E., Drapeau, P. and Rouleau, G. A. (2011) 'Systematic resequencing of X-chromosome synaptic genes in autism spectrum disorder and schizophrenia', *Mol Psychiatry,* 16(8), 867-80.

Pujol, N., Link, E., Liu, L., Kurz, C., Alloing, G., Tan, M., Ray, K., Solari, R., Johnson, C. and Ewbank, J. (2001) 'A reverse genetic analysis of components of the Toll signaling pathway in Caenorhabditis elegans', *Curr Biol,* 11, 809 - 21.

Putnam, F. W. and Takahashi, N. (1988) 'Structural characterization of glycoproteins', *J Chromatogr,* 443, 267-84.

Qin, C. and Luo, M. (2009) 'Neurochemical phenotypes of the afferent and efferent projections of the mouse medial habenula', *Neuroscience,* 161(3), 827-37.

Quina, L. A., Wang, S., Ng, L. and Turner, E. E. (2009) 'Brn3a and Nurr1 mediate a gene regulatory pathway for habenula development', *J Neurosci,* 29(45), 14309-22.

Rabenau, K. E., O'Toole, J. M., Bassi, R., Kotanides, H., Witte, L., Ludwig, D. L. and Pereira, D. S. (2004) 'DEGA/AMIGO-2, a leucine-rich repeat family member, differentially expressed in human gastric adenocarcinoma: effects on ploidy, chromosomal stability, cell adhesion/migration and tumorigenicity', *Oncogene,* 23(29), 5056-67.

Racine, R. J. (1972) 'Modification of seizure activity by electrical stimulation: II. Motor seizure', *Electroencephalography and Clinical Neurophysiology,* 32(3), 281-294.

Rafael, J. A., Nitta, Y., Peters, J. and Davies, K. E. (2000) 'Testing of SHIRPA, a mouse phenotypic assessment protocol, on Dmd(mdx) and Dmd(mdx3cv) dystrophin-deficient mice', *Mamm Genome,* 11(9), 725-8.

Rajakumar, N., Elisevich, K. and Flumerfelt, B. A. (1994) 'Parvalbumin-containing GABAergic neurons in the basal ganglia output system of the rat', *J Comp Neurol,* 350(2), 324-36.

Reichelt, A. C., Rodgers, R. J. and Clapcote, S. J. (2012) 'The role of neurexins in schizophrenia and autistic spectrum disorder', *Neuropharmacology,* 62(3), 1519-26.

Reitz, C., Conrad, C., Roszkowski, K., Rogers, R. S. and Mayeux, R. (2012) 'Effect of Genetic Variation in LRRTM3 on Risk of Alzheimer Disease', *Arch Neurol.*

Richards, J. G., Schoch, P., Haring, P., Takacs, B. and Mohler, H. (1987) 'Resolving GABAA/benzodiazepine receptors: cellular and subcellular localization in the CNS with monoclonal antibodies', *J Neurosci,* 7(6), 1866-86.

Rose, D., Zhu, X., Kose, H., Hoang, B., Cho, J. and Chiba, A. (1997) 'Toll, a muscle cell surface molecule, locally inhibits synaptic initiation of the RP3 motoneuron growth cone in Drosophila', *Development,* 124(8), 1561-71.

Roubin, R., Pizette, S., Ollendorff, V., Planche, J., Birnbaum, D. and Delapeyriere, O. (1996) 'Structure and developmental expression of mouse Garp, a gene encoding a new leucine-rich repeat-containing protein', *Int J Dev Biol,* 40(3), 545-55.

Rougon, G. and Hobert, O. (2003) 'New insights into the diversity and function of neuronal immunoglobulin superfamily molecules', *Annu Rev Neurosci,* 26, 207-38.

Roussigne, M., Bianco, I. H., Wilson, S. W. and Blader, P. (2009) 'Nodal signalling imposes left-right asymmetry upon neurogenesis in the habenular nuclei', *Development,* 136(9), 1549-57.

Rudy, B., Fishell, G., Lee, S. and Hjerling-Leffler, J. (2011) 'Three groups of interneurons account for nearly 100% of neocortical GABAergic neurons', *Dev Neurobiol,* 71(1), 45-61.

Sabatier, C., Plump, A. S., Le, M., Brose, K., Tamada, A., Murakami, F., Lee, E. Y. and Tessier-Lavigne, M. (2004) 'The divergent Robo family protein rig-1/Robo3 is a negative regulator of slit responsiveness required for midline crossing by commissural axons', *Cell,* 117(2), 157-69.

Sadek, A. R., Magill, P. J. and Bolam, J. P. (2007) 'A single-cell analysis of intrinsic connectivity in the rat globus pallidus', *J Neurosci,* 27(24), 6352-62.

Sagane, K., Ishihama, Y. and Sugimoto, H. (2008) 'LGI1 and LGI4 bind to ADAM22, ADAM23 and ADAM11', *Int J Biol Sci,* 4(6), 387-96.

Sagvolden, T., Johansen, E. B., Aase, H. and Russell, V. A. (2005a) 'A dynamic developmental theory of attention-deficit/hyperactivity disorder (ADHD) predominantly hyperactive/impulsive and combined subtypes', *Behav Brain Sci,* 28(3), 397-419; discussion 419-68.

Sagvolden, T., Russell, V. A., Aase, H., Johansen, E. B. and Farshbaf, M. (2005b) 'Rodent models of attention-deficit/hyperactivity disorder', *Biol Psychiatry,* 57(11), 1239-47.

SAH, P., FABER, E. S. L., LOPEZ DE ARMENTIA, M. and POWER, J. (2003) 'The Amygdaloid Complex: Anatomy and Physiology', *Physiological Reviews,* 83(3), 803-834.

Satoh, K., Hata, M., Shimizu, T., Yokota, H., Akatsu, H., Yamamoto, T., Kosaka, K. and Yamada, T. (2005) 'Lib, transcriptionally induced in senile plaque-associated astrocytes, promotes glial migration through extracellular matrix', *Biochem Biophys Res Commun,* 335(2), 631-6.

Schindowski, K., Belarbi, K. and Buee, L. (2008) 'Neurotrophic factors in Alzheimer's disease: role of axonal transport', *Genes Brain Behav,* 7 Suppl 1, 43-56.

Scott, P., McEwan, P., Dodd, C., Bergmann, E., Bishop, P. and Bella, J. (2004) 'Crystal structure of the dimeric protein core of decorin, the archetypal small leucine-rich repeat proteoglycan', *Proc Natl Acad Sci USA,* 101, 15633 - 8.

Seabold, G. K., Wang, P. Y., Chang, K., Wang, C. Y., Wang, Y. X., Petralia, R. S. and Wenthold, R. J. (2008) 'The SALM family of adhesion-like molecules forms heteromeric and homomeric complexes', *J Biol Chem,* 283(13), 8395-405.

Sebe, J. Y. and Baraban, S. C. (2011) 'The promise of an interneuron-based cell therapy for epilepsy', *Dev Neurobiol,* 71(1), 107-17.

Sedaghat, K., Shen, P. J., Finkelstein, D. I., Henderson, J. M. and Gundlach, A. L. (2008) 'Leucine-rich repeat-containing G-protein-coupled receptor 8 in the rat brain: Enrichment in thalamic neurons and their efferent projections', *Neuroscience,* 156(2), 319-33.

Seppala, E. H., Jokinen, T. S., Fukata, M., Fukata, Y., Webster, M. T., Karlsson, E. K., Kilpinen, S. K., Steffen, F., Dietschi, E., Leeb, T., Eklund, R., Zhao, X., Rilstone, J. J., Lindblad-Toh, K., Minassian, B. A. and Lohi, H. (2011) 'LGI2 truncation causes a remitting focal epilepsy in dogs', *PLoS Genet,* 7(7), e1002194.

Shao, Z., Browning, J., Lee, X., Scott, M., Shulga-Morskaya, S., Allaire, N., Thill, G., Levesque, M., Sah, D. and McCoy, J. (2005) 'TAJ/TROY, an orphan TNF

receptor family member, binds Nogo-66 receptor 1 and regulates axonal regeneration', *Neuron,* 45, 353 - 9.

Shepard, P. D., Holcomb, H. H. and Gold, J. M. (2006) 'Schizophrenia in translation: the presence of absence: habenular regulation of dopamine neurons and the encoding of negative outcomes', *Schizophr Bull,* 32(3), 417-21.

Shibata, H. and Suzuki, T. (1984) 'Efferent projections of the interpeduncular complex in the rat, with special reference to its subnuclei: a retrograde horseradish peroxidase study', *Brain Res,* 296(2), 345-9.

Shimada, S., Inagaki, S., Kubota, Y., Ogawa, N., Shibasaki, T. and Takagi, H. (1989) 'Coexistence of peptides (corticotropin releasing factor/neurotensin and substance P/somatostatin) in the bed nucleus of the stria terminalis and central amygdaloid nucleus of the rat', *Neuroscience,* 30(2), 377-83.

Shimogori, T., Lee, D. A., Miranda-Angulo, A., Yang, Y., Wang, H., Jiang, L., Yoshida, A. C., Kataoka, A., Mashiko, H., Avetisyan, M., Qi, L., Qian, J. and Blackshaw, S. (2010) 'A genomic atlas of mouse hypothalamic development', *Nat Neurosci,* 13(6), 767-75.

Shinza-Kameda, M., Takasu, E., Sakurai, K., Hayashi, S. and Nose, A. (2006) 'Regulation of layer-specific targeting by reciprocal expression of a cell adhesion molecule, capricious', *Neuron,* 49(2), 205-13.

Shishido, E., Takeichi, M. and Nose, A. (1998) 'Drosophila Synapse Formation: Regulation by Transmembrane Protein with Leu-Rich Repeats, CAPRICIOUS', *Science,* 280(5372), 2118-2121.

Shmelkov, S. V., Hormigo, A., Jing, D., Proenca, C. C., Bath, K. G., Milde, T., Shmelkov, E., Kushner, J. S., Baljevic, M., Dincheva, I., Murphy, A. J., Valenzuela, D. M., Gale, N. W., Yancopoulos, G. D., Ninan, I., Lee, F. S. and Rafii,

S. (2010) 'Slitrk5 deficiency impairs corticostriatal circuitry and leads to obsessive-compulsive-like behaviors in mice', *Nat Med,* 16(5), 598-602, 1p following 602.

Silva, J. P. and Ushkaryov, Y. A. (2010) 'The latrophilins, "split-personality" receptors', *Adv Exp Med Biol,* 706, 59-75.

Sirerol-Piquer, M. S., Ayerdi-Izquierdo, A., Morante-Redolat, J. M., Herranz-Perez, V., Favell, K., Barker, P. A. and Perez-Tur, J. (2006) 'The epilepsy gene LGI1 encodes a secreted glycoprotein that binds to the cell surface', *Hum Mol Genet,* 15(23), 3436-45.

Smits, G. and Kajava, A. (2004) 'LRRC8 extracellular domain is composed of 17 leucine-rich repeats', *Mol Immunol,* 41, 561 - 2.

Sollner, C. and Wright, G. J. (2009) 'A cell surface interaction network of neural leucine-rich repeat receptors', *Genome Biol,* 10(9), R99.

Sousa, I., Clark, T. G., Holt, R., Pagnamenta, A. T., Mulder, E. J., Minderaa, R. B., Bailey, A. J., Battaglia, A., Klauck, S. M., Poustka, F. and Monaco, A. P. (2010) 'Polymorphisms in leucine-rich repeat genes are associated with autism spectrum disorder susceptibility in populations of European ancestry', *Mol Autism,* 1(1), 7.

Stamatakis, A. M. and Stuber, G. D. (2012) 'Activation of lateral habenula inputs to the ventral midbrain promotes behavioral avoidance', *Nat Neurosci,* 15(8), 1105-7.

State, M. W. (2011) 'The genetics of Tourette disorder', *Curr Opin Genet Dev,* 21(3), 302-9.

Steiner, H., Fuchs, S. and Accili, D. (1997) 'D3 dopamine receptor-deficient mouse: evidence for reduced anxiety', *Physiol Behav,* 63(1), 137-41.

Stephenson-Jones, M., Floros, O., Robertson, B. and Grillner, S. (2012) 'Evolutionary conservation of the habenular nuclei and their circuitry controlling the dopamine and 5-hydroxytryptophan (5-HT) systems', *Proc Natl Acad Sci U S A,* 109(3), E164-73.

Stocco, A., Lebiere, C. and Anderson, J. R. (2010) 'Conditional routing of information to the cortex: a model of the basal ganglia's role in cognitive coordination', *Psychol Rev,* 117(2), 541-74.

Strack, S., Barban, M. A., Wadzinski, B. E. and Colbran, R. J. (1997) 'Differential Inactivation of Postsynaptic Density-Associated and Soluble Ca2+/Calmodulin-Dependent Protein Kinase II by Protein Phosphatases 1 and 2A', *J Neurochem,* 68(5), 2119-2128.

Stringer, J. L. (1993) 'Alterations in both excitation and inhibition occur before the onset of seizure activity in the hippocampus', *Epilepsy Res,* 16(2), 99-109.

Sulzer, D. (2011) 'How addictive drugs disrupt presynaptic dopamine neurotransmission', *Neuron,* 69(4), 628-49.

Sutherland, R. J. (1982) 'The dorsal diencephalic conduction system: a review of the anatomy and functions of the habenular complex', *Neurosci Biobehav Rev,* 6(1), 1-13.

Swanson, L. W. and Cowan, W. M. (1979) 'The connections of the septal region in the rat', *J Comp Neurol,* 186(4), 621-655.

Sylwestrak, E. L. and Ghosh, A. (2012) 'Elfn1 Regulates Target-Specific Release Probability at CA1-Interneuron Synapses', *Science.*

Takahashi, H., Shoji, H., Ando, S., Kanayama, Y., Kusano, T., Takeshita, M., Suzuki, M. and Masuta, C. (2012) 'RCY1-mediated resistance to Cucumber

mosaic virus is regulated by LRR domain-mediated interaction with CMV(Y) following degradation of RCY1', *Mol Plant Microbe Interact,* 25(9), 1171-85.

Takeichi, M. (2007) 'The cadherin superfamily in neuronal connections and interactions', *Nat Rev Neurosci,* 8(1), 11-20.

Tanji, H., Ohto, U., Shibata, T., Miyake, K. and Shimizu, T. (2013) 'Structural reorganization of the Toll-like receptor 8 dimer induced by agonistic ligands', *Science,* 339(6126), 1426-9.

Tasheva, E., Klocke, B. and Conrad, G. (2004) 'Analysis of transcriptional regulation of the small leucine rich proteoglycans', *Mol Vis,* 10, 758 - 72.

Tautz, D. and Pfeifle, C. (1989) 'A non-radioactive in situ hybridization method for the localization of specific RNAs in Drosophila embryos reveals translational control of the segmentation gene hunchback', *Chromosoma,* 98(2), 81-5.

Tepper, J. M. and Lee, C. R. (2007) 'GABAergic control of substantia nigra dopaminergic neurons', *Prog Brain Res,* 160, 189-208.

Tessier-Lavigne, M. and Goodman, C. S. (1996) 'The molecular biology of axon guidance', *Science,* 274(5290), 1123-33.

Tsuji, L., Yamashita, T., Kubo, T., Madura, T., Tanaka, H., Hosokawa, K. and Tohyama, M. (2004) 'FLRT3, a cell surface molecule containing LRR repeats and a FNIII domain, promotes neurite outgrowth', *Biochem Biophys Res Commun,* 313(4), 1086-91.

Turner, C. P., DeBenedetto, D., Ware, E., Stowe, R., Lee, A., Swanson, J., Walburg, C., Lambert, A., Lyle, M., Desai, P. and Liu, C. (2010) 'Postnatal exposure to MK801 induces selective changes in GAD67 or parvalbumin', *Exp Brain Res,* 201(3), 479-88.

Tusnady, G. and Simon, I. (2001) 'The HMMTOP transmembrane topology prediction server', *Bioinformatics,* 17, 849 - 50.

Ullrich, A. and Schlessinger, J. (1990) 'Signal transduction by receptors with tyrosine kinase activity', *Cell,* 61(2), 203-12.

Vacher, C.-M., Gassmann, M., Desrayaud, S., Challet, E., Bradaia, A., Hoyer, D., Waldmeier, P., Kaupmann, K., Pévet, P. and Bettler, B. (2006) 'Hyperdopaminergia and altered locomotor activity in GABAB1-deficient mice', *J Neurochem,* 97(4), 979-991.

Valiente, M. and Marin, O. (2010) 'Neuronal migration mechanisms in development and disease', *Curr Opin Neurobiol,* 20(1), 68-78.

van den Buuse, M. and de Jong, W. (1989) 'Differential effects of dopaminergic drugs on open-field behavior of spontaneously hypertensive rats and normotensive Wistar-Kyoto rats', *J Pharmacol Exp Ther,* 248(3), 1189-96.

Van Vactor, D., Krantz, D., Reinke, R. and Zipursky, S. (1988) 'Analysis of mutants in chaoptin, a photoreceptor cell-specific glycoprotein in Drosophila, reveals its role in cellular morphogenesis', *Cell,* 52, 281 - 90.

Viggiano, D., Ruocco, L. A. and Sadile, A. G. (2003) 'Dopamine phenotype and behaviour in animal models: in relation to attention deficit hyperactivity disorder', *Neurosci Biobehav Rev,* 27(7), 623-37.

Vilarino-Guell, C., Wider, C., Ross, O. A., Jasinska-Myga, B., Kachergus, J., Cobb, S. A., Soto-Ortolaza, A. I., Behrouz, B., Heckman, M. G., Diehl, N. N., Testa, C. M., Wszolek, Z. K., Uitti, R. J., Jankovic, J., Louis, E. D., Clark, L. N., Rajput, A. and Farrer, M. J. (2010) 'LINGO1 and LINGO2 variants are associated with essential tremor and Parkinson disease', *Neurogenetics,* 11(4), 401-8.

Vitek, J. L. and Giroux, M. (2000) 'Physiology of hypokinetic and hyperkinetic movement disorders: model for dyskinesia', *Ann Neurol,* 47(4 Suppl 1), S131-40.

Vogel, C., Teichmann, S. and Chothia, C. (2003) 'The immunoglobulin superfamily in Drosophila melanogaster and Caenorhabditis elegans and the evolution of complexity', *Development,* 130, 6317 - 28.

Wadachi, R. and Hargreaves, K. (2006) 'Trigeminal nociceptors express TLR-4 and CD14: a mechanism for pain due to infection', *J Dent Res,* 85, 49 - 53.

Walker, D. L., Toufexis, D. J. and Davis, M. (2003) 'Role of the bed nucleus of the stria terminalis versus the amygdala in fear, stress, and anxiety', *Eur J Pharmacol,* 463(1-3), 199-216.

Walker, M. C., White, H. S. and Sander, J. W. (2002) 'Disease modification in partial epilepsy', *Brain,* 125(Pt 9), 1937-50.

Walsh, R. N. and Cummins, R. A. (1976) 'The Open-Field Test: a critical review', *Psychol Bull,* 83(3), 482-504.

Wang, K., Kim, J., Sivasankaran, R., Segal, R. and He, Z. (2002a) 'P75 interacts with the Nogo receptor as a co-receptor for Nogo, MAG and OMgp', *Nature,* 420, 74 - 8.

Wang, K., Koprivica, V., Kim, J., Sivasankaran, R., Guo, Y., Neve, R. and He, Z. (2002b) 'Oligodendrocyte-myelin glycoprotein is a Nogo receptor ligand that inhibits neurite outgrowth', *Nature,* 417, 941 - 4.

Wang, R. Y. and Aghajanian, G. K. (1977) 'Physiological evidence for habenula as major link between forebrain and midbrain raphe', *Science,* 197(4298), 89-91.

Wang, W., Yang, Y., Li, L. and Shi, Y. (2003) 'Synleurin, a novel leucine-rich repeat protein that increases the intensity of pleiotropic cytokine responses', *Biochem Biophys Res Commun,* 305(4), 981-8.

Wang, Y., Zhang, J., Mori, S. and Nathans, J. (2006) 'Axonal growth and guidance defects in Frizzled3 knock-out mice: a comparison of diffusion tensor magnetic resonance imaging, neurofilament staining, and genetically directed cell labeling', *J Neurosci,* 26(2), 355-64.

West, A., Koblansky, A. and Ghosh, S. (2006) 'Recognition and signaling by toll-like receptors', *Annu Rev Cell Dev Biol,* 22, 409 - 37.

Whitman, S. P., Archer, K. J., Feng, L., Baldus, C., Becknell, B., Carlson, B. D., Carroll, A. J., Mrozek, K., Vardiman, J. W., George, S. L., Kolitz, J. E., Larson, R. A., Bloomfield, C. D. and Caligiuri, M. A. (2001) 'Absence of the wild-type allele predicts poor prognosis in adult de novo acute myeloid leukemia with normal cytogenetics and the internal tandem duplication of FLT3: a cancer and leukemia group B study', *Cancer Res,* 61(19), 7233-9.

Wills, Z. P., Mandel-Brehm, C., Mardinly, A. R., McCord, A. E., Giger, R. J. and Greenberg, M. E. (2012) 'The nogo receptor family restricts synapse number in the developing hippocampus', *Neuron,* 73(3), 466-81.

Winberg, M. L., Mitchell, K. J. and Goodman, C. S. (1998) 'Genetic analysis of the mechanisms controlling target selection: complementary and combinatorial functions of netrins, semaphorins, and IgCAMs', *Cell,* 93(4), 581-91.

Wirtshafter, D., Asin, K. E. and Pitzer, M. R. (1994) 'Dopamine agonists and stress produce different patterns of Fos-like immunoreactivity in the lateral habenula', *Brain Res,* 633(1-2), 21-6.

Woo, J., Kwon, S. K. and Kim, E. (2009) 'The NGL family of leucine-rich repeat-containing synaptic adhesion molecules', *Mol Cell Neurosci,* 42(1), 1-10.

Wree, A., Zilles, K. and Schleicher, A. (1981) 'Growth of fresh volumes and spontaneous cell death in the nuclei habenulae of albino rats during ontogenesis', *Anat Embryol (Berl),* 161(4), 419-31.

Wu, H. F., Cen, J. S., Zhong, Q., Chen, L., Wang, J., Deng, D. Y. and Wan, Y. (2013) 'The promotion of functional recovery and nerve regeneration after spinal cord injury by lentiviral vectors encoding Lingo-1 shRNA delivered by Pluronic F-127', *Biomaterials,* 34(6), 1686-700.

Wu, Y. W., Prakash, K. M., Rong, T. Y., Li, H. H., Xiao, Q., Tan, L. C., Au, W. L., Ding, J. Q., Chen, S. D. and Tan, E. K. (2011) 'Lingo2 variants associated with essential tremor and Parkinson's disease', *Hum Genet,* 129(6), 611-5.

Xu, B., Woodroffe, A., Rodriguez-Murillo, L., Roos, J. L., van Rensburg, E. J., Abecasis, G. R., Gogos, J. A. and Karayiorgou, M. (2009) 'Elucidating the genetic architecture of familial schizophrenia using rare copy number variant and linkage scans', *Proceedings of the National Academy of Sciences,* 106(39), 16746-16751.

Yamagishi, S., Hampel, F., Hata, K., Del Toro, D., Schwark, M., Kvachnina, E., Bastmeyer, M., Yamashita, T., Tarabykin, V., Klein, R. and Egea, J. (2011) 'FLRT2 and FLRT3 act as repulsive guidance cues for Unc5-positive neurons', *EMBO J,* 30(14), 2920-33.

Yang, J., Liu, X., Zhao, Y., Adamian, M., Pawlyk, B., Sun, X., McMillan, D. R., Liberman, M. C. and Li, T. (2010) 'Ablation of whirlin long isoform disrupts the USH2 protein complex and causes vision and hearing loss', *PLoS Genet,* 6(5), e1000955.

Yang, L. M., Hu, B., Xia, Y. H., Zhang, B. L. and Zhao, H. (2008) 'Lateral habenula lesions improve the behavioral response in depressed rats via

increasing the serotonin level in dorsal raphe nucleus', *Behav Brain Res,* 188(1), 84-90.

Yoshihara, S.-i., Takahashi, H., Nishimura, N., Naritsuka, H., Shirao, T., Hirai, H., Yoshihara, Y., Mori, K., Stern, P. L. and Tsuboi, A. (2012) '5T4 Glycoprotein Regulates the Sensory Input-Dependent Development of a Specific Subtype of Newborn Interneurons in the Mouse Olfactory Bulb', *The Journal of Neuroscience,* 32(6), 2217-2226.

Ypsilanti, A. R., Zagar, Y. and Chedotal, A. (2010) 'Moving away from the midline: new developments for Slit and Robo', *Development,* 137(12), 1939-1952.

Yuste, R. and Bonhoeffer, T. (2001) 'Morphological changes in dendritic spines associated with long-term synaptic plasticity', *Annu Rev Neurosci,* 24, 1071-89.

Zhou, Y. D., Lee, S., Jin, Z., Wright, M., Smith, S. E. and Anderson, M. P. (2009) 'Arrested maturation of excitatory synapses in autosomal dominant lateral temporal lobe epilepsy', *Nat Med,* 15(10), 1208-14.